Thermodynamic studies on Semi-Clathrate Hydrates of TBAB + gases containing Carbon Dioxide

Ali Eslamimanesh

Ecole doctorale n° 432 : Sciences des Métiers de l'Ingénieur

Doctorat ParisTech

T H È S E

pour obtenir le grade de docteur délivré par

l'École Nationale Supérieure des Mines de Paris

Spécialité " Génie des Procédés "

En vue de sa soutenance publique

le 14 Août 2012

Ali ESLAMIMANESH

Études Thermodynamiques sur les Semi-Clathrate Hydrates de TBAB + Gaz Contenant du Dioxyde de Carbone

Thermodynamic Studies on Semi-Clathrate Hydrates of TBAB + Gases Containing Carbon Dioxide

Directeur de thèse I: **Dominique RICHON**
Directeur de thèse II: **Amir H. MOHAMMADI**

Jury
Mme Josefa FERNANDEZ, Professor, Dept. de Física Aplicada, Universidade de Santiago de Compostela *Rapporteur*
M. Georgios M. KONTOGEORGIS, Professor, Dept. of Chemical and Biochemical Engineering, DTU   *Rapporteur*
M. Nicolas von SOLMS, Professor, Dept. of Chemical and Biochemical Engineering, DTU   *Rapporteur*
M. Abbas FIROOZABADI, Professor, Dept. of Chemical & Environmental Engineering, Yale University   *Examinateur*
M. Amir H. MOHAMMADI, Doctor (HDR), CEP/TEP, MINES ParisTech   *Examinateur*
M. Deresh RAMJUGERNATH, Professor, School of Chemical Engineering, UKZN   *Examinateur*
M. Dominique RICHON, Professor, CEP/TEP, MINES ParisTech   *Examinateur*
M. Dendy SLOAN, Professor, Chemical Engineering Dept., Colorado School of Mines   *Examinateur*

MINES ParisTech
Centre Énergétique et Procédés - Laboratoire CEP/TEP
35, rue Saint Honoré, 77305 Fontainebleau cedex, France

T
H
E
S
E

تقدیم به خانواده عزیزتر از جانم که به من عشق را آموختند...

Acknowledgements

Significant thanks should be dedicated to my dear friends in France: Amir A. Karimi, Marco Campestrini, Dr. Moussa Dicko, Dr. Chien Bin Soo, Haifan Liu, and Veronica Belandria. I wish you all success in your entire life.

In this step, I wish to state my highest gratitude to the jury members, whose names and fames have resulted in my great honor. Many thanks for taking their valuable time.

Finally, I would like to emphasize my interest in solving problems of humanity by application of what I gained throughout my studies as this is the best way of using the abilities that have been bestowed on every man.

Paris, August 2012

Ali ESLAMIMANESH

Table of contents

List of Figures

List of Tables

List of Abbreviations and Symbols

A = area in Eq. (7.5); parameter of Henry's constant correlation in Eq. (4.22); parameter in Eq. (7.35)

A_{12} & A_{21} = NRTL model parameters

AD = absolute deviation, %

$AARD$ = average absolute relative deviation, %

ANN = artificial neural network

ARD = absolute relative deviation, %

a = attractive parameter of the equation of state, ($MPa.m^6/mol^2$); activity of water; estimated value of an unknown variable in Eq. (6.12); parameter in Eq. (7.34)

aa = parameter of Langmuir constant correlation in Eq. (4.14)

$\bar{a}$ = parameter of equation of state in Eq. (A.3)

B = Parameter of Henry's constant correlation in Eq. (4.22), (K); tightening bolts; parameter in Eq. (7.35)

b = repulsive parameter of the equation of state, (m^3/mol); parameter in Eq. (7.34)

bb = parameter of Langmuir constant correlation in Eq. (4.14)

C = Langmuir constant; parameter in Eq. (7.35)

C_P = molar heat capacity, ($kJ.mol^{-1}.K^{-1}$)

$C^{'}$ = Parameter of Henry's constant correlation in Eq. (4.22)

c = third parameter of the equation of state, (m^3/mol); parameter of Langmuir constant correlation in Eq. (4.12)

CBF = conventional blast furnace

CBM = cold bed methane

16

CC_{1-3} = Mathias-Copeman alpha function parameters

CCS = carbon dioxide capture and sequestration (storage)

$CSMGem$ = Colorado School of Mines Gibbs Energy Minimization

D = Parameter of Henry's constant correlation in Eq. (4.22), (K^{-1}); parameter in Eq. (7.35)

DAU = data acquisition unit

DE = differential evolution optimization strategy

DW = degassed water

d = parameter of Langmuir constant correlation in Eq. (4.12); derivative operator

E = error; parameter in Eq. (7.35)

EC = equilibrium cell

EoS = equation of state

e = parameter of Langmuir constant correlation in Eq. (4.12)

F = coefficient of the equation of state in Eq. (A.7); parameter in Eq. (7.35)

FF = primary objective function before introducing the constraints

f = fugacity, (MPa); non-linear function

f' = parameter of Langmuir constant correlation in Eq. (4.13)

G = gas cylinder

GC = group contributions; gas chromatograph

g = parameter of Langmuir constant correlation in Eq. (4.13)

gg = inequality constraint

H = hydrate; heat of dissociation; Henry's constant defined in Eq. (4.8); Hat matrix in Eq. (7.33)

HDP = hydrate dissociation point

HFC = hydrofluorocarbons

HPT = high pressure transducer

h = enthalpy, (kJ/mol); adjustable parameter in Eq. (4.11)

I = Ice

IL = ionic liquid

i = parameter of Langmuir constant correlation in Eq. (4.13)

J = Jacobian Matrix

K = vapor-solid distribution coefficient defined by Eq. (3.1)

k = binary interaction parameter; Boltzmann's constant in Eq. (3.9)

L = liquid

LB = liquid bath

LD = lattice dynamics

LNG = liquefied natural gas

LPT = low pressure transducer

LSSVM = least-squares support vector machine

LTX = low temperature extraction

l = binary interaction parameter for the asymmetric term of the VPT-EoS

MB = main body

MC = monte carlo

MD = molecular dynamic

MEA = monoethanolamine

MR = magnetic rod

M_w *= molecular weight, (g.mol^{-1})*

m = molality, (mol.kg^{-1}); gas mixture in Eq. (6.1)

N = number of experimental data points

N_A *= Avogadro's number*

N_w^{MT} *= number of water molecules per hydrate cell*

NFC = not fully consistent

NMR = nuclear magnetic resonance

NRTL = non-random two-liquid model

n = hydrate number in Eq. (3.2); mole number in Eq. (6.1); number of training points

ndp = number of data points

OF = objective function

P = pressure, (MPa)

PG = protection grid

PP = platinum probe

PR = Peng-Robinson

PT = pressure transducer

PVT = pressure-volume-temperature

p = number of model input parameters

q = hydration number

$q_{1,2}$ *= parameters in Eq. (4.25)*

QSPR = quantitative structure-property relationships

R = universal gas constant, $(MPa.m^{3.}mol^{-1}.K^{-1})$; standardized cross-validated residuals

Ref. = reference

ROLSI ^{TM} = rapid on-line sampler-injector

RS = ROLSI ^{TM}

r = distance measured from centre of a spherically symmetric hydrate cell

$r_{1,2}$ = parameters in Eq. (4.25)

$\bar{R}$ = cavity radius

R-134a = 1,1,1,2-tetrafluoroethane

SA = stirring assembly

SAFT-VR = statistical associating fluid theory with variable range for electrolytes

SD = stirring device

SV = isolation valve

SVM = support vector machine

SW = sapphire windows

s = hydrate structure

$s_{1,2,3}$ = parameters in Eq. (4.25)

T = temperature, (K)

TBAB = tetra-n-butyl ammonium bromide

TBAC = tetra-n-butyl ammonium chloride

TC = thermodynamically consistent

THF = tetrahydrofuran

TI = thermodynamically inconsistent

TR = temperature regulator

V = vapor; volume; valve

VP = vacuum pump

v = molar volume, ($m^3.mol^{-1}$)

vp = vapor pressure, (MPa)

v'_m = number of cavities of type m per water molecule in the unit hydrate cell

vdW-P = van der Waals and Platteeuw solid solution theory

WP = high pressure pump

w = weight fraction

X = two-dimensional matrix

XRD = X-ray diffraction analysis

x = mole fraction in liquid phase

y = mole fraction in vapor phase

Z = compressibility factor

z = mole fraction in water-free solid hydrate; coordination number of the cavity in Eq. (3.10)

Greek letters

α = alpha function of the equation of state; the radius of spherical molecular core in Eq. (3.11)

γ = activity coefficient

φ = fugacity coefficient

Δ = difference value

Ψ = coefficient in Eq. (A.11)

ω = acentric factor

Ω = coefficients in Eqs. (A.3) to (A.5)

μ = chemical potential

π = π number

ε = characteristic energy; specified tolerance during the calculation steps of the Newton's numerical method in Eq. (6.15)

δ = Kihara potential parameter in Eq. (3.10)

σ = collision diameter

∞ = infinite dilution

ρ = density, $(g.cm^{-3})$

β = parameter in Eq. (4.28)

θ = cage occupancy

Subscripts

A = area

c = critical state

cal. = calculated

exp. = experimental

g = gas

H = hydrate

HC = hydrocarbon hydrate former

I = ice

i = i^{th} component in a mixture; i^{th} experimental data set

j = j^{th} component in a mixture; j^{th} individual calculated area

large = large cavity

m = numbers of particular functions

n = numbers of related variables

P = index of polar components

p = gas hydrate formation promoter; experimental P-T-x/y data in Eq. (7.5)

pred. = predicted

r = reduced property

s = dissolution

small = small cavity

w = water; spherically symmetric cell potential in the cavity

φ = calculated parameters of the model for evaluations of the integrals in Eq. (7.6)

0 = reference property

1 = refers to methane, occupation of large tetrakaidecahedra cavities in Eq. (4.10)

2 = refers to water, occupation of large pentakaidecahedra cavities in Eq. (4.10)

Superscripts

A = refers to asymmetric interaction

C = attractive term of the VPT-EoS defined by classical quadratic mixing rules

calc. = calculated

diss = dissociation

E = excess property

exp. = experimental

H = hydrate

G = gas

g = gas

I = ice

L = liquid state

L_w = liquid water

large = large cavity

MT = hypothetical empty hydrate lattice

pred. = predicted

sat = saturated state

small = small cavity

t = total; transpose matrix in Eq. (7.33)

V = vapor

v = vapor

Ψ = parameter in Eq. (A.6)

0 = first parameter of asymmetric binary interaction parameter

1 = second parameter of asymmetric binary interaction parameter

*= *warning Leverage*

1. Introduction

Introduction: Contexte Historique

Le piégeage d'une molécule (ou molécules) d'un composé dans une structure formée par les molécules d'un autre composé génère des structures nommées clathrates ou composés d´inclusion.[1,2] Les caractéristiques remarquables des molécules d'eau donnent lieu à la formation de réseaux tridimensionnels de liaisons hydrogènes capables d´enfermer en leur sein des types particuliers de molécules.[3] Le composé final qui est appelé hydrate a fait l'objet de nombreuses études depuis le 19ième siècle.[1-3]

Les premières études sur les hydrates sont attribuées à Sir Humphrey Davy,[4] et à Michael Faraday,[5] qui a découvert l'hydrate du chlore. Sir Humphrey Davy a déclaré que le solide qu´il avait découvert, semblable à de la glace (pas seulement composé de molécules d'eau), avait été formé à des températures supérieures au point de congélation de l´eau.[1,2] Michael Faraday a fourni la composition de l'hydrate de chlore (sans doute pour la première fois).

Au cours des périodes suivantes, deux groupes d'hydrates, comprenant les hydrates d'alkylamine et les hydrates de sel d'ammonium quaternaire ont été identifiés [3,6,7] Toutefois, les hydrates les plus importants pour l'industrie, qui sont « les hydrates de gaz (ou clathrate) » ont commencé à être considérés après la présentation de Davy en 1811.[2,4] Les hydrates de gaz sont des solides cristallins composés d'eau et de petites molécules.[1,2] Dans le cadre des « clathrates hydrates » (réseau solide ouvert), les molécules d'eau sont considérées comme « hôtes » tandis que les autres molécules, qui sont capturées dans les réseaux des liaisons hydrogènes de l'eau (cages), sont appelées « invitées ».[2] Les molécules invitées peuvent être celles de gaz de taille appropriée, de certains liquides volatils, etc.[2,8,9] Les hydrates de gaz se forment généralement à des températures relativement basses mais supérieures au point de congélation de l´eau et à des pressions élevées, dû à l´effet stabilisant de la molécule invitée.[2]

Dans ce chapitre, nous trouvons une brève description des clathrates hydrates, de leurs différentes structures, de certaines de leurs caractéristiques et de leur rôle dans l'industrie pétrolière.

1.1. Historical background

Trapping of a molecule (or molecules) of a compound in a structure formed by the molecules of another compound normally generates clathrate structures or inclusion compounds.[1,2] The unique characteristics of the water molecules result in formation of hydrogen-bonded three-dimensional networks able to encage particular kinds of molecules.[3] The final compound is called the "hydrate", which has been the subject of many studies from the 19th century.[1-3]

The first investigations on the hydrate compounds are attributed to the Sir Humphrey Davy,[4] and Michael Faraday,[5] who discovered the hydrate of chlorine. The former scientist stated that the discovered ice-like solid (which also composed of other molecules than those of water) were formed even at temperatures greater than the freezing point of water.[1,2] The latter researcher reported the composition of the chlorine hydrate (perhaps for the first time).

Throughout the later periods, two groups of hydrates including the alkylamine hydrates and the quaternary ammonium salt hydrates were noticed.[3,6,7] However, the most significant hydrates for the industry, which are "gas (or clathrate) hydrates" were begun to be noted after Davy's lecture in 1811.[2,4] Gas hydrates are crystalline solid compounds composed of water and smaller molecules.[1,2] In the clathrate hydrate framework (open solid lattice), water molecules are considered as the "hosts" and the other ones, which are captured in the water hydrogen-bonded networks (cages) are called the "guests".[2] The guest molecules can be of appropriate size gases, some volatile liquids, etc.[2,8,9] Gas hydrates generally form at low temperatures and elevated pressures stabilized by the guest molecules.[2]

It is currently clear that the clathrate hydrates are nonstoichiometric compounds and distinguished from ice, which has a normal hexagonal structure. In earlier times, the difference between ice and hydrate was clarified using the effects of the two structures on the polarized light due to the fact that hydrates do not have any effects on the polarized light while the effects of ice are obvious.[2]

In this chapter, description of clathrate hydrates, their different structures, some particular characteristics as well as their role in petroleum industry are briefly presented.

1.2. Clathrate hydrates of hydrocarbons

The French chemists, Villard[10] and de Forcrand,[11] might be the premier scientists to contribute a lot in discovery of hydrates of hydrocarbons.[1,2] Villard noticed the existence of hydrates of methane (CH_4), ethane (C_2H_6), and propane (C_3H_8) for the first time.[1,2] In addition, de Forcrand[11] measured the equilibrium temperature of clathrate hydrates of 15 different substances including natural gas species at 1 atm.[2]

The primary researches in the fields of hydrates of hydrocarbons were mostly dealing with the estimation of number of water molecules per guest molecule in hydrate crystalline structure. For instance, Villard[10] reported a hydrate structure containing 6 water molecules per guest molecule.[1] Later, Schroeder[12] stated that the previous discovered structure can be only applied to 15 substances (hydrate formers).[2] However, it is nowadays obvious that there are many exceptions for the Villard's theory.[2]

1.3. Natural gas hydrates

Formation of clathrate hydrates from the natural gas constituents can be well observed in petroleum industry (or found abundantly in nature). Water is often associated with natural gas in the reservoirs. Thus, produced natural gas is, in most cases, saturated with water.[2,13,14] As the temperature and pressure change during the production of the gas, water can condense from the flow of the gas. Moreover, natural gas sweetening process (in order to remove hydrogen sulfide and carbon dioxide, the so-called "acid gases") often employs aqueous solutions.[1] The subsequent sweet gas (i.e. the product of the sweetening process) can be saturated with water.[15] Several processes are designed to remove water from natural gas streams. This association of water and natural gas means that gas hydrates may be encountered during the production and processing of natural gas. With this knowledge, engineers working in the natural gas industry know whether hydrates will be a problem in their application. The detection of hydrates in pipelines marked the importance of hydrates in industry and began the new hydrate research era.[2]

1.4. Hydrate structures

Hydrates are classified by the arrangement of the water molecules in the crystal, and hence, the crystal structures. Two types of hydrate structures are observed in the industry (or in the nature): Structure I (sI) and structure II (sII). A third less common type of hydrate structure is structure H (sH), which needs a small molecule (like methane) and a larger hydrate former (like cyclopentane) for stabilization although there may be possibility of formation of other hydrate structures e.g. sIII, sT etc.; however, they are not generally observed in natural gas industry.[2] Table 1.1 shows the characteristics of the different hydrate structures.[1]

1.4.1. Structure I

Structure I is treated as the simplest hydrate structure.[1,2] It is composed of dodecahedron and tetrakaidecahedron cages. Dodecahedron cages can be explained as twelve-sided polyhedron with a pentagon for each face (labeled as 5^{12}, in which 5 stands for the number of edges in a face type, and 12 is the number of faces with 5 edges)[*] while tetrakaidecahedron cages are fourteen-sided polyhedron with twelve pentagonal faces and two hexagonal faces (6^2).[1] Because the dodecahedron cavities are smaller than the tetrakaidecahedron ones, they are normally considered as small cages compared to the latter cavities, which are referred as large ones. Methane, carbon dioxide, and hydrogen sulfide can, for instance, form hydrate sI, in which the hydrate former can occupy both the small and the large cages though only large cavities are occupied by the ethane molecules in the corresponding hydrate compound.[1,2]

1.4.2. Structure II

There are also two kinds of cavities in a unit hydrate cell of sII including a similar dodecahedron as in sI, and hexakaidecahedron consisting of a sixteen-sided polyhedron with twelve pentagonal faces and four hexagonal faces ($5^{12}6^4$). Indeed, the dodecahedral cages are smaller than the hexakaidecahedron cavities in this structure.[1,2] Among the constituents of natural gas, propane, isobutene, and (probably) nitrogen form the sII hydrates. The latter hydrate former occupies both the large and small cavities; however, propane and isobutane only occupy the large ones.[1,2]

1.4.3. Structure H

Three types of cavities can be found in hydrate sH: A regular dodecahedron, an irregular dodecahedron, and an irregular icosahedron. There are constructed from a twelve-sided polyhedron (5^{12}) as in sI and sII, three square faces, six pentagonal faces accompanied by three hexagonal faces that can be presented as ($4^35^66^3$), and a twenty-sided polyhedron as ($5^{12}6^8$), respectively. The cavities of second type are designated as medium cavities.

Generally, the small guest molecules occupy the small and medium cavities in a unit cell of sH clathrate hydrates and larger molecules occupy the large one. 2-methylbutane, 2,2-dimethylbutane, and cycloheptane are examples of the sH hydrate formers.[1,2,16,17] The three types of hydrate structures and their cage arrangements are shown in Figure 1.1.[18]

---

[*] After Jeffrey, 1984.[3]

Table 1.1: The characteristics of 3 types of clathrate hydrate structures. (Reproduced from Carroll[1])

Structure	I	II	H
Water molecules per unit cell	46	136	34
Cages per unit cell			
Small	6	16	3
Medium	-	-	2
Large	2	8	1
Theoretical formula			
All cages filled	X^{*}.5 3/4 H_2O	X.5 2/3 H_2O	5X. Y^{**}. 34 H_2O
Mole fraction of hydrate former	0.1481	0.15	0.15
Only large cages filled	X.7 2/3 H_2O	X. 17 H_2O	-
Mole fraction of hydrate former	0.1154	0.0556	-
Cavity diameter (Å)			
Small	7.9	7.8	7.8
Medium	-	-	8.1
Large	8.6	9.5	11.2
Volume of unit cell (m^3)	1.728×10^{-27}	5.178×10^{-27}	
Typical formers	CH_4, C_2H_6, H_2S, CO_2	N_2, C_3H_8, iC_4H_{10}	2-methylbutane, 2,2-dimethylbutane, etc.

*Hydrate former
** Structure H former

1.4.4. Size of the guest molecule

The relationship between the size of the guest molecules (or the largest van der Waals diameters) and the corresponding structures of the clathrate hydrates can be well represented through a chart firstly reported by Von Stackelberg,[19] which is depicted in Figure 1.2, as reproduced by Sloan and Koh.[2] It is worth pointing out that hydrogen and helium (which have small diameters of about 2.72 and 2.28 Å, respectively) are declared, in this figure, not to form any clathrate hydrates because their diamters are less than 3.8 Å. However, it is currently well demonstrated that extremely high pressures (typically 100 to 360 MPa) can stabilize the sII H_2 clathrate hydrate.[20-23(a,b)] Another element to consider is that the molecules larger than about 7 Å do not form sI or sII clathrate hydrates e.g. pentane, and larger paraffin hydrocarbons. However, these large molecules can be enclathrated in sH hydrates with the help of smaller hydrate former molecules.
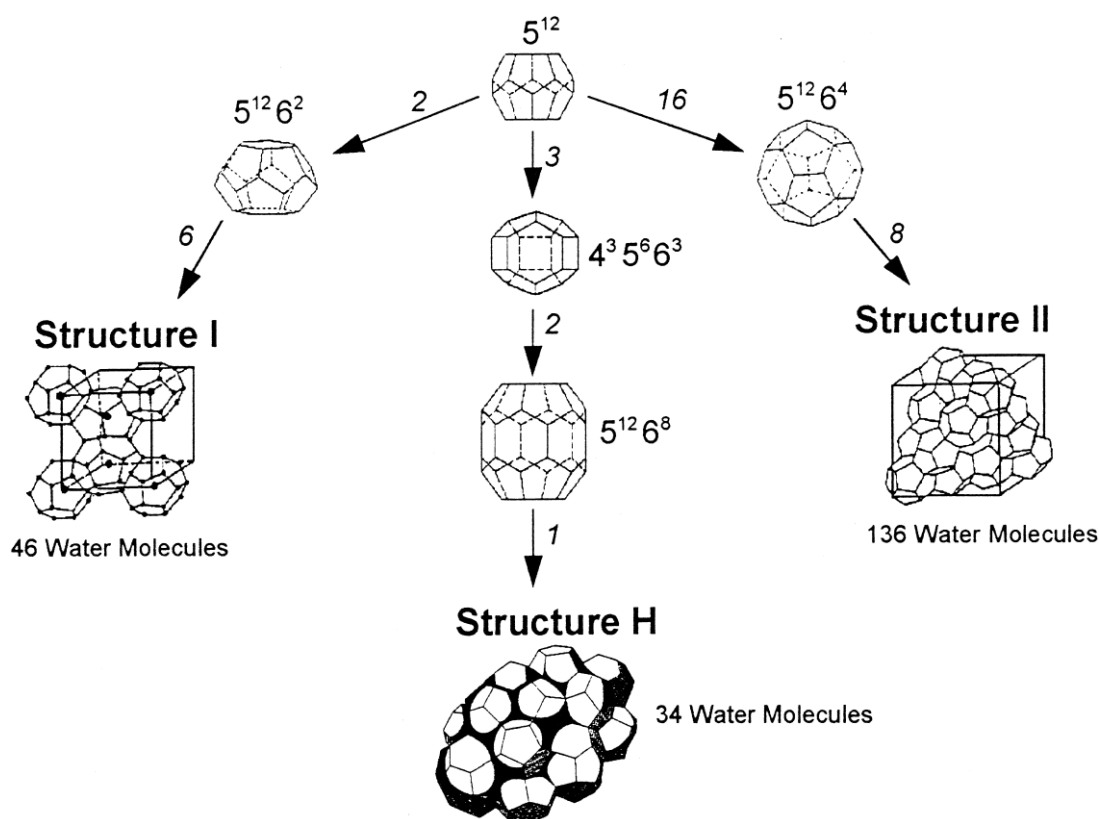
Figure 1.1: Three types of hydrate structures accompanied with their cage arrangements. (Reproduced from Khokhar et al. [18])

1.4.5. Semi-clathrate hydrates

Toward crystallographic studies and X-ray structure analysis, it was found that alkylamines can form particular kinds of clathrates with some broken bonds in the hydrogen-bonded water framework.[3,24,25] These groups of compounds are called "semi-clathrate" hydrates because their structures are more or less similar to those of clathrate hydrates; though, with an incomplete (or immature) water cavities. As a matter of fact, amine group forms a part of the bonded water network and the alkyl may occupy the cavities for stabilization of the hydrate.[3] The quaternary ammonium (like tetra-*n*-butyl ammonium or TBA) salts can also form semi-clathrate hydrates.[3]
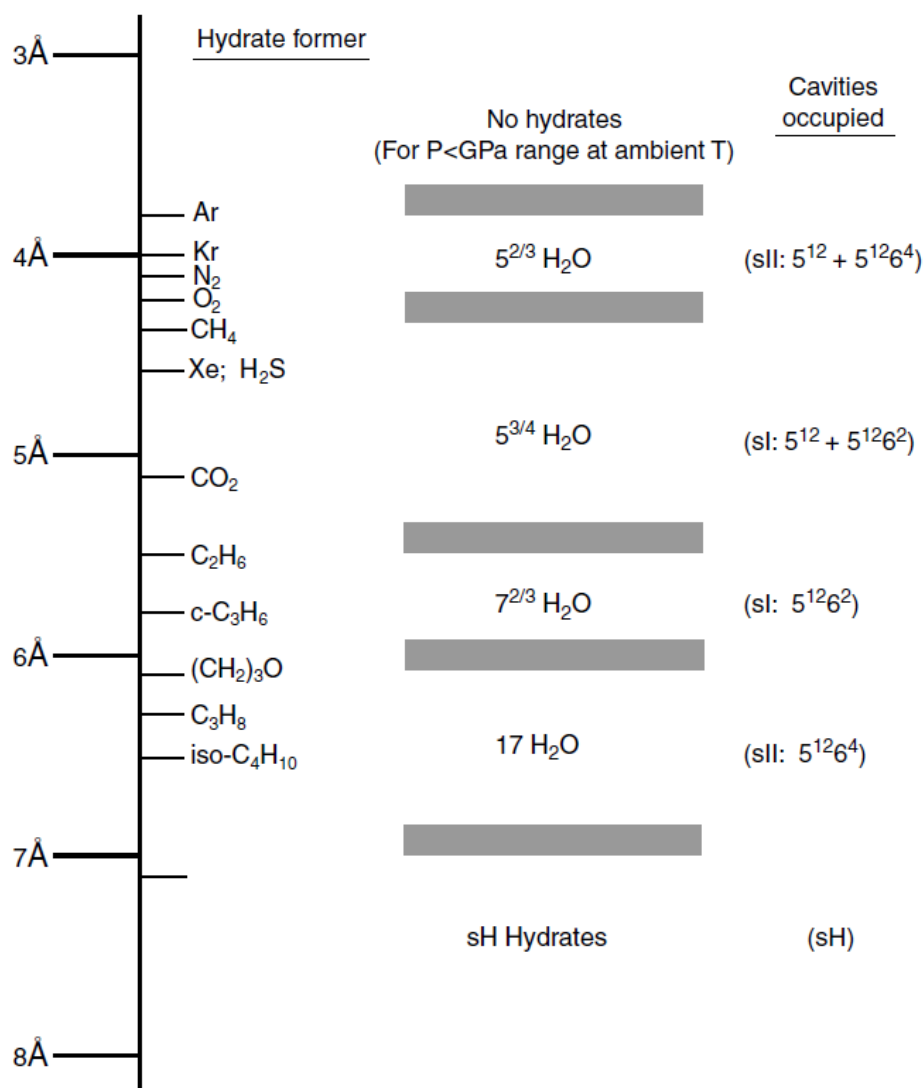
Figure 1.2: Relationships between the molecular sizes of different simple hydrate formers and the corresponding hydrate structures. (Reproduced from Sloan and Koh[2])

In these semi-clathrates, a part of the cage structure is broken in order to enclose the large tetra-*n*-butyl ammonium ion while the halogen anion (e.g. Br⁻, Cl⁻, etc.) may participate in the hydrogen-bonded water network. There are several evidences[26-29] showing that the semi-clathrate hydrates of TBAB (tetra-*n*-butyl ammonium bromide), TBAC (tetra-*n*-butyl ammonium chloride) and so forth can be used as molecular sieves to trap the molecules of particular kinds of hydrate formers, which will be described in detail later. A typical three-dimensional view of the TBAB semi-clathrate hydrate is shown in Figure 1.3.[28]
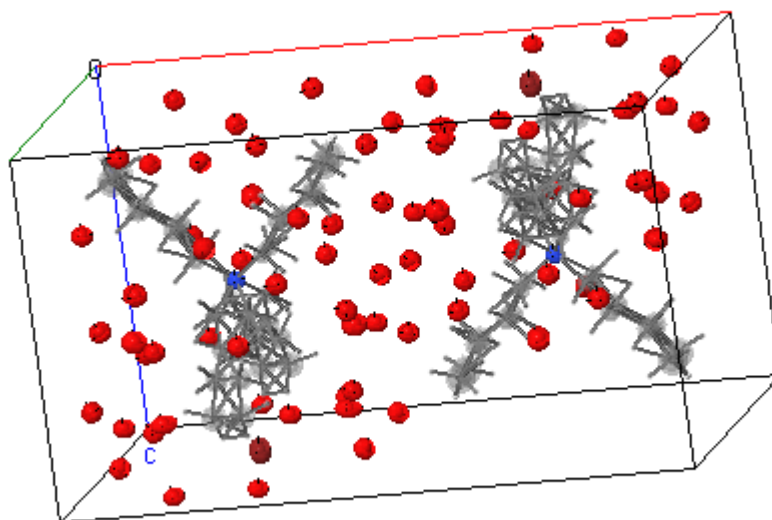
Figure 1.3: A typical three-dimensional view of tetra-n-butyl-ammonium bromide hydrate unit cell. This structure is composed of one molecule of TBAB and 38 molecules of water as: $C_{16}H_{36}N^+ \cdot Br^- \cdot 38H_2O$. (Reproduced from Shimada et al.[28] applying the schematic representation in the online version)

The readers can refer to the book entitled "*Clathrate Hydrates of Natural Gases*" by Sloan and Koh[2] for a comprehensive study on the structures of clathrate hydrates.

2. Application of Gas Hydrates in Separation Processes

Utilisation des hydrates de gaz dans les procédés de séparation

Les premières activités de recherche industrielle sur les hydrates de gaz, qui ont été lancées au début du XXe siècle, sont attribuées à l'exigence de l'industrie pétrolière pour une meilleure compréhension des effets de l'eau dans le cadre de l'exploitation des canalisations de gaz, de pétrole et de traitement de gaz.[30] Comme mentionné précédemment, le contact de l'eau et du gaz naturel fraichement extrait semble être inévitable. Il y a donc une forte probabilité de formation d´hydrates de gaz et/ou condensat d'eau au cours de la production et lors du traitement du gaz naturel.[30] Dans les années 1930, Hammerschmidt[31] annonce que les hydrates de gaz naturel pourraient entraîner le blocage des lignes de transport de gaz. La formation de ces composés contribue à une réduction de la section interne des pipelines et par conséquent à une augmentation de la chute de pression en ligne, conduisant à des coûts plus élevés de production, de transformation et de transport, et des débits plus faibles.[2,30] Le besoin d´inhiber la formation d'hydrates de gaz dans les pipelines a donc focalisé l'attention des ingénieurs au cours du siècle dernier.[1,2,30] La formation des hydrates de gaz peut se produire dans les pipelines bien au-dessous du niveau de la mer où la pression est élevée, ou dans les zones froides, où la température est suffisamment basse.[30] Ce phénomène a également été signalé dans les boues de forage,[32-34] les gisements de pétrole,[35-38] à partir du contenu en eau des gaz naturels,[13,39-51] à l'intérieur de la croûte terrestre,[52-55] à l'extérieur de l'atmosphère terrestre (Mars et Saturne).[2,30,56,57] Partout où les hydrates de gaz ont tendance à se former, il faut scrupuleusement prévenir/résoudre/utiliser les fonctionnalités utiles ou nocives de ces structures chimiques. Les ingénieurs qui rencontrent des problèmes avec les hydrates de gaz (problème de blocages de pipeline) ont généralement recourt à l'une des méthodes suivantes: élimination mécanique des clathrates; réchauffage des pipelines; modification du point de rosée de l'eau dans les unités de déshydratation.[30] Ils sont aidés en cela par les modèles thermodynamiques/cinétiques de prédiction des conditions de dissociation.

La formation des hydrates de gaz, même si c'est quelque chose qui a une connotation négative dans le pétrole et l'industrie de transformation du gaz, a certes le potentiel pour de nombreuses applications positives, par exemple l'utilisation des clathrates hydrates comme moyen de stockage de gaz. De nombreuses applications positives des clathrates hydrates, comme dans le cadre de la capture du dioxyde de carbone et de sa séquestration, du stockage de gaz, des systèmes de climatisation sous la forme de coulis d'hydrates, des technologies de dessalement et de traitement de l'eau, de la concentration des solutions aqueuses diluées, de la séparation des différents gaz contenus dans les effluents de combustion, et de bien d'autres exemples ont été signalées, surtout au cours de ces dernières années.[2,30,58,59]

Dans ce chapitre, nous présentons une brève étude des diverses applications positives des hydrates de gaz, en mettant l'accent sur un examen exhaustif des études réalisées à ce jour

concernant la formation de clathrates/semi-clathrates hydrates comme nouvelle approche pour les procédés de séparation.

The first industrial research activities on gas hydrates, which were initiated in the early 20th century, are attributed to the requirement from the petroleum industry for a better understanding of the effects of water in the operation of gas pipelines, and petroleum and gas processing.[30] As mentioned earlier, association of water with the fresh extracted natural gas streams seems to be inevitable. This phenomena indicates that there is high probability of formation of gas hydrate and/or water condensate during the production and processes of natural gas.[30] In the early 1930s, Hammerschmidt[31] firstly reported that natural gas hydrates might result in blockage of gas transmission lines. Formation of these compounds contributes to a reduction in the pipelines' cross sectional area and consequently increases the pressure drop in the processing of natural gases leading to higher production, processing, and transportation costs and the corresponding lower flow rates.[2,30] Inhibition of gas hydrate formation in pipelines has therefore attracted the attention of engineers in the field over the past century.[1,2,30] Gas hydrate formation may occur in pipelines well below sea level where the pressure is high, or in cold areas, where the temperature is suitably low.[30] This phenomenon has also been reported to occur in drilling muds,[32-34] oil reservoirs,[35-38] from water content of natural gas,[13,39-51] inside the earth's crust,[52-55] and outside the earth's atmosphere (Mars and Saturn).[2,30,56,57] Wherever gas hydrates tend to be formed, significant care should be taken to prevent/solve/use the harmful or useful features of these chemical structures. Engineers encountering problems with gas hydrates generally have to employ one of the following methods to overcome the issue of pipeline blockages: mechanical removal of the clathrates; warming up the pipelines; prediction of the dissociation conditions via thermodynamic/kinetic models; or modifying the dew point of water in dehydration units.[30]

Gas hydrate formation, even though it is something that has negative connotations in the petroleum and gas processing industry, also has the potential for numerous positive applications, e.g. the use of clathrate hydrates as means of gas storage. Many positive applications of clathrate hydrates such as in carbon dioxide capture and sequestration, gas storage, air-conditioning systems in the form of hydrate slurry, water desalination/treatment technology, concentration of dilute aqueous solutions, separation of different gases from flue gas streams, and many other examples have been reported, especially in recent years.[2,30,58,59]

In this chapter, a brief study of the various positive applications of gas hydrates is presented, focusing on a comprehensive review of studies undertaken to date with regard to the application of clathrate/semi-clathrate hydrate formation as a novel approach for separation processes.

2.1. Some positive uses of gas hydrates

2.1.1. Gas supply

Natural reserves of gas hydrates in the earth can be used as a gas/natural gas supply by providing the increasing amounts of energy needed by the world economy.[30] The estimated amount of methane in-situ gas reserves is approximately 10^{16} m^3.[60,61] Furthermore, some estimations show that there are more organic carbon reserves present globally as methane hydrates than all other forms of fossil fuels.[62] It is currently believed that if only about 1% of the estimated reserves of methane from methane hydrate reserves are recovered, it may be enough for the United States to satisfy its energy demands for the next eight decades.[30,63] There are generally three methods of methane production from these hydrate reserves:[30,64]

1. Pressure reduction in the reservoirs to conditions below the gas hydrate equilibrium pressure;

2. Increasing the temperature of the reservoir by heating up to a temperature above that needed for equilibrium (or hydrate dissociation temperature);

3. Addition of alternate gases or inhibitors such as CO_2 or methanol which would replace methane within the hydrate structures or change the stability conditions of the corresponding hydrates.

Although methane (or natural gas) has, perhaps, not yet been produced from gas hydrate reserves on a commercial scale and also interestingly it has not been included in the EPPA model in MITEI's Future of Natural Gas report,[65] it is still considered as a promising approach which should begin to be exploited within the next 15 years, mainly due to the fact that conventional natural gas reservoirs are being depleted very rapidly.[30,65] Detailed experimental and theoretical studies on this issue (e.g. thermodynamic and kinetic models, effects of the physical parameters on the gas hydrate reservoirs fluids, exploitation of the reserves, methods of gas recovery, economic study of the process of extraction of methane/natural gas from gas hydrate reserves) have been well-established in the literature.[62-111]

2.1.2. Gas storage

Many investigations indicate that the gas hydrate structures have considerable potential as storage media for various gases. For instance, they can be used for natural gas/hydrogen storage and transportation, as cool storage media in air conditioning systems, etc.[22,112-192] Storage and transportation in the form of gas hydrates have the advantage of safety for the corresponding processes, as well as much lower process volumes in comparison with conventional storage methods like liquefaction. An economic study shows that the capital cost for natural gas transportation in the form of gas hydrates is lower than that for the liquefied

natural gas (LNG) technique, mainly because of lower investment in infrastructure and equipment.[30,126] However, LNG-type gas transportation is currently preferred for distant markets or transportation of natural gases produced from huge gas fields because of expensive capital investment.[30,126] There is evidence, on the other hand, (e.g. Mitsui Shipbuilding & Engineering Company Pilot Plant, Hiroshima, Japan) showing that gas hydrates are economically more cost-effective for storage and transportation of standard gas (gas streams of small quantity, especially those far from the pipeline) compared to the LNG method.[127-129,136] As for the application of gas hydrates for hydrogen storage, it is worth it to point out that a comprehensive review has been already published by Strobel and coworkers.[182] It is revealed that the capacity of the clathrate hydrate cages to absorb hydrogen must be determined, or at least estimated, before starting industrial design of the related processes for hydrogen storage. In addition, use of this technique for cool storage in air conditioning processes has been well-discussed by Chatti et al.[57]

2.2. Separation processes through gas hydrate formation

2.2.1. Separation of greenhouse gases

Truth be told, the ever-growing energy needs of human beings, which resulted from rapid industrialization and population growth, has to date been satisfied mainly by using fossil fuels such as coal, oil, and natural gas.[30,193-198] Many studies demonstrate that large amounts of carbon dioxide, carbon monoxide, and hydrogen sulfide (called ''greenhouse gases'') are emitted every year into the atmosphere[30,193-198] due to combustion of fossil and fossil-based fuels. Over the last few decades, there has been growing concern as to the effects of the increased concentration of these gases in the earth's atmosphere and their contribution to global warming. Due to the potential for harmful environmental effects, including climate change, there has been public and political pressure to reduce the amount of ''greenhouse'' gas emitted. Therefore, separation of these gases from their corresponding gas mixtures, generally found in flue gas streams of most industrial processes, has generated great interest and a number of research studies recently.

2.2.1.a. Separation of CO_2

How are we to account for reducing the amounts of CO_2 emissions worldwide? The capture and sequestration (storage) of carbon dioxide (CCS) is considered, as an academic and industrial curiosity, to be the issue of many studies because around 64% of the greenhouse gas effects in the atmosphere are related to carbon dioxide emissions.[30,193-198] The main objective of these studies may focus on developing environmental friendly and energy efficient technologies to capture CO_2 emitted from power-plants, where flue gas streams normally contain CO_2 and N_2.[30,193-198]

Three general (or commercial) methods have been proposed in open literature for CO_2 capture from flue gases as follows:[198]

1. Post-combustion processes: One of the most widely used methods for post-combustion carbon dioxide removing (or at least mitigating) is the chemical MEA (monoethanolamine) absorption. Estimations show that an economical MEA process is supposed to capture more than 2000 ton CO_2 per year (with the approximate cost of 120 $ for each ton of CO_2 captured). The aforementioned technique is normally suitable for flue gases containing CO_2 and N_2, which is mostly emitted from the refineries. Generally-simple design of the corresponding process is also one of its advantages. Another approach is the PSA (pressure swing absorption) process, in which CO_2 can be removed from a flue gas containing $CO_2 + H_2$. This method seems to be less energy intensive compared to the MEA process accompanied by H_2 production; however, with less selectivity for CO_2 absorption. In addition to the preceding technologies, cryogenic and membrane processes have been also designed for CO_2 capture, which seem to be more expensive and needs more scrutiny. More detailed comparison between these methods can be found elsewhere.[198-200]

2. Pre-combustion techniques: Removing CO_2 prior to combustion is the main goal of these methods. IGCC (integrated gasification combined cycle), as one of the practical processes, generally synthesizes a syngas stream from coal. Therefore, the impurities in coal are removed (or reduced) from the syngas before it is further combusted by pre-combustion CO_2 capture technique. High concentration of carbon dioxide in the final syngas may be the most significant advantages of this process. However, new processes equipment need to be installed to make use of this method.[198-200]

3. Oxy-combustion process: This technique involves burning a fuel using oxygen with high purity. Compared to the conventional burning phenomenon in the presence of air, oxy-combustion method requires less fuel and reduced volume of flue gas regarding the absence of air with excess nitrogen compound. In general, the oxygen-rich stream is first fed to a combustion chamber to produce an exhaust gas stream containing a higher concentration of CO_2. Since this process contains a costly air separation process, several researches are now being undergone to make it more economical.[198]

However, one novel approach to separate carbon dioxide from combustion flue gas (it may be categorized in either the first group of the preceding methods or in the second one) is through gas hydrate crystallization technique.[197,201-229] The affinity of various hydrate formers to be trapped in the water hydrogen-bonded cages is different. Therefore, due to the difference in the tendency of CO_2 and other gases to be captured in the hydrate cages, when clathrate/semi-clathrate hydrate crystals are formed from a corresponding mixture, the hydrate phase can be enriched in CO_2 while the concentration of other gases can be increased in the gas phase. As a consequence, the hydrate phase can be later dissociated by depressurization and/or heating resulting the recovery of CO_2.[30,59] Detailed experimental results indicate that CO_2 selectivity in the hydrate phase would be at least four times higher than that in the gas phase.[204] Table 2.1 reports most of the corresponding experimental studies undertaken to date on gas hydrates for the (CO_2 + other gas/gases + water) systems in the absence of hydrate promoters.

Since high pressure conditions are generally required for gas hydrate formation technique, hydrate promoters can be typically used as chemical additives in such processes.[30] The promoters generally reduce the required hydrate formation pressure and/or increase the formation temperature. They may also modify the selectivity of hydrate cages to encage particular gas molecules. The proposed gas hydrate formation promoters can be categorized into two groups:[30]

1. Chemical additives that have no effect on the structures of the water hydrogen-bonded networks e.g. tetrahydrofuran (THF), anionic/non-ionic surfactants, cyclopentane, acetone etc.[177-182,190,192,230-236] and

2. Additives that take part in the structures of the ordinary water cages in the traditional clathrates networks such as tetra-n-butylammonium salts (e.g. TBAB and tetra-n-butylammonium borohydride).[27,184,237–266]

THF from the first, and TBAB from the second category are well known thermodynamic promoters that have been employed (in non-industrial scale) recently.[30] As a matter of fact, the second group of promoters consists mainly of environmental friendly tetra-n-butylammonium salts and form semi-clathrate hydrates, in which a part of the cage structure is broken in order to trap the large tetra-n-butyl ammonium molecule, as mentioned earlier. This characteristic of the semi-clathrate hydrates may lead to generation of such structures having more gas storage capacity than those produced from promoters such as THF. Although promoters like THF can significantly decrease the hydrate formation pressure, they are volatile and this may lead to non-negligible amounts of their loss during the corresponding storage/separation/transportation processes.[30,58] Experimental studies performed to date on the separation of CO_2 from different gas mixtures via clathrate/semi-clathrate hydrates in the presence of promoters are reported in Table 2.2.

Table 2.1: Experimental studies for gas hydrates of the carbon dioxide + gas/gas mixture systems in the presence of liquid water.[30]

Author(s)	Gas System	Study
Ohgaki et al.[217]	$CO_2 + CH_4$	PVT studies on dissociation conditions + compositions of vapor and hydrate phases
Seo and Kang[211]	$CO_2 + CH_4$	PVT studies on dissociation conditions + composition of vapor and hydrate phases
Bruusgaard et al.[219]	$CO_2 + CH_4$	PVT studies on dissociation conditions + composition of vapor phase in equilibrium with hydrate phase
Belandria et al.[23(b)]	$CO_2 + CH_4$	PVT studies on dissociation conditions of gas hydrates
Belandria et al.[426]	$CO_2 + CH_4$	PVT studies on dissociation conditions + compositions of vapor, liquid, and hydrate phases
Unruh and Katz[213]	$CO_2 + CH_4$	PVT studies on dissociation conditions of gas hydrates
Adisasmito et al.[214]	$CO_2 + CH_4$	PVT studies on dissociation conditions of gas hydrates
Hachikubo et al.[216]	$CO_2 + CH_4$	PVT studies on dissociation conditions of gas hydrates
Seo et al.[210]	$CO_2 + CH_4$	PVT studies on dissociation conditions of gas hydrates
Uchida et al.[144]	$CO_2 + CH_4$	Kinetic study: Investigation of the change of vapor-phase composition and cage occupancies using gas chromatography and Raman spectroscopy.
Seo et al.[210]	$CO_2 + N_2$	PVT studies on dissociation conditions + compositions of vapor and hydrate phases
Kang et al.[220]	$CO_2 + N_2$	PVT studies on dissociation conditions + compositions of vapor and hydrate phases
Seo and Lee[221]	$CO_2 + N_2$	PVT studies on dissociation conditions + compositions of vapor and hydrate phases
Bruusgaard et al.[222]	$CO_2 + N_2$	PVT studies on dissociation conditions + compositions of vapor in equilibrium with gas hydrate

Table 2.1: continued…

Park et al.[209]	$CO_2 + N_2$	PVT studies in an equilibrium cell for measurements of gas hydrate phase equilibria and NMR spectroscopy for measurements of the cage occupancies of CO_2 and consequently the molar compositions of hydrate phase
Belandria et al.[59]	$CO_2 + N_2$	PVT studies on dissociation conditions + compositions of vapor, liquid, and hydrate phases
Sugahara et al.[223]	$CO_2 + H_2$	Raman spectroscopy using quartz windows on cage occupancy by hydrogen molecules and direct gas release method
Kumar et al.[207]	$CO_2 + H_2$	Powder X-Ray Diffraction on cage occupancy by hydrogen molecules, gas chromatography of released gas from hydrate, 13C NMR, Raman spectroscopy
Seo and Kang[211]	$CO_2 + H_2$	13C NMR on cage occupancy by hydrogen molecules in hydrate formed in silica gel particles
Kim and Lee[225(a)]	$CO_2 + H_2$	1H MAS NMR on cage occupancy by hydrogen molecules, gas chromatography of released gas from hydrate on cage occupancy by hydrogen molecules
Rice[226]	$CO_2 + H_2$	Designing a process in which methane is burnt to produce energy and H_2 and CO_2. Later, CO_2 can be separated from a flue containing H_2 using gas hydrate formation process.
Belandria et al.[23(a)]	$CO_2 + H_2$	PVT studies on dissociation conditions + compositions of vapor phase
Zhang et al.[227(a)]	$CO_2 + H_2$ +cyclopentane	The hydrate-liquid-liquid-vapor equilibria of a pre-combustion gas sample have been measured using a high pressure DSC technique. Cyclopentane has been added to the system as a more beneficial promoter than THF.
Surovtseva et al.[228(a)]	$CO_2+H_2+N_2+CH_4+Ar$	Combination of a gas hydrate formation process with a low temperature cryogenic one for capturing CO_2 from a coal gas stream. The operational conditions and the amount of captured CO_2 have been reported.

44

Table 2.1: continued…

Tajima et al.[229(a)]	$CO_2 + N_2 + O_2 + H_2O$ (vapor)	Design of a process for separation of CO_2 from a flue gas sample using a hydrate forming reactor. The kinetic and energy consumption parameters of the process have been also measured and calculated.
Lee et al.[229(c)]	$CO_2 + NO_x + SO_x$	A separation process has been presented to separate CO_2 from flue gas. Thermodynamic and kinetic studies have been performed on the hydrate formation process.

Table 2.2: Experimental studies on clathrate/semi-clathrate hydrate for the carbon dioxide + gas/gases systems in the presence of hydrate promoters.[30]

Authors	System	Study
Beltrán and Servio[218]	$CO_2 + CH_4$ + water/neohexane emulsion	PVT studies on dissociation conditions + composition of vapor phase in equilibrium with hydrate phase
Linga et al.[212]	$CO_2 + N_2$ + THF aqueous solution	PVT and kinetic studies on CO_2 capture from its mixture with N_2 via clathrate hydrate structures. Induction times, hydrate formation rates, CO_2 uptake amount accompanied with molar compositions of hydrate and vapor phases have also been measured.
Fan et al.[215]	$CO_2 + CH_4$ + water/aqueous sodium chloride solution	PVT studies on dissociation conditions of gas hydrates
Lu et al.[233(a)]	$CO_2 + N_2$ + TBAB/THF aqueous solutions	PVT studies on dissociation conditions of gas hydrates
Deschamps and Dalmazzone[248]	$CO_2 + N_2$ + TBAB aqueous solution and $CO_2 + CH_4$ + TBAB aqueous solution	Measurements of enthalpy of dissociations via differential scanning calorimetry (DSC) under pressure
Fan et al.[258]	$CO_2 + H_2$ + TBAB aqueous solution and $CO_2 + H_2$ + THF aqueous solution	Measurements of semi-clathrate hydrate formation conditions and the effects of different additives through using equilibrium cell

Table 2.2: continued…

Li et al.[252]	$CO_2 + N_2$ + TBAB aqueous solution in the presence of dodecyl trimethyl ammonium chloride (DTAC)	Measurement of induction time, pressure drop, split fraction via a crystallizer cell
Ma et al.[262]	$H_2 + CH_4$, $H_2+N_2+CH_4$, $CH_4+C_2H_4$, $CH_4+C_2H_4$ in the presence of water and aqueous solution of THF	Measurements of gas and liquid phases compositions in equilibrium with gas hydrates through an equilibrium cell
Fan et al.[258]	$CO_2 + N_2$ + TBAB/TBAF aqueous solution	PVT studies on measurement of induction time, dissociation conditions, space velocity, and vapor and hydrate compositions using a two- stage hybrid hydrate membrane separation process
Meysel et al.[430]	$CO_2 + N_2$ + TBAB aqueous solution	PVT studies on equilibrium conditions of semi-clathrate hydrate in a jacketed isochoric cell reactor
Li et al.[253]	$CO_2 + H_2$ + TBAB aqueous solution	Measurement of dissociation condition, gas consumption, induction time of semi-clathrate gas hydrates of a flue gas containing $CO_2 + H_2$ in a hydrate crystallizer. The effect of water memory has been also studied.
Kim et al.[263]	$CO_2 + H_2$ + TBAB aqueous solution	PVT and kinetic studies on hydrate formation conditions, gas consumption, induction time of semi-clathrate gas hydrates of a flue gas containing $CO_2 + H_2$ in a hydrate formation reactor. Enclathration of the semi-clathrate hydrate with the CO_2 molecules have been also observed using Raman Spectroscopy.
Li et al.[252]	$CO_2 + H_2$ + TBAB aqueous solution/Cyclopentane	Measurements of CO_2 separation efficiency, gas consumption, and induction time for a CO_2 capture process from a flue gas of $CO_2 + H_2$ in a hydrate crystallizer.
Kamata et al.[265]	$CO_2 + H_2S$ + TBAB aqueous solution	Constructing a high pressure equilibrium cell for separation of mixtures of different gases through semi-clathrate hydrate formation processes.

46

Table 2.2: continued…

Li et al.[229(b)]	$CO_2 + N_2$ +cyclopentane/water emulsion	The kinetics of hydrate formation in a flue gas sample containing $CO_2 + N_2$ have been studied in a reactor along with measurements of vapor and hydrate compositions at equilibrium.
Mohammadi et al.[427]	$CO_2 + N_2$ + TBAB aqueous solution	PVT studies on dissociation conditions of gas hydrates
Belandria et al.[199]	$CO_2 + N_2$ + TBAB aqueous solution	PVT studies on dissociation conditions of gas hydrates

Assuming that there are no losses of gas hydrate promoters (such as TBAB) and water (if water is re-circulated in the corresponding process); 80% efficiency for pumps, compressors, and expanders; a typical economic study shows the energy cost of CO_2 capture using gas hydrates would be approximately 30 € per ton of CO_2.[30,204] The cost is comparable to conventional CO_2 capture methods such as amine absorption, etc. Further simulation results suggest that other costs associated with carbon dioxide separation processes using gas hydrate crystallization, such as equipment, total capital investment, maintenance and depreciation, would lead to estimated capture cost of approximately 40.8 € per ton of CO_2 from a conventional blast furnace (CBF) flue gas.[30,204] Two points should however be kept in mind regarding the costing of hydrate separation processes: First, there is the possibility for designing more efficient and economical separation processes through suitable utilization of the energy available in the fluid streams of the processes (i.e. pinch technology can be applied to re-design the aforementioned processes); and secondly, economic simulation results show that gas separation by hydrate formation techniques may be more competitive in applications where there are high pressure feed gas streams to the separation process, such as in the oil and gas industry. Hydrate separation method for CO_2 capture is still considered as a long-term capturing technology.[264]

2.2.1.b Separation of methane

Methane is a greenhouse gas with a greenhouse effect 21 times greater than that of CO_2 and it contributes to around 18 % of the global greenhouse effects.[30,234(a),267] This component is the major constituent of natural gas streams and natural gas reserves in the form of hydrates in the earth, as well as emissions in the form of cold bed methane (CBM) discharging from

coal seams.[2,30,58,234,268] Consequently, separation of methane from emitted industrial gases has attracted significant attention in the last few decades. Recently, novel separation processes using gas hydrate formation phenomenon have been proposed, similar to that of used for separation of CO_2. Table 2.3 lists the corresponding experimental studies undertaken and available in open literature. Economic studies for such processes would focus mainly on the price of the gas hydrate promoters needed to reduce the pressure and increase the temperature of the separation steps because the design of other required equipment is generally simple.[30] It seems that the industry will be interested in such investments whenever the environmental regulations are rigid and when the natural gas reserves tend to reach their half-lives.[30]

Table 2.3: Experimental studies on clathrate/semi-clathrate hydrates for the methane + gas/gas mixture systems in the presence/absence of hydrate promoters.[30]

Author(s)	System	Study
Zhao et al.[235(a)]	CH_4 + oxygen-containing coal bed gas + THF aqueous solution	Separation of CH_4 using a reactor in different concentration of feed gas and pressures
Lu et al.[233(a)]	CH_4 + N_2 + TBAB/THF aqueous solutions	PVT studies on dissociation conditions
Zhang and Wu[232(a)]	CH_4 + N_2 + O_2 + THF aqueous solution	Separation of methane from a coal mine methane using a high pressure reactor
Kondo et al.[232(b)]	CH_4 + C_2H_6 + C_3H_8 + pure water	Measurements of dissociation conditions and the composition of vapor phases in equilibrium with gas hydrate in a high pressure cell
Ng[233(b)]	CH_4 + C_3H_8, CH_4 + C_2H_6 + C_3H_8, CH_4 + C_3H_8 + C_4H_{10} + CO_2, CH_4 + C_2H_6 + C_3H_8 + C_4H_{10} + CO_2, CH_4 + C_2H_6 + C_3H_8 + C_4H_{10} + CO_2 in the presence of water	Measurements of compositions of hydrate phase by gas chromatography in an equilibrium variable-volume cell
Sun et al.[230]	CH_4 + C_2H_6 + THF aqueous solution	Measurements of hydrate formation conditions of a sample consisting of CH_4 and C_2H_6 for observing the appropriate conditions of a separation process of CH_4. The structures of the hydrates formed have been also investigated using Raman spectroscopy.

Table 2.3: continued…

Ma et al.[234(b)]	$CH_4 + C_2H_6$ + THF aqueous solution, $CH_4 + C_2H_4$ + THF aqueous solution	PVT study on hydrate formation conditions and molar compositions of vapor and hydrate phases for separation of methane from its mixture with ethane and ethylene in a high pressure equilibrium cell
Lee et al.[235(b)]	$CH_4 + N_2$ + water	PVT studies and 13C solid-state NMR spectroscopy along with powder XRD measurement have been performed for investigation of the equilibrium conditions and phase transitions of clathrate hydrates of mixture of $CH_4 + N_2$
Sun et al.[237]	$CH_4 + N_2$ + TBAB / (TBAB + SDS (sodium dodecyl sulfate)) aqueous solutions	Measurement of phase equilibrium conditions of semi-clathrate hydrates of mixtures of methane + nitrogen + TBAB aqueous solution in a hydrate forming reactor. Gas storage capacity and recovery factor of CH_4 have also been reported.
Kamata et al.[266(a)]	$CH_4 + C_2H_6$ + TBAB aqueous solution, $CH_4 + H_2$ + TBAB aqueous solution, $CH_4 + N_2$	High pressure equilibrium studies for separation of methane from its mixtures with different gases.

2.2.1.c Separation of other greenhouse gases

Beside carbon dioxide and methane, gas hydrate separation processes have been investigated for other greenhouse gases such as hydrogen sulfide (H_2S), sulfur hexafluoride (SF_6), and 1,1,1,2-tetrafluoroethane (R-134a).[30] Separation of hydrogen sulfide from gas streams may be an imperative task for the petroleum industry mainly because high hydrogen sulfide concentration in gas streams increases the possibility of solid sulfur precipitation during the production of sour natural gases in the formation, in well bores, and in production facilities especially at high temperatures and pressures (besides its corrosive potential).[30,269]

SF$_6$-containing gases are widely used in industry because SF$_6$ has good electrical insulating properties.[269] Its mixtures with N$_2$ are used as an insulating filler gas for underground cables, a protective, and an etching agent in the semiconductor industry.[269] Because it has a very long lifetime in the atmosphere (3200 years) and significant global warming potential, separation of this component is of great interest. Utilization of gas hydrates for the separation of refrigerant gases, which have extreme greenhouse effects, has also been recently studied in the literature. Table 2.4 reports experimental studies available in open literature on separation of the aforementioned gases from their corresponding mixtures via gas hydrate formation processes. Careful attention should be paid to materials of construction and health and safety issues in the design of process equipment for separation of these gases, especially H$_2$S and SF$_6$, because they are toxic and corrosive.[30] Therefore, the main factor in an economic study would be focused on these issues. From studies performed to date, it seems that these types of separations, through gas hydrate formation, would only be considered as economical alternative approach by industry by the end of this decade.[30, 63,195-197,201,204,235,267]

2.2.2. Hydrogen separation

Hydrogen is considered as a clean and novel energy resource. As a result, separation, storage, and transportation of this component are among the latest industrial technology developments. For instance, a dual-effect process can be pursued to capture CO$_2$ and separate H$_2$ simultaneously from the generated gas stream after the steam reforming operation applying gas hydrate crystallization.[23,30,58] Extremely high pressures normally in the range of 100 to 360 MPa, as stated in the previous chapter, are needed to stabilize the sII H$_2$ clathrate hydrate while CO$_2$ is enclathrated in hydrate cages at moderate pressure conditions.[30,58] The difference between hydrate formation pressures of these two substances is the main reason for considering the potential of gas hydrate technology for the aforementioned process.[224-226] The experimental studies undertaken to date on the separation of hydrogen from different gas mixtures through gas hydrate crystallization processes are reported in Table 2.5.

2.2.3. Nitrogen separation

Since N$_2$ is one of the major components of flue gas emitted from power-plants,[30,59,210] efficient processes should be proposed for its separation from the accompanied gases. Gas hydrate formation method has been studied as an alternative nitrogen separation process in industry. Table 2.6 summarizes experimental studies undertaken in this area, which are available in open literature.

2.2.4. Oil and gas separation

Due to the fact that the composition of a hydrate-forming mixture is different from the composition of the hydrate phase, gas hydrate formation can be applied as an alternative approach to conventional gas-liquid separation (fractionation) technique.[30,61,271] A low temperature extraction (LTX) process designed by Dorsett [272] and separation of oil and gas in a hydrate rig by Østergaard et al.[271]using the gas hydrate crystallization method, in which the kinetic parameters of the proposed process have been reported, may be the only two proposed processes for this purpose to date.

Table 2.4: Experimental studies on clathrate/semi-clathrate hydrates for mixtures of greenhouse gases with other gases in the presence/absence of hydrate promoters.[30]

Authors	System	Study
Shiojiri et al.[266(b)]	HFC-134a (R-134a) + N_2 + water	Measurements of hydrate formation conditions and vapor and hydrate molar compositions in a porous media for separation of R-134a greenhouse gas
Tajima et al.[229(a)]	HFC-134a (R-134a) + air + water, SF_6 + N_2 + pure water	Design of a process for separation of R-134a refrigerant from air, and SF_6 from N_2 using a hydrate forming reactor. The kinetic and energy consumption parameters of the process have been also measured and calculated.
Tajima et al.[231(b)]	R-134a + N_2 + water	Study on the effects of concentration of feed gas on kinetic parameters of HFC hydrate formation and its separation from its mixture with N_2 in a hydrate forming reactor.
Vorotyntsev et al.[208]	SF_6 + SO_2 + water, SF_6 + CCl_2F_2 + water	Separation of SF_6 greenhouse gas from its corresponding mixtures in a batch isobaric gas hydrate crystallization process. The separation factors of the compounds have been reported along with relevant kinetic study.
Dong et al.[227(b)]	CH_4 + NH_3 + water / THF aqueous solution	Measurements of equilibrium conditions, vapor phase compositions in equilibrium with gas hydrates in a hydrate forming reactor for separation of ammonia from methane

Table 2.4:
continued…

Cha et al.[270]	$SF_6 + N_2$ + water	Hydrate dissociation conditions of mixture of $SF_6 + N_2$ in the presence of pure water and Raman Spectroscopy of cage occupancies by the corresponding hydrate formers in a high pressure equilibrium cell.
Kamata et al.[266(a)]	$CH_4 + H_2S$ + TBAB aqueous solution, $CO_2 + H_2S$ + TBAB aqueous solution, $CH_4 + CO_2 + H_2S$ + TBAB aqueous solution	A high pressure cell has been designed and constructed to separate H_2S from a flue gas via gas hydrate formation process. The effects of different operational parameters on recovery of H_2S have been reported.

Table 2.5: Experimental studies on clathrate/semi-clathrate hydrates for the hydrogen + gas/gas mixture systems in the presence/absence of hydrate promoters.

Authors	System	Study
Wang et al.[225(b)]	$H_2 + CH_4$ + diesel oil + THF aqueous solution + anti-agglomeration system	Measurements of gas-hydrate phase equilibria in a variable-volume cell for observing the conditions of separation of H_2 from a flue sample. A surfactant has been added to the system to disperse hydrate particles into the condensate phase.
Lee et al.[228(b)]	$H_2 + CH_4$ + pure water	Hydrate formation conditions for a mixture of pre-combustion flue gas containing $H_2 + CH_4$ has been investigated in a semi-batch stirred vessel
Sun et al.[268]	$H_2 + CH_4$ + water/THF aqueous solution	A one-stage hydrogen separation unit has been constructed based on hydrate formation process. In addition, the separation efficiency of the proposed process has been reported.

Table 2.6: Experimental studies on clathrate hydrates for the nitrogen + gas/gas mixtures.

Authors	System	Study
Johnson et al.[245(b)]	N_2 + industrial gas mixtures + water	Designing a new economical and efficient process for separation of N_2 from gas mixtures in a constructed multi-stage reactor to form gas hydrates.
Happel et al.[267]	N_2 + CH_4 + pure water	A novel apparatus for separation of N_2 from its mixture with CH_4 using a hydrate forming reactor has been constructed, in which the vapor and hydrate molar compositions and kinetic parameters like the rate of hydrate formation can be measured.

2.2.5. Desalination process

Water desalination/treatment technology using clathrate hydrates with different hydrate formers e.g. refrigerants can perform well when compared with traditional desalination processes.[273–277] The technique is of particular interest because only water and an appropriate refrigerant can form clathrate hydrates at ambient temperature and atmospheric pressure. The clathrate hydrate can then be dissociated and pure water phase can be produced while the released refrigerant may be recycled in the hydrate formation unit. From the 1940s to date, numerous studies have been undertaken to design desalination processes efficiently and economically via formation of gas hydrates.[30,278–294] For instance, a detailed economic study[275] including total capital investment, operational and maintenance costs, and depreciation (amortized) costs demonstrates that the total cost of potable water production through the propane hydrate formation method is between 2.8 and 4.2 US$ per ton of fresh water depending on the yield (number of moles of the potable water produced by the process per mole of seawater fed to the process) and temperature of the inlet seawater.[30] These results indicate that formation of the gas hydrates in the absence of any hydrate promoters may not be an economical method for a desalination process compared with the traditional methods.[273–277] Though, it is obvious that an appropriate hydrate promoter can reduce the energy cost of the process and may finally lead to a lower fresh water production cost.[30]

2.2.6. Biotechnology

The possible formation of clathrate hydrates in animal/plant tissues and gas hydrate formation in protein containing micellar solutions, as well as applications in controlling enzymes in biological systems, recovery of proteins, application in drug delivery systems, etc. are just some examples of importance of gas hydrate formation in the bioengineering/biotechnology field.[295–307] This area is relatively new and has the potential for tremendous growth in terms of the study of applications.[30]

2.2.7. Food industry

The concentration of dilute aqueous solutions using clathrate hydrate formation is, similar to but, seems to be more economically feasible than freeze concentration because clathrate hydrates can be formed at temperatures above the normal freezing point of water.[30,61,308] The characteristics of refrigerant hydrates in a variety of aqueous solutions containing carbohydrates, proteins, or lipids and the concentration of apple, orange, and tomato juices via hydrate formation have already been reported.[30,309,310]

2.2.8. Separation of ionic liquids

Ionic liquids (ILs) are organic salts which are generally liquid at room temperatures.[311] They are normally composed of a large organic cation and organic or inorganic anions.[311] The applications of ionic liquids have generated numerous discussions and studies since the past decade. This is mainly due to their physico-chemical properties which are able to be adjusted through combination of cations and anions. This phenomenon can be utilized to design particular solvents for application in the development of efficient processes and products[30, 311] Non-flammability, high thermal stability, a wide liquid range, and their electric conductivity are all physical properties[311] which make ionic liquids very attractive in terms of application as separating solvents and catalysts. In the synthesis of ionic liquids, one of the key steps is their purification. Ionic liquids are also expensive to synthesize and therefore their recovery via regeneration is essential.[30] Recovery of these solvents from aqueous solutions will certainly be beneficial for the future potential of these solvents in the separation industry.[30, 311,312] Recently, a novel separation technique has been proposed regarding the separation of ionic liquids from dilute aqueous solutions using clathrate hydrates of carbon dioxide.[313] The fundamental concept of this method is based on the phenomenon of hydrophobic hydration taking place when a gas dissolves in water and results in formation of both structured water and gas hydrates under suitable operational conditions.[313]

2.3. Concluding remarks and experimental objective

In this chapter, we have focused on reviewing the applications of clathrate/semi-clathrate hydrates for separation processes, including experimental studies on separation of greenhouse gases; separation of hydrogen and nitrogen; oil and gas fractionation; desalination processes; separation of different substances from living organisms; and separation of ionic liquids from their dilute aqueous solutions. The studies preformed to date show diverse fields of research in chemistry, physics, earth and environmental sciences, bioengineering, and pharmaceutical processes to name a few.

It is evident that gas hydrate formation technology will play a significant role in the future in separation processes and has the potential to be, perhaps, a more sustainable technique than current comparable commercial technologies for separation (particularly for CO_2 capture and sequestration). So far, application of gas hydrate for storage and transportation of gas streams has found to be used in industrial practice, as already mentioned. In addition, CO_2 capture and sequestration (due to its eventual high recovery of CO_2) and cool storage in the form of hydrate slurry (due to considerable latent heat of hydrate formation/dissociation) through this technique may be the most promising positive application of gas hydrate formation among the investigated ones. Although the proposed processes are still in the form of batch operations though there are some efforts to design semi-batch or continuous gas hydrate formation processes. However, this review demonstrates that the experimental phase equilibrium measurements required for efficient design of such processes are still rare. These data are imperatively needed in order to clarify the novel aspects and applications of gas clathrate/semi-clathrate hydrates in separation of CO_2 from flue gas streams and consequently persuade the industry to invest in this in near future.

As a consequence, the phase equilibria of clathrate/semi-clathrate hydrates of significant systems for the aforementioned processes including the CO_2 + N_2/CH_4/H_2 + liquid water/ TBAB aqueous solution systems are measured and reported in this work, which are considered to be the experimental objectives of the thesis. These experimental works can be considered as the major contributions of this work for understanding the different aspects of use of semi-clathrate hydrates in CO_2 capture processes.

3. Review of Gas Hydrate Phase Equilibrium Models

Examen des modèles d'équilibres de phases des hydrates de gaz

Depuis le siècle dernier, il y a eu un nombre considérable d'études théoriques pour représenter et prédire les données d'équilibres de phases expérimentales des systèmes contenant des hydrates de gaz de composés purs ou en mélanges. Les modèles qui sont proposés ici peuvent être appliqués afin de prédire le comportement de phase pour d'autres systèmes à des conditions particulières (dans le domaine de leur applicabilité) par exemple, l'inhibition de la formation des hydrates dans les pipelines de gaz et de pétrole, séquestration de CO_2 sur le plancher océanique, capture du CO_2 par utilisation de la méthode de formation d'hydrate, analyse de la salinité des inclusions de fluides et ainsi de suite. Une étude bibliographique préliminaire a montré que les modèles thermodynamiques pour la prévision des équilibres de phase hydrates rentrent généralement dans cinq catégories principales: « Techniques d'Estimation », «Calculs de Flash Multi-phases », « Minimisation de l'énergie de Gibbs », « Modèles Numériques » et « Méthodes Moléculaires ». L'objectif principal de ce chapitre est d'aborder brièvement ces méthodes afin de justifier la nécessité impérieuse d'élaborer une approche thermodynamique simple pour modéliser les équilibres de phases des semi-clathrate hydrates.

Since the past century, there have been considerable number of theoretical studies to represent/predict the existing experimental phase equilibria data for the systems containing gas hydrates of simple hydrate formers and/or their mixtures. The subsequent proposed models can be later applied to predict the corresponding phase behaviors for other systems at specific conditions (within the domain of their applicability) *e.g.* inhibition of the formation of hydrates in oil and gas pipelines, sequestrating CO_2 on the ocean floor, capturing CO_2 utilizing the hydrate formation method, analyzing the salinity of fluid inclusions and so forth.[314] A preliminary literature survey shows that the thermodynamic models for prediction of hydrates phase equilibria generally fall into five main categories: "*Estimation Techniques*", "*Multi-Phase Flash Calculations*", "*Gibbs Energy Minimization*", "*Numerical Models*", and "*Molecular Methods*". The main objective of this chapter is to briefly address about these methods in order to clarify the imperative need for developing a simple thermodynamic approach for modeling the phase equilibria of semi-clathrate hydrates.

3.1. Estimation techniques

Perhaps, the simplest method for estimation (or calculation) of the phase behavior of simple hydrates is the exponential correlation proposed by Kamath in 1984.[315] This correlation can be applied for calculation/estimation of three-phase liquid water (L_w)-hydrate (H)-Vapor (V) and Ice (I)-H-V phase equilibria regarding hydrate formers such as methane, carbon dioxide, ethane, nitrogen etc. It should be noted that this correlation should be used in definite applicability domains (refer to the original article or reference[2] to see the applicability domains).[2]

Katz[316] was the first to present the gas gravity charts to estimate the (L_w-H-V) equilibrium conditions. Gas gravity stands for the ratio of molecular weight of the gas to that of air.[2] The Katz[316] chart is presented in Figure 3.1, as reproduced by and from Sloan and Koh here.[2] Once the gas gravity is defined, the hydrate formation pressure can be straightforwardly determined at a given temperature from the chart. This easy-to-use technique is generally applied as rough estimation in industry.
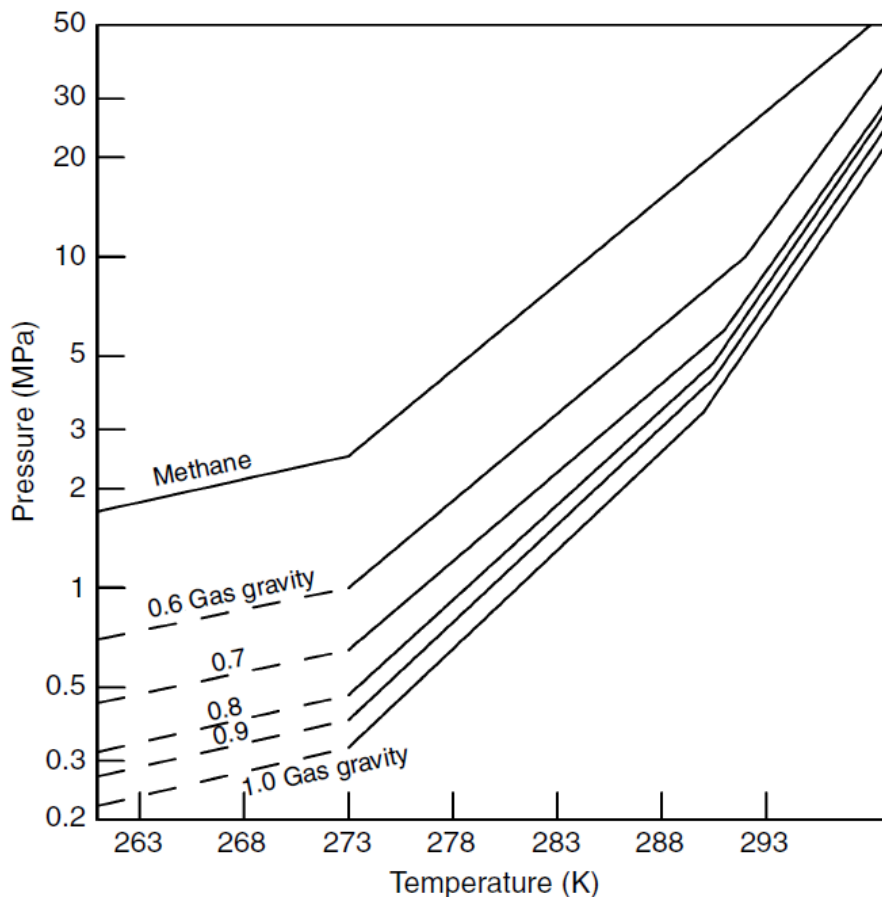
Figure 3.1: The Katz[316] gas gravity chart (Reproduced from Sloan and Koh[2]).

59

The other famous method is based on the distribution coefficient (K-value) presented first by Wilcox et al.[317] and later completed by Carson and Katz.[318] The method is based on vapor-solid distribution coefficient as follows:[2]

$$K_i = \frac{y_i}{z_i} \tag{3.1}$$

where y_i and z_i denote the mole fractions of component i in the water-free vapor and water-free solid hydrate, respectively. The higher the value for K, the higher the tendency of the hydrate former to concentrate in the vapor phase than that in the hydrate phase would be expected. The values of the distribution coefficient are sketched as functions of temperature and pressure for conventional simple hydrate formers present in natural gas. These values are finally collapsed into a single 18-parameter correlation, which have been well-argued elsewhere.[2]

The thermodynamically correct Clapeyron equation can be normally applied to determine the phase boundary of the clathrate hydrate systems, in the case of availability of hydrate dissociation enthalpy (heat) values.[2,9] The sketch of logarithm of dissociation pressure ($\log(P)$) vs. reciprocal temperature ($1/T$) generally exhibits a straight line for (L_w-H-V) and (I-H-V) equilibria regions (which shows the value of the enthalpy of hydrate dissociation). However, for three-phase (L_w-H-liquid hydrate former (L_{HC})) equilibrium region, the hydrate dissociation pressure is generally a strong function of the system temperature.[2,9] This is because of the fact that all three phases are incompressible and immiscible, so that only a small thermal expansion is required to cause a large pressure change.[2,9] As a consequence, accurate determination of pressure–temperature diagrams is a stringent test for even the most accurate equations of state (EoS) to predict both the density and the solubility of the liquid hydrate former phase and the aqueous phase. It is worth pointing out that the Clapeyron equation can be applied to deal with this issue. However, it has been previously argued[9] that taking into account the effects of solubility of gases (especially for CO_2 and H_2S) and variation of the hydrate volume with temperature brings about a change in the slope of the $\log(P)$ vs. $1/T$ curve in (L_w-H- L_{HC}) region. In this regard, Eslamimanesh et al.[9] proposed an improved Clapeyron model taking into account the mentioned criteria as follows:

$$\frac{dP}{dT} = \frac{\Delta H_H + nx\Delta H_S}{T\Delta V} \tag{3.2}$$

where n is the hydrate number, x is the mole fraction of a hydrate former in water, and subscript H represent hydrate. In the above equation, ΔH_H is the heat of dissociation of gas hydrates and ΔH_S stands for the heat of dissolution of hydrate former in water. ΔV is defined as follows:[7]

$$\Delta V = V_{L_{HC}} + nV_{L_w} - V_H \tag{3.3}$$

where subscripts L_{HC} and L_w refer to liquid hydrate former and liquid water, respectively. The preceding equations have been successfully checked for the phase boundary of simple hydrates of CO_2, H_2S, and C_2H_6.[9]

3.2. Multi-phase flash calculations

The basic statistical thermodynamic model for representation/prediction of the phase equilibrium of gas hydrates was derived from the solid solution theory of van der Waals and Platteeuw (vdW-P),[319,320] which was generalized by Parrish and Prausnitz.[321] Later, Holder et al.[322] simplified the Parrish and Prausnitz model[321] so that the reference hydrate was eliminated from the model by introducing universal reference properties for each type of hydrate structure. This led to an established methodology for most of the later thermodynamic models for dealing with phase behavior of gas hydrates.

3.2.1. Equality of chemical potentials

These kinds of models have been developed on the basis of the equality of the chemical potential of water in hydrate phase with that in water-rich liquid phase assuming negligible amounts of water in vapor phase (water content):[322]

$$\mu_w^{I/L_w}(T,P) = \mu_w^{H}(T,P) \tag{3.4}$$

where μ is the chemical potential, subscript w denotes water, and superscripts I/L_w and H stand for the ice/liquid water (or aqueous) and hydrate phases, respectively. If the chemical potential of an empty hydrate lattice is taken as reference, Eq. (3.4) becomes:

$$\Delta\mu_w^{I/L_w} = \Delta\mu_w^{H} \tag{3.5}$$

where,

$$\Delta\mu_w^{I/L_w} = \mu_w^{MT} - \mu_w^{I/L_w} \tag{3.6}$$

$$\Delta\mu_w^{H} = \mu_w^{MT} - \mu_w^{H} \tag{3.7}$$

where superscript MT refers to the empty hydrate lattice. The chemical potential of water in hydrate phase can be evaluated using the vdW-P theory:[2,319,320]

$$\mu_w^H = \mu_w^{MT} - RT \sum_m v_m' \ln\left(1 + \sum_j C_{mj} f_j\right) \tag{3.8}$$

where R is the universal gas constant, v_m' stands for the number of cavities of type m per water molecule in a unit hydrate cell, f_j denotes the fugacity of the hydrate former j, and C_{mj} is the Langmuir constant. Fugacity values are calculated using appropriate equations of state (EoS). Numerical values for the Langmuir constant can be calculated by choosing a model for the guest-host interaction:[2,322,323]

$$C_{mj}(T) = \frac{4\pi}{kT} \int_0^\infty \exp\left(-\frac{w(r)}{kT}\right) r^2 dr \tag{3.9}$$

where k is the Boltzmann's constant. The function $w(r)$ is the spherically symmetric cell potential in the cavity, with r measured from centre and depends on the intermolecular potential function chosen for describing the encaged gas-water interaction. A potential function can be employed to determine the Langmuir constant. The following relation can be written in the case of application of the Kihara[324,325] potential function:[326]

$$w(r) = 2z\varepsilon\left[\frac{(\sigma^*)^{12}}{\overline{R}^{11} r}\left(\delta^{10} + \frac{\alpha}{\overline{R}}\delta^{11}\right) - \frac{(\sigma^*)^6}{\overline{R}^5 r}\left(\delta^4 + \frac{\alpha}{\overline{R}}\delta^5\right)\right] \tag{3.10}$$

where,

$$\delta^{\overline{N}} = \frac{1}{\overline{N}}\left[\left(1 - \frac{r}{\overline{R}} - \frac{\alpha}{\overline{R}}\right)^{-\overline{N}} - \left(1 + \frac{r}{\overline{R}} - \frac{\alpha}{\overline{R}}\right)^{-\overline{N}}\right] \tag{3.11}$$

In the two preceding equations, z is the coordination number of the cavity (the number of oxygen molecules at the periphery of each cavity), ε would be characteristic energy, α is the radius of spherical molecular core, $\overline{R}$ stands for the cavity radius, and $\overline{N}$ is an integer equals to 4, 5, 10, or 11. Additionally, $\sigma^* = \sigma - 2\alpha$, where σ is the collision diameter.[2,322,323] The Kihara[324,325] potential parameters (including α, ε, and σ) are generally regressed against the gas hydrate dissociation data for particular system of interest (although there are other theoretical approaches for their determination).[2]

Eq. (3.12) is normally used for determining the chemical potential difference of water in empty hydrate lattice and liquid water or ice:[322]

$$\frac{\Delta\mu_w^{MT-I/L_w}}{RT} = \frac{\mu_w^{MT}}{RT_0} - \frac{\mu_w^{I/L_w}}{RT_0} = \frac{\Delta\mu_w^0}{RT_0} - \int_{T_0}^T \frac{\Delta h_w^{MT-I/L_w}}{RT^2} dT + \int_0^P \frac{\Delta v_w^{MT-I/L_w}}{RT} dP - \ln a_w \tag{3.12}$$

where superscripts 0 refers to reference property and *MT-I/L_w* stands for the difference property between empty hydrate lattice and water in liquid state or in ice. $\Delta\mu_w^0$ is the reference chemical potential difference between water in empty hydrate lattice and pure water in the ice phase at standard condition (here it is 273.15 K) and a_w stands for the activity of water. In addition, Δv is the molar volume difference, and Δh stands for the enthalpy difference, which can be generally calculated by the following expression:[2,323]

$$\Delta h_w^{\beta-I/L} = \Delta h_w^0 + \int_{T_0}^{T} \Delta C_{P_w} dT \tag{3.13}$$

where C_{P_w} stands for the molar heat capacity, and Δh^0 is the enthalpy difference between the empty hydrate lattice and ice, at the ice point and zero pressure. Additionally, the difference between the heat capacity of the empty hydrate lattice and the pure liquid water can be evaluated by the following equation:[2,323]

$$\Delta C_{P_w} = -37.32 + 0.179\,(T - T_0) \qquad\qquad T > T_0 \tag{3.14}$$

The heat capacity difference is assumed to be zero when $T \le T_0$. The values of the reference properties have been already reported for the three different hydrate structures (sI, sII, and sH).[2] Consequently, the following summarized equation can be written resulting from the equality of chemical potential of water in the phases present (ignoring water-content of vapor phase, as already mentioned):[323]

$$\frac{\Delta\mu_w^0}{RT_0} - \int_{T_0}^{T} \frac{\Delta h_w^{MT-I/L_w}}{RT^2} dT + \int_0^{P} \frac{\Delta v_w^{MT-I/L_w}}{RT} dP - \ln a_w - \sum_m v_m' \ln\left(1 + \sum_j C_{mj} f_j\right) = 0 \tag{3.15}$$

Application of the described method for modeling various systems has been the subject of many studies. For instance, Clarke et al.[327] were among the first researchers who used this method to predict the conditions of hydrate formation especially in porous media. They stated that the proposed method, along with application of Trebble-Bishnoi[328] EoS, results in maximum deviations of 15 % for methane hydrate and 29 % for propane hydrate formation condition predictions in the presence of porous media. Trying to improve the accuracy of the original model, Lee and Holder[329] took into account the effects of lattice structure distortion by the enclathrated molecules through introducing the "second" and "third" shells into the Kihara potential function[324,325] relation. Their model contributed to predictions with deviation ranges of (0.07 to 1.36) % and (0.2 to 1.47) % for hydrates sI and sII compared with the corresponding experimental data. However, the method of equality of the chemical potential of water in liquid phase (or ice) and that in hydrate phase has a drawback, which is ignoring the equality of the aforementioned chemical potentials to the chemical potential of water in vapor phase.

3.2.2. Equality of fugacities

The general phase equilibrium criterion that is the equality of fugacity of each component throughout all phases present is utilized by the methods grouped in this category. Considering the equality of fugacity of water in the phases present (including hydrate phase), the final equilibrium criteria would be as follows:[323,330-333]

$$f_i^v = f_i^{L_w}$$
(3.16)

$$f_w^v = f_w^{L_w} = f_w^H$$
(3.17)

where f is the fugacity, subscript i represent i^{th} component in the mixture (except water), and superscripts v stands for the vapor phase. An equation of state is normally used to calculate the fugacity of water in vapor and aqueous phases. The equations required for pursuing this method are discussed in detail in next chapter along with the model presented in this work.

The equality of fugacities approach has been also followed by many authors to model the phase equilibria of hydrate-containing systems. For instance, Anderson and Prausnitz[331] used this method to present a molecular-thermodynamic model in order to calculate the inhibition effect of methanol on the formation of hydrates in moist gas mixtures. Their model can be used to compute the hydrate dissociation pressure as well as relative amounts and compositions of all coexisting phases. Good agreement was obtained in comparison with existing experimental data reported in the literature.

In 1996, Avlonitis and Varotsis[332] investigated the gas hydrate formation in three important industrial systems including natural gases, gas condensates, and black oils applying a multi-flash algorithm. Acceptable convergence of the applied algorithm was observed in gas systems containing methanol up to 20 % weight percent in the water-rich liquid phase. However, they stated that since reservoir fluids always contain various dissolved salts that may have appreciable effects on the corresponding phase equilibria, it is necessary to account for these compounds as well.

Another attempt was undertaken by Klauda and Sandler.[333] Their model is capable of accurate prediction of hydrate equilibrium pressures as a function of temperature for the CH_4, C_2H_6, C_3H_8, N_2, H_2, or CO_2 containing systems and their mixtures. The model parameters were fitted to equilibrium pressure data for single guest hydrates (simple hydrates) allowing the prediction of phase behaviors in the mixed guest hydrates. In the case of calculations for single hydrate formers, the average absolute relative deviation (AARD%) of the results compared to the experimental data was about 5.7 % whereas it was almost 12 % in the case of prediction for mixed-guest hydrates.

Phase equilibrium of gas hydrates of carbon monoxide (CO) has been also modeled by Mohammadi and coworkers[323] for the first time applying the aforementioned method. They also measured and reported the phase equilibria data of the CO, CO + CO$_2$, and CO + C$_3$H$_8$ clathrate hydrate systems. Their obtained results show that the maximum absolute deviation (AD%) of their predictions from the measured equilibrium values is 0.8 %. Some other researches on the same category of thermodynamic models can be found elsewhere.[335-336] In addition, one is able to find a detailed description of these thermodynamic models in series of publications by Ballard and Sloan[337-340] and Jager et al.[341] Development of the multi-flash thermodynamic models for calculation/estimation of the phase equilibria of gas hydrates seems to be still in progress in order to extend the previous models for the new systems or other structures of hydrates (like semi-clathrate hydrates) or to decrease the sources of probable errors in calculation steps.

3.3. ab initio intermolecular potential method

In recent years, some researchers tried to determine the potentials between the atoms and molecules in hydrate phase through the *ab initio* intermolecular potential instead of Lennard-Jones[342] or Kihara[324,325] potential functions.[2,343-345] Some of the advantageous of the *ab inito* method are as follows, as mentioned by Sloan and Koh:[2]

"1. Potential parameters (such as the Kihara[324,325] or Lennard-Jones[342] potential parameters) can be calculated from a small set of fundamental, ab initio intermolecular energies, rather than fits of the potentials to phase equilibria and spectroscopic data.

2. Potential parameters are well-defined and do not extend over a wide range of values.

3. Nonspherical shells are readily included in generating the Langmuir constants.

4. Water molecules beyond the first shell are readily included in Langmuir constants.

5. Guest–guest interactions between cages can be easily included.

6. Critical hydrate parameters, such as cage occupancies and structural transitions can be predicted a priori, without fitting the model to spectroscopic measurements."

Cao et al.[343,344] estimated the *ab initio* potential energy surface for CH$_4$-H$_2$O dimer and applied it to predict phase equilibrium of methane hydrate. Their developed model is able to predict the equilibrium pressure of CH$_4$ hydrate accurately; however, it gives unreasonable cage occupancies. The failure in predicting cage occupancies clarifies that the previous determined averaged *ab initio* potential[343] was not enough to account for all types of orientations between CH$_4$ and H$_2$O. Sun and Duan[314] found that there are two major problems in the treatment of Cao et al.[343,344] In the first place, they only chose two types of orientations between CH$_4$ and H$_2$O during calculating *ab initio* potential, which may not be sufficient for obtaining an accurate potential energy surface.[314] Secondly, spherical average on the intermolecular potential with the Boltzmann averaging algorithm was performed before

computing Langmuir constants. This treatment causes the loss of the quality of *ab initio* potential since *ab initio* intermolecular potential is strongly angle dependent.[314] Anderson et al.[345] stated that angle-averaged potential results in large errors in the prediction of the cage occupancies in the study of Cao and his coworkers.[344] They used a site-site potential model to fit the *ab initio* potentials for CH_4-H_2O and improved the prediction of cage occupancies of methane hydrate.

Although the *ab initio* model normally contributes to accurate predictions of phase equilibria of many of hydrate systems, its application seems not to be very common among the researchers. High computer RAM capacity, much time consumption, and probable divergence of the algorithm may be general disadvantages of this approach[2] compared to the original vdW-P model.[319,320]

3.4. Gibbs energy minimization

To establish an equilibrium between phases present in a closed system, the Gibbs energy of the system must be at a minimum at constant pressure and temperature condition. This phenomenon results, indirectly, from the second law of thermodynamics. Satisfaction of the following conditions:

(1) Temperature equilibrium of all phases,
(2) Pressure equilibrium of all phases, and
(3) Equality of chemical potential of a component in each phase

ensures that the system of interest is at equilibrium (with known phases).[2] However, it is not adequate for the minimization of the Gibbs energy.[2] The latter issue is generally encountered when dealing with complex systems including multi-phases, which are not known in advance. [2,346] In such systems, minimization of the Gibbs energy can be applied to estimate the number and quality of the phases present at any temperature and pressure conditions. The described method is able to calculate the formation (or dissociation) conditions for any phases (including the hydrate) as well.[2]

Detailed calculation procedure of the Gibbs energy minimization method can be also found in the article by Avlonitis and Varotsis.[332] These two researchers investigated the indirect use of Gibbs energy minimization called "Gibbs tangent plane criterion" for gas hydrate phase equilibria modeling. The Sloan's hydrate research group in the Colorado School of Mines has had a major contribution for the Gibbs energy minimization method.[2] They developed the well-known software named "CSMGem" on the basis of the explained technique.[2] A comparison between the results of simulations by this software (including phase equilibrium modeling of different gas hydrates) and other commercial hydrate softwares show that the CSMGem[2] generally leads to less average absolute relative deviations of the obtained results from the selected experimental data available in the literature for many of the common industrial applications.[2]

3.5. Numerical models

In the recent decades, use of numerical models like Artificial Neural Network (ANN), Support Vector Machine (SVM) and so forth has generated lots of interest in the scientific community. These models (networks) are composed of simple elements working in a parallel computational strategy. These elements are inspired by biological nervous systems and are called neurons.[347-353]

One of the most-widely used numerical models is the ANN one. ANN models lie merely on mathematical concepts, which is to establish a relationship (linear or non-linear one) between the input data and desired output properties of a system. These networks are extensively used in various scientific and engineering problems.[347] For instance, calculations/estimations of physico-chemical properties of different pure compounds[354] or mixtures (fluids) [354] phase behavior representation/predictions of various (generally complex or multi-component) systems, etc. [348,349,355]

As a groundbreaking work, Elgibaly and Elkamel[356] developed an ANN model for representing (and predicting) hydrate formation conditions for various gas mixtures + inhibitor systems. This approach was later continued by Gu et al. [352] and comprehensively studied by Mohammadi and Richon,[357-359] Chapoy et al.,[360] and Mohammadi and coworkers[361,362] for determination of phase equilibria of the systems containing gas hydrates from various hydrate formers (in the presence/absence of hydrate promoters) or water content of natural gases. The reported results show acceptable deviations from the corresponding experimental values.

However, the ANN models may lead to the random initialization of the networks and variation of the stopping criteria during optimization of the model parameters.[363-366] The aforementioned characteristics may discourage the application of the ANN models for external predictions (external inputs excluding those applied in training and optimization procedures of treatment of the corresponding networks). The Support Vector Machine is a powerful strategy developed from the machine-learning community. [363-366] A "SVM" is a tool, mainly discussed in computer science, for a set of related supervised learning methods that analyze data and recognize patterns, used for regression analysis. [363] The SVM is considered as a non-probabilistic binary linear classifier. The following criteria may indicate most of the advantages of the SVM-based methods over the traditional methods based on the ANNs:[16,17,363-366]

1. They are more probable to converge to the global optimum;

2. They normally find a solution that can be quickly obtained by a standard algorithm (quadratic programming);

3. Such models do not require a priori determination of the network topology; which can be automatically determined as the training process ends;

4. Over-fitting complications are less probable in SVM schemes;

5. There is no need to choose the number of hidden nodes;

6. They have acceptable generalization performance;

7. These methods generally contain fewer adjustable parameters;

8. They require convex optimization procedures.

Due to the specific formulation of the SVM algorithm, sparse solutions can be found and both linear and nonlinear regressions can be pursued for solving the corresponding problems.[16,17,363-366] These features motivate to develop numerical models for phase equilibrium calculations/estimations on the basis of the SVM strategy. Thus far, phase equilibria of clathrate hydrates of methane, carbon dioxide, nitrogen, and hydrogen + "water soluble" organic promoters have been modeled successfully through this method.[363]

Omitting several elements from our discussion in this sub-section would be an oversight. As stated earlier, these numerical models are generally mathematical black boxes, in which the scientific aspects (e.g. thermodynamic issues) of the investigated systems do not play much role in their development and/or final application. Implication (or development) of such models are recommended in the case that the thermodynamic models have significant drawbacks in correlating or predicting the properties of particular systems or there is no other method for this purpose. In any case, extrapolations using such models may not be normally advised.

3.6. Molecular models

Molecular simulations including Molecular Dynamics and Monte Carlo simulations, Lattice Dynamics (LD), Group Contributions (GC), and Quantitative Structure-Property Relationships (QSPR) are generally able to relate the microscopic properties of molecules of compounds (fluids) to their macroscopic properties. Interests to apply these models have been undergone significant improvements toward recent years resulting from progresses in the capabilities of the computers not only due to their speed but also because of enhancement in parallel computing opportunities.

3.6.1. Molecular Dynamics

Investigation of the water hydrogen-bonded structures and intermolecular forces through molecular dynamics have been pursued by several research groups thus far. Tse et al.[367(a)-(d)] were, perhaps, the first to apply molecular dynamic simulation to clathrate hydrate compounds. The later works have been focused mainly on calculation of Langmuir constants,

368,369 the characteristics of the systems at water-hydrate interface,[370] and modeling hydrate kinetic inhibitors effects on the surface of the hydrate crystals.[2,371-374] and so forth. More details on the molecular dynamics models have been discussed elsewhere.[2]

3.6.2. Monte Carlo

Calculating the total energy of the molecules moving randomly in a definite space, Monte Carlo methods are capable of determination of time-independent thermodynamic properties (un-like the molecular dynamics methods).[2] Studies on interaction between the guest molecules and the hydrate cavities,[375,376] guest-guest interactions within the hydrogen-bonded networks,[377,378] and evaluation of Langmuir constants[379] have been the prominent attempts to apply Monte Carlo techniques to gas hydrate field.[2]

3.6.3. Group Contributions

The GC algorithms divide a molecule into small parts (generally named as "segments"). Each of these segments is considered as a functional group and has a contribution to the physicochemical properties of the specified molecule.[17] Finally, the value of the property is defined through calculating the summation of the contributions of all functional groups in a molecule.[17] The functional groups can be normally applied to represent many of the existing chemicals for determinations of their properties/phase behaviors particularly at the conditions of interest, where experimental measurements are difficult to conduct. To the best of our knowledge, there may be only one study applying the GC method to gas hydrate domain, in which Eslamimanesh and co-workers[17] coupled special functional groups with the least-squares support vector machine (LSSVM) mathematical algorithm[16,17,363-366] to develop a model for representation/prediction of the dissociation conditions of sH clathrate hydrates of methane with 21 hydrocarbon promoters namely as water "insoluble" hydrate formers (promoters). Acceptable accuracy of the proposed model with respect to the existing experimental data was observed.[17]

3.6.3. QSPR

In QSPR approaches, the numerical characteristics of molecules are treated to look for their effects on particular physicochemical properties, phase behaviors etc. These numerical factors, which are associated with chemical structures are called "Molecular Descriptors". They are, as a matter of fact, basic molecular properties of a compound and normally determined from the chemical structure.[16,380,381] Each type of molecular descriptors is related to a specific type of interactions between chemical groups in a particular molecule. Computations of molecular descriptors are generally performed using powerful computer software like "Dragon".[381] Since the values of many descriptors are related to the bond lengths, bond angles, etc., each chemical structure is generally optimized before calculation of its molecular descriptors. Later, a mathematical algorithm is applied to select the most

efficient molecular descriptors for evaluating a property/phase behavior of a compound/mixture of interest. Recently, this approach was followed by Eslamimanesh et al.[16] to present two molecular models for determination of the sH hydrate dissociation conditions with methane as help gas and some water "insoluble" hydrocarbon promoters as hydrate formers.

Models to determine phase equilibria of semi-clathrate hydrates

Theoretical attempts for calculation/estimation of the phase equilibria of semi-clathrate hydrates have been rarely undertaken and may be limited to two recent works. Mohammadi et al.[362] studied the application of Artificial Neural Networks (ANNs) for acceptable representation/prediction of the hydrate dissociation conditions of the systems including H_2 + TBAB aqueous solution. Application of these kinds of numerical models requires enough expertise in mathematics. Moreover, development of these models generally requires the use of many experimental data in order to be capable of predicting the structural changes of the cavities. Recently, Paricaud[382] successfully presented a thermodynamic model based on the use of the statistical associating fluid theory with variable range for electrolytes (SAFT-VRE)[383,384] to model the aqueous phase and vdW-P[319,320] solid solution theory for dealing with the solid (hydrate) phase for the hydrates formed in the carbon dioxide + TBAB aqueous solution system. The latter model requires enough expertise in SAFT molecular theory to make its extension to account for the representation/prediction of phase behavior of semi-clathrate systems formed from other hydrate formers/promoters.

3.7. Concluding remarks and theoretical objectives

According to the aforementioned description, which results from a preliminary literature review, it can be stated that:

- ✓ Estimation techniques like the Katz[316] chart have been widely used in industry for rough estimations.

- ✓ The calculation steps of the models on the basis of evaluating chemical potentials or fugacity coefficients are almost similar. Both of them apply the solid solution theory of vdW-P[319,320] for modeling the hydrate phase. The differences generally include models used for representation of the fluid phase behaviors and Langmuir constants as well as the assumptions made during the calculations. These models are, perhaps, the most interesting ones for industrial applications.

- ✓ The improved relations for determination of the Langmuir constants in *ab initio* methods seem to be more accurate than the conventional equations; however, more complex and may not be of interest of engineers.

- ✓ The Gibbs energy minimization model may be the most flexible predictive tool among the studied models due to capability of multi-phase flash calculations and stability tests. The developed CSMGem[2] software is now of much attraction for the petroleum industry.

- ✓ Numerical models such as ANN and SVM techniques[347-353] are generally applied in the case that the thermodynamic models are not found to be reliable for representing the phase behavior of a system of interest, as previously described.

- ✓ Molecular models are capable techniques for phase equilibrium predictions. Their applications are normally recommended especially when dealing with new systems. However, they need enough expertise about the molecular theories and generally more calculation time as well.

The presented theoretical approaches to model phase equilibria of clathrate hydrates seem to became mature toward the past decades while the corresponding methods to model the phase behavior of semi-clathrate hydrate systems are still at the demonstrating stage. Therefore, it is of much significance to develop an easy-to-use, reliable, and simple thermodynamic model for calculation/estimation of the corresponding phase equilibria, which is the main theoretical objective of this work. Furthermore, a mathematical approach is proposed to determine the molar composition of hydrate phase in equilibrium with liquid water and vapor for the systems containing carbon dioxide. Finally, two approaches are presented to evaluate the selected experimental phase equilibria data of significant systems for industry (generally contain fluid phases in equilibrium with gas hydrates, liquid water, or ice). The two latter elements consist other portions of the theoretical section of the thesis.

4. Presentation of the Developed Thermodynamic Model

Présentation du modèle thermodynamique développé

Dans ce chapitre, nous proposons un modèle thermodynamique pour la représentation et la prédiction des équilibres de phases des clathrate/semi-clathrates hydrates de CO_2, CH_4 et N_2 en présence de solutions aqueuses de bromure de tétra-n-butyl ammonium (TBAB). Pour la modélisation de la phase semi-clathrate hydrate, nous utilisons la théorie des solutions solides de van der Waals et Platteeuw (vdW-P)[319,320] avec deux modifications relatives aux évaluations des constantes de Langmuir et de la pression de vapeur d'eau dans le réseau de l'hydrate vide, dans lequel ces valeurs sont censées être fonction de la concentration en TBAB en solution aqueuse. L'équation d'État de Peng-Robinson (PR-EoS)[393] avec les paramètres réajustés de la fonction alpha de Mathias-Copeman[394] est utilisée pour le calcul de la fugacité des gaz précurseurs d'hydrates. Pour déterminer le coefficient d'activité de l'espèce non électrolyte dans la phase aqueuse, nous utilisons le modèle NRTL.[399] Pour calculer les coefficients d'activité moyens de la partie électrolyte, nous utilisons une corrélation basée sur les valeurs du coefficient osmotique et des coefficients d'activité.

In this chapter, a thermodynamic model is proposed for representation/prediction of phase equilibria of the CO_2, CH_4, or N_2 semi-clathrate hydrates in the presence of tetra-n-butyl ammonium bromide (TBAB) aqueous solution. For modeling the hydrate phase, the van der Waals - Platteeuw (vdW-P) [319,320] solid solution theory is used, revised with two modifications for evaluations of Langmuir constants and vapor pressure of water in the empty hydrate lattice, in which these values are supposed to be a function of TBAB concentration in aqueous solution. The Peng-Robinson equation of state (PR-EoS)[393] along with re-tuned parameters of Mathias-Copeman[394] alpha function is applied for calculation of the fugacity of gaseous hydrate former. For determination of the activity coefficient of the non-electrolyte species in the aqueous phase, the Non-Random Two-Liquid (NRTL)[399] activity model is used. To calculate the mean activity coefficients of the electrolyte portion, a correlation on the basis of existing osmotic coefficient and activity coefficient values is employed.

4.1. Model development

The liquid water- hydrate- gas/vapor (L_w-H-G/V) equilibrium conditions are calculated by equating the fugacity of water in the aqueous (f_w^L) and in the hydrate (f_w^H) phases:[2,312,385-389]

$$f_w^L = f_w^H \tag{4.1}$$

The fugacity of water in the hydrate phase is related to the chemical potential difference of water in the filled and empty hydrate lattice ($\Delta\mu_w^{MT-H}$) by the following relation: [2,312,385-389]

$$f_w^H = f_w^{MT} \exp(\frac{-\Delta\mu_w^{MT-H}}{RT}) \tag{4.2}$$

The fugacity of the hypothetical empty hydrate lattice (f_w^{MT}) is given by the following equation: [2,312,331,385-390]

$$f_w^{MT} = P_w^{MT}\varphi_w^{MT} \exp \int_{P_w^{MT}}^{P}(\frac{v_w^{MT}dP}{RT}) \tag{4.3}$$

where φ is fugacity coefficient and P_w^{MT} is the vapor pressure of water in empty hydrate lattice. The fugacity coefficient of water in empty hydrate lattice (φ_w^{MT}) is taken to be unity because the vapor pressure of the water phase is low. The partial molar volume of water in the empty hydrate lattice (v_w^{MT}) in the Poynting correction term of Eq. 4.3 is assumed to be pressure independent. Hence, the preceding equation can be written as follows: [2,312,385-390]

$$f_w^{MT} = P_w^{MT}\exp(\frac{v_w^{MT}(P - P_w^{MT})}{RT}) \tag{4.4}$$

In Eq. 4.2, $\Delta\mu_w^{MT-H}$ is calculated using Eq. 3.7 and 3.8.

The aqueous phase of the systems of interest contains liquid water, low concentrations of dissolved gas, and TBAB (hydrate promoter). The fugacity of water in the aqueous phase (f_w^L) can be determined using the following equation: [312,385-390]

$$f_w^L = x_w^L \gamma_w P_w^{sat} \exp(\frac{v_w^L(P - P_w^{sat})}{RT})$$ (4.5)

where x_w^L, γ_w, P_w^{sat}, and v_w^L stand for mole fraction of water in the aqueous phase, activity coefficient of water, water vapor pressure, and molar volume of liquid water, respectively, and superscript *sat* represents the saturation condition. Since we are dealing with an electrolyte solution (aqueous solution of TBAB), the concentration of water in aqueous phase can be determined applying the following equation:[382]

$$x_w^L = \frac{1}{1 + 0.001 \times 2 \times m \times M_w} - x_g^L$$ (4.6)

where *m* stands for the molality of aqueous solution in ($mol.kg^{-1}$), M_w is the molecular weight of water in ($g.mol^{-1}$) and x_g^L stands for the solubility of the gaseous hydrate former in the aqueous phase, and subscript *g* represent the gaseous hydrate former. Eq. 4.6 is obtained assuming total dissociation of TBAB in water, which yields anions of Br⁻ and cations of TBA⁺. The molality of the solution (defined as number of moles of TBAB per kg mass of water) can be calculated by the following relation: [382,389]

$$m = \frac{18.0153 \, x_{(TBA^+)}}{1000 \, x_w}$$ (4.7)

The solubility of gases in the aqueous phase is calculated using the Krichevsky-Kasarnovsky[391] equation:

$$x_g^L = \frac{f_g}{H_{g-w} \exp\left(\frac{v_g^\infty}{RT}(P - P_w^{sat})\right)}$$ (4.8)

where H_{g-w} is the Henry's constant of gas in water, subscript *g* stand for gas, and superscript ∞ represents infinite dilution condition. An experimental study has argued that the effects of the existing ions in the aqueous phase on the gas solubility are relatively small for the similar systems to those investigated in this work.[392]

The fugacity of gaseous hydrate former in the gas phase have been evaluated using the Peng-Robinson (PR)[393] EoS accompanied by the Mathias-Copeman alpha function[394] with re-tuned parameters, as discussed later. This alpha function has been proven to improve the performance of the equations of state to represent/predict the vapor pressure of pure compounds (generally polar ones).[394] Additionally, the water content of the gas phase is assumed to be negligible at the pressure-temperature conditions studied in this work.

The crystallographic data[28,395] show that each unit hydrate cell of the investigated semi-clathrate is composed of 2 TBA$^+$ and 2 Br$^-$ along with 76 water molecules. Furthermore, TBA$^+$ also plays the role of a guest species (along with the gaseous hydrate former) in the hydrate cavities, where the TBA$^+$ is encaged in tetrakaidecahedra and pentakaidecahedra (large) cages (50 % of each) and the gaseous component is trapped in dodecahedral small cages.[28,395] The subsequent hydrate structures could be either type A or type B with different hydration numbers that are described in the next section. As a consequence, the values of the fugacity of the hydrate promoter in the aqueous phase need to be determined as well. Eq. 4.9 can be applied for this purpose:

$$f_p^L = x_p^L \gamma_p P_p^{sat} \exp(\frac{v_p^L (P - P_p^{sat})}{RT}) \tag{4.9}$$

where γ_p represents the activity coefficient of the hydrate promoter in the aqueous (electrolyte) solution, and the subscript p stands for the hydrate promoter, respectively.

Substitution of the preceding equations in Eq. 4.1, the following expression is finally obtained:

$$\left[\frac{P_w^{MT} \exp(\frac{v_w^{MT}(P - P_w^{MT})}{RT})}{x_w^L \gamma_w^L P_w^{sat} \exp(\frac{v_w^L(P - P_w^{sat})}{RT})} \right] \times [\left(1 + C^{small} f_g\right)^{-v' small_{typeA/B}} \times \left(1 + C^{large_1} f_p^L\right)^{-v' large_{1typeA/B}}$$

$$\times \left(1 + C^{large_2} f_p^L\right)^{-v' large_{2typeA/B}}] = 1 \tag{4.10}$$

where superscripts/subscripts small and large stand for small and large cavities, respectively, and subscript type A/B represents the formation of types A or B semi-clathrate hydrates, respectively. Furthermore, subscripts 1 and 2 refer to occupation of large tetrakaidecahedra and pentakaidecahedra cages by TBA$^+$ cations. The hydrate dissociation pressure at a given temperature can be determined by solving the latter equation.

4.2. Model parameters

A typical structure of a TBAB semi-clathrate hydrate is depicted in Figure 4.1. Existence of TBAB in the system has non-negligible effects on the vapor pressure of water in empty hydrate lattice, consequently, in this work, the method of Dharmawardhana et al.[396] for evaluation of the saturated vapor pressure of water in empty hydrate lattice has been modified on the basis of the assumption that the vapor pressure is inversely proportional to TBAB concentration in aqueous phase because the hydrogen bonds, which form the cavities networks, elongate (Br⁻ takes part in the hydrate hydrogen-bonded network, as mentioned earlier). As a result, the following equation is proposed:

$$P_w^{MT} = 0.1\exp(17.44 - \frac{6003.9}{T} + h \times w_p) \tag{4.11}$$

where the units of P_w^{MT} and T are, respectively, MPa and K, h is an adjustable parameter, and w_p is the weight fraction of the TBAB in aqueous solution. It seems, from the structural formation of semi-clathrate hydrates, that the values of h may be generally a reverse function of w_p. It should be noted that Eq. 4.11 has not been developed on the basis of the assumption of Dharmawardhana et al.[396] which considers a fixed shape of the hydratre structure and consequently evalutes only temperature-dependent vapor pressure of water in empty hydrate lattice.

To determine the Langmuir constants, the method proposed by Parrish and Prausnitz[321] have been applied along with a correction factor to account for the disorders in the structures of the cavities resulted from Br⁻ bond to the molecules of water and interactions between the large molecules of TBAB (or their dissociated ions in aqueous solution) with each other as follows:

For tetrakaidecahedra cages:

$$C^{large\,1} = \left(\frac{c}{T} \times \exp\left(\frac{d}{T}\right)\right) \times (1 + e \times w_p) \tag{4.12}$$

For pentakaidecahedra cages:

$$C^{large\,2} = \left(\frac{f'}{T} \times \exp\left(\frac{g}{T}\right)\right) \times (1 + i \times w_p) \tag{4.13}$$
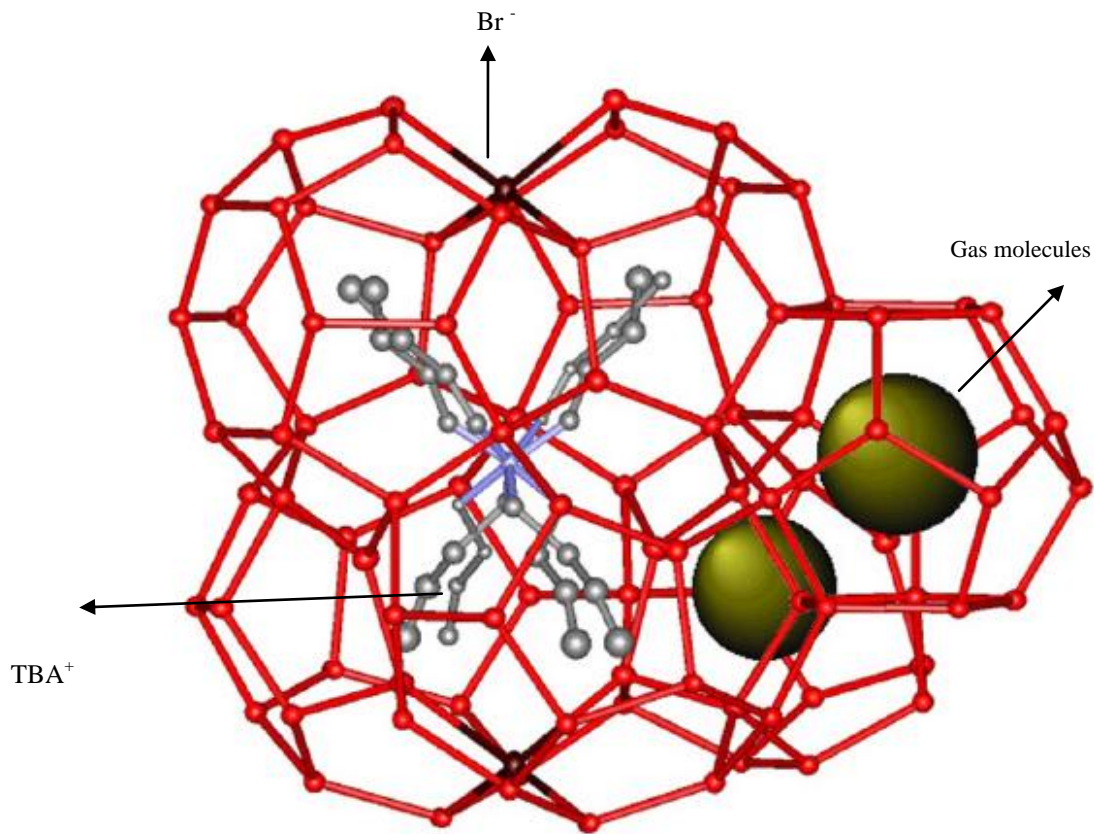
Figure 4.1: The schematic picture of a typical semi-clathrate hydrate formed from a gaseous hydrate former + TBAB aqueous solution (reproduced from Shimada et al.[28] with permission from Crystallography Journals Online, http://journals.iucr.org/).

In addition, the expression proposed by Parrish and Prausnitz[321] has been used for the dodecahedral small cages, which include the gas molecules:

$$C^{small} = \frac{aa}{T} \times \exp\left(\frac{bb}{T}\right) \tag{4.14}$$

In the preceding equations, c, d, and e are adjustable parameters for tetrakaidecahedra cavities, f', g, and i are those related to pentakaidecahedra cages, and aa and bb are the parameters recommended by Parrish and Prausnitz[321] for each gaseous hydrate former encaged in small dodecahedral cages (reported in Table 4.1).

On the basis of the so far knowledge about the structures of the semi-clathrate hydrates formed in the presence of the aqueous solutions of TBAB,[28,395,397] the following assumptions have been made for determination of the Langmuir constants:[389]

1. Hydration numbers = 26 for type A and 38 for type B;

2. The enclathrated gas molecules are located in the small dodecahedral cages;

3. The TBA^+ cations are trapped in two large tetrakaidecahedra and two large pentakaidecahedra cages.

4. Each type of semi-clathrates have two large cavities and one small cavity. As a result, the number of cages of the specified type per water molecule in a unit hydrate cell are calculated as follows:

- $v'_{\text{large 1type A}} = 4/(2 \times 26) = 1/13$ (4.15)

- $v'_{\text{large 2type A}} = 4/(2 \times 26) = 1/13$ (4.16)

- $v'_{\text{small type A}} = 6/(2 \times 26) = 3/26$ (4.17)

- $v'_{\text{small type B}} = 6/(2 \times 38) = 3/38$ (4.18)

- $v'_{\text{large 1type B}} = 4/(2 \times 38) = 1/19$ (4.19)

- $v'_{\text{large 2type B}} = 4/(2 \times 38) = 1/19$ (4.20)

Table 4.1: Constants *aa* and *bb* in Eq. 4.14. [321]

Hydrate former	*aa* /(K.MPa^{-1})	*bb* / (K)
CO_2	0.0011978	2860.5
CH_4	0.0037237	2708.8
N_2	0.0038087	2205.5

The value of v_W^{MT} is obtained using the following expressions, assuming that the volume of the empty hydrate lattice is similar to that for hydrate structure I:[398]

$$v_w^{MT} = (11.835 + 2.217 \times 10^{-5} T + 2.242 \times 10^{-6} T^2) \frac{10^{-30} N_A}{N_w^{MT}} - 8.006 \times 10^{-9} P + 5.448 \times 10^{-12} P^2 \qquad (4.21)$$

where N_A is Avogadro's number, N_w^{MT} stands for the number of water molecules per hydrate cell. The unit of pressure in Eq. 4.21 is MPa and the unit of temperature is K. It should be noted that the values of the pressure dependent terms in the preceding equation are very small and negligible. Therefore, they have very small effects on the values of the integral in Eq. 4.3.

The activity coefficient of water in aqueous phase has been determined using the NRTL[399] model with interaction parameters for our systems of interest reported in Table 4.2.

Table 4.2: The interaction parameters of the NRTL[399] model used in this work.

Compound	A_{12} (kJ.mole^{-1})	A_{21} (kJ.mole^{-1})	α
CO_2	5.82	6.81	0.3
CH_4	4.00	2.15	0.6
N_2	7.11	7.12	0.3

The following expression for calculation of the Henry's constants of gas-water can be used in Krichevsky-Kasarnovsky[391] equation: [312,385,388,389]

$$H_{g\text{-}w} = (10^{A + B(T)^{-1} + C' \times \log(T) + D \times T}) \times 0.1 \qquad (4.22)$$

where the Henry's constant is calculated in MPa and T is in K. The parameters of Eq. 4.22 are reported in Table 4.3. The values of partial molar volumes at infinite dilution (and at 298.15 K) to be applied in Eq. 4.8 for CO_2, CH_4, and N_2 have been considered as 33.9, 34.5, and 35.7 (cm^3.mol^{-1}), respectively, from the experimental work of Moore et al.[400]

Table 4.3: Constants A to D in Eq. 4.22. [312,385,388,389]

Solute	A	B / K	C'	D / K^{-1}
CO_2	21.6215	-1499.8	-5.6495	0.000206
CH_4	147.788	-5768.3	-52.295	0.018616
N_2	78.852	-3745	-24.832	0.000291

The activity coefficient of TBAB is calculated through the corresponding values proposed by Lindenbaum and Boyd,[401] and Amado and Blanco,[402] as function of molality of the aqueous solution at 298.15 K and 0.101 MPa. Applying Eq. 4.7 and the mentioned

osmotic pressure and activity coefficient values[401,402] leads to obtaining the following correlation to calculate the activity coefficient of the utilized hydrate promoter (TBAB):

$$\gamma_p = -0.5057 w_p^3 + 1.1603 w_p^2 - 1.3689 w_p + 0.7655 \tag{4.23}$$

In this work, it has not been tried to go deeply into the modeling of the electrolyte solution mainly due to the following reasons:

1. At the time of preparation of the dissertation manuscript, no experimental data of activity coefficient of TBAB in aqueous solution at various temperatures or pressures were available. This fact assigns some limitations to obtain the optimum values of the required parameters for modeling the electrolyte solution.

2. Modeling such systems are still a challenge (including selection of the most suitable electrolyte model, estimation of the required parameters, obtaining the interaction parameters etc.).

3. The main objective of the proposed model has been focusing on considering the effects of the applied promoter on the hydrate cages (or hydrate structures).

The density (ρ) of the TBAB aqueous solution (and consequently the molar volume (v_p^L)) has been determined using the correlation of Söhnel and Novotny[403] with the values recommended by Belandria and co-workers:[404]

$$\rho_p = \rho_w + o_1(100w_p) + o_2(100w_p)^2 + o_3(100w_p)^3 \tag{4.24}$$

where,

$$o_i = q_i + r_i(T) + s_i(T)^2 \tag{4.25}$$

In Eqs. 4.24 and 4.25, ρ_p is calculated in (g.cm^{-3}) and T is in K. Additionally, subscript i stands for the three sets of parameters reported in Table 4.4.

Table 4.4: Constants in Eq. 4.25.[404]

Constants	Values	Constants	Values
q_1	-1.707×10^{-8}	r_3	4.088×10^{-8}
q_2	4.570×10^{-9}	s_1	4.549×10^{-4}
r_1	5.693×10^{-6}	s_2	5.304×10^{-4}
r_2	-3.099×10^{-6}	s_3	-7.091×10^{-6}

In addition, partial molar volume of water has been calculated using Eq. 4.26, on the basis of the available data for a wide range of temperatures:[405]

$$v_w^L = (5.459 / 0.30542^{\ (1+(1-T/647.13)^{0.081})})^{-1}$$ (4.26)

where molar volume is in $cm^3.mol^{-1}$ and T is in K.

As already mentioned, fugacity of the gaseous hydrate former is calculated by the PR EoS.[393] The values of the Mathias-Copeman alpha function[394] parameters have been herein re-tuned to accurately represent the vapor pressure of the pure compounds (CO_2, CH_4, N_2, and H_2O) from triple point to the critical point accurately. The probable global optimum values of these parameters are reported in Table 4.5 and the applied critical properties and acentric factors of the studied compounds are indicated in Table 4.6.

Table 4.5: The optimal values of the Mathias-Copeman alpha function[394] * obtained and used in this study (CC_1 to CC_3 are the three parameters of the alpha function[394]).

| Component | Temperature range / K | Optimal values of parameters | | | |
		CC_1	CC_2	CC_3	$AARD^a$ / %
CO_2	217 to 304	0.709	-0.317	1.91	0.5
N_2	64 to 126	0.449	-0.158	0.469	0.6
CH_4	91 to 190	0.416	-0.173	0.348	0.4

^{a} $AARD = \dfrac{100}{N} \sum\limits_{i}^{N} \dfrac{|P_{i,cal.}^{vp} - P_{i,exp.}^{vp}|}{P_{i,exp.}^{vp}}$, where N is the number of the experimental data points, superscript vp denotes the

vapor pressure, and subscripts $cal.$ and $exp.$ stand for the calculated and experimental values, respectively.

*
$$\alpha(T) = \left[1 + cc_1\left(1 - \sqrt{\frac{T}{T_c}}\right) + cc_2\left(1 - \sqrt{\frac{T}{T_c}}\right)^2 + cc_3\left(1 - \sqrt{\frac{T}{T_c}}\right)^3\right]^2 \quad for\ T < Tc$$

otherwise,

$$\alpha(T) = \left[1 + cc_1\left(1 - \sqrt{\frac{T}{T_c}}\right)\right]^2$$

To determine the optimal values of the model parameters including those in Eqs. 4.11, 4.12, and 4.13 and also the Mathias-Copeman[394] alpha function parameters, the Differential Evolution (DE) optimization strategy[406,407] has been used. This optimization technique has been previously shown to have high capability in phase equilibrium calculations.[408-413] Apart from that, the DE algorithm[406,407] generally satisfies the following criteria:

Table 4.6: Critical properties and acentric factor of the pure compounds used in this study.[405]

Compound	$P_c{}^a$ / MPa	$T_c{}^b$ / K	$Z_c{}^c$	$\omega{}^d$
CH_4	4.599	190.56	0.2862	0.0114
CO_2	7.377	304.13	0.2744	0.2239
N_2	3.399	126.20	0.2917	0.0377
H_2O	22.055	647.13	0.2294	0.3449

^{a} Critical pressure
^{b} Critical temperature
^{c} Critical compressibility factor
^{d} Acentric factor

1. More probability for convergence to the global optimum;

2. High probability of finding a mathematically-correct solution;

3. No requirement for determination of the network topology in advance; which can be automatically determined as the training process ends;

4. Low probability to face over-fitting/under-fitting problems;

5. Acceptable generalization performance;

6. Fewer adjustable parameters;

7. Relying on the population-based initialization;

8. Use of the basis of stochastic evolutionary principles;

9. Ability to handle non-differentiable, nonlinear, and multimodal cost functions;

10. Few, robust, and easy to choose control variables to steer the minimization of the objective function;

11. No sensitivity to starting points i.e. starting decision variables or objective function values; and

12. Consistent and consecutive modification of the solutions in each generation.

The probable global optimum values of these parameters are obtained on the basis of the minimization of the following objective function:

$$function = \frac{100}{ndp} \sum_i^{ndp} \frac{|P_{i,cal.}^{diss./vp} - P_{i,exp.}^{diss./vp}|}{P_{i,exp.}^{diss./vp}} \tag{4.27}$$

where *ndp* is the number of data points used in the optimization procedure, superscript *diss./vp* denotes the hydrate dissociation pressure or vapor pressure of pure compound, and subscripts *i*, *cal.* and *exp.* stand for i^{th} calculated or experimental value, the calculated, and the experimental hydrate dissociation pressure or vapor pressure values, respectively. The above

objective function has been subjected to the following constraints (only for optimizing the Mathias-Copeman alpha function parameters):

$$(Z - \beta) > 0 \tag{4.28}$$

$$(\frac{Z + (1 - \sqrt{2})\beta}{Z + (1 + \sqrt{2})\beta}) > 0 \tag{4.29}$$

where Z is the compressibility factor and:

$$\beta = \frac{bP^{vp}}{RT} \tag{4.30}$$

In the preceding equation, b is the repulsive parameter of the PR EoS.[393] These two constraints have been taken into account to avoid trivial results from the exponential terms of the fugacity expressions during the calculation steps because the DE algorithm[406,407] is a population-based optimization method on the basis of random search algorithm and may consequently contribute to obtaining negative values of the corresponding arguments (Eqs. 4.28 and 4.29). The penalty functions are generally employed in the case of constrained optimization, which penalize infeasible solutions (eliminate the unexpected results).[408-414] The penalty function takes a finite value when a constraint is violated and zero value when it is satisfied.[408-414] The penalized function (objective function after imposing the penalty function criteria) can be expressed as follows:

$$PF(P^{diss./vp}) = function\ (P^{diss./vp}) + PP\left[\sum_{l=1}^{L} \langle gg_l(P^{vp}) \rangle + \sum_{m=1}^{M} |hh_m(P^{vp})| \right] \tag{4.31}$$

where PF is the penalized function, $gg_l(P^{vp})$ is the inequality constraint, $hh_m(P^{vp})$ represents the equality constraint, L and M are the number of inequality and equality constraints, respectively, and PP denotes the penalty parameter which can be defined by the user. The value of this parameter depends on the order of magnitude of the functions values involved in the problem and normally lies between 1 and 10^6.[408-414] Greater values of PP lead to more penalized effects of the constraints on the values of the objective function. In the present work, the penalty parameter has been set to 10. The bracket-operator $\langle \rangle$ represents the absolute value of the operand, if operand is negative. Therefore, the final formulation of the objective function is written as follows:

$$OF(P^{diss./vp}) = function(P^{diss./vp}) + 10 \sum_{l=1}^{2} \langle gg_l(P^{vp}) \rangle \tag{4.32}$$

where,

$$gg_1(P^{vp}) = \max\{0, (Z - \beta)\} \tag{4.33}$$

$$gg_2(P^{vp}) = \max\{0, (\frac{Z + (1 - \sqrt{2})\beta}{Z + (1 + \sqrt{2})\beta})\} \qquad (4.34)$$

The vapor pressure values of the DIPPR 801[415] database have been used in the optimization procedure of the Mathias-Copeman[394] alpha function. Moreover, selected experimental dissociation pressures of semi-clathrate hydrates of CO_2 in the presence of TBAB aqueous solutions[58,416] at various concentrations (mostly generated in our laboratory)[58] have been utilized for obtaining the optimal values of the parameters in Eqs. 4.11, 4.12, and 4.13. The probable global optimum values of the aforementioned parameters are reported in Table 4.7.

Table 4.7: Optimal values of the parameters in Eqs. 4.11, 4.12, and 4.13.

Parameter	Values[*]	
	Type A[a]	Type B[b]
c / (K.MPa^{-1})	0.501813	0.998105
d / (K)	3835.7	6999.5
e	-0.7342	-0.0076
f' / (K.MPa^{-1})	0.619810	0.738929
g / (K)	6518.8	4940.5
i	-0.971250	-0.040894
h	0.2078	0.3606

[*] The numbers of the digits of the parameters have been determined by a sensitivity analysis of the final results to their values and their orders of magnitudes are in agreement with the corresponding values proposed by Parrish and Prausnitz[321] for clathrate hydrates.
[a] Calculations were performed assuming formation of semi-clathrate hydrate of type A.
[b] Calculations were performed assuming formation of semi-clathrate hydrate of type B.

4.3. Results of the proposed model

The performance of the model for prediction of the clathrate hydrate dissociation conditions for the CO_2/CH_4/N_2 + water systems in L_w-H-G/V equilibrium region has been first examined. The obtained results are shown in Table 4.8. They demonstrate acceptable accuracy of the model results in wide ranges of temperatures and pressures compared with selected experimental data (available in the NIST gas hydrate database).[417]

It is worth pointing out that the phase behavior calculations of the studied semi-clathrate hydrates have been undertaken in two steps assuming formation of type A and type B, respectively. Later, the represented/predicted hydrate dissociation pressures possessing the lowest values of the objective function or average absolute relative deviation (AARD) from the experimental values can be applied to designate which type of semi-clathrate hydrate is

formed at the conditions of interest (i.e. pressure-temperature-concentration of TBAB in aqueous solution).

Table 4.8: Summary of the model results for prediction of the hydrate dissociation conditions of $CO_2/CH_4/N_2$ in the presence of water in L_w-H-V equilibrium region.

System	Number of data	Temperature range / K	Pressure range / MPa	AARD[a] / %
CO_2 + water	160	273.3 to 283.0	1.35 to 4.40	1.8
CH_4 + water	107	273.2 to 291.2	2.65 to 18.55	2.3
N_2 + water	14	273.2 to 292.0	16.27 to 101	4.0

[a] $AARD = \dfrac{100}{N} \sum_{i}^{N} \dfrac{|P_{i,pred.}^{diss.} - P_{i,exp.}^{diss.}|}{P_{i,exp.}^{diss.}}$, where N is the number of the experimental data points, and subscript *pred.* stands for the predicted values.

Figure 4.2 shows the predicted (for clathrate hydrates)/represented (for semi-clathrate hydrates) hydrate dissociation conditions for the CO_2 + TBAB aqueous solution systems. It should be noted that only these experimental data[58,416] (the data shown in Fig. 2) have been applied for obtaining the optimal values of the model parameters. These parameters have been later utilized for prediction of the dissociation conditions of $CO_2/CH_4/N_2$ semi-clathrate hydrates in the presence of TBAB aqueous solution. In other words, the parameters in Eqs. 4.11, 4.12, and 4.13 for evaluation of the vapor pressure of water in empty hydrate lattice and the Langmuir constants in large hydrate cavities remain as global values for other systems (CH_4/N_2 + TBAB aqueous solution) for further calculations.

The predicted phase equilibria of the $CO_2/CH_4/N_2$ + water/TBAB aqueous solution systems are sketched in Figures 4.3 to 4.5. It should be again pointed out that no experimental hydrate dissociation data for the CH_4/N_2 + TBAB aqueous solution systems have been used in tuning process. A summary of the obtained results are reported in Table 4.9. It is interpreted that the developed model can acceptably represent/predict the TBAB hydrate promotion effects (i.e. shifting the hydrate phase boundaries to lower pressures and higher temperatures) for the three investigated systems.

A recent comprehensive research study[424] argues that the phase behavior of semi-clathrate hydrates may be complicated and difficult to analyze, as stated earlier.[30] This is mainly because the semi-clathrate structure can be changed from type A to type B[424] or vice versa.[30,389,424] The type of the structure depends normally on the hydration number of the hydrate which results from particular gases investigated in the presence of TBAB aqueous solutions.[30,389,424] Generally, the deviations of the calculated/estimated results of the proposed model in this work from the experimental data seem to be less assuming formation of semi-clathrate hydrates of type B with respect to those obtained assuming formation of semi-

clathrate hydrates of type A. It is worth it to point out that the model seems to be capable of prediction of the structural change of the investigated semi-clathrates at some (limited) conditions of "temperature-pressure-concentration of TBAB" triplets. For instance, at around 283 K and 0.4 MPa, there may be a structural change from type A to B in the phase equilibrium of the CO_2 + 0.0702 mass fraction TBAB aqueous solution system.

It may be also the case at about 289 K and 7 MPa for the hydrate dissociation conditions of the N_2 + 0.40 mass fraction TBAB aqueous solution system. However, various experimental studies such as RAMAN spectroscopy and calorimetry have revealed that there may be much more occasions where the structural changes happen for the investigated systems.[424] On the other hand, the former experimental technique has also proposed formation of a new type of semi-clathrates in the N_2 + TBAB aqueous solution system.[424]

In addition, recent studies have shown[30,424] that there are some discrepancies in the produced experimental data for the semi-clathrate hydrate systems so far. Therefore, it may not be expected that the developed model is able to predict such structural changes, proposed by the experimental efforts.

Another element to consider is that, the developed model can acceptably predict the hydrate inhibition effects of TBAB at the concentrations greater than that of stoichiometric ratios (around 0.427 mass fraction TBAB in aqueous solution).[30,424]

The average absolute relative deviations of the model results from the corresponding experimental hydrate dissociation values for the N_2 + TBAB aqueous solution system assuming formation of type A or type B hydrate structures are almost the same (around 11 %). It may suggest that there are few structural changes (from type A to type B vice versa) expected in this system compared to the other two investigated systems (i.e. semi-clathrate hydrates of CO_2 or CH_4).

One significant factor should not be omitted from our discussion. The main goal here has been to determine the phase behavior of semi-clathrate hydrates formed from gaseous hydrate former + TBAB aqueous solution. The developed model is not able to represent/predict the solid (S)-liquid (L) equilibria of the TBAB + water system (TBAB hydrate + TBAB aqueous solution phase equilibria). In other words, it seems not to be applicable for determination of the "temperature-composition" diagram of the aforementioned system at a specified pressure. Furthermore, the proposed model for the liquid phase cannot be used for complete liquid phase calculations.
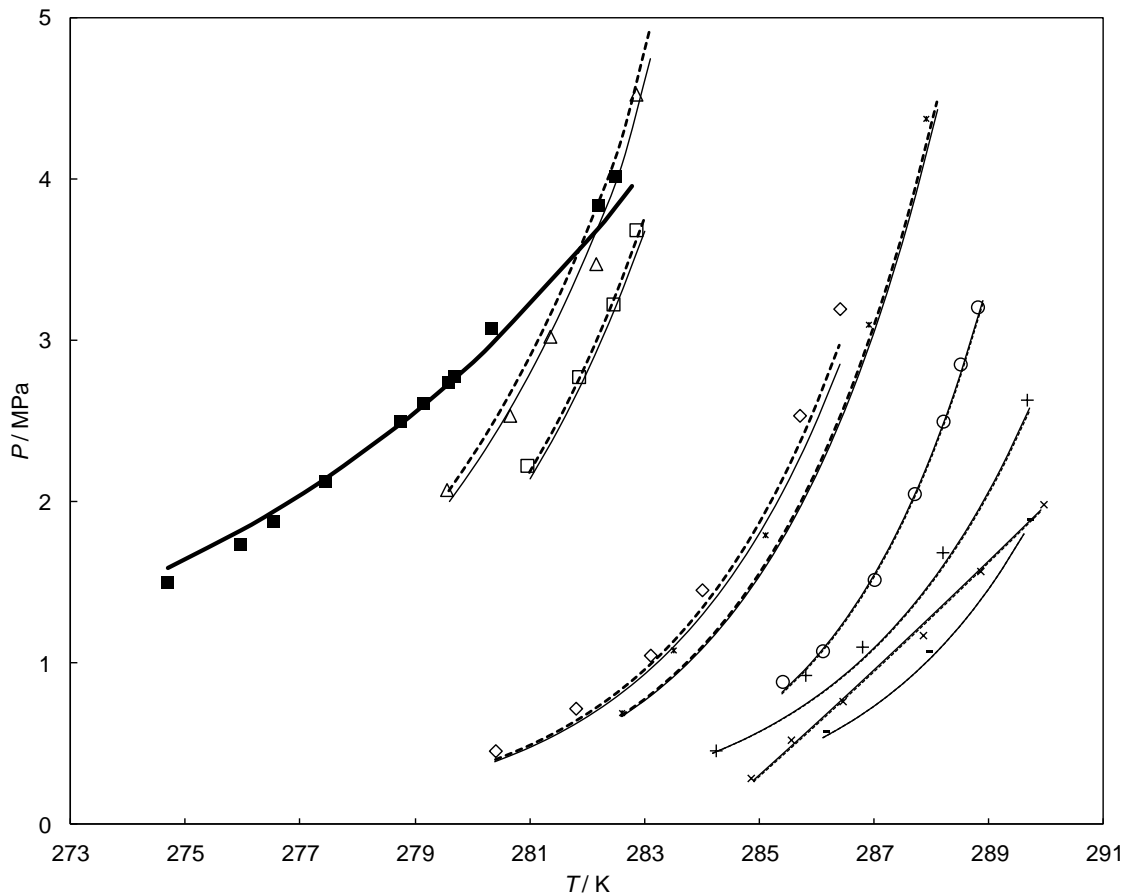
Figure 4.2: Dissociation conditions of clathrate/semi-clathrate hydrates for the carbon dioxide + water/TBAB aqueous solution systems. Symbols stand for the experimental data and curves (lines) refer to the predicted (for clathrate hydrates)/represented (for semi-clathrate hydrates) values using the developed thermodynamic model. ■, CO_2 + water system;[215,323,418,419] Δ, CO_2 in the presence of 0.01 mass fraction TBAB aqueous solution;[416] □, CO_2 in the presence of 0.02 mass fraction TBAB aqueous solution;[416] ◊, CO_2 in the presence of 0.05 mass fraction TBAB aqueous solution;[58] *, CO_2 in the presence of 0.50 mass fraction TBAB aqueous solution;[58] ○, CO_2 in the presence of 0.10 mass fraction TBAB aqueous solution;[58] +, CO_2 in the presence of 0.167 mass fraction TBAB aqueous solution;[58] ×, CO_2 in the presence of 0.25 mass fraction TBAB aqueous solution;[58] -, CO_2 in the presence of 0.35 mass fraction TBAB aqueous solution.[58] Bold solid Curve, model predicted results for the CO_2 + water system; Solid curves, model represented results assuming the formation of type B semi-clathrate hydrates (AARD = 3.1 %); Dashed curves, model represented results assuming the formation of type A semi-clathrate hydrates (AARD = 3.2 %).
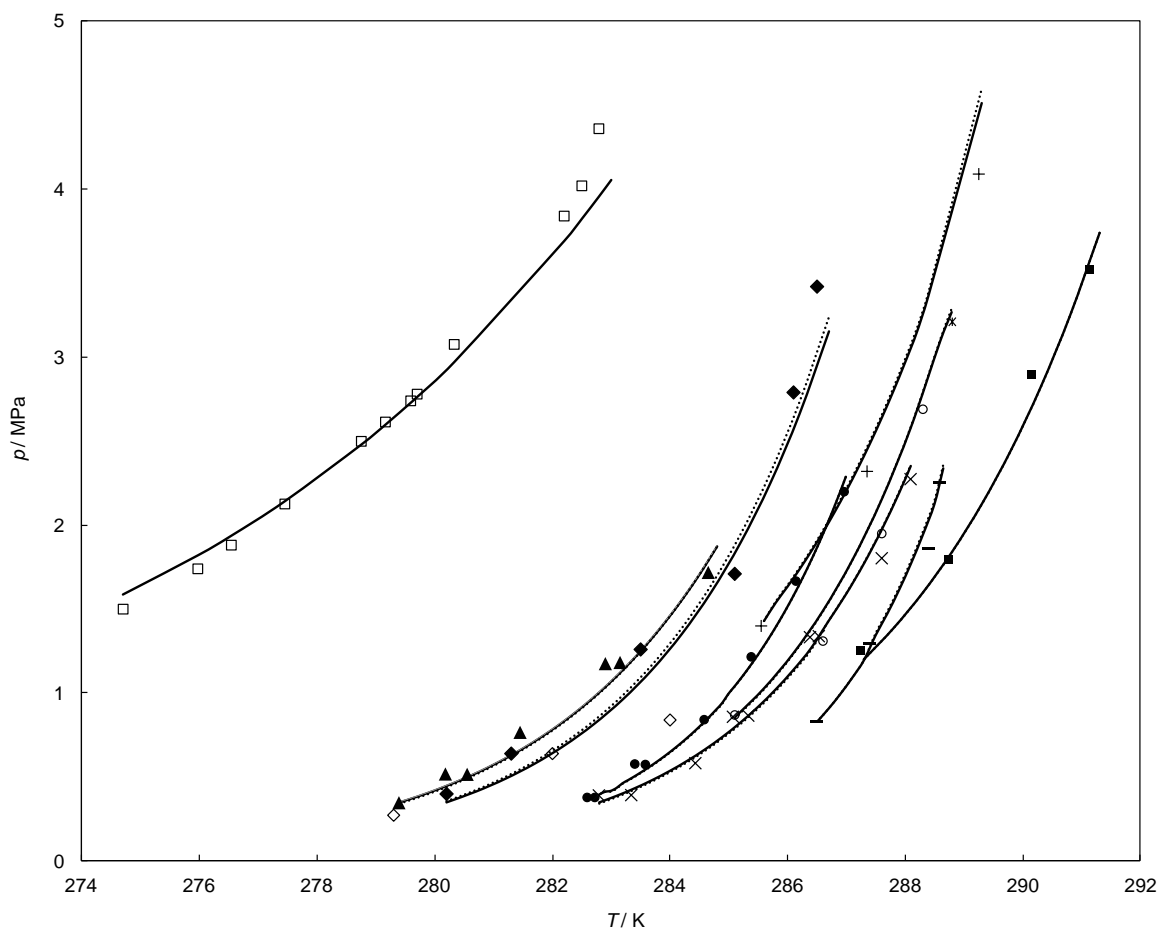
Figure 4.3: Dissociation conditions of clathrate/semi-clathrate hydrates for the carbon dioxide + water/TBAB aqueous solution systems. Symbols stand for experimental data and curves (lines) refer to the predicted values using the developed thermodynamic model. □, CO_2 + water system;[215,323,418,419] ▲, CO_2 in the presence of 0.0443 mass fraction TBAB aqueous solution;[392] ♦, CO_2 in the presence of 0.05 mass fraction TBAB aqueous solution;[420] ◊, CO_2 in the presence of 0.05 mass fraction TBAB aqueous solution;[204] ●, CO_2 in the presence of 0.0702 mass fraction TBAB aqueous solution;[392] ×, CO_2 in the presence of 0.0901 mass fraction TBAB aqueous solution;[392] +, CO_2 in the presence of 0.10 mass fraction TBAB aqueous solution;[421] ○, CO_2 in the presence of 0.10 mass fraction TBAB aqueous solution;[420] ■, CO_2 in the presence of 0.427 mass fraction TBAB aqueous solution;[421] -, CO_2 in the presence of 0.40 mass fraction TBAB aqueous solution;[257] Solid curves, model predicted results assuming the formation of type B semi-clathrate hydrates (AARD = 7.7 %); Dashed curves, model predicted results assuming the formation of type A semi-clathrate hydrates (AARD = 8.2 %).
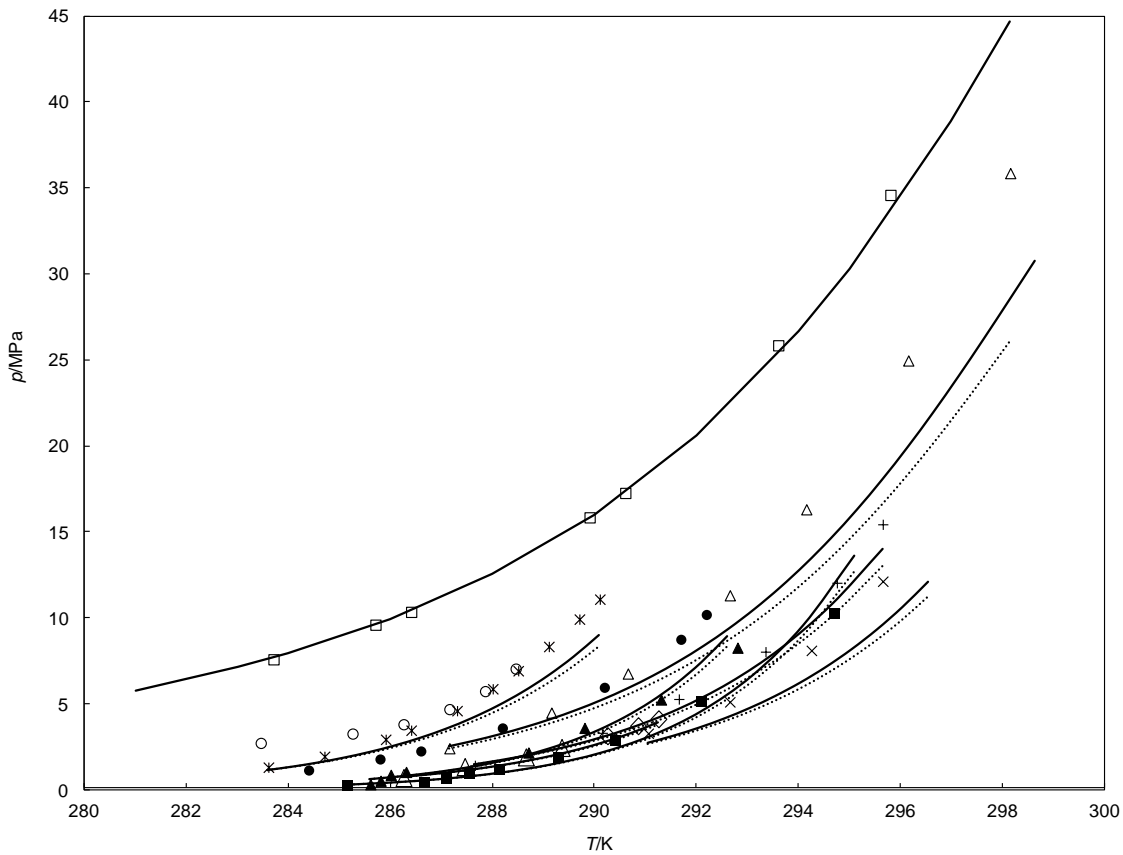
Figure 4.4: Dissociation conditions of clathrate/semi-clathrate hydrates for the methane + water/TBAB aqueous solution systems. Symbols stand for experimental data and curves (lines) refer to the predicted values using the developed thermodynamic model. □, CH$_4$ + water system;[323] *, CH$_4$ in the presence of 0.05 mass fraction TBAB aqueous solution;[422] ○, CH$_4$ in the presence of 0.05 mass fraction TBAB aqueous solution;[25] ●, CH$_4$ in the presence of 0.10 mass fraction TBAB aqueous solution;[58] Δ, CH$_4$ in the presence of 0.10 mass fraction TBAB aqueous solution;[421] ▲, CH$_4$ in the presence of 0.50 mass fraction TBAB aqueous solution;[58] +, CH$_4$ in the presence of 0.20 mass fraction TBAB aqueous solution;[421] ◊, CH$_4$ in the presence of 0.45 mass fraction TBAB aqueous solution;[25] ■, CH$_4$ in the presence of 0.25 mass fraction TBAB aqueous solution;[58] ×, CH$_4$ in the presence of 0.30 mass fraction TBAB aqueous solution;[421] Solid curves, model predicted results assuming the formation of type B semi-clathrate hydrates (AARD = 5.6 %); Dashed curves, model predicted results assuming the formation of type A semi-clathrate hydrates (AARD = 13 %).
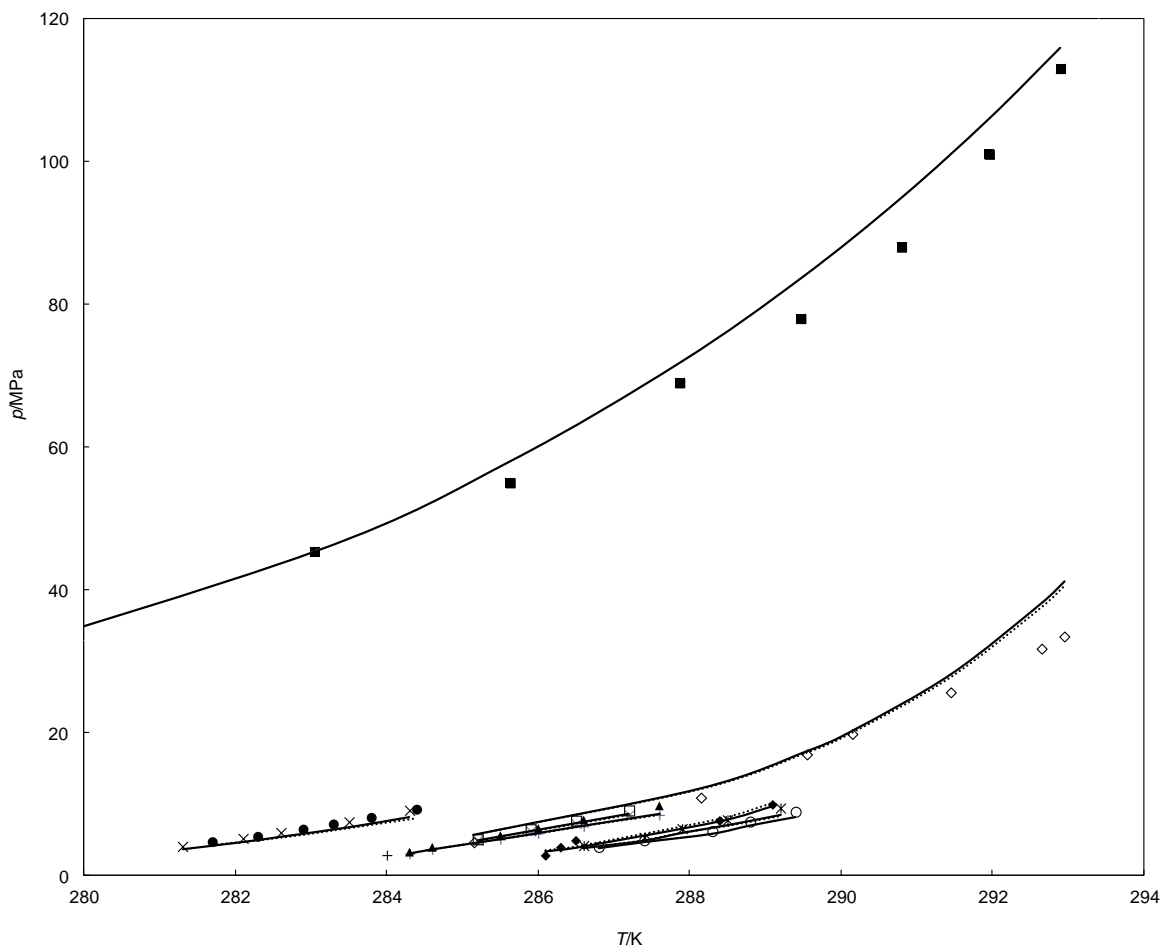
Figure 4.5: Dissociation conditions of clathrate/semi-clathrate hydrates for the nitrogen + water/TBAB aqueous solution systems. Symbols stand for experimental data and curves (lines) refer to the predicted values using the developed thermodynamic model. ■, N_2 + water system;[423] ×, N_2 in the presence of 0.05 mass fraction TBAB aqueous solution;[206] ●, N_2 in the presence of 0.05 mass fraction TBAB aqueous solution;[58] ◊, N_2 in the presence of 0.10 mass fraction TBAB aqueous solution;[421] +, N_2 in the presence of 0.10 mass fraction TBAB aqueous solution;[204] ▲, N_2 in the presence of 0.10 mass fraction TBAB aqueous solution;[58] □, N_2 in the presence of 0.60 mass fraction TBAB aqueous solution;[206] ♦, CH_4 in the presence of 0.50 mass fraction TBAB aqueous solution;[58] *, N_2 in the presence of 0.20 mass fraction TBAB aqueous solution;[206] ○, N_2 in the presence of 0.40 mass fraction TBAB aqueous solution;[206] Solid curves, model predicted results assuming the formation of type B semi-clathrate hydrates (AARD = 11 %); Dashed curves, model predicted results assuming the formation of type A semi-clathrate hydrates (AARD = 11 %).

It is worth pointing out that the equality of fugacities approach especially adopted in this work, have been already demonstrated to be reliable for phase equilibrium predictions of the following systems: gas hydrate phase behavior in the presence of different inhibitors[331] (methanol etc.), ionic liquid,[312] promoters (THF etc.),[388] phase equilibria of gas hydrates of refrigerant.[387] The aforementioned criteria led us to select the basis of this thermodynamic model for its extension to the semi-clathrate hydrate systems.

Another element to consider is that the performance of the same thermodynamic model without modifications for the vapor pressure of water in empty hydrate lattice and Langmuir constants (the thermodynamic model for conventional clathrate hydrates) for prediction of phase behavior of semi-clathrate hydrates have been also checked in this work without acceptable results. It was inferred that introducing all the adjusting parameters are needed to reliably predict the phase equilibria of the investigated systems. It also merits to point out that the model may be more appropriate for interpolation of the invesitgated data, but not for extrapolation.

To recapitulate, there is still a need to conduct considerable efforts for developing accurate and predictive models for representation/prediction of the phase equilibria of semi-clathrate hydrates.

Table 4.9: Summary of the model results for prediction of the dissociation conditions of semi-clathrate hydrates of $CO_2/CH_4/N_2$ + TBAB aqueous solution in the L_w-H-G/V equilibrium region.

System	Number of data	Temperature range / K	Pressure range / MPa	TBAB concentration in aqueous solution / mass fraction	AARD[a] / %	
					Type A [b]	Type B [c]
CO_2 + TBAB aqueous solution[*]	54	279.3 to 291.2	0.273 to 4.09	0.0443, 0.05, 0.0702, 0.0901, 0.1, 0.4, 0.427, 0.65	8.2	7.7
CH_4 + TBAB aqueous solution	66	281.75 to 298.15	0.235 to 35.853	0.05, 0.1, 0.2, 0.25. 0.3, 0.45, 0.50	13	5.6
N_2 + TBAB aqueous solution	55	279.84 to 292.95	0.47 to 35.503	0.05, 0.10, 0.20, 0.25, 0.40, 0.50, 0.60	11	11

[a] $AARD = \dfrac{100}{N} \sum\limits_{i}^{N} \dfrac{|P_{i,pred.}^{diss.} - P_{i,exp.}^{diss.}|}{P_{i,exp.}^{diss.}}$, where N is the number of the experimental data points, and subscript *pred.* stands for the predicted values.

[b] Calculations were performed assuming formation of semi-clathrate hydrate of type A.
[c] Calculations were performed assuming formation of semi-clathrate hydrate of type B.
[*] The model proposed by Paricaud[382] has been shown to give the AARD of about 10 % for the same system; however, using less experimental data to check.

5. Experimental Measurements

Mesures expérimentales

Certaines études théoriques et observations de terrain suggèrent que la forte consommation d'énergie, des coûts d´investissement élevés ou la probabilité de corrosion dans les installations seraient peut-être les inconvénients potentiels relatifs aux procédés de séparation du CO_2.[30] En conséquence, la recherche de procédés de séparation moins gourmands en énergie, respectueux de l'environnement et plus économiques est en cours au sein de divers groupes de recherche, et ce, à l'échelle mondiale. La méthode de cristallisation (formation) de l'hydrate de gaz a récemment attiré beaucoup d'attention en vue de séparer le dioxyde de carbone des gaz de combustion (voir chapitre 2 pour plus de détails).

Certains gaz industriels peuvent avoir des quantités considérables de dioxyde de carbone, d'hydrogène, de méthane, d'azote, etc.. Par exemple, les gaz de combustion émis par les centrales à grande échelle contiennent généralement N_2 et CO_2. Les procédés de reformage à la vapeur et la partie de gazification des procédés "ICGC" (integrated coal gasification cycle) produisent des effluents contenant des mélanges de CO_2 et de H_2. Les veines de charbon produisent des émissions considérables de méthane froid (CBM, Cold Bed Methane).[425]

Afin de concevoir des procédés de séparation faisant appel à la cristallisation sous forme de clathrates/semi-clathrates hydrates, des données fiables d'équilibres de phases sont requises. Les Tableaux 5.1 à 5.3 fournissent un résumé de presque tous les résultats des études expérimentales disponibles dans la littérature sur les clathrates/semi-clathrates hydrates concernant les mélanges: CO_2 + H_2/CH_4/N_2 en présence de promoteurs d'hydrates. Il semble évident qu'il y a un grand enthousiasme pour générer plus de données expérimentales d'équilibres de phases afin de clarifier le comportement de phase complexe des semi-clathrates, ajuster les paramètres des futurs modèles thermodynamiques et enquêter sur les réelles capacités de séparation liées à l'application de ces structures. Ainsi, dans cette étude, les conditions de dissociation des clathrates/semi-clathrates hydrates ont été mesurées pour les systèmes suivants:

1. CO_2 (fractions molaires : 0,151/0,399) + N_2 (fractions molaires : 0,849/0,601) + eau et + solutions aqueuses de TBAB (0,05/0,15/0,30 en fractions massiques).

2. CO_2 (fraction molaire : 0,4029) + CH_4 (fraction molaire : 0,5971) + solutions aqueuses de TBAB (fractions massiques : 0,05/0,10).

3. CO_2 (fractions molaires : 0,1481/0,3952/0,7501) + H_2 (fractions molaires : 0,8519/0,6048/0,2499) + eau et + solutions aqueuses de TBAB (0,05/0,30 en fractions massiques).

Divers mélanges de gaz contenant du CO_2 ont été étudiés pour représenter le grand domaine de compositions généralement rencontré dans les applications industrielles.

Some field observations/theoretical studies argue that relatively high energy consumption, high costs, or probability of corrosions in the processes facilities may be the potential drawbacks of the current CO_2 separation processes.[30] Consequently, searching for less energy-intensive, environmental-friendly, and more economic separation processes are being undergone by various research groups world-wide. Gas hydrate crystallization (formation) method has recently attracted much attention to separate carbon dioxide from combustion flue gases (refer to Chapter 2 for details).

Some industrial gas streams may have considerable amounts of carbon dioxide, hydrogen, methane, or nitrogen etc. For instance, flue gases emitted from large scale power plants typically contain N_2 and CO_2, steam reforming processes and the gasifier section of the integrated coal gasification cycle (ICGC) processes produce gas flows containing mixtures of CO_2 and H_2, and emissions in the form of cold bed methane (CBM) discharging from coal seams contain considerable amounts of CH_4.[425]

In order to design separation processes using clathrate/semi-clathrate hydrate crystallization, reliable phase equilibrium data are required. Tables 5.1 to 5.3 provide a summary of almost all experimental studies on semi-clathrate hydrates for mixtures of $CO_2 + N_2/CH_4/H_2$ in the presence of hydrate promoters that are available in open literature to date. It seems to be obvious that it is of great attraction to generate more experimental phase equilibrium data to clarify complex phase behavior of semi-clathrates, tune the future thermodynamic models, and for the investigation of the relevant separation capabilities through application of these structures. Consequently, in this study, the clathrate/semi-clathrate hydrate dissociation conditions for the following systems have been measured and reported:

1. CO_2 (0.151/0.399 mole fraction) + N_2 (0.849/0.601 mole fraction) + TBAB aqueous solution (0.05/0.15/0.30 mass fraction) or water.

2. CO_2 (0.4029 mole fraction) + CH_4 (0.5971 mole fraction) + TBAB aqueous solution (0.05/0.10 mass fraction).

3. CO_2 (0.1481/0.3952/0.7501 mole fraction) + H_2 (0.8519/0.6048/0.2499 mole fraction) + TBAB aqueous solution (0.05/0.30 mass fraction) or water.

Various gas mixtures containing CO_2 have been investigated to represent wide compositional ranges generally encountered in industrial applications.

Table 5.1: Experimental hydrate dissociation data available in open literature for the carbon dioxide + nitrogen + TBAB aqueous solution system at various concentrations of TBAB.

Authors	System	TBAB mass fraction	T range / K	P range / MPa	Number of points
Deschamps and Dalmazzone[257]	CO_2 (0.249 mole fraction) + N_2 (0.751 mole fraction)	0.4	284.8 to 293.3	Up to 9.180	5
Meysel et al.[430]	CO_2 (0.75 mole fraction) + N_2 (0.15 mole fraction)	0.05, 0.1, 0.2	284.1to 290.0	1.964 to 3.822	14
Meysel et al.[430]	CO_2 (0.50 mole fraction) + N_2 (0.50 mole fraction)	0.05, 0.1, 0.2	282.3 to 290.4	1.956 to 5.754	16
Meysel et al.[430]	CO_2 (0.20 mole fraction) + N_2 (0.80 mole fraction)	0.05, 0.1, 0.2	281.8 to 288.3	2.976 to 5.901	12
Lu et al.[233(a)]	CO_2 (0.159 mole fraction) + N_2 (0.841 mole fraction)	0.05, 0.153, 0.348, 0.407, 0.457	278.05 to 287.85	1.17 to 5.84	12

Table 5.2: Experimental hydrate dissociation data available in open literature for the carbon dioxide + methane + TBAB aqueous solution system at various concentrations of TBAB.

Authors	System	TBAB mass fraction	T range / K	P range / MPa	Number of points
Deschamps and Dalmazzone[257]	CO_2 (0.501 mole fraction) + CH_4 (0.499 mole fraction)	0.4	284.8 to 292.4	Atmospheric pressure up to 3.20	5

Materials

Table 5.4 reports the chemicals used in the present work, their suppliers and purities. The chemicals were used without any further purification. Aqueous solutions were prepared following the gravimetric method, using an accurate analytical balance (mass uncertainty ± 0.0001 g). Consequently, uncertainties on the basis of mole fraction are estimated to be less than 0.01.

Table 5.3: Experimental hydrate dissociation data available in open literature for the carbon dioxide + hydrogen + TBAB aqueous solution system at various concentrations of TBAB.

Authors	System	TBAB mass fraction	T range / K	P range / MPa	Number of points
Li et al.[253]	CO_2 (0.185/0.392 mole fraction) + H_2 (0.815/0.608 mole fraction)	0.024, 0.036, 0.050, 0.083, 0.153, 0.329	274.45 to 288.55	0.25 to 7.26	63

Table 5.4: Purities and suppliers of chemicals.[*]

Chemical	Supplier	Purity
Carbon Dioxide (0.151 mole fraction) + Nitrogen (0.849 mole fraction)	Air Liquide	Purity of each gas > 0.99[**] (mole fraction)
Carbon Dioxide (0.399 mole fraction) + Nitrogen (0.601 mole fraction)	Air Liquide	Purity of each gas > 0.99 (mole fraction)
Carbon Dioxide (0.749 mole fraction) + Nitrogen (0.251 mole fraction)	Air Liquide	Purity of each gas > 0.99 (mole fraction)
Carbon Dioxide (0.4029 mole fraction) + Methane (0.5971 mole fraction)	Air Liquide	Purity of each gas > 0.99 (mole fraction)
Carbon Dioxide (0.1481 mole fraction) + Hydrogen (0.8519 mole fraction)	Air Liquide	Purity of each gas > 0.99 (mole fraction)
Carbon Dioxide (0.3952 mole fraction) + Hydrogen (0.6048 mole fraction)	Air Liquide	Purity of each gas > 0.99 (mole fraction)
Carbon Dioxide (0.7501 mole fraction) + Hydrogen (0.2499 mole fraction)	Air Liquide	Purity of each gas > 0.99 (mole fraction)
TBAB	Sigma-Aldrich	0.99 (mass fraction)

[*] Deionized water was used in all experiments. [**] The measurement uncertainty reported by the supplier.

5.1. Apparatuses

5.1.a. Apparatus 1

The schematic diagram of this apparatus is given in Figure 5.1. This in-house designed and built apparatus is based on the "static-analytic" technique with capillary gas phase sampling (ROLSI[TM]). Suitability for working with corrosive fluids, strong agitation, accurate measuring devices, compositional analysis of the gas phase in equilibrium with liquid water and hydrate phases, and visual observation through the equilibrium cell during the experiments are among the main features of this apparatus.[58,59,426] In addition, it is suitable for measurements at temperatures ranging from 233 to 373 K. The main part of the apparatus is a cylindrical equilibrium cell, made of austenitic stainless steel to withstand hydrogen embrittlement and pressures up to 60 MPa.[58] Figures 5.2 and 5.3 show cross and lateral sections of the equilibrium cell, respectively. It is worth to point out that, the grid support, which is installed inside the cell, is to protect the capillary sampler from plugging by hydrate particles. Since the objective of the measurements in this work has been determination of the phase equilibria of semi-clathrates hydrates (without measuring the molar compositions of the vapor phase), the ROLSI[TM] has not been herein employed.

The equilibrium cell has an inner volume of 201.5 ± 0.5 cm^3 and two sapphire windows. A motor-driven turbine agitation system (Top Industrie) ensures sufficient agitation to facilitate reaching equilibrium even during the hydrate formation. However, this system may have serious drawbacks: significant dead volumes, leak issues, and/or frequent seizing which should be taken into account during the measurements. Temperature of equilibrium cell is controlled using a thermostatic bath (Tamson Instruments, TV4000LT), which allows the visual observation of the cell content throughout the experiments. One platinum resistance sensor (Pt100), inserted in the cell interior, is used to in situ measure the temperature within $\pm$ 0.1 K uncertainty estimated after calibration against a 25-Ω reference platinum resistance thermometer. This 25-Ω reference probe was calibrated, following the ITS 90 protocol, by Laboratoire National d'essais (Paris). Pressure is measured using a pressure transducer (Druck, type PTX611): High pressure sensor (HPT) for pressures up to 40 MPa. Resulting from calibration against a dead weight balance (Desgranges & Huot 5202S CP, Aubervilliers, France), pressure instrumental uncertainty is estimated to be less than 5 kPa.
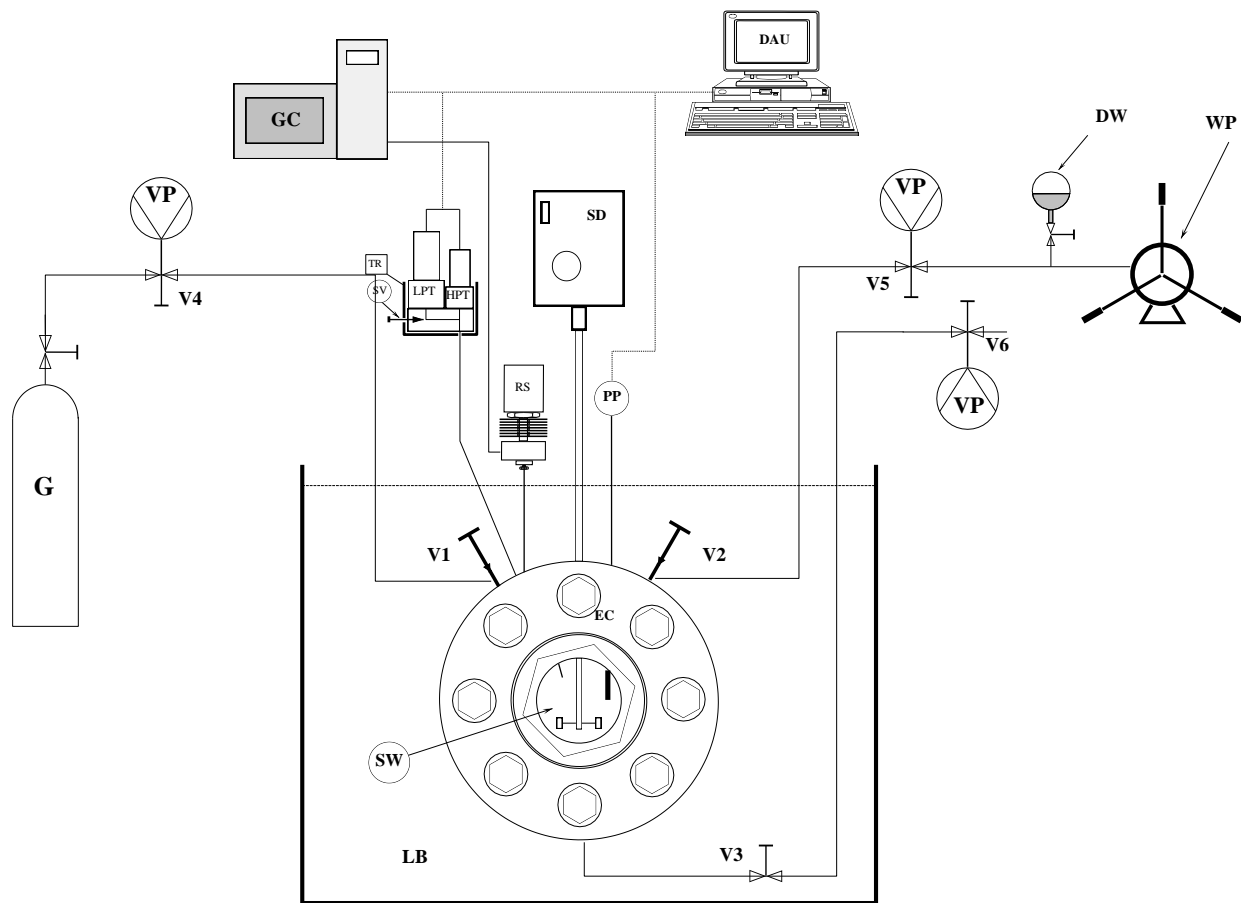
Figure 5.1: Schematic diagram of the apparatus 1:[58,426] DAU, data acquisition unit; DW, degassed water; EC, equilibrium cell; G, gas cylinder; GC, gas chromatograph; HPT, high pressure transducer; LB, liquid bath; LPT, low pressure transducer; PP, platinum probe; RS, ROLSI[TM] sampler; SD, stirring device; SW, sapphire windows, TR, temperature regulator; V1, V2, V4, V5, feeding valves; V3, V6, purge valves; VP, vacuum pump; SV, isolation valve for LPT; WP, high pressure pump. The VP signs stand for only one vacuum pump, which can be connected to the system through V4, V5, and V6 valves.

5.1.b. Apparatus 2

The main part of this apparatus is a cylindrical vessel made of Hastelloy, which can withstand pressures up to 20 MPa.[58,199,425,427] The volume of the vessel is approximately 30 cm^3. A magnetic stirrer is installed in the vessel to agitate the fluids and hydrate crystals formed during the measurements.[58] Two platinum resistance thermometers (Pt100) are inserted into the vessel to measure temperatures and check for their equality within temperature measurement

uncertainty, which is estimated to be about 0.1 K and ensure temperature homogeneity inside the equilibrium cell.[58] Temperature uncertainty estimation comes from calibration against a 25 Ω
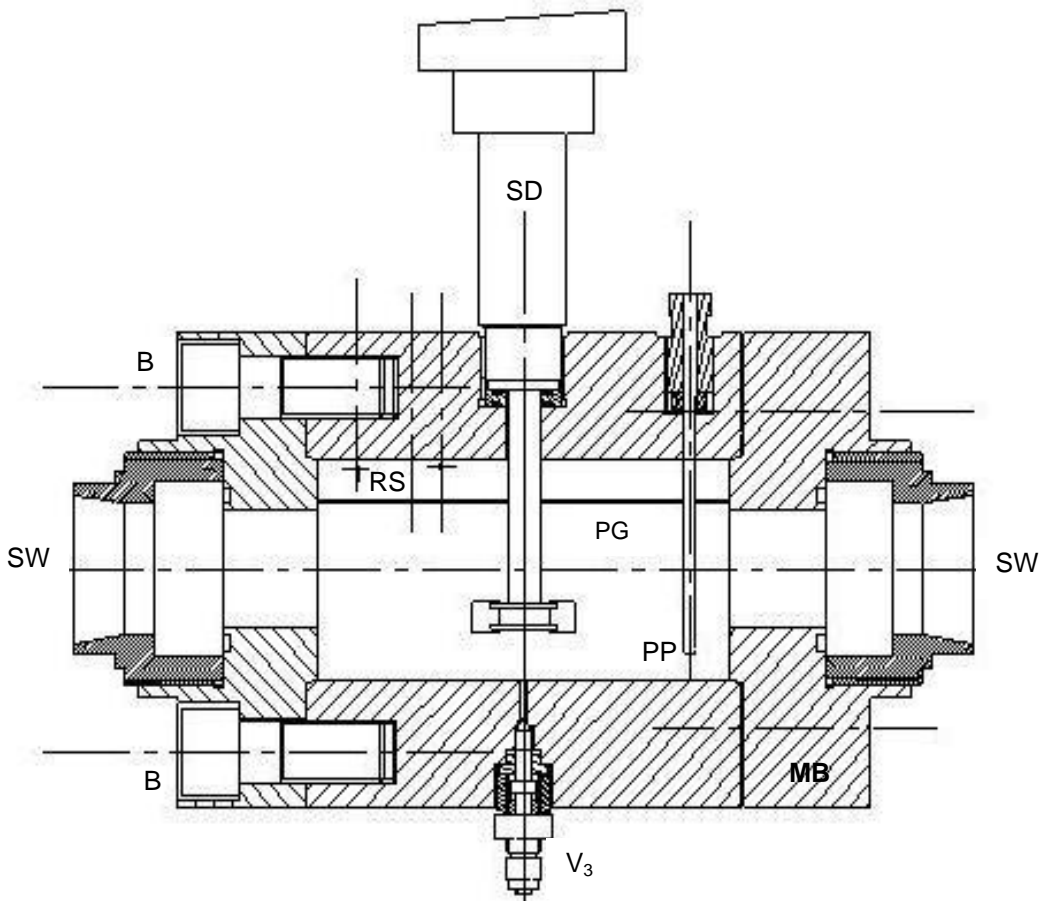
Figure 5.2: Cross section of the equilibrium cell (used in the first apparatus):[426] B, tightening bolts; MB, main body; PG, protection grid; PP, platinum probe; RS, ROLSI^{TM} sampler; SD, stirring device; SW, sapphire windows; V3, purge valve.

reference platinum resistance thermometer, as described in the section 5.1.a. Pressure in the vessel is measured with a DRUCK pressure transducer (Druck, type PTX611 for pressure ranges up to 16 MPa). Pressure measurement uncertainties are estimated to be less than 5 kPa, as a result of careful calibration against a dead weight balance (Desgranges and Huot, model 520). The schematic diagram of this experimental apparatus is shown in Figure 5.4.

5.2. Common experimental procedure

The hydrate dissociation conditions were measured (applying both apparatuses) through an isochoric pressure search method.[58,59,199,312,425-429] as implemented by Ohmura and co-workers.[429] The reliability of this method for measurement of phase equilibria of clathrate/semi-clathrate hydrates has been demonstrated in the literature.[58,59,199,312,425-429] The vessel containing
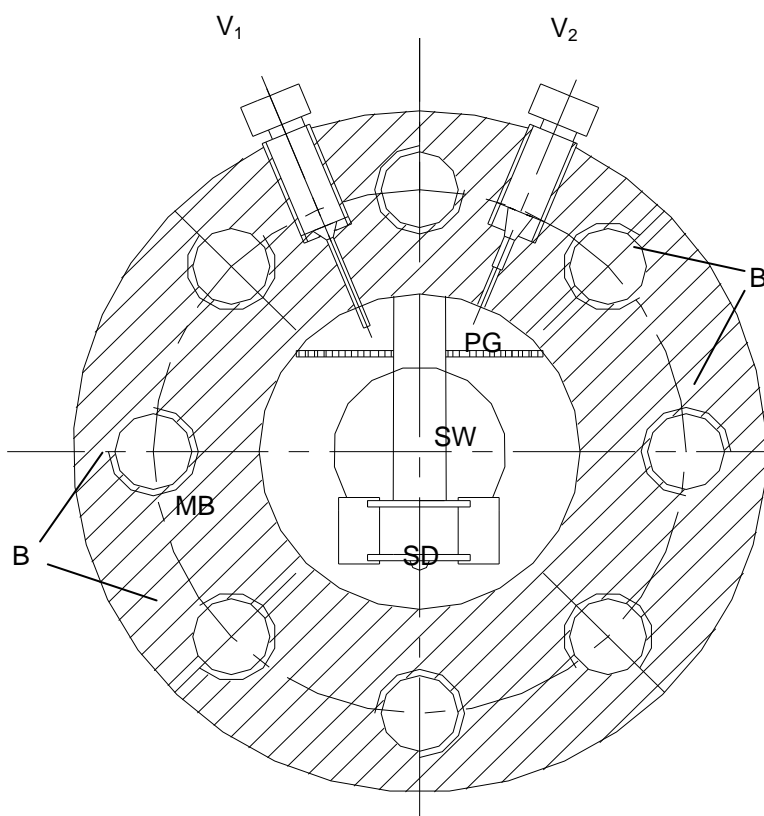
Figure 5.3: Lateral section of the equilibrium cell (used in the first apparatus):[426] B, tightening bolts; MB, main body; PG, protection grid; SD, stirring device; SW, sapphire windows; V1 and V2, feeding valves.

aqueous solution (approximately 10 % by volume of the vessel is filled with aqueous solution) is immersed into the temperature-controlled bath, and the gas is supplied from a cylinder through a pressure-regulating valve into the vessel. Note that the vessel is evacuated before the introduction of any aqueous solution and gas.[58] After obtaining temperature and pressure stability (far enough from the hydrate formation region), the valve in the line connecting
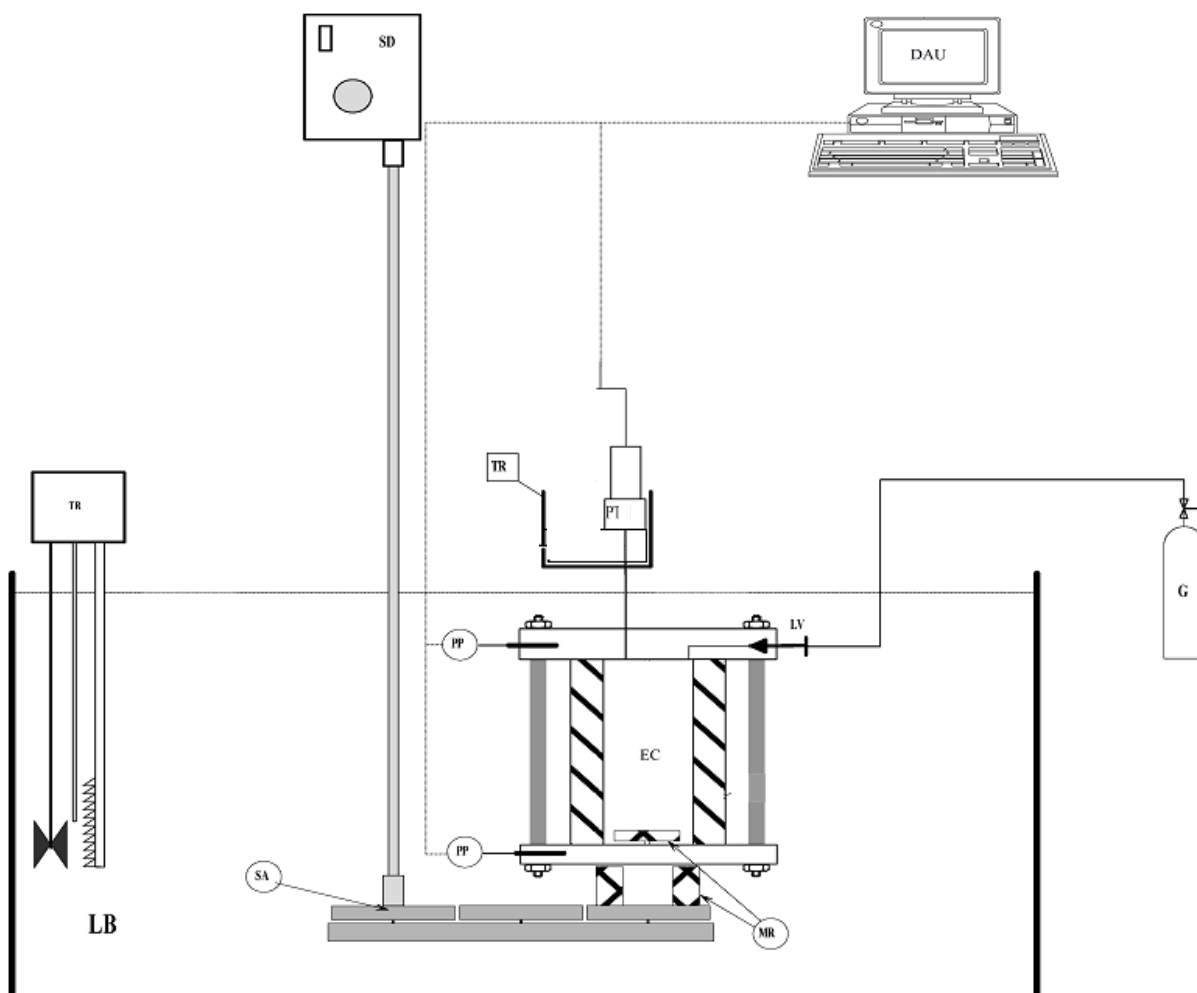
Figure 5.4: Schematic diagram of the experimental apparatus 2. DAU, data acquisition unit; EC, equilibrium cell; G, gas cylinder; LB, liquid bath; LV, loading valve; MR, magnetic rod; PP, platinum probe (temperature sensor); PT, pressure transducer; SA, stirring assembly; SD, stirring device with variable speed motor; TR, temperature controller.

the vessel and the cylinder is closed. Subsequently, temperature is slowly decreased to form the hydrate.[58] Hydrate formation in the vessel is observed when a pressure drop at constant temperature is detected using the data acquisition unit. The temperature is then increased with steps of 0.1 K. At every temperature step, the temperature is kept constant with enough time to obtain an equilibrium state in the cell.

Therefore, a pressure-temperature diagram is sketched for each experimental run, from which we determine the hydrate dissociation point.[58,59,199,312,425-429] During the dissociation of the hydrate crystals inside hydrate formation region, the pressure is gradually increased by increasing the temperature. However, outside this region, a slight pressure increase is observed during the increase of temperature.[58,59,199,312,425-429] Consequently, the hydrate dissociation point is displayed when the slope of the pressure temperature diagram changes suddenly.[58,59,199,312,425-429] A typical diagram of this experimental method is shown in Figure 5.5. The maximum uncertainties for the measured hydrate dissociation temperatures and pressures are expected to be 0.2 K and 0.05 MPa due to graphical determination of the corresponding values.
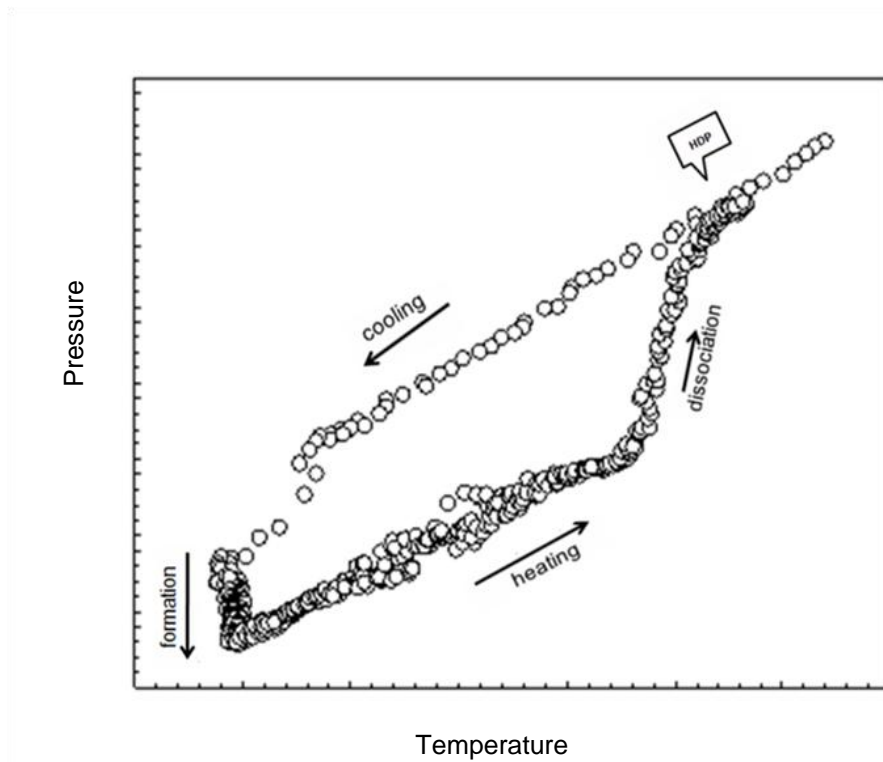
Figure 5.5: Typical diagram obtained using the isochoric pressure search method.[58,59,199,312,425-429] The down arrow callout (HDP) indicates the gas hydrate dissociation point.

5.3. Experimental results

The results of the experimental measurements of the clathrate/semi-clathrate hydrate dissociation conditions for the aforementioned systems (systems 1 to 3) are depicted in Figures 5.6 to 5.11. A semi-logarithmic scale is used for better studying the hydrate promotion effects of TBAB aqueous solutions and the trend of the experimental data as well. The predictions of the phase equilibria of clathrate hydrates of the same gas mixtures (except the $CO_2 + H_2$ mixtures) in the presence of water (pure water) using the well-known CSMGem[2] thermodynamic model are also shown in these figures for comparison reasons. In addition, all the obtained experimental data are reported in Tables 5.5 to 5.7. Analysis of the experimental data, shown in these figures, indicates some interesting findings. It is clearly seen that TBAB has drastic promotion effects on the formation of the semi-clathrate hydrates of the systems concerned, i.e. the formation conditions are shifted to high temperatures and low pressures in comparison with the clathrate hydrates of ($CO_2 + N_2/CH_4/H_2$) in the presence of water. Furthermore, it may suggest the improved selectivity of hydrate cages (semi-clathrate hydrate cages) for trapping the CO_2 molecules. These effects should lead to a more efficient separation (recovery) process for CO_2 from gas mixtures using hydrate crystallization (lower energy consumption compared with processes using conventional clathrate hydrate approaches in the presence of liquid water). It is also revealed from the measured data for the $CO_2 + N_2/H_2$ +TBAB aqueous solution system that the required pressure for semi-clathrate hydrates formation (dissociation) is increased as the concentration of nitrogen and hydrogen in the feed gas increases under the same concentration of TBAB and temperature.

Another element to consider is that the promotion effect of the TBAB aqueous solution is generally enhanced at low concentrations of the TBAB aqueous solution. In other words, by increasing the amount of TBAB in the feed aqueous solution (in the concentration ranges studied in this work), the shift in temperature/pressure conditions of the hydrate formation is reduced. Therefore, economic studies should be performed to find the optimum value of TBAB addition to the process. It is also found that a small increase in temperature results in a large equilibrium pressure increase. This fact reveals that such measurements have to be done very carefully to avoid high experimental errors during the measurements including errors in calibration of temperature probes and pressure transducers, etc. (The effects of experimental errors on the quality of the phase equilibrium data will be discussed later).

Table 5.5: Experimental clathrate/semi-clathrate hydrate dissociation conditions measured in this study for the carbon dioxide + nitrogen + TBAB aqueous solution or water system.

System	TBAB mass fraction	T / K	P / MPa
CO_2 (0.151 mole fraction) + N_2 (0.849 mole fraction)	0	275.2	10.10
		276.6	11.93
		277.7	14.09
		278.6	15.70
		278.9	16.74
CO_2 (0.151 mole fraction) + N_2 (0.849 mole fraction)	0.05	284.5	6.67
		285.6	9.04
		286.4	11.70
		287.6	14.08
CO_2 (0.151 mole fraction) + N_2 (0.849 mole fraction)	0.15	285.0	1.83
		287.5	5.54
		288.6	7.71
		289.0	8.81
		290.0	11.37
		291.6	15.94
CO_2 (0.151 mole fraction) + N_2 (0.849 mole fraction)	0.30	285.7	1.57
		288.5	4.64
		290.5	8.01
		292.1	12.04
		293.2	16.21
CO_2 (0.399 mole fraction) + N_2 (0.601 mole fraction)	0	275.6	4.92
		276.3	5.27
		277.3	5.97
		277.7	6.27
CO_2 (0.399 mole fraction) + N_2 (0.601 mole fraction)	0.05	277.1[*]	1.12
		282.6	2.78
		284.0	4.22
		285.6	5.93

[*] Likely represents semi-clathrate hydrate of (TBAB + water).

Table 5.5: Continued…

		284.3	1.42
CO_2 (0.399 mole fraction) + N_2 (0.601 mole fraction)	0.15	286.6	2.89
		288.2	4.50
		289.2	6.06
		286.4	1.71
CO_2 (0.399 mole fraction) + N_2 (0.601 mole fraction)	0.30	288.0	3.20
		289.5	4.35
		290.2	5.72
		290.6	6.17
		275.1	2.35
		275.6	2.48
CO_2 (0.749 mole fraction) + N_2 (0.251 mole fraction)	0	277.0	2.91
		278.0	3.33
		278.2	3.45

[*] Likely represents semi-clathrate hydrate of (TBAB + water).

As mentioned in Chapter 3, meticulous scrutiny of experimental data and findings from recent research studies[424] reveal that the phase behavior of semi-clathrate hydrates may be complicated and difficult to analyze. This is mainly due to the fact that the semi-clathrate structure can change from type A to type B or vice versa by increasing/decreasing the amounts of TBAB in aqueous solutions or by increasing/decreasing the dissociation pressure of the system.[30,389,424] The type of the structure depends normally on the hydration number of the hydrate which results from particular gas mixtures investigated in the presence of TBAB aqueous solutions. Furthermore, some data obtained from RAMAN spectroscopy show that there may be two co-existing phases in the phase equilibria of particular semi-clathrate hydrates such as those hydrates formed from the CO_2 + TBAB aqueous solution system.[424] It may not be possible to conclude about the hydrate structure change from phase equilibrium measurements by PVT studies only (as performed in this work). It is therefore proposed that NMR, crystallography, X-Ray diffraction, and calorimetry studies should be undertaken simultaneously to clarify different aspects of this issue.[427]
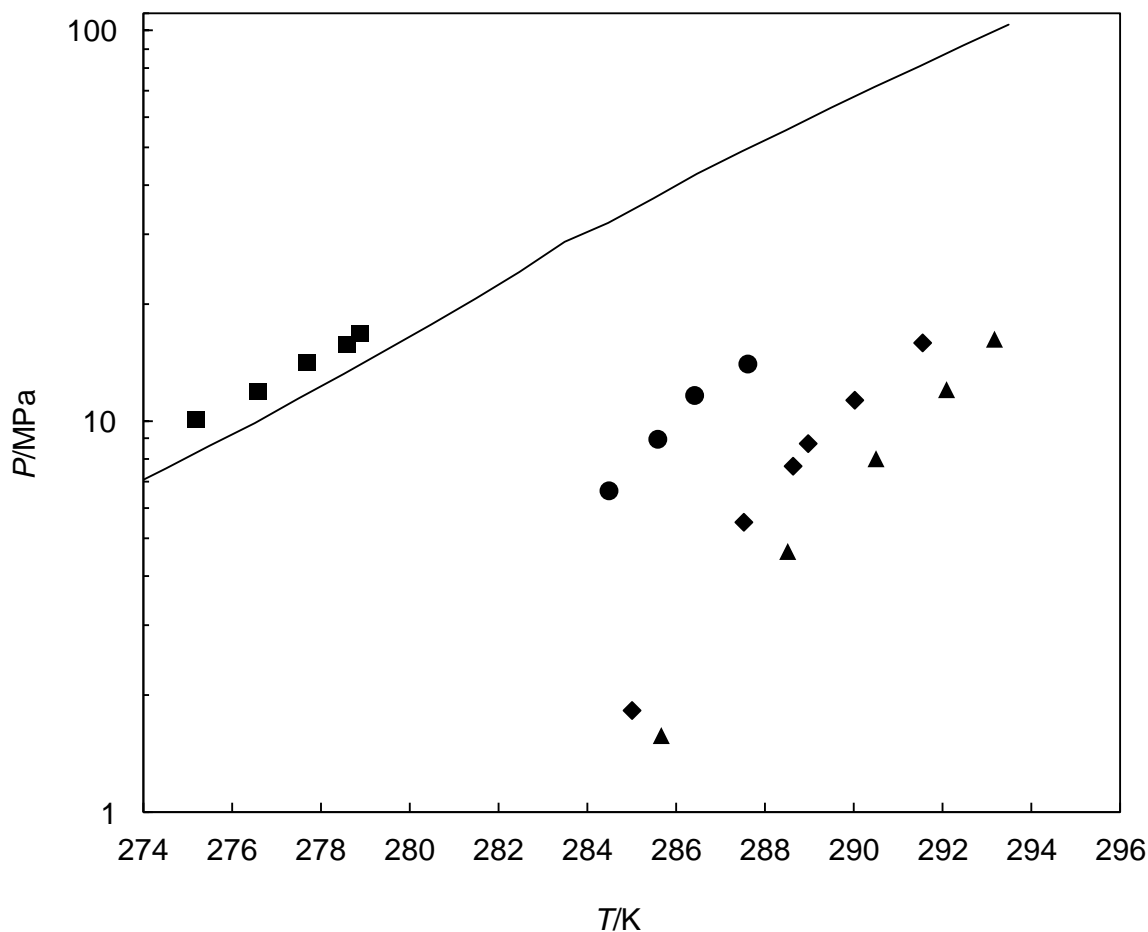
Figure 5.6: Phase equilibrium of clathrate/semi-clathrate hydrates for the carbon dioxide (0.151 mole fraction) + nitrogen (0.849 mole fraction) + water or TBAB aqueous solution systems. ■, This work, in the presence of water; ●, This work in the presence of TBAB 0.05 mass fraction aqueous solution; ♦, This work in the presence of TBAB 0.15 mass fraction aqueous solution; ▲, This work in the presence of TBAB 0.30 mass fraction aqueous solution; Curve, Predictions of CSMGem hydrate model[2] in the presence of water, Feed gas composition (0.151 mole fraction CO_2 + 0.849 mole fraction N_2).

Omitting one point from our discussion seems to be an oversight. The whole measured data have been checked with the temperature-composition phase diagram of TBAB semi-clathrate hydrates[26,27] ensuring our hydrate dissociation conditions are outside of the dissociation conditions of semi-clathrate hydrates of the TBAB + water system. It should be noted that comparing semi-clathrate hydrate phase equilibrium data from different sources on the same basis is generally not an easy task because the compositions of the feed gases are quite different.

As already stated, the available experimental phase equilibrium data for the three binary gas mixtures investigated in this work are limited to those reported in Tables 5.1 to 5.3.
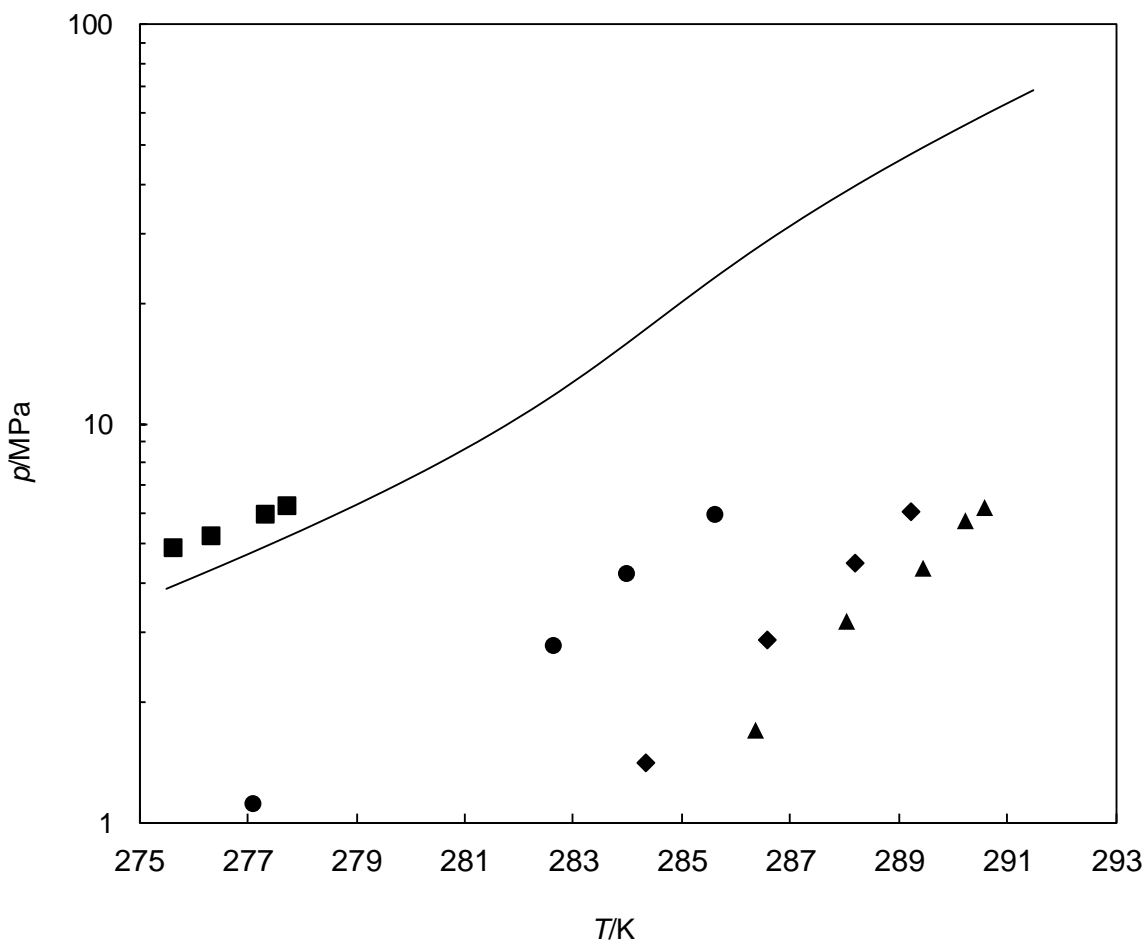
Figure 5.7: Phase equilibrium of clathrate/semi-clathrate hydrates for the carbon dioxide (0.399 mole fraction) + nitrogen (0.601 mole fraction) + water or TBAB aqueous solution systems. ■, This work, in the presence of water; ●, This work in the presence of TBAB 0.05 mass fraction aqueous solution; ♦, This work in the presence of TBAB 0.15 mass fraction aqueous solution; ▲, This work in the presence of TBAB 0.30 mass fraction aqueous solution; Curve, Predictions of CSMGem hydrate model[2] in the presence of water, Feed gas composition (0.399 mole fraction CO_2 + 0.601 mole fraction N_2).

Table 5.6: Experimental semi-clathrate hydrate dissociation conditions measured in this study for the carbon dioxide + methane + TBAB aqueous solution or water system.

System	TBAB mass fraction	T / K	P / MPa
CO_2 (0.4029 mole fraction) + CH_4 (0.5971 mole fraction)	0.05	283.3	1.59
		284.1	2.36
		285.0	2.95
		286.8	3.88
		287.8	4.86
CO_2 (0.4029 mole fraction) + CH_4 (0.5971 mole fraction)	0.3	286.7	1.59
		288.6	2.43
		289.5	3.30
		290.2	4.09
		291.0	5.02
		291.6	5.92

In the final analysis, it is of importance to mention that the effects of addition of the TBAB to the CO_2 + N_2 and CO_2 + H_2 systems seem to be more sensible with respect to those observed for CO_2 + CH_4 system. In other words, TBAB leads to larger shifts in the phase boundaries of the two former systems than in the latter one. This point would be of great interest for the industry regarding the decision making of the future projects/processes modifications.

It should also be noted that at the time of preparation of this manuscript, there were no similar experimental data to show in the figures for comparison purposes.
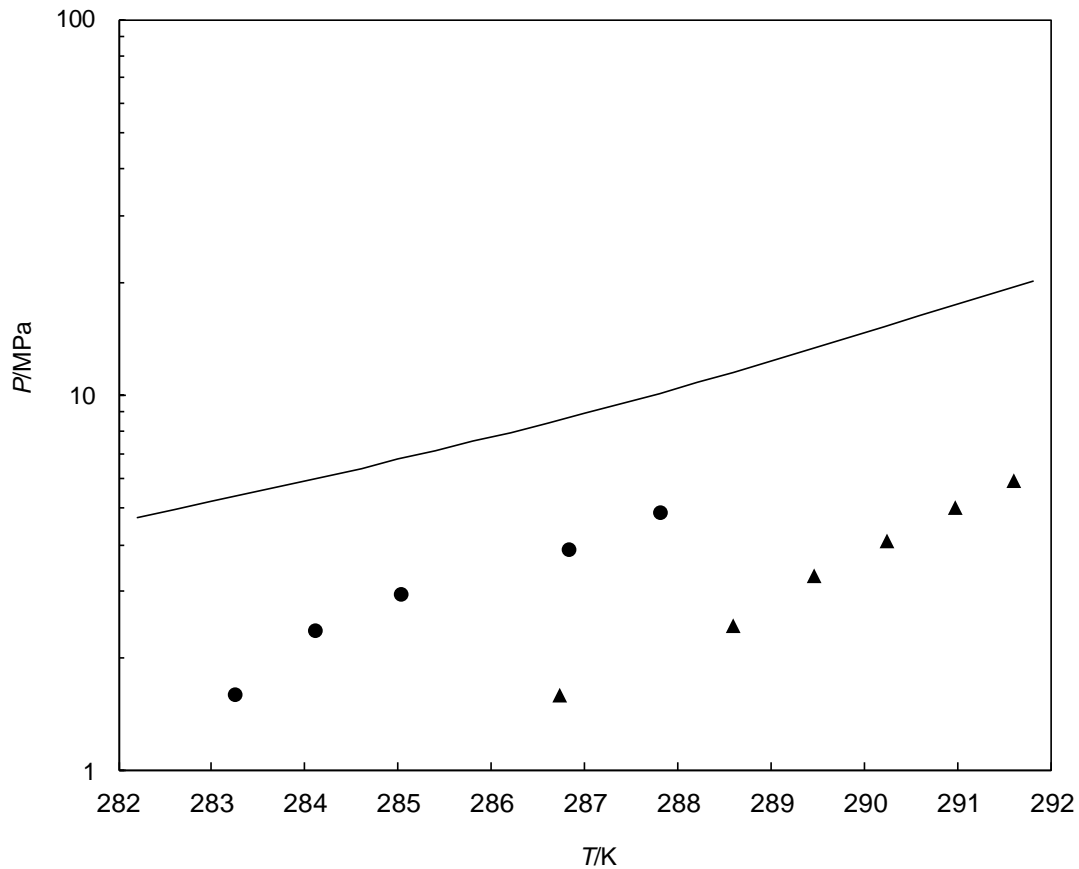
Figure 5.8: Phase equilibrium of clathrate/semi-clathrate hydrates for the carbon dioxide (0.4029 mole fraction) + methane (0.5971 mole fraction) + water or TBAB aqueous solution systems. ●, This work in the presence of TBAB 0.05 mass fraction aqueous solution; ▲, This work in the presence of TBAB 0.30 mass fraction aqueous solution; Curve, Predictions of CSMGem hydrate model[2] in the presence of water, Feed gas composition (0.4029 mole fraction CO_2 + 0.5971 mole fraction CH_4).

Table 5.7: Experimental clathrate/semi-clathrate hydrate dissociation conditions measured in this study for the carbon dioxide + hydrogen + TBAB aqueous solution or water system.

System	TBAB mass fraction	T / K	P / MPa
CO_2 (0.1481 mole fraction) + H_2 (0.8519 mole fraction)	0.05	282.9	7.89
		283.8	10.52
		285.6	15.91
CO_2 (0.1481 mole fraction) + H_2 (0.8519 mole fraction)	0.30	286.0	4.70
		287.7	8.72
		288.8	12.01
		289.7	15.85
CO_2 (0.3952 mole fraction) + H_2 (0.6048 mole fraction)	0	277.2	8.55
		277.5	9.05
		278.4	10.5
CO_2 (0.3952 mole fraction) + H_2 (0.6048 mole fraction)	0.05	280.7	2.31
		286.1	6.69
		286.6	9.16
		288.6	12.17
CO_2 (0.3952 mole fraction) + H_2 (0.6048 mole fraction)	0.30	288.9	4.07
		290.3	7.01
		292.1	10.87
		292.8	12.19
CO_2 (0.7501 mole fraction) + H_2 (0.2499 mole fraction)	0	278.4	3.71
		275.6	2.56
		275.7	2.59
		276.1	2.60
CO_2 (0.7501 mole fraction) + H_2 (0.2499 mole fraction)	0.05	281.4	1.32
		283.2	1.99
		285.8	3.45
		286.0	3.67
CO_2 (0.7501 mole fraction) + H_2 (0.2499 mole fraction)	0.30	289.1	1.98
		289.8	2.59
		290.0	3.45
		289.2	2.27
		290.0	3.16
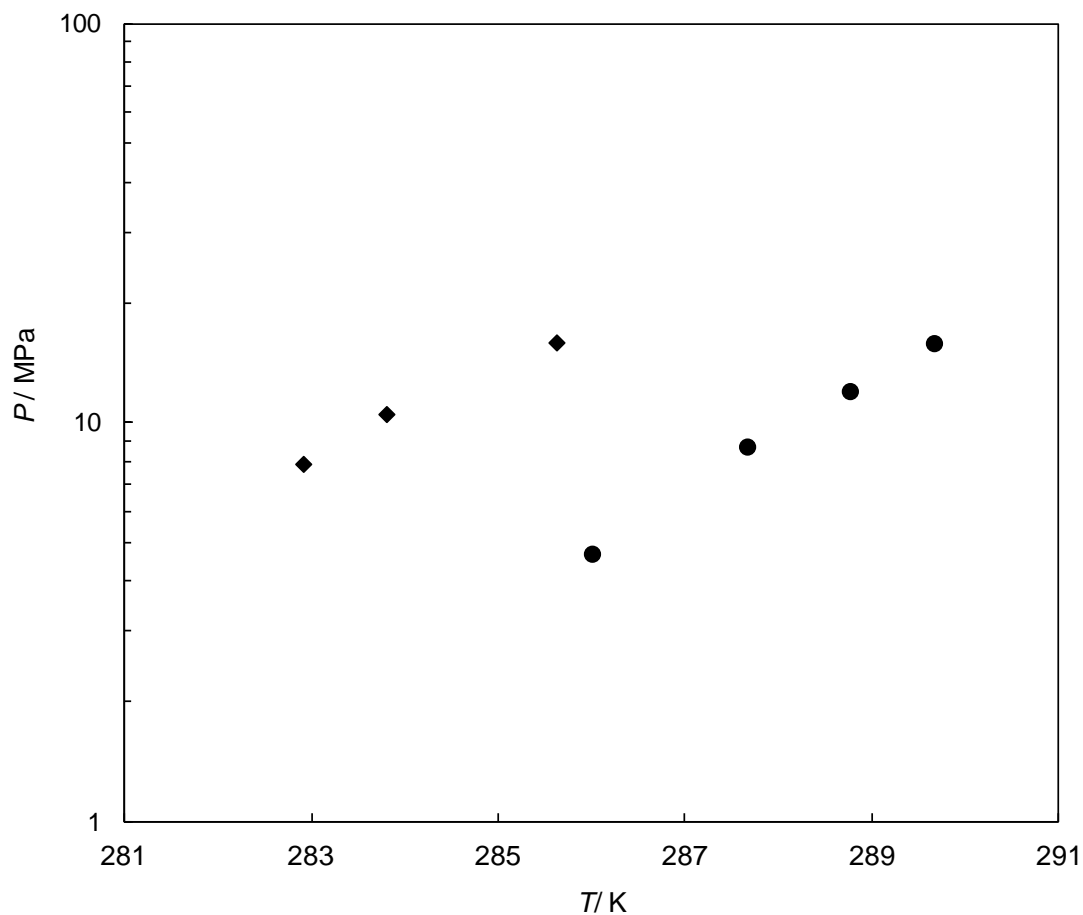
Figure 5.9: Dissociation conditions (this work) of semi-clathrate hydrates for the CO_2 (0.1481 mole fraction) + H_2 (0.8519 mole fraction) + TBAB aqueous solution system. ♦, 0.05 mass fraction TBAB aqueous solution; ●, 0.30 mass fraction TBAB aqueous solution. Hydrate dissociation data of the corresponding mixture in the presence of pure water have not been measured in the present study due to very high formation pressure that would be required.
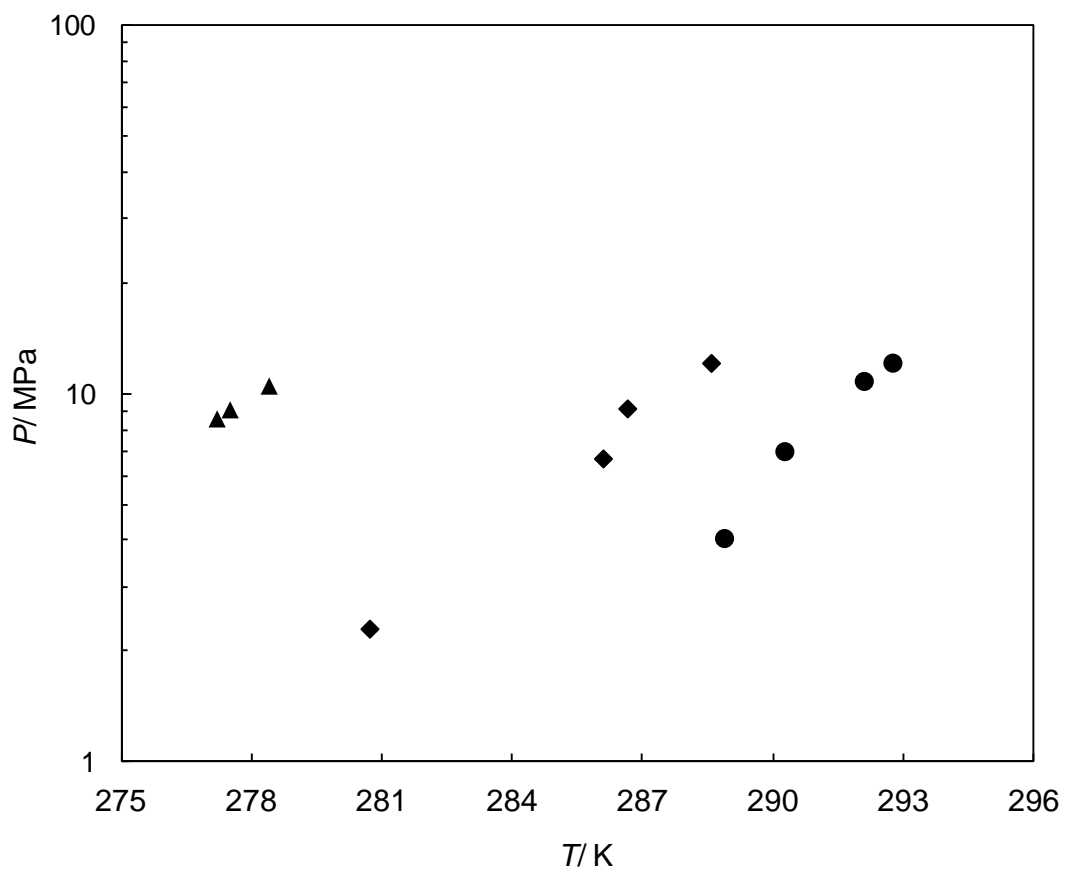
Figure 5.10: Dissociation conditions (this work) of clathrate/semi-clathrate hydrates for the CO$_2$ (0.3952 mole fraction) + H$_2$ (0.6048 mole fraction) + TBAB aqueous solution system. ▲, pure water; ♦, 0.05 mass fraction TBAB aqueous solution; ●, 0.30 mass fraction TBAB aqueous solution.
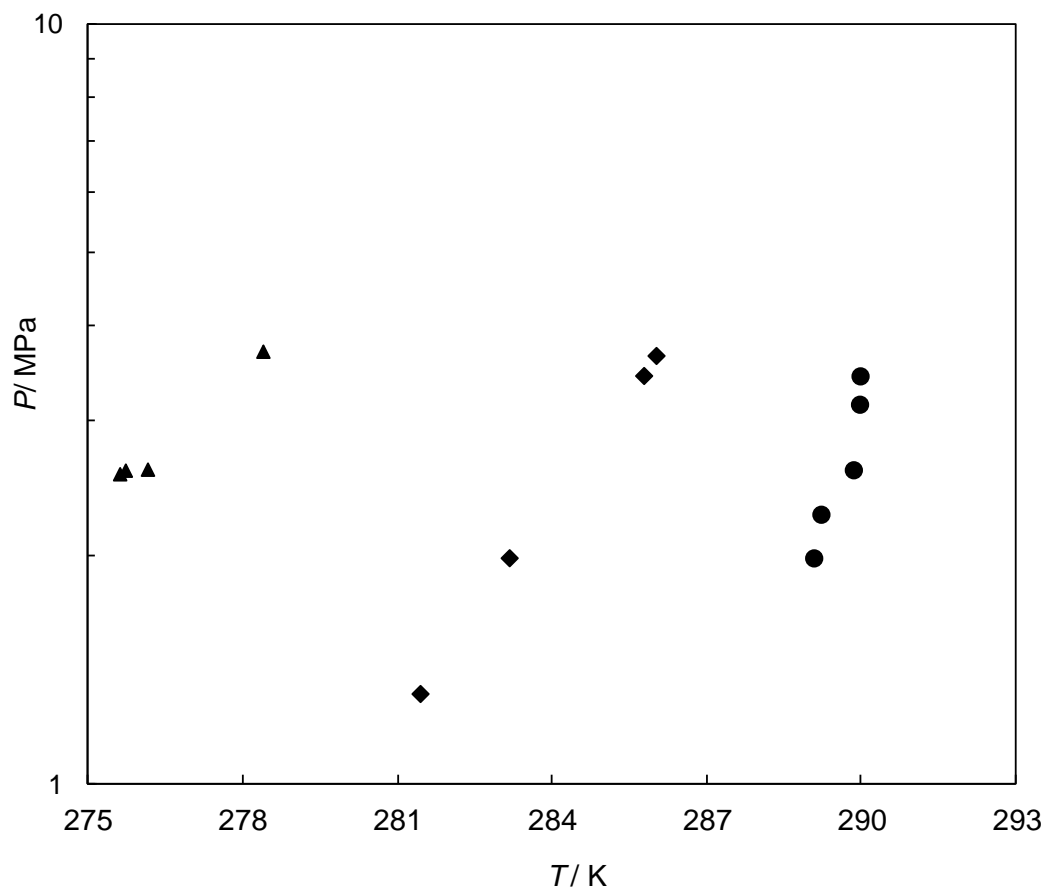
Figure 5.11: Dissociation conditions (this work) of clathrate/semi-clathrate hydrates for the CO$_2$ (0.7501 mole fraction) + H$_2$ (0.2499 mole fraction) + TBAB aqueous solution system. ▲, − pure water; ♦, 0.05 mass fraction TBAB aqueous solution; ●, 0.30 mass fraction TBAB aqueous solution.

6. Determination of the Hydrate Phase Composition

Détermination de la Composition de la Phase Hydrate

Personne ne peut nier l'importance de la détermination de la composition molaire des clathrates hydrates dans le cadre de la conception de procédés de formation d'hydrate de gaz pour la capture et la séquestration du CO_2. Connaissant la composition de la phase hydrate, tout ingénieur est capable d'évaluer la quantité de CO_2 piégée dans les cavités de l'hydrate. En d'autres termes, des informations fiables de compositions molaires dans un large domaine de températures et pressions conduisent finalement à la sélection des conditions opérationnelles optimales: T et p appropriées pour atteindre la purification souhaitée des gaz ainsi traités. À cet égard, une démarche de calcul par bilans de masses a été appliquée ici afin de déterminer la composition molaire de la phase hydrate pour les systèmes: le $CO_2 + N_2$ et $CO_2 + CH_4$ en présence d'eau.

No one can ever deny the importance of determination of the molar composition of the clathrate hydrates in design of the gas hydrate formation processes with the aim of CO_2 capture and sequestration. Having calculated the composition of the hydrate phase, an engineer is able to evaluate the amount of the CO_2 trapped in the hydrate cavities. In other words, reliable molar composition information eventually leads to selection of the optimal operational conditions such as appropriate pressures and temperatures to reach a desired purification of the outlet gas streams from such processes. In this regard, a mass balance approach has been herein applied to determine the molar composition of the hydrate phase for the $CO_2 + N_2$ and $CO_2 + CH_4$ systems in the presence of water.

6.1. Experimental information

During previous measurements in our laboratory[59,426] pursuing isochoric pressure search method[58,59,199,312,425-429] accompanied by the gas phase sampling using the ROLSI[TM] and gas chromatography, the following quantities had been measured for the two aforementioned systems:

1. Total volume of the equilibrium cell (V),

2. Total quantity (moles) of carbon dioxide, methane/nitrogen, and water (n_1^t, n_2^t, n_3^t, respectively),

3. Mole fractions of gas phase (y_1 and y_2 where subscripts 1 and 2 refer to CO_2 and CH_4/N_2, respectively, and

4. The equilibrium temperature (T) and pressure (P).

6.2. Mass balance equations

The compositions of the hydrate and aqueous phases are determined using a material balance approach reported by Ohgaki et al.[217] in combination with the experimental data and the volumetric properties evaluated from a thermodynamic model (using an appropriate equation of state). Considering that all types of molecules have the same gaseous molar volume (v_i^G which is replaced by v_m^G), the following volume balance equation can be written:[59,217,426]

$$V = \sum n_i^G v_m^G + \sum n_i^L v_i^L + n^H v^H \qquad (6.1)$$

where the subscript m denotes the gas mixture and the superscripts H, L, and G represent the hydrate, liquid, and gas phases, respectively, as designated in previous chapters. The volumetric properties for the gas mixture (v_m^G), liquid (v_i^L) and the molar volume of ideal hydrate (v_i^H) have been calculated using the reliable CSMGem[2] thermodynamic model (refer to reference[2] and section 3.4 of this thesis to see more details about this model).

In addition, Eqs. 6.2 to 6.4 are derived according to the material balances for the three present components in the system as follows:[59,217,426]

$$n_1^t = n_1^G + n_1^L + z\,n^H \tag{6.2}$$
$$n_2^t = n_2^G + n_2^L + (1-z)\,n^H \tag{6.3}$$
$$n_3^t = n_3^L + q\,n^H \tag{6.4}$$

where z is water-free mole fraction in hydrate phase and q stands for hydration number. The total amount of each component once measured, can be partitioned into gas, liquid (aqueous phase), and hydrate (z) phases for CO_2 and CH_4/N_2 (n_1^t, n_2^t, respectively), and liquid and hydrate phases for water (n_3^t).

The expressions for mole fractions of CO_2 in the gas phase (y_1) and CO_2 (x_1) and CH_4/N_2 (x_2) in the liquid phase are given by the following equations:

$$y_1 = n_1^G / \sum n_i^G \tag{6.5}$$
$$x_1 = n_1^L / \sum n_i^L \tag{6.6}$$
$$x_2 = n_2^L / \sum n_i^L \tag{6.7}$$

The values of x_1 and x_2 have been estimated applying the CSMGem[2] thermodynamic model, as first guesses. Eqs. (6.1) to (6.7) have been solved simultaneously using the numerical approach described in the next section.

6.3. Mathematical approach

6.3.1. Newton's method

For obtaining the values of the seven unknown variables including n_1^G, n_2^G, n_1^L, n_2^L, n_3^L, n^H, and z, the Newton's method[431] has been used. Among the numerical methods for solving

non-linear equations (such as interval halving, fixed point iteration *etc.*), the Newton's numerical method[431] can be reliably extended to solve systems of non-linear equations, which are generally required in scientific and engineering problems.[432]

Consider the system of N non-linear equations with N unknowns as follows:

$$f_1(x_{i-1}, x_i, ...) = 0 \qquad i = 1,...N \tag{6.9}$$

$$f_2(x_{i-1}, x_i, ...) = 0 \qquad i = 1,...N \tag{6.10}$$

.

.

.

$$f_N(x_{i-1}, x_i, ...) = 0 \qquad i = 1,...N \tag{6.11}$$

where f stands for the function and x stands for the unknowns. Solving for values of the unknowns is followed up by presenting the preceding functions as Taylor series and appropriate mathematical derivations following by some rearrangements as:

$$\begin{bmatrix} x_{0(a+1)} \\ x_{1(a+1)} \\ . \\ . \\ . \\ x_{N(a+1)} \end{bmatrix} = \begin{bmatrix} x_{0(a)} \\ x_{1(a)} \\ . \\ . \\ . \\ x_{N(a)} \end{bmatrix} - \begin{bmatrix} f_1(x_{(i-1)a}, x_{(i)a}, ...) \\ f_2(x_{(i-1)a}, x_{(i)a}, ...) \\ . \\ . \\ . \\ f_N(x_{(i-1)a}, x_{(i)a}, ...) \end{bmatrix} \begin{bmatrix} \dfrac{\partial f_1}{\partial x_{i-1}} & \dfrac{\partial f_1}{\partial x_i} & ... \\ \dfrac{\partial f_2}{\partial x_{i-1}} & \dfrac{\partial f_2}{\partial x_i} & ... \\ . & . & \\ . & . & \\ . & . & \\ \dfrac{\partial f_N}{\partial x_{i-1}} & \dfrac{\partial f_N}{\partial x_i} & ... \end{bmatrix}_{(x_{(i-1)a}, x_{(i)a}, ...)}^{-1} \qquad i = 1,...N \tag{6.12}$$

where a denotes the estimated value of an unknown variable. Finally, the following expression is used applying the Jacobian matrix:[432]

$$x_{N(a+1)} = x_{Na} - J_a^{-1} f(x_{Na}) \tag{6.13}$$

where J refers to the Jacobian Matrix and is calculated by the expression below:[432]

$$J_a(m,n) = \left[\frac{\partial fm}{\partial x_n} \right]_{x_{Na}} \tag{6.14}$$

In the preceding equation, *m* and *n* are the numbers of particular functions and related variables, respectively. Equations (6.13) and (6.14) are repetitively used until the following convergence criteria are satisfied:

$$\left\| \begin{bmatrix} x_{0(a+1)} - x_{0(a)} \\ x_{1(a+1)} - x_{1(a)} \\ . \\ . \\ . \\ x_{N(a+1)} - x_{N(a)} \end{bmatrix} \right\| \leq \begin{bmatrix} \varepsilon_1 \\ \varepsilon_2 \\ . \\ . \\ . \\ \varepsilon_N \end{bmatrix} \tag{6.15}$$

where ε stands for a specified tolerance during the calculation steps of the Newton's numerical method, which is normally defined by the user (it can be a small value depending of the order of magnitudes of the solution values).

6.3.2. Constraint handling

According to the mass conservation law, some constraints should be taken into account for solving the system of equations of the interest as follows:

$$n_1^G \leq n_1^t \tag{6.16}$$
$$n_2^G \leq n_2^t \tag{6.17}$$
$$n_1^L \leq n_1^t \tag{6.18}$$
$$n_2^L \leq n_2^t \tag{6.19}$$
$$n_3^L \leq n_3^t \tag{6.20}$$

Due to the fact that the mentioned Newton's method is not, normally, able to handle the following constraints, we have considered an objective function that is supposed to be minimized by an appropriate optimization method as follows:

$$FF(x_{i-1}, x_i, ...) = \sum_i^N f_i(x_{i-1}, x_i, ...) \tag{6.21}$$

where *FF* stands for the primary objective function before introducing the constraints. It should be noted that the other constraint ($0 \leq z \leq 1$) is satisfied intrinsically through solving the equations. In this work, the DE[406,407] optimization algorithm has been used for minimization of the objective function (Eq. 6.21).

6.3.3 Problem formulation

The constraints of the problem are considered to be inequality constraints and written as follows:[426]

$$n_1^t - n_1^G \geq 0 \tag{6.22}$$

$$n_2^t - n_2^G \geq 0 \tag{6.23}$$

$$n_1^t - n_1^L \geq 0 \tag{6.24}$$

$$n_2^t - n_2^L \geq 0 \tag{6.25}$$

$$n_3^t - n_3^L \geq 0 \tag{6.26}$$

Taking the advantage of penalty functions (similar to those described in section 4.2.), the final formulation of the objective function is given by:[426]

$$OF = FF(x_{i-1}, x_i, \ldots) + (1) \sum_{l=1}^{5} \left\langle g_l^2 \right\rangle \tag{6.27}$$

where,

$$g_1 = \max\{ 0, n_1^t - n_1^G \} \tag{6.28}$$

$$g_2 = \max\{ 0, n_2^t - n_2^G \} \tag{6.29}$$

$$g_3 = \max\{ 0, n_1^t - n_1^L \} \tag{6.30}$$

$$g_4 = \max\{ 0, n_2^t - n_2^L \} \tag{6.31}$$

$$g_5 = \max\{ 0, n_3^t - n_3^L \} \tag{6.32}$$

Therefore, Newton's numerical method[431] has been coupled with the DE[406,407] strategy to obtain the values of the unknown variables. The calculation steps are continued until the convergence criterion of the Newton's method and all of the constraints of the objective function are satisfied.

6.4. Results of solving the mass balance equations

The previously measured hydrate equilibrium conditions[59,426] (temperature, pressure, molar composition of vapor phase) for the $CO_2 + CH_4/N_2 + H_2O$ systems at various compositions of CO_2 in the gas feed have been treated in this work. The described mathematical approach has been pursued to determine the compositions of hydrate (and liquid) phases. Figures 6.1 to 6.10 depict the pressure-composition diagrams for the $CO_2 + CH_4/N_2 +$ water systems containing the CO_2 molar compositions in the vapor and hydrate phases at selected isothermal conditions. It is observed that the mole fractions of CO_2 in the gas and hydrate phases generally decrease as pressure increases. This suggests that considerable enrichment of CO_2 in the hydrate phase takes place in the studied systems. It is also interpreted that the composition of CO_2 in the gas phase increases as temperature increases, which translates in less amount of CO_2 trapped in the hydrate phase at high temperatures.[59,426] It is worth it to mention that sketching such figures (Figures 6.1 to 6.10) is essential in designing the adsorption/desorption units (multi-stage operations) in CO_2 capture processes.

Compositional analysis of the hydrate and liquid phases for the ternary $CO_2 + CH_4/N_2 + H_2O$ systems are also illustrated in Table 6.1 and Table 6.2. As can be seen in these tables, the predictions of the CSMGem model[2] for the mole fraction of CO_2 in the gas phase generally agree with the applied experimental data.[59,426] However, the thermodynamic model[2] shows higher deviations when predicting the molar compositions of CO_2 in the hydrate phase with respect to the results of compositional analysis using the mass balance approach. This suggests that the parameters of the thermodynamic model may require re-adjustment using fully compositional analysis + hydrate dissociation conditions experimental data since the optimal values of such model parameters have generally been obtained using mainly experimental hydrate dissociation data (and perhaps not compositional three-phases data). As for the unspecified points shown in Table 6.1 and Table 6.2 related to the predictions of the CSMGem model,[2] it should be noted that the model is not able to predict the three-phase equilibrium (L_w-H-G) properties at the studied conditions. It should be noted that the uncertainty in the results of the molar compositions of the hydrate phase is calculated to be around 15 % applying the error propagation method.
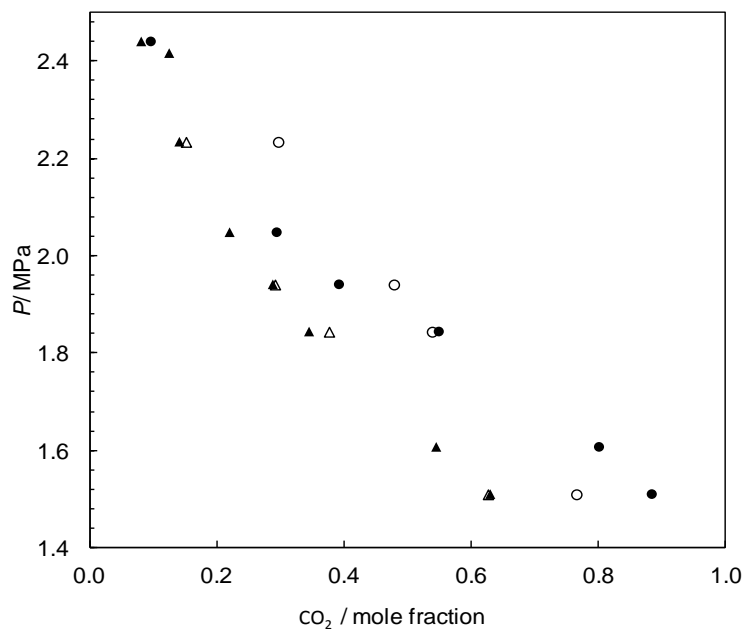
Figure 6.1: Pressure-composition diagram for the methane + carbon dioxide + water system under L_w-H-G equilibrium at 273.6 K. Experimental: yCO_2 (▲);[426] This work: zCO_2 (●). CSMGem model[2] predictions: yCO_2 (△); zCO_2 (○).
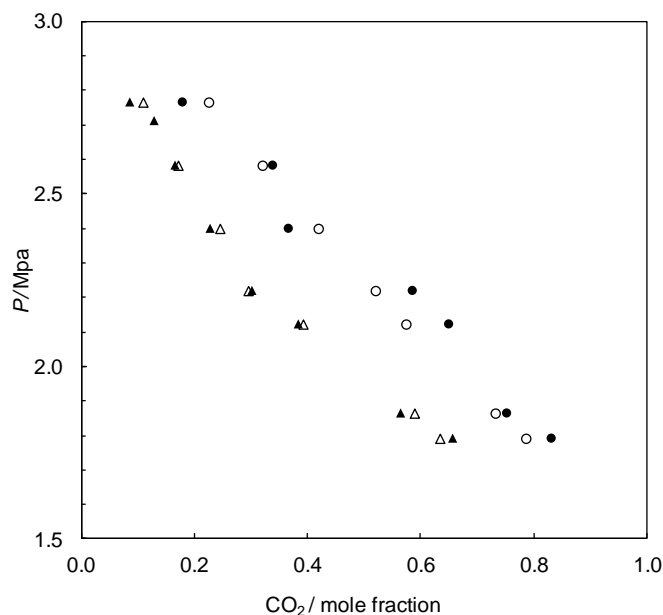
Figure 6.2: Pressure-composition diagram for the methane + carbon dioxide + water system under L_w-H-G equilibrium at 275.2 K. Experimental: yCO_2 (▲);[426] This work: zCO_2 (●). CSMGem model[2] predictions: yCO_2 (△); zCO_2 (○).
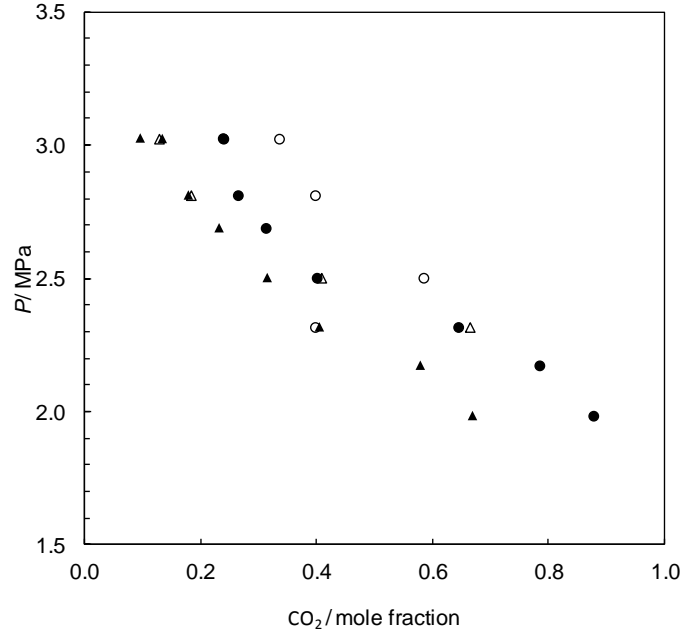
Figure 6.3: Pressure-composition diagram for the methane + carbon dioxide + water system under L_w-H-G equilibrium at 276.1 K. Experimental: yCO_2 (▲);[426] This work: zCO_2 (●). CSMGem model[2] predictions: yCO_2 (Δ); zCO_2 (○).
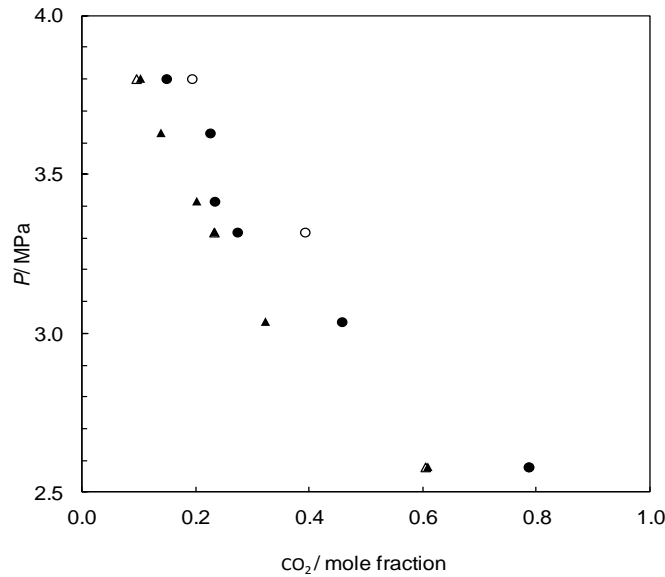
Figure 6.4: Pressure-composition diagram for the methane + carbon dioxide + water system under L_w-H-G equilibrium at 278.1 K. Experimental: yCO_2 (▲);[426] This work: zCO_2 (●). CSMGem model[2] predictions: yCO_2 (Δ); zCO_2 (○).
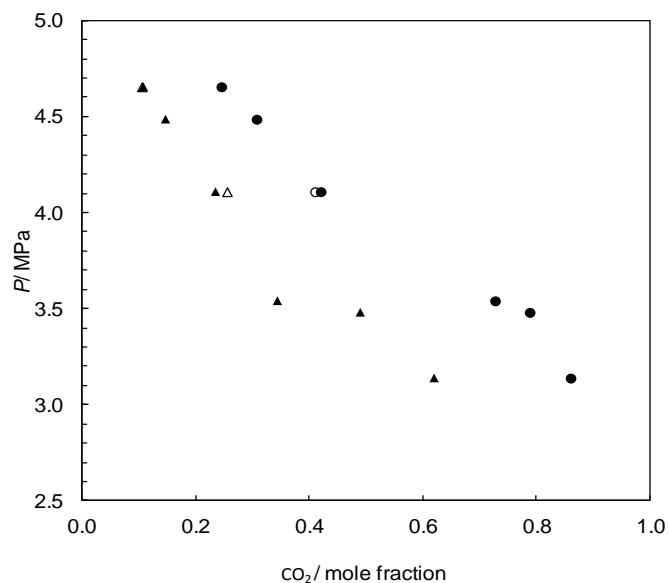
Figure 6.5: Pressure-composition diagram for the methane + carbon dioxide + water system under L_w-H-G equilibrium at 280.2 K. Experimental: yCO_2 (▲);[426] This work: zCO_2 (●). CSMGem model[2] predictions: yCO_2 (△); zCO_2 (○).
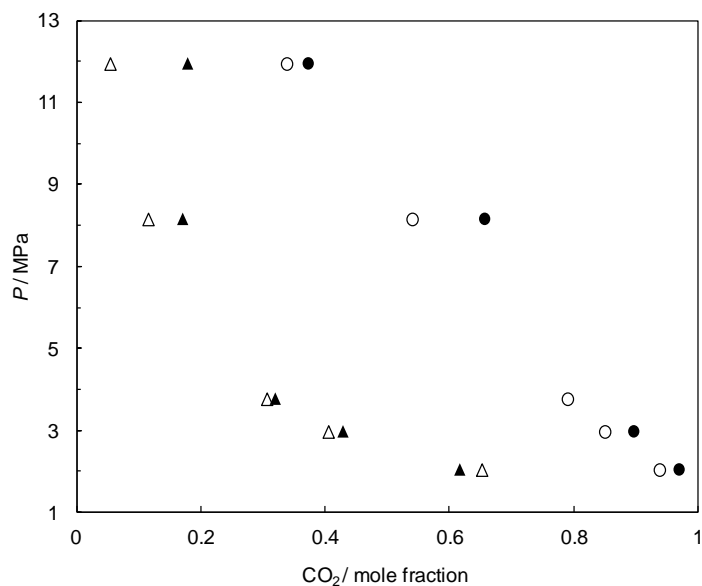
Figure 6.6: Pressure-composition diagram for the nitrogen + carbon dioxide + water system under L_w-H-G equilibrium at 273.6 K. Experimental: yCO_2 (▲);[59] This work: zCO_2 (●). CSMGem model[2] predictions: yCO_2 (△); zCO_2 (○).
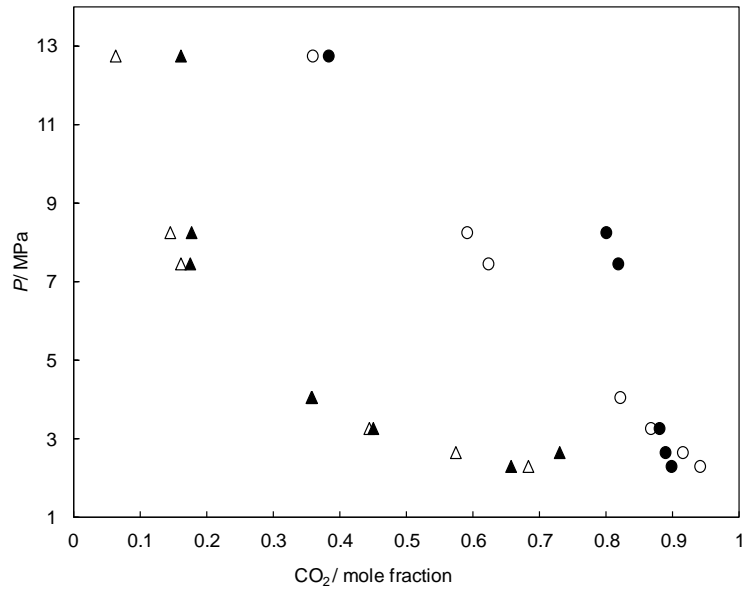
Figure 6.7: Pressure-composition diagram for the nitrogen + carbon dioxide + water system under L_w-H-G equilibrium at 275.2 K. Experimental: yCO_2 (▲);[59] This work: zCO_2 (●). CSMGem model[2] predictions: yCO_2 (Δ); zCO_2 (○).
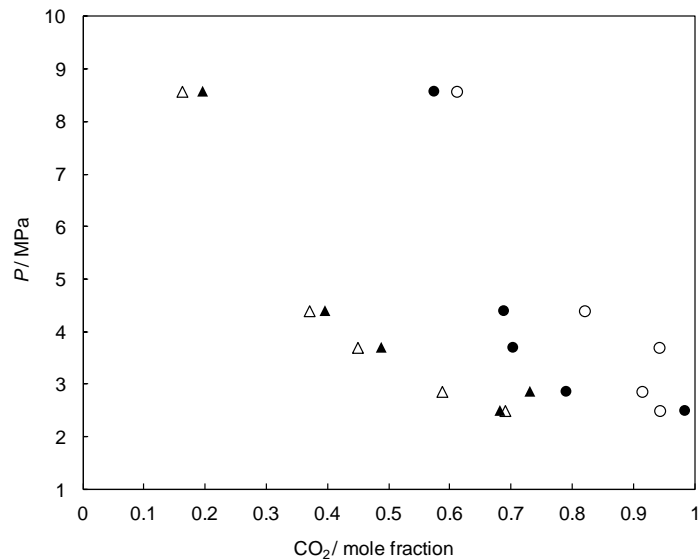
Figure 6.8: Pressure-composition diagram for the nitrogen + carbon dioxide + water system under L_w-H-G equilibrium at 276.1 K. Experimental: yCO_2 (▲);[59] This work: zCO_2 (●). CSMGem model[2] predictions: yCO_2 (Δ); zCO_2 (○).
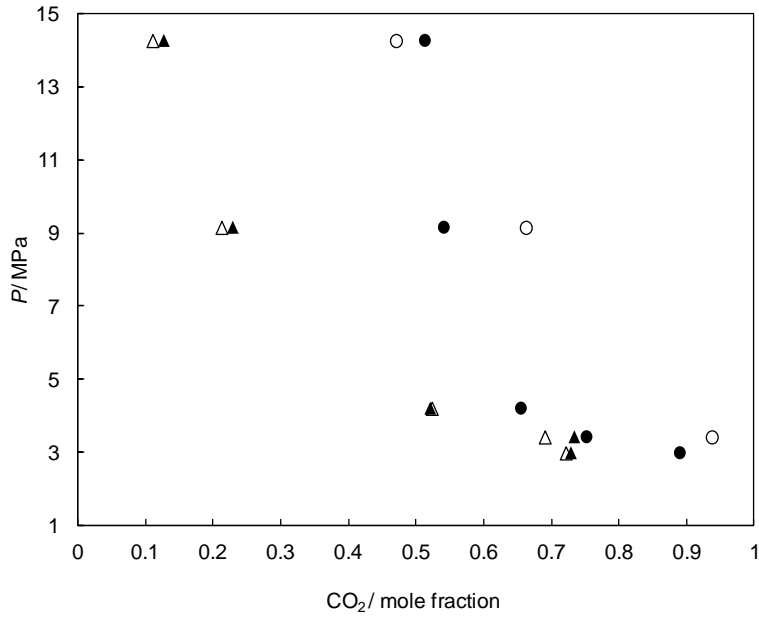
Figure 6.9: Pressure-composition diagram for the nitrogen + carbon dioxide + water system under L_w-H-G equilibrium at 278.1 K. Experimental: yCO_2 (▲);[59] This work: zCO_2 (●). CSMGem model[2] predictions: yCO_2 (Δ); zCO_2 (○).
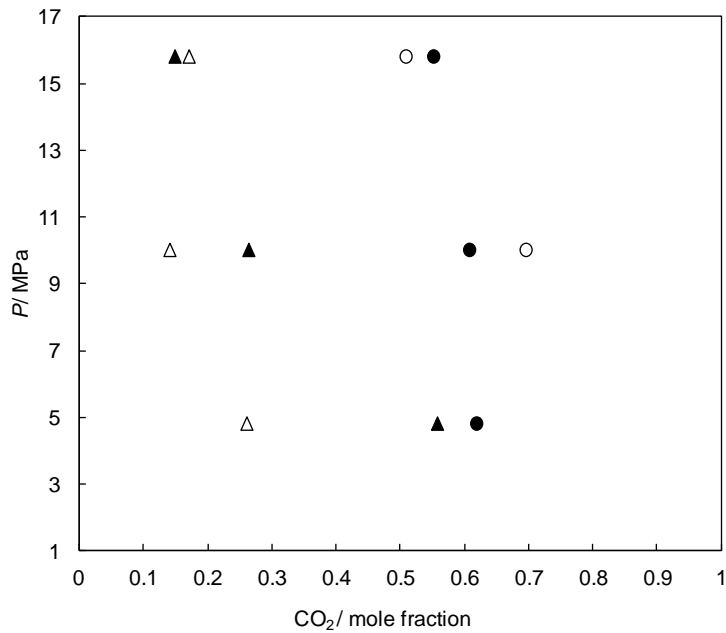
Figure 6.10: Pressure-composition diagram for the nitrogen + carbon dioxide + water system under L_w-H-G equilibrium at 279.7 K. Experimental: yCO_2 (▲);[59] This work: zCO_2 (●). CSMGem model[2] predictions: yCO_2 (Δ); zCO_2 (○).

Table 6.1: Three-phase (L_w-H-G) equilibrium data/mass balance approach results for gas mixtures of CO_2 + CH_4 in the presence of water at various temperatures and pressures.

CO₂ / mole	CH₄ / mole	H₂O / mole	T / K	p / MPa	y_CO2/ mole fraction	z_CO2/ mole fraction (water free base)	CO₂/ mole fraction	CH₄/ mole fraction	H₂0 / mole fraction	y_CO2/ mole fraction	z_CO2/ mole fraction (water free base)	x_CO2/ mole fraction	x_CH4/ mole fraction	x_H2O/ mole fraction	y_CO2/ mole fraction	z_CO2/ mole fraction (water free base)	x_CO2/ mole fraction	x_CH4/ mole fraction	x_H2O/ mole fraction
0.048	0.165	1.43	273.6	2.234	0.141	a	a	a	a	0.151	0.296	0.0036	0.0008	0.9956	7.1	-	-	-	-
0.048	0.165	5.236	273.6	2.416	0.125	a	a	a	a	b	b	b	b	b	-	-	-	-	-
0.048	0.165	8.185	273.6	2.440	0.081	0.096	0.0055	0.0006	0.994	b	b	b	b	b	-	-	-	-	-
0.116	0.115	1.65	273.6	1.844	0.345	0.549	0.0099	0.0003	0.9898	0.376	0.538	0.0075	0.0005	0.992	9.0	2.0	24	67	0.2
0.116	0.115	5.355	273.6	1.941	0.288	0.392	0.0062	0.0006	0.9932	0.291	0.478	0.0062	0.0006	0.9932	1.0	22	0.0	0.0	0.0
0.116	0.115	8.48	273.6	2.048	0.220	0.294	0.0095	0.0003	0.9902	b	b	b	b	b	-	51	-	-	-
0.181	0.057	1.696	273.6	1.510	0.63	0.884	0.0127	0.0001	0.9872	0.626	0.765	0.0107	0.0002	0.9891	0.6	13	16	100	0.2
0.181	0.057	5.182	273.6	1.607	0.545	0.801	0.0128	0.0001	0.9871	b	b	b	b	b	-	-	-	-	-
0.048	0.165	1.43	275.2	2.583	0.166	0.338	0.0071	0.0008	0.9921	0.171	0.32	0.0044	0.0008	0.9948	3.0	5.3	38	0.0	0.3
0.048	0.165	5.236	275.2	2.712	0.129	a	a	a	a	b	b	b	b	b	-	-	-	-	-
0.048	0.165	8.185	275.2	2.766	0.086	0.179	0.003	0.0009	0.9961	0.109	0.225	0.003	0.0009	0.9961	27	26	0.0	0.0	0.0
0.116	0.115	1.65	275.2	2.123	0.384	0.65	0.0108	0.0003	0.9889	0.392	0.574	0.0085	0.0005	0.991	2.1	12	21	67	0.2
0.116	0.115	5.355	275.2	2.220	0.302	0.586	0.0075	0.0006	0.9919	0.295	0.52	0.0075	0.0006	0.9919	2.3	11	0.0	0.0	0.0
0.116	0.115	8.48	275.2	2.400	0.228	0.366	0.0108	0.0003	0.9889	0.245	0.419	0.0059	0.0007	0.9934	7.5	14	45	133	0.5
0.181	0.057	1.696	275.2	1.792	0.657	0.831	0.0123	0.0002	0.9875	0.634	0.786	0.0123	0.0002	0.9875	3.5	5.4	0.0	0.0	0.0
0.181	0.057	5.182	275.2	1.865	0.565	0.752	0.0113	0.0003	0.9884	0.589	0.732	0.0113	0.0003	0.9884	4.2	2.7	0.0	0.0	0.0
0.048	0.165	1.43	276.1	2.813	0.179	0.264	0.0062	0.0007	0.9931	0.183	0.397	0.0049	0.0008	0.9943	2.2	50	21	14	0.1
0.048	0.165	5.236	276.1	3.025	0.134	0.239	0.0034	0.0009	0.9957	0.128	0.335	0.0034	0.0009	0.9957	4.5	40	0.0	0.0	0.0
0.048	0.165	8.185	276.1	3.027	0.096	0.238	0.0062	0.0007	0.9931	b	b	b	b	b	-	-	-	-	-
0.116	0.115	1.65	276.1	2.318	0.405	0.644	0.0113	0.0004	0.9883	0.664	0.397	0.0092	0.0005	0.9903	64	38	19	25	0.2

0.116	0.115	5.355	276.1	2.503	0.315	0.4	0.0113	0.0004	0.9883	0.408	0.584	0.0074	0.0006	0.992	29	46	34	50	0.4
0.116	0.115	8.48	276.1	2.69	0.232	0.312	0.0113	0.0004	0.9883	*b*	*b*	*b*	*b*	*b*	-	-	-	-	-
0.181	0.057	1.696	276.1	1.985	0.669	0.877	0.0158	0.0002	0.984	*b*	*b*	*b*	*b*	*b*	-	-	-	-	-
0.181	0.057	5.182	276.1	2.174	0.579	0.784	0.0114	0.0004	0.9882	*b*	*b*	*b*	*b*	*b*	-	-	-	-	-
0.048	0.165	1.43	278.1	3.416	0.202	0.233	0.0088	0.0021	0.989	*b*	*b*	*b*	*b*	*b*	-	-	-	-	-
0.048	0.165	5.236	278.1	3.631	0.139	0.225	0.0074	0.0009	0.9917	*b*	*b*	*b*	*b*	*b*	-	-	-	-	-
0.048	0.165	8.185	278.1	3.802	0.103	0.148	0.0068	0.0008	0.9924	0.095	0.193	0.003	0.0011	0.9959	7.8	30	56	37	0.4
0.116	0.115	5.355	278.1	3.037	0.323	0.457	0.0124	0.0004	0.9871	*b*	*b*	*b*	*b*	*b*	-	-	-	-	-
0.116	0.115	8.48	278.1	3.319	0.233	0.273	0.0126	0.0004	0.987	0.232	0.392	0.0066	0.0009	0.9926	0.4	44	48	125	0.6
0.181	0.057	1.696	278.1	2.450	0.694	*a*	*a*	*a*	*a*	*b*	*b*	*b*	*b*	*b*	-	-	-	-	-
0.181	0.057	5.182	278.1	2.580	0.609	0.786	0.0137	0.0004	0.9859	0.604	0.786	0.0137	0.0004	0.9859	0.8	0.0	0.0	0.0	0.0
0.048	0.165	1.43	279.2	3.565	0.202	0.266	0.0071	0.0009	0.992	*b*	*b*	*b*	*b*	*b*	-	-	-	-	-
0.048	0.165	5.236	280.2	4.486	0.147	0.307	0.0023	0.0079	0.9898	*b*	*b*	*b*	*b*	*b*	-	-	-	-	-
0.048	0.165	8.185	280.2	4.655	0.108	0.245	0.0013	0.007	0.9917	*b*	0.41	*b*	*b*	*b*	-	-	-	-	-
0.116	0.115	5.355	280.2	3.541	0.344	0.727	0.0146	0.0005	0.9849	*b*	*b*	*b*	*b*	*b*	-	-	-	-	-
0.116	0.115	8.48	280.2	4.109	0.235	0.339	0.0114	0.0005	0.9881	0.255	0.409	0.0078	0.0009	0.9912	8.5	21	32	80	0.3
0.181	0.057	5.182	280.2	3.139	0.62	0.86	0.0167	0.0004	0.983	*b*	*b*	*b*	*b*	*b*	-	-	-	-	-
0.181	0.057	8.395	280.2	3.481	0.49	0.788	0.015	0.0002	0.9848	*b*	*b*	*b*	*b*	*b*	-	-	-	-	-
0.048	0.165	8.185	282.2	5.767	0.114	0.276	0.0065	0.0016	0.9919	*b*	*b*	*b*	*b*	*b*	-	-	-	-	-
0.048	0.165	8.185	284.2	7.190	0.115	0.107	0.0067	0.0012	0.9921	*b*	*b*	*b*	*b*	*b*	-	-	-	-	-
AARD %															10	22	20	41	0.2

[a] Some/all of constraints are not satisfied.

[b] No three phase flash convergence using CSMGem model.[2]

[c] $ARD\% = 100 \times \dfrac{\left| (y/x/z)_i^{exp.} - (y/x/z)_i^{pred.} \right|}{(y/x/z)_i^{exp.}}$, where superscript *exp.* stands for the values resulting from the experimental measurements for the gas phase or compositional analysis using mass balance approach, and superscript *pred.* refers to the predicted values applying the CSMGem model.[2]

Table 6.2: Three-phase (L_w-H-G) equilibrium data/mass balance approach results for gas mixtures of $CO_2 + N_2$ in the presence of water at various temperatures and pressures.

| Feed | | | | | Experimental data for the gas phase/Compositional analysis of the liquid and hydrate phases | | | | | CSMGem model[2] predictions | | | | | | | | | | absolute relative deviation (ARD %)[a] | | | | |
| | | | | | gas phase | hydrate phase | aqueous phase | | | gas phase | hydrate phase | | | | | | aqueous phase | | | gas phase | hydrate phase | aqueous phase | | |
CO_2 / mole	N_2 / mole	H_2O / mole	T / K	p / MPa	yCO_2 / mole fraction (water content free base)	zCO_2 / mole fraction (water free base)	CO_2 / mole fraction	N_2 / mole fraction	H_2O / mole fraction	yCO_2 / mole fraction (water content free base)	zCO_2 / mole fraction (water free base)	S^*	$\theta^{**}CO_{2-S}$	$\theta^{***}CO_{2-L}$	θN_{2-S}	θN_{2-L}	CO_2 / mole fraction	N_2 / mole fraction	H_2O / mole fraction	yCO_2 / mole fraction (water content free base)	zCO_2 / mole fraction (water free base)	CO_2 / mole fraction	N_2 / mole fraction	H_2O / mole fraction
0.2086	0.0695	1.543	273.6	2.032	0.617	0.97	0.0136	0.0001	0.9862	0.618	0.938	I	0.4416	0.9277	0.1407	0.033	0.0140	0.0001	0.9857	0.2	3.3	2.9	0.0	0.1
0.1947	0.5842	1.5516	273.6	8.149	0.171	0.657	0.0123	0.0009	0.9868	0.109	0.537	I	0.1312	0.6096	0.6557	0.3451	0.0069	0.0012	0.9919	36	18	44	33	0.5
0.1947	0.5842	6.6615	273.6	11.943	0.179	0.373	0.0037	0.0018	0.9945	0.045	0.261	I	0.0396	0.307	0.7986	0.6417	0.0036	0.0018	0.9946	75	30	3.2	0.8	0.0
0.2086	0.0695	7.649	273.6	2.962	0.429	0.897	0.0123	0.0003	0.9874	0.405	0.855	I	0.3625	0.8814	0.2768	0.0775	0.0123	0.0003	0.9874	5.6	4.7	0.0	0.0	0.0
0.1845	0.196	1.553	273.6	3.761	0.32	b	b	b	b	0.306	0.797	I	0.3066	0.8402	0.3685	0.1175	0.0112	0.0005	0.9883	4.4	-	-	-	-
0.2547	0.0898	2.7525	274.6	2.543	0.728	0.739	0.0141	0.0002	0.9857	0.552	0.909	I	0.433	0.9177	0.1844	0.0448	0.0141	0.0002	0.9857	24	23	0.0	0.0	0.0
0.4371	0.1472	2.0555	274.9	5.204	0.717	0.788	0.0277	0.0002	0.972	c	c	c	c	c	c	c	c	c	c	-	-	-	-	-
0.2086	0.0695	1.543	275.2	2.29	0.656	0.897	0.0154	0.0001	0.9845	0.682	0.941	I	0.478	0.9369	0.1244	0.0277	0.0202	0.0001	0.9797	4.0	4.9	31	0.0	0.5
0.2547	0.0898	2.7525	275.2	2.643	0.729	0.888	0.0148	0.0002	0.985	0.574	0.914	I	0.4476	0.922	0.1762	0.0419	0.0148	0.0002	0.9850	21	2.9	0.0	0.0	0.0
0.2086	0.0695	7.649	275.2	3.256	0.449	0.879	0.014	0.0003	0.9857	0.443	0.866	I	0.3994	0.8959	0.2549	0.0671	0.0140	0.0003	0.9860	1.3	1.5	0.0	0.0	0.0
0.1845	0.196	1.553	275.2	4.045	0.357	b	b	b	b	0.356	0.820	I	0.3457	0.8614	0.34	0.1006	0.0130	0.0004	0.9866	0.3	-	-	-	-
0.1845	0.196	6.273	275.2	7.45	0.174	0.817	0.0139	0.0062	0.9799	0.166	0.622	I	0.1889	0.7034	0.5822	0.2556	0.0091	0.0010	0.9899	4.6	24	34	84	1.0
0.1947	0.5842	1.5516	275.2	8.246	0.176	0.799	0.0086	0.0011	0.9903	0.144	0.590	I	0.1641	0.6646	0.6204	0.2939	0.0120	0.0010	0.9871	18	26	39	9.1	0.3
0.1947	0.5842	6.6615	275.2	12.745	0.16	0.382	0.011	0.0014	0.9876	0.066	0.370	I	0.0697	0.4338	0.7685	0.5227	0.0050	0.0020	0.9930	59	3.2	54	43	0.5
0.2547	0.0898	2.7525	275.6	2.714	0.73	0.764	0.0153	0.0002	0.9845	0.590	0.917	I	0.4573	0.9248	0.1708	0.04	0.0153	0.0001	0.9844	19	20	0.1	50	0.0
0.4371	0.1472	2.0555	275.8	5.381	0.719	0.802	0.0359	0.0003	0.9638	c	c	c	c	c	c	c	c	c	c	-	-	-	-	-
0.2086	0.0695	1.543	276.1	2.5	0.682	0.984	0.0164	0.0001	0.9835	0.690	0.943	I	0.4952	0.94	0.1211	0.0264	0.0164	0.0001	0.9835	1.2	4.2	0.0	0.0	0.0
0.2547	0.0898	2.7525	276.1	2.865	0.731	0.79	0.0177	0.0002	0.9821	0.595	0.917	I	0.465	0.926	0.1715	0.0398	0.0158	0.0002	0.9840	19	16	11	0.0	0.2

0.2086	0.0695	7.649	276.1	3.703	0.488	0.703	0.0156	0.0003	0.9841	0.449	0.864	I	0.4027	0.8933	0.2707	0.0715	0.0147	0.0003	0.9850	8.0	23	5.8	0.0	0.1
0.1845	0.196	1.553	276.1	4.401	0.396	0.688	0.015	0.0004	0.9817	0.370	0.823	I	0.3579	0.8653	0.3398	0.0987	0.0137	0.0005	0.9859	6.6	20	8.7	25	0.4
0.1947	0.5842	1.552	276.1	8.58	0.196	0.574	0.0095	0.0011	0.9894	0.162	0.611	I	0.181	0.6872	0.6071	0.2739	0.0095	0.0011	0.9894	17	6.4	0.0	0.0	0.0
0.2086	0.0695	7.6487	276.7	3.703	0.488	0.703	0.0156	0.0003	0.9841	0.489	0.878	I	0.4269	0.9038	0.2469	0.0625	0.0156	0.0003	0.9841	0.2	25	0.0	0.0	0.0
0.2086	0.0695	1.543	277.1	2.706	0.705	0.838	0.0177	0.0001	0.9822	c	c	c	c	c	c	c	c	c	c	c	-	-	-	-	-
0.2547	0.0898	2.7525	277.3	3.13	0.732	0.83	0.0185	0.0002	0.9814	0.639	0.927	I	0.4938	0.9336	0.1564	0.0349	0.0174	0.0002	0.9824	13	12	5.9	0.0	0.1
0.4371	0.1472	2.0555	277.8	6.159	0.747	0.864	0.0336	0.0057	0.9607	c	c	c	c	c	c	c	c	c	c	c	-	-	-	-	-
0.2086	0.0695	1.543	278.1	2.974	0.729	0.89	0.0213	0.0068	0.9719	c	c	c	c	c	c	c	c	c	c	c	-	-	-	-	-
0.2547	0.0898	2.7525	278.1	3.411	0.734	0.752	0.0185	0.0002	0.9814	0.692	0.937	I	0.5075	0.9358	0.1554	0.0342	0.0184	0.0002	0.9814	5.7	25	0.5	0.0	0.0
0.2086	0.0695	7.649	278.1	4.194	0.521	0.655	0.0173	0.0003	0.9824	c	c	c	c	c	c	c	c	c	c	c	-	-	-	-	-
0.1947	0.5842	1.552	278.1	9.146	0.229	0.541	0.0121	0.0011	0.9869	0.212	0.662	I	0.2303	0.743	0.5627	0.2234	0.0118	0.0011	0.9870	7.4	22	2.5	0.0	0.0
0.1947	0.5842	6.6615	278.1	14.26	0.127	0.513	0.008	0.0017	0.9903	0.110	0.474	I	0.1145	0.5529	0.7303	0.412	0.0080	0.0017	0.9904	13	7.6	0.0	0.0	0.0
0.2086	0.0695	7.649	279.7	4.817	0.557	0.698	0.0167	0.0003	0.983	c	c	c	c	c	c	c	c	c	c	c	-	-	-	-	-
0.1845	0.196	6.273	279.7	10.021	0.263	0.607	0.0137	0.0083	0.9781	0.261	0.695	I	0.2644	0.7723	0.5373	0.1977	0.0141	0.0011	0.9848	0.8	14	2.9	87	0.7
0.1947	0.5842	6.6615	279.7	15.816	0.148	0.551	0.0095	0.0018	0.9887	0.140	0.508	I	0.135	0.5915	0.7178	0.3773	0.0095	0.0018	0.9887	5.4	7.8	0.0	0.0	0.0
0.1947	0.5842	6.6615	281.2	17.628	0.176	0.584	0.0112	0.0018	0.987	0.170	0.536	I	0.1547	0.6229	0.7065	0.3494	0.0112	0.0018	0.9870	3.4	8.2	0.0	0.0	0.0
0.4371	0.1472	2.0555	281.7	6.329	0.746	0.806	0.0207	0.0006	0.9788	c	c	c	c	c	c	c	c	c	c	c	-	-	-	-	-
AARD %																				14	14	9.8	13	0.2

[a] $ARD\% = 100 \times \dfrac{\left|(y/x/z)_i^{exp.} - (y/x/z)_i^{pred.}\right|}{(y/x/z)_i^{exp.}}$, where superscript *exp.* stands for the values resulting from the experimental measurements for the gas phase or compositional analysis using mass balance approach, and superscript *pred.* refers to the predicted values applying the CSMGem model.[2]

[b] Some/all of constraints are not satisfied.
[c] No three phase flash convergence using CSMGem[2] model.
[*] Gas hydrate structure.
[**] Small cage occupancy.
[***] Large cage occupancy.

7. Assessment of Experimental Phase Equilibrium Data

Evaluation des données expérimentales d'équilibres de Phases

Il est maintenant bien accepté que les procédés efficaces des industries chimiques, pétrolières, pharmaceutiques et des polymères sont généralement conçus lorsqu´il est possible de disposer de valeurs thermo-physiques, physico-chimiques et de propriétés thermodynamiques des produits concernés ou de leurs mélanges, ainsi que des équilibres de phases aussi précis que possible.[433-435] On peut espérer obtenir les valeurs de ces propriétés/équilibres de phases par des mesures via des procédures/techniques expérimentales associées à des appareillages appropriés dans des laboratoires fiables. En général, la mesure précise des équilibres de phases est d'une grande importance surtout pour remplir les objectifs suivants :

1. Pour offrir à l'industrie des données fiables afin de concevoir des procédés efficaces dans le cadre d´applications industrielles potentielles;

2. Pour évaluer les paramètres des modèles thermodynamiques, qui sont censés être applicables pour les prédictions des équilibres de phases de systèmes d´intérêt aux diverses conditions opératoires.

Les gros efforts expérimentaux, entrepris depuis les deux siècles passés, ont permis de s´apercevoir que les données de ce type sont générées avec des incertitudes non négligeables probablement en raison des conditions de température et de pression très élevées (ou très faibles), des compositions extrêmement faibles de certaines espèces dans les mélanges, de la conception inappropriée des appareils, de techniques expérimentales non fiables, de transitions de phase trop lentes, de gradients compositionnels, de phénomènes d´hystérésis, d´erreurs humaines pendant les mesures, d´un manque de soin au cours de l'étalonnage des instruments (notamment les capteurs de pression, les sondes de température, les détecteurs de chromatographes, etc.).[13,14,413,436-439] Par conséquent, la cohérence des données expérimentales d'équilibres de phases doit être vérifiée soigneusement avant toute utilisation.

Le but de ce chapitre est l'évaluation des données d'équilibres de phases des systèmes contenant des hydrates de gaz, et ce, à l'aide de deux approches:

I. Tests de cohérence thermodynamique au moyen d'une méthode fondée sur l´équation de Gibbs-Duhem;[440-443]

II. Évaluation des données par application de la méthode statistique basée sur l'effet de levier.[444-446]

It is currently well-accepted that the efficient processes in chemical, petroleum, pharmaceutical, and polymer industries are generally designed in the case of availability of the values of the thermo-physical, physico-chemical, and thermodynamic properties of the involved components or their relevant mixtures as well as accurate phase equilibrium data.[433-435] This can be expected by the corresponding experimental measurements of such properties/phase behaviors (indeed, beside the integrity of the processes' design), which are obtained through accurate experimental procedures/techniques and appropriate apparatuses in reliable laboratories. In general, measuring accurate experimental phase equilibrium data is of great significance mainly to fulfill the following objectives:

1. To provide the industry with reliable data, which have potential industrial applications in order to design efficient processes;

2. Evaluation of the optimal parameters of the thermodynamic models, which are supposed to be applicable for predictions of the phase equilibria of the systems of interest at various operational conditions.

However, broad experimental efforts, since the past two centuries, indicate that generating these kinds of data are intrinsically with probable non-negligible uncertainties mainly due to very high (or very low) temperature/pressure conditions, extremely low compositions of particular species in the mixtures, inappropriate design of the apparatuses, unreliable experimental techniques, time-consuming phase transitions, compositional gradients, hysteresis human mistakes during the measurements, carelessness in calibration of the instruments (including pressure transducers, temperature probes, detectors of gas chromatographs and so forth) etc.[13,14,413,436-439] Therefore, the consistency of the experimental phase equilibrium data need to be checked prior to their further applications.

This chapter aims at assessment of phase equilibrium data of the systems containing gas hydrates using two approaches:

I. Thermodynamic consistency tests using a method on the basis of the "Gibbs-Duhem equation";[440-443]

II. Data evaluation applying the statistical method of the Leverage approach.[444-446]

7.1. Thermodynamic consistency test

The thermodynamic relationship, which is frequently used to analyze thermodynamic consistency of experimental phase equilibrium data is the fundamental ''Gibbs-Duhem equation.'' [440-443] This equation, as normally presented in the literature, interrelates the activity/fugacity coefficients of all components in a given mixture. If the equation is not obeyed within the defined criteria, then the data may be declared to be thermodynamically inconsistent i.e. this relation imposes a constraint on the activity/fugacity coefficients that has not been satisfied by the experimental data. [13,14,413,436-439] The latter phenomenon is mainly due to probable errors during the experimental phase equilibrium measurements, as already described.

The ways in which the ''Gibbs-Duhem equation'' [440-443] is arranged and applied to the experimental data have given origin to several ''consistency test methods'', most of them developed for low-pressure data. Among these, are the ''slope test,'' the ''integral test,'' the ''differential test,'' and the ''tangent-intercept test''. [440-443] Good reviews of these methods are given elsewhere. [443]

In recent years, Valderrama and coworkers [447-451] have investigated the applications of numerical thermodynamic consistency method to various systems including incomplete phase equilibrium data of high-pressure gas–liquid mixtures, [447] high pressure ternary mixtures of compressed gas and solid solutes, [448] high pressure gas-solid solubility data of binary mixtures, [449] vapor-liquid equilibrium data for mixtures containing ionic liquids, [450] and high pressure gas–liquid equilibrium data including both liquid and gas phases. [447] More recently, our aim has been focused on application of almost the same method on important systems for petroleum industry [13,14,413,436-439] including water content of methane in equilibrium with gas hydrate, liquid water or ice, [13] solubility data of carbon dioxide and methane with water inside and outside gas hydrate formation region, [14] sulfur content of hydrogen sulfide vapor, [413] compositional data of vapor phase in equilibrium with gas hydrate and liquid water for carbon dioxide + methane or nitrogen + water system, [436] solubility of waxy paraffins in natural gas systems, [437] diamondoids solubility [438] and glycol loss data [438] in gaseous systems.

The applied thermodynamic consistency test method has been developed on the basis of rewriting the ''Gibbs-Duhem equation'' [440-443] in terms of fugacity coefficients. [452] The employed method can be considered as a modeling procedure. This is because a thermodynamic model that can reliably represent the experimental data must be used to apply the consistency test. Fitting of the experimental data requires the calculation of some model parameters using a defined objective function that must be minimized.

As stated by Valderrama and Alvarez, [447] a good consistency test method to analyze high pressure data is supposed to fulfill 10 basic requirements: [13] (i) uses the ''Gibbs-Duhem equation'' [440-443]; (ii) uses the fundamental equation of phase equilibrium; (iii) be used for

testing all the experimental *P-T-y* data available; (iv) not necessarily requires experimental data for the whole concentration range and be applicable for data in any range of concentration; (v) be able to correlate the data within acceptable limits of deviations, deviations that must be evenly distributed; (vi) requires few additional calculated properties; (vii) be able to detect erroneous experimental points; (viii) makes appropriate use of necessary statistical parameters; (ix) be simple to be applied, with respect to the complexity of the problem to be solved; and (x) be able to conclude about consistency taking into account appropriate criteria.

7.1.1. Equations

The ''Gibbs-Duhem equation''[440-443] for a binary homogeneous mixture at constant temperature can be written as: [13,14,413,436-439,447-451]

$$\left[\frac{v^E}{RT}\right]dP = y_1 d(\ln \gamma_1) + y_2 d(\ln \gamma_2)$$
(7.1)

where v^E is the excess molar volume, y represents the mole fraction of species present, γ is the activity coefficient, and d is the derivative symbol. In this equation, subscripts 1 and 2 refer to components 1 and 2 in the phase of interest, respectively. Eq. 1 can be written in terms of the fugacity coefficients as follows:[13,14,413,436-439,447-451]

$$\left[\frac{Z-1}{P}\right]dP = y_1 d(\ln \varphi_1) + y_2 d(\ln \varphi_2)$$
(7.2)

where Z is the compressibility factor of the phase of concerned (the phase, on which the consistency test is supposed to be undertaken) and φ stands for the fugacity coefficient, as already designated. This equation can be written in terms of solubility of one of the components of the mixture in the phase of interest. For instance, if the water is considered as component 2 in the binary mixture of methane/nitrogen + water, the latter equation becomes: [13,14,413,436-439,447-451]

$$\frac{1}{P}\frac{dP}{dy_2} = \frac{y_2}{(Z-1)}\frac{d(\ln \varphi_2)}{dy_2} + \frac{(1-y_2)}{(Z-1)}\frac{d(\ln \varphi_1)}{dy_2}$$
(7.3)

or in integral form as follows:

$$\int \frac{1}{Py_2}dP = \int \frac{1}{(Z-1)\varphi_2}d\varphi_2 + \int \frac{(1-y_2)}{y_2(Z-1)\varphi_1}d\varphi_1$$
(7.4)

The properties φ_1, φ_2, and Z can be calculated using an appropriate thermodynamic model. In Eq. 7.4, the left hand side is designated by A_p and the right hand side by A_φ, as follows:[13,14,413,436-439,447-451]

$$A_p = \int \frac{1}{Py_2} dP \tag{7.5}$$

$$A_\varphi = A_{\varphi 1} + A_{\varphi 2} \tag{7.6}$$

$$A_{\varphi 1} = \int \frac{(1-y_2)}{y_2(Z-1)\varphi_1} d\varphi_1 \tag{7.7}$$

$$A_{\varphi 2} = \int \frac{1}{(Z-1)\varphi_2} d\varphi_2 \tag{7.8}$$

Thus, if a set of data is considered to be consistent, A_p should be equal to A_φ within acceptable defined deviations. To set the margins of errors, an individual percent area deviation ($\Delta A_i\%$) is defined as:[13,14,413,436-439,447-451]

$$\Delta A_i\% = 100\left[\frac{\left| A_{\varphi_i} - A_{p_i} \right|}{A_{p_i}} \right] \tag{7.9}$$

where i refers to the data set number. The maximum values accepted for these deviations regarding the proposed systems are discussed later.

7.1.2. Methodology

To evaluate the parameters required for the consistency test including the compressibility factors, activity coefficients, molar compositions of the phase(s) of interest, a suitable thermodynamic model should be applied, which is able to represent/predict the phase behavior of the corresponding systems within an acceptable deviation, which is evaluated using the following equation:

$$ARD\% = 100\frac{\left| y_i^{cal./pred.} - y_i^{exp.} \right|}{y_i^{exp.}} \tag{7.10}$$

where superscript *cal./pred.* stands for calculated/predicted values. The acceptable range of

the absolute relative deviations for each investigated system is determined on the basis of the general capabilities of the applied model(s) to represent/predict the concerned experimental data.

The following steps are later pursued:[13,14,413,436-439,447-451]

1. Determine A_p from Eq. 7.5 using the experimental P (pressure)-T (temperature)-y/x (composition) data. Use a numerical integration for this purpose. In this work, Simpson's 3/8 rule [431] has been used for the whole systems. Valderrama and Alvarez [447] have demonstrated that the deviations between the calculated values of the integrals by the simple trapezoidal integration rule and a fitted polynomial function are below 2%. Therefore, a simple numerical integration method e.g. trapezoidal rule can be applied for the cases that there are only two available experimental data points.

2. Evaluate A_φ by Eqs. 7.6 to 7.8 using the obtained values for φ_2 and Z from the selected thermodynamic model for the proposed system and y_2/x_2 from experimental data.

3. For every set of the experimental data, determine an individual absolute percent area deviation ($\Delta A_i\%$) between experimental and calculated values by Eq. 7.9.

7.1.3. Consistency criteria

For determination of the acceptable percentages of the two evaluated areas deviations from each other, the error propagation was performed on the existing experimental data. This has been done herein using the general equation of error propagation,[461] considering the temperature and molar composition of the phase of interest as the independent measured variables.[13] The calculated individual area (A_φ) is the dependent variable. The error in the calculated areas, E_A and the percent error $E_A\%$ are calculated as follows:[13,14,413,436-439,447-451]

$$E_A = \left[\frac{\partial A_{\varphi j}}{\partial T}\right]\Delta T + \left[\frac{\partial A_{\varphi j}}{\partial y}\right]\Delta y \tag{7.11}$$

$$E_A\% = 100\left[\left|\frac{E_A}{A_{\varphi j}}\right|\right] \tag{7.12}$$

where subscript j refers to j^{th} individual calculated area. We generally assume maximum uncertainties of 0.1 K for the experimental temperature and 10% for the experimental compositional data. However, these uncertainties depend on the method of experimental measurements and the systems investigated. The maximum acceptable errors are much dependent on uncertainty of compositional (or solubility) measurements and one can also

neglect the first right hand side term of Eq. 7.11 because the corresponding uncertainty is normally high (or at least higher than the uncertainty of temperature measurements).

The partial derivatives of the two preceding equations have been evaluated using the Central Finite Difference method as implemented by Constantinides and Moustofi.[431] The range of the maximum acceptable error for the calculated areas ($\Delta A_i\%$ or $E_A\%$) depends on the investigated system and the applied thermodynamic model.

The thermodynamic consistency test criteria are applied through the following instructions:[13,14,413,436-439,447-451]

1. Check that the absolute relative deviations of the model results (evaluated by Eq. 7.10) are not outside of the margins of errors (*ARD* %). If so, eliminate the weak predictions until the ARDs lie within the acceptable range.

2. If the model correlates the data within the acceptable error ranges of the compositional data and the assessment test (consistency test) is fulfilled for all points in the data set, the proposed model is reliable and the data seem to be thermodynamically consistent.

3. In the case that the model correlates the data acceptably and the area test is not accomplished for most of the data set (about 75% of the areas), the applied model is reliable; however, the experimental data seem to be thermodynamically inconsistent.

4. In the case that the model acceptably correlates the data and some of the area deviations (equal to or less than 25% of the areas) are outside the error range ($E_A\%$), the applied method declares the experimental values as probable not fully consistent.

7.1.4. Consistency test for experimental data of water content of methane in equilibrium with gas hydrate, liquid water or ice

As mentioned earlier, natural gases may contain some quantities of undesired dissolved water, which may condense during production, transportation, and processing operations altering the physical state from vapor to condensed water, gas hydrates, and/or ice. Condensed phase may lead to corrosion and/or two-phase flow problems. The formation of gas hydrates and/or ice could result in equipment blockage and shutdown. A gas phase with dissolved water can form gas hydrates/ice at the gas hydrates/ice-gas boundaries without the presence of a free water phase from a thermodynamic standpoint. However, gas hydrate/ice formation process from the dissolved water in the gas phase (in the absence of free water) is a very time consuming process.[2,13] Moreover, because of the low concentration of dissolved water in the gaseous phase, the determination of water content of gas in equilibrium with gas hydrate, ice, or liquid water (near gas hydrate or ice formation region) is difficult.[13] Figure 7.1 shows the typical *P-T* phase diagram for the methane + water system.[13,453,454]

Unfortunately, most of the experimental data for water content of natural gas components in equilibrium with gas hydrate, ice, or liquid water (near gas hydrate or ice formation region) were found to be scarce and often rather dispersed.[1,2,13] Literature survey reveals the availability of few sets of experimental data for water content of gases in equilibrium with gas hydrate/ice.[2] Therefore, few predictive methods for the water content of gases in equilibrium with gas hydrate/ice have been recommended in the literature as these methods are generally developed based on experimental data for their correlation.[13] To present accurate thermodynamic models for estimation of the water content of natural gases, reliable experimental data sets are required. This section aims at testing the thermodynamic consistency of literature data for methane (the main component of natural gases) water content at conditions of equilibrium with gas hydrate, ice, or liquid water (near gas hydrate or ice formation region) to verify their reliability.
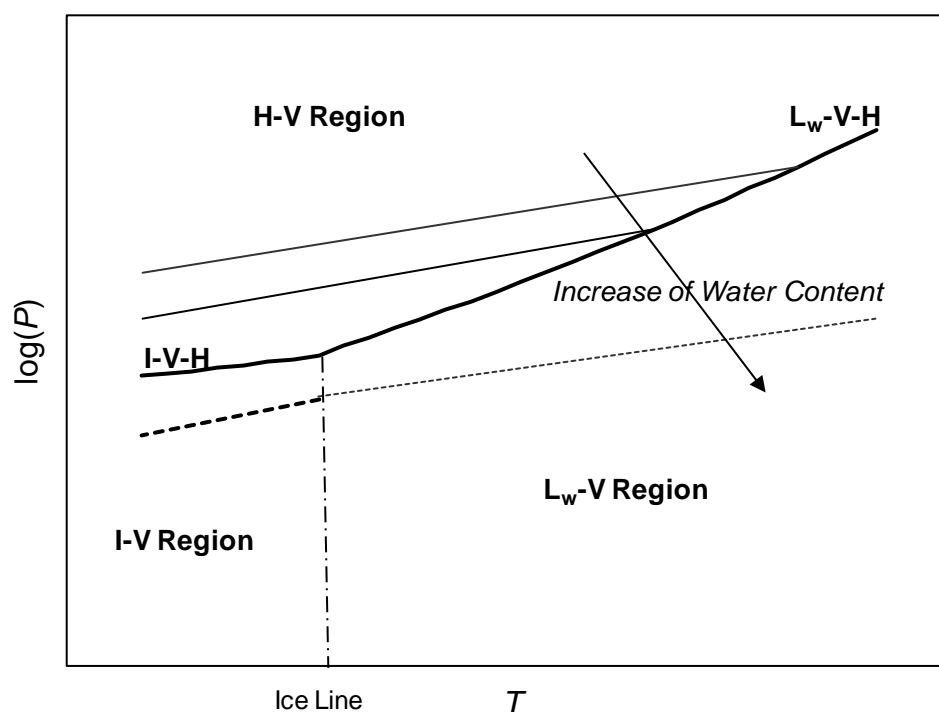
Figure 7.1: Typical H-G, I-G, and L_w-G equilibria regions for water (limiting reactant) single (pure and supercritical) hydrate former system. [13,453,454] Bold solid lines: L_w-G-H and I-G-H equilibria; Solid lines: water content of gas inside hydrate stability zone; Dashed line: water content of gas outside hydrate or ice stability zone; Bold dashed line: water content of gas inside ice stability zone; Solid-dashed line: Ice line representing L_w-G-I equilibrium.

143

Hydrate-Gas Equilibrium

The water content of a single hydrate former in equilibrium with its gas hydrate up to intermediate pressures can be estimated using the following expression:[13,453-455]

$$y_2 = \frac{P_2^{MT}}{\varphi_2 P} \times \exp[\frac{v_2^{MT}(P - P_2^{MT})}{RT}] \times [(1 + C_{small}P)^{-v'_{small}} \times (1 + C_{l\,arg\,e}P)^{-v'_{l\,arg\,e}}] \tag{7.13}$$

where y_2 is the mole fraction of water in vapor phase (water content), subscript 2 stands for water, and the superscripts *small* and *large* refer to two types of cavities, as designated in previous chapters. The Langmuir constants for methane's interaction with each type of cavity have been determined as a function of temperature, which are expressed from statistical mechanics as well as from data at the three-phase line by Parrish and Prausnitz:[321]

For pentagonal dodecahedra (small cavity):[13,453]

$$C_{small} = \frac{3.7237 \times 10^{-2}}{T} \exp(\frac{2.7088 \times 10^3}{T}) \tag{7.14}$$

For tetrakaidecahedra (large cavity): [13,453]

$$C_{large} = \frac{1.8373 \times 10^{-1}}{T} \exp(\frac{2.7379 \times 10^3}{T}) \tag{7.15}$$

where T is in K and C has unit of reciprocal MPa. Dharmawardhana *et al.* [396] obtained the following equation for the vapor pressure of the empty hydrate structure I: [2,13,453]

$$P_2^{MT} = 0.1 \times \exp(17.440 - \frac{6003.9}{T}) \tag{7.16}$$

where P_2^{MT} is in MPa and T in K. In the above equation, the following values can be used:

$v_2^{MT} = 0.022655$ m^3.kgmol^{-1} (von Stackelberg and Müller[456])

$v'_{small} = 1/23$ (Sloan and Koh[2])

$v'_{large} = 3/23$ (Sloan and Koh[2])

Liquid Water/Ice-Gas Equilibrium

The water content of a gas in equilibrium with liquid water up to intermediate pressures can be estimated using the following expression: [13,453]

$$y_2 = \frac{P_2^{sat}}{\varphi_2 P} exp(\frac{v_2^L(P - P_2^{sat})}{RT})$$ (7.17)

where P_2^{sat} and v_2^L are saturation pressure of water and molar volume of liquid water, respectively. As can be seen, water content is determined primarily by the fugacity coefficient of water in the gas phase, temperature and pressure. In other word, the non-ideality of the gas phase is the critical factor determining water content in the intermediate pressure range.[13,453]

To estimate vapor pressure and molar volume of water in Eq. 7.17, the relations reported by Daubert and Danner [457] and McCain [458] can be used, respectively: [13,453]

$$P_2^{sat} = 10^{-6} exp(73.649 - 7258.2/T - 7.3037 \ln(T) + 4.1653 \times 10^{-6} T^2)$$ (7.18)

$$v_2^L = 18.015 \times (1 - 1.0001 \times 10^{-2} + 1.33391 \times 10^{-4} \times [1.8(T - 273.15) + 32] + 5.50654 \times 10^{-7}$$

$$\times [1.8(T - 273.15) + 32]^2) \times 10^{-3}$$ (7.19)

where, T, P_2^{sat}, v_2^L are, respectively, in K, MPa and m^3.kgmol^{-1}. Eqs. 7.18 and 7.19 are valid at $T < 400\ K$, and $P < 34.5$ MPa even over a wide range of salt concentration in aqueous solution.[13,453,459,460]

Ice-gas equilibrium normally reaches at low-intermediate pressures and therefore Eq. 7.17 can be used for estimating water content of gases in equilibrium with ice. [13,453] For this purpose, the following relations for molar volume of ice and ice vapor pressure can be used: [13,459,460]

$$v_2^I = (19.655 + 0.0022364 \times (T - 273.15)) \times 10^{-3}$$ (7.20)

$$P_I^{sat} = [10^{(-1032.558/T + 51.056 \times \log(T) - 0.0977 \times T + 7.0357 \times 10^{-5} \times T^2 - 98.512)}]/7600$$ (7.21)

where v_2^I and P_I^{sat} stand for molar volume and saturation pressure of ice, respectively. In the above equations, T, v_2^I and P_I^{sat} are in K, m^3.kgmol^{-1} and MPa, respectively.

Eq. 7.17 can be applied directly to estimate the water content of gas in equilibrium with liquid water or ice using an appropriate expression for the fugacity coefficient of water in the gas phase.[13,454,455] The ice-gas equilibrium normally reaches at relatively low-pressures, as mentioned earlier, and therefore the fugacity coefficient of water in the gas phase can be set to unity as a good approximation. In other word, the Ideal model (Raoult's law) or ideal model + Poynting correction can be used to estimate water content of a gas in equilibrium with ice.[13,454,455]

To evaluate the rest of the required parameters, a previously tuned thermodynamic model [323,462-464] has been applied. The Valderrama modification of the Patel and Teja equation of state (VPT EoS) [465] with non-density-dependent (NDD) mixing rules [466] has been used to calculate the compressibility factor and fugacity coefficients of components in the gas phase. The formulations of the VPT EoS [465] with the NDD mixing rules [466] is given in the Appendix A. In addition, the error propagation[461] method results in the absolute relative deviations range between 0 to 58%. Therefore, the range [0,60] % has been established as the maximum acceptable error for the calculated areas ($\Delta A_i\%$ or E_A %) for the consistency test of the experimental data of water content of methane in equilibrium with gas hydrate, liquid water or ice.

As discussed earlier, the experimental data for the water content of gas in equilibrium with gas hydrate, ice or liquid water (near gas hydrate or ice formation region) are limited. In this work, 29 (isothermal) experimental data sets have been treated for consistency test (it was tried to gather all the isothermal data available in open literature). Table 7.1 summarizes the ranges of the data along with their references. Previous studies have shown that the thermodynamic model used in this work results in reliable predictions of water content of various gas samples, as pointed out earlier.[453,454,460,467] Table 7.2 indicates the results of the thermodynamic consistency test for all the experimental data sets presented in Table 7.1. As can be seen, almost all of the deviations lie near the maximum acceptable limit for being thermodynamically consistent. This is partly because of the difficulty of experimental measurements for such systems.[2,13] The percentage of the probable consistent data, inconsistent data, and not fully consistent data are around 48, 28, and 24%, respectively. It can also be indicated that the thermodynamic consistency test is a useful procedure to determine the accuracy of the measurements. For instance, the sets 16-23 are the revised data measured by Chapoy et al.[468] previously reported as the data sets 8-15.[469] The results show that the revised data are reported with more accuracy and this has led the experimental data to be more thermodynamically consistent. Typical calculation results for the forth data set are shown in Table 7.3. It is also obvious that using more modified (or improved) experimental apparatus can lead to more reliable experimental data. As for this, consider the data sets 1-4 reported by Aoyagi et al.[470] in 1980, which have been shown to be probable thermodynamically inconsistent data (three sets out of four ones) partly due to the mentioned point.

It is worth pointing out some important factors about the obtained results of such consistency test, which will be discussed at the end of the chapter.

Table 7.1: The experimental data ranges used for consistency test on water content of methane in equilibrium with gas hydrate, liquid water or ice.

System	Set No.	T/K	N^a	P range/MPa	y_2 range/mole fraction $\times 10^8$	Reference
H-G-E[*]						
	1	240.00	3	3.45 to 10.34	272 to 1230	470
	2	250.00	3	3.45 to 10.34	846 to 3217	
	3	260.00	3	3.45 to 10.34	2423 to 7824	
	4	270.00	3	3.45 to 10.34	6422 to 17809	
	5	283.08	2	10.01 to 14.24	15000 to 21300	468
	6	288.11	3	17.49 to 34.46	9200 to 16700	
	7	293.11	2	24.95 to 35.09	16800 to 22500	
L_w-G-E[**]	8	283.08	2	1.006 to 6.03	10800 to 124000	469
	9	288.11	3	1.044 to 10.03	8760 to 178000	
	10	293.11	4	0.992 to 17.68	7990 to 236000	
	11	298.11	6	1.01 to 34.42	7790 to 330000	
	12	303.11	6	1.10 to 34.56	15100 to 390000	
	13	308.11	6	1.10 to 34.58	28000 to 582000	
	14	313.12	6	1.10 to 34.61	42400 to 746000	
	15	318.12	6	1.003 to 34.61	56000 to 989000	
	16	283.08	2	1.006 to 6.03	29200 to 124000	471
	17	288.11	3	1.044 to 10.03	27300 to 178000	
	18	293.11	4	0.992 to 17.68	33800 to 236000	
	19	298.11	6	1.01 to 34.42	26500 to 330000	
	20	303.11	6	1.10 to 34.56	33100 to 444000	
	21	308.11	6	1.10 to 34.58	44700 to 111400	
	22	313.12	6	1.10 to 34.61	57500 to 746000	
	23	318.12	6	1.003 to 34.61	69100 to 989400	
	24	254.00	2	3.45 to 6.900	2070 to 4240	468
	25	293.01	2	0.51 to 0.992	241000 to 464000	472
	26	298.01	2	0.608 to 2.846	121800 to 519300	
	27	258.15	2	0.50 to 1.50	11000 to 31000	473
I-G-E[***]	28	263.15	2	0.50 to 1.50	19000 to 52000	
	29	268.15	2	0.50 to 1.50	28000 to 83000	

[a] Number of experimental data points.
[*] Hydrate-Gas Equilibria.
[**] Liquid Water-Gas Equilibria.
[***] Ice-Gas Equilibria.

Table 7.2: Results of the consistency test on water content of methane in equilibrium with gas hydrate, liquid water, or ice.

Set No.	$\Delta A_i\%$	Test result
1	62.5	TI^*
2	35.2	TC^{**}
3	62.5	TI
4	63.6	TI
5	49.5	NFC^{***}
6	49.0	TC
7	65.2	TI
8	74.9	TI
9	58.6	NFC
10	53.4	TC
11	48.9	TC
12	63.8	TI
13	67.2	TI
14	51.2	NFC
15	49.1	TC
16	57.9	NFC
17	46.5	TC
18	53.1	TC
19	50.0	TC
20	52.1	TC
21	61.7	TI
22	52.3	NFC
23	46.2	TC
24	52.3	TC
25	51.6	TC
26	58.7	NFC
27	50.7	TC
28	52.4	NFC
29	49.8	TC

[*] *Probable Thermodynamically Inconsistent Data.*
[**] *Probable Thermodynamically Consistent Data.*
[***] *Probable Thermodynamically Not Fully Consistent Data.*

Table 7.3: Typical detailed calculation results for the data set 4 defined in Table 7.1.

T /K	P/MPa	$y_2^{exp.}/ \times 10^8$	$y_2^{cal.}/ \times 10^8$	$\Delta y_2\%$	Z	φ_1^G	φ_2^G	A_p	A_φ	$\Delta A\%$
270	3.45	17809	15700	12	0.910	0.912	0.863	1.08×10^4	1.77×10^4	64
	6.9	9443	8340	12	0.831	0.836	0.742			
	10.34	6422	6210	3.3	0.774	0.774	0.639			

7.1.5. Consistency test for experimental solubility data in carbon dioxide/methane + water system inside and outside gas hydrate formation region

Accurate knowledge of the solubility in the carbon dioxide/methane + water system over a wide range of temperatures and pressures is especially necessary to tune thermodynamic models as such mixtures are of major systems in the petroleum industry, as described in previous chapters. Figure 7.2 shows a typical solubility-temperature diagram for a water-pure hydrate former (limiting reactant) system.[14,386] As can be seen, the temperature and pressure dependencies of the pure hydrate former (e.g., carbon dioxide and methane) solubility in pure water being in the liquid water-gas/vapor (depending on whether the component is in supercritical state or not) equilibrium region are different from the corresponding dependency in the liquid water-hydrate equilibrium region.[14,386] The L_w-G/V equilibrium is a strong function of temperature and pressure, while the L_w-H equilibrium is a strong function of temperature but a very weak function of pressure.[14,386]

On the other hand, the pure hydrate former solubility in pure water in the L_w-G/V equilibrium region generally increases with decreasing the temperature at given pressure, while the corresponding solubility in pure water in the liquid water-hydrate equilibrium region decreases with decreasing the temperature at the same pressure.[14,386] Furthermore, the meta-stable liquid water-vapor equilibrium may extend well into the gas hydrate formation zone.[14,386] Low solubilities of carbon dioxide/methane gases in water (especially methane) result in some significant experimental measurement difficulties. Although many experimental works have been done to obtain solubilities of carbon dioxide/methane in water in L_w-G/V region, the experimental data for describing the L_w-H equilibrium are limited mainly due to two factors: the possible extension of the meta-stable L_w-G/V equilibrium into the gas hydrate region and the experimental restraint that the existing analytical methods require modifications.[14,386]

Literature surveys reveal the availability of few sets of experimental data for the L_w-H equilibrium.[14,386] Consequently, few reliable models are available in the literature for representing the L_w-H equilibrium data.[14,386] These models are generally based on cubic equations of state, different mixing rules, and mathematical correlations. To check the existing thermodynamic models or to develop new ones, if necessary, for an accurate estimation of the solubility in the carbon dioxide/methane + water system, reliable

experimental data sets are required. This section aims at testing the thermodynamic consistency of such literature solubility data in the wide range of available temperatures and pressures including L_w-G/V and L_w-H equilibria concerning their reliability. Note that we consider the mole fraction of carbon dioxide/methane in the vapor/gas phase for performing thermodynamic consistency test on the mentioned phase. A similar method can be applied, of course, on the water content of the vapor/gas phase.

Liquid Water/Ice-Gas Equilibrium

To evaluate the parameters for the consistency test in this region (Z, φ_1, and φ_2), a previously tuned thermodynamic model[323,462-464] was applied. The general phase equilibrium criterion of equality of fugacities of each component throughout all phases was considered to model the phase behavior as follows:
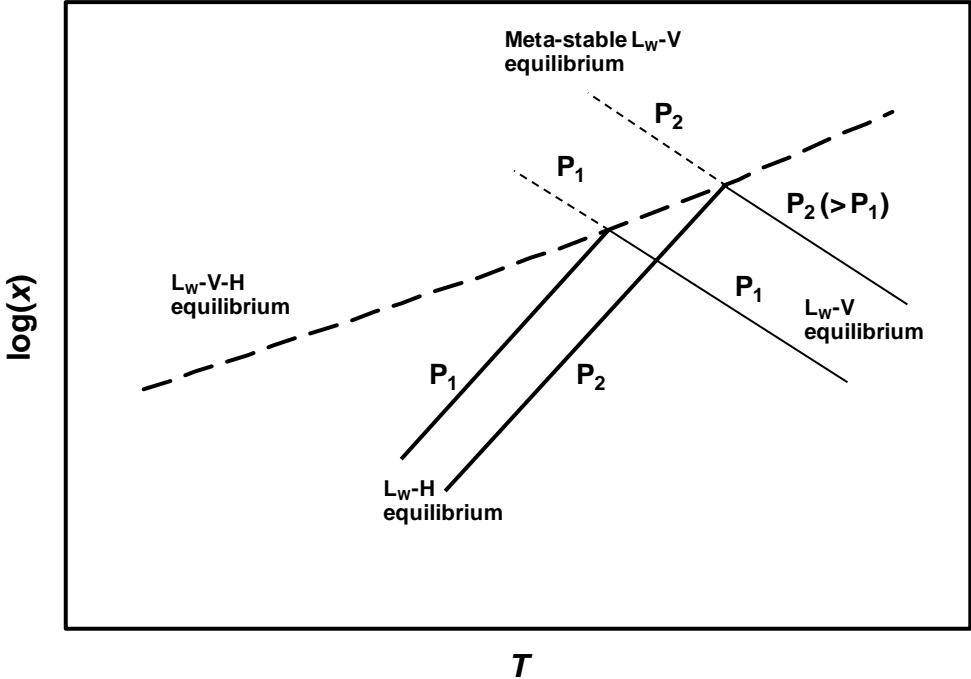
Figure 7.2: Typical *x* (solubility) - *T* diagram for water-single (pure) hydrate former (limiting reactant) system. [14,386] Bold solid lines: L_W -H equilibrium; Solid lines: L_w-V equilibrium; Dashed lines: Meta-stable L_w-V equilibrium; Bold dashed lines: L_w-V-H equilibrium.

$$f_i{}^{G/V} = f_i{}^{L} \qquad\qquad\qquad (7.22)$$

where i refers to the ith component in the mixture. The VPT EoS[465] with nondensity-dependent (NDD) mixing rules[466] was used to calculate the compressibility factor, fugacity coefficients, and the mole fractions of components in liquid and gas/vapor phases.[14,323,462-464]

Liquid water- hydrate equilibrium

Almost a similar model to those described in chapter 3 and 4 (on the basis of equating the fugacities of water in the liquid water phase and in the hydrate phase) has been herein applied; though, with the following equations to evaluate the fugacities:[14,385,386]

$$f_w^H = P_w^{MT} \times [(1 + C_{small} f_{HC}^L)^{-v'_{small}} \times (1 + C_{l \arg e} f_{HC}^L)^{-v'_{l \arg e}}] \tag{7.23}$$

where subscript HC stands for hydrate formers (methane/carbon dioxide) and:

$$f_w^L = x_w^L \gamma_w^L P_w^{sat} \tag{7.24}$$

In the intermediate pressure range, the liquid water is an incompressible fluid, the methane solubility is very small compared with unity; consequently the activity coefficient of water can be approximated to unity[14,385,386] (however, it is necessary to be careful, as it is not the case at high pressures where the nonideality of the liquid water phase and solubility of methane become important[14,385,386]). Therefore, Eq. 7.24 can be satisfactorily written as below:[14,385,386]

$$f_w^L \cong P_w^{sat} \tag{7.25}$$

Using the preceding equations, the following expression is obtained:[14,385,386]

$$P_w^{sat} = P_w^{MT} \times [(1 + C_{small} f_{HC}^L)^{-v'_{small}} \times (1 + C_{l \arg e} f_{HC}^L)^{-v'_{l \arg e}}] \tag{7.26}$$

or

$$1 - (\frac{P_w^{MT}}{P_w^{sat}}) \times [(1 + C_{small} f_{HC}^L)^{-v'_{small}} \times (1 + C_{l \arg e} f_{HC}^L)^{-v'_{l \arg e}}] = 0 \tag{7.27}$$

The fugacity of hydrocarbon hydrate former (here, methane) in the liquid water phase up to intermediate pressures can be calculated using the following equation:[14,385,386]

$$f_{HC}^L = x_{HC}^L H_{HC-w} \tag{7.28}$$

where H_{HC-w} represents Henry's constant for hydrocarbon hydrate former-water system. Therefore, the following final expression is obtained for estimating the solubility of pure hydrocarbon hydrate former in liquid water phase being in equilibrium with gas hydrates: [14,385,386]

$$1-(\frac{P_w^{MT}}{P_w^{sat}}) \times [(1+C_{small}x_{HC}^L H_{HC-w})^{-v'_{small}} \times (1+C_{large}x_{HC}^L H_{HC-w})^{-v'_{large}}] = 0 \quad (7.29a)$$

Equation 7.29a allows easy calculation of the solubility of pure hydrocarbon hydrate former in the liquid water being in equilibrium with gas hydrates. Its main advantages are the availability of necessary input data and the simplicity of the calculations that can be done even in Microsoft Excel $^{®}$ spreadsheets (without requirement of long programming codes).[2,4] Furthermore, as can be seen in this equation, almost all terms are temperature dependent while not pressure dependent, indicating the solubility of pure hydrocarbon hydrate former in liquid water phase being in equilibrium with gas hydrate is strong function of temperature and only weak function of pressure. For the CO_2 (and other highly soluble gases like H_2S)- water system, the solubility of CO_2 in the water phase cannot be ignored and consequently, the water activity cannot be set to unity. Taking into account the CO_2 solubility in the water phase and also the water activity, the following equation can be derived:[14]

$$1-[\frac{P_w^{MT}}{(1-x_{CO_2}^L)\gamma_w^L P_w^{sat}}] \times [(1+C_{small}x_{CO_2}^L H_{C0_2-w})^{-v'_{small}} \times (1+C_{large}x_{CO_2}^L H_{CO_2-w})^{-v'_{large}}] = 0 \,(7.29b)$$

Model parameters for L_w-H region

In equations (7.29a) and (7.29b), the following values of v_i' for sI hydrates can be used:[14,385,386,456]

$$v'_{small} = 1/23$$
$$v'_{large} = 3/23$$

and for sII:

$$v'_{small} = 2/17$$
$$v'_{large} = 1/17$$

Note that carbon dioxide and methane form sI clathrate hydrates. The Langmuir constants accounting for the interaction between the hydrate former and water molecules in the cavities were reported by Parrish and Prausnitz[321] for a range of temperatures and hydrate formers. [14,385,386] However, the integration procedure was followed in obtaining the

Langmuir constants for wider temperatures using the Kihara[324,325] potential function with a spherical core according to the study by McKoy and Sinanoĝlu.[326] In this work, the Langmuir constants for the hydrate former's interaction with each type of cavity have been determined using the equations of Parrish and Prausnitz:[321]

For pentagonal dodecahedra cavity (small one):

$$C_{small} = \frac{a}{T} \times exp(\frac{b}{T})$$ (7.30)

For tetrakaidecahedra cavity (large one):

$$C_{large} = \frac{c}{T} \times exp(\frac{d}{T})$$ (7.31)

where T is in K and C has reciprocal MPa unit. These values for methane hydrate are: $a = 0.0037237$ K.MPa^{-1}, $b = 2708.8$ K, $c = 0.018373$ K.MPa^{-1}, and $d = 2737.9$ K; and for CO_2 hydrate are: $a = 0.0011978$ K.MPa^{-1}, $b = 2860.5$ K, c = 0.008507 K.MPa^{-1}, and d = 3277.9 K.[14,385,386]

The following equation[396] has been used for calculation of the vapor pressure of the empty hydrate sI:[14, 385,386]

$$P_w^{MT} = 0.1 \times exp(17.440 - \frac{6003.9}{T})$$ (7.32a)

and for sII:

$$P_w^{MT} = 0.1 \times exp(17.332 - \frac{6017.6}{T})$$ (7.32b)

where P_w^{MT} is in MPa and T is in K. It should be mentioned that the non-ideality of water vapor pressure of the empty hydrate at saturation seems to be negligible due to the small quantity (typically, 10^{-3} to 10^{-5} MPa).[14]

To determine the Henry's constant of hydrate former in water (assuming that the activity coefficient is unity due to small solute concentration), Eq. 4.22 along with the values reported in Table 4.3 have been applied. In addition, the water vapor pressure can be obtained using Eq. 7.18. Moreover, Table 4.6 shows the critical properties and acentric factor of the pure compounds used in the VPT EoS.[456] The interaction parameters of the NDD mixing rules[457] are given elsewhere.[463]

For this system, it has been assumed maximum uncertainties of 0.1 K for the experimental temperature and 10 % for the experimental solubility data outside of hydrate region while 20 % regarding the data inside of hydrate formation region. Evaluating the partial derivatives in Eq. 7.11, the range (0 to 40) % is established as the maximum

acceptable error for the areas ($\Delta A_i\%$ or $E_A\%$, below the curves calculated from the numerical integration) related to outside of hydrate formation region and (0 to 50) % for the corresponding areas related to the data of inside the hydrate formation region. The high uncertainty in measurements of the mutual solubilities of the investigated gases with water and also low concentrations of these components in liquid phase at hydrate forming conditions, lead to obtaining this wide range of acceptable area deviations for the data to be probable thermodynamically consistent.

The calculation steps of the thermodynamic consistency tests explained earlier have been pursued to check the reliability of the investigated data. Forty-nine (isothermal) experimental data sets have been investigated for consistency test in this work. Table 7.4 summarizes the ranges of the data along with their references.[14]

As can be observed in Tables 7.5 and 7.6, the thermodynamic models used in this section generally result in reliable predictions/representations of mutual solubilities for investigated equilibrium conditions. Table 7.7 reports the typical results of the thermodynamic consistency test for solubility of carbon dioxide in water. The typical results of the consistency test for the experimental data of the carbon dioxide + water in gas phase are reported in Table 7.8.[14]

These results show that about 47 % of the investigated experimental data of solubility of carbon dioxide in water seem to be thermodynamically consistent; meanwhile this percentage is around 53 % for inconsistent data and 0 % for not fully consistent data. These percentages are about 31 %, 46 %, and 23 % for the data of concentrations of carbon dioxide in the gas phase, respectively.[14]

Table 7.9 shows the typical results of the thermodynamic consistency test for the data of solubility of methane in water. It is found out from these results that around 16 % of the investigated experimental data of solubilities of methane in water seem to be thermodynamically consistent while this percentage is around 78 % for inconsistent data and about 6 % for not fully consistent data.[14] It is inferred that the area deviations of these sets of data are higher than those ones for solubility of carbon dioxide.[14] This is mainly because of lower solubility of methane in water and therefore the expected difficulties of experimental measurements for such systems.[14] The typical results of the consistency test for the experimental data of the methane + water gas phase are reported in Table 7.10. The percentages of consistent, inconsistent, and not fully consistent data seem to be around 0 %, 50 %, and 50 %, respectively, regarding these data.

It is obvious that using more developed experimental apparatuses results in more accurate measurements of solubilities of carbon dioxide/methane in water especially in equilibrium with gas hydrates.

Table 7.4: The experimental data ranges used for experimental solubility data in carbon dioxide/methane + water system inside and outside gas hydrate formation region.

System	Set No.	T/K	N^a	Range of experimental data			Ref.[b]
				P/MPa	$x_2{}^c \times 10^5$ / mole fraction	$y_2{}^d \times 10^5$ / mole fraction	
carbon dioxide + water							
L_w-G/V-E*							
	1	323.15	7	6.82 to 17.68	1651 to 2262	99661 to 99357	474
	2	298.20	3	3.63 to 6.42	1830 to 2470	99860 to 99890	475
	3	323.20	7	7.08 to 14.11	1760 to 2170	99660 to 99390	476
	4	333.20	10	4.05 to 14.11	960 to 2080	99340 to 99220	476
	5	353.10	9	4.05 to 13.10	800 to 1840	98570 to 99000	476
	6	308.80	7	1.166 to 7.957	800 to 5060	89900 to 99000	477
	7	373.15	6	0.60 to 2.307	98 to 414	84500 to 95500	478
	8	393.15	5	0.599 to 2.848	181 to 428	84000 to 92600	478
	9	413.15	3	2.01 to 3.247	258 to 43	80000 to 87200	478
	10	323.15	7	6.82 to 17.68	1651 to 2262	99357 to 99661	479
	11	383.15	15	10 to 150	1400 to 4000	96969 to 97399	480
	12	423.15	15	10 to 150	1350 to 4800	75200 to 88000	480
	13	473.15	14	20 to 150	1300 to 7200	69000 to 82000	480
L_w-H-E**							
	14	274.05	2	4.2 to 5.0	1560 to 1630		481
	15	280.50	8	4.99 to 14.20	2560 to 2600		482
	16	278.50	4	6.10 to 10.41	2210 to 2350		482
	17	279.50	5	6.10 to 10.44	2620 to 2410		482
methane + water							
L_w-G-E							
	1	298.15	10	2.351 to 44.402	49.7 to 417	-§	483
	2	310.93	12	2.275 to 68.223	44.0 to 465	-	483
	3	344.26	9	6.501 to 68.017	34.0 to 424	-	483
	4	377.59	13	2.296 to 68.086	32.3 to 451	-	483
	5	310.93	9	3.516 to 2.965	6.4 to 58.8	-	484
	6	327.59	7	0.779 to 3.592	12.8 to 56.4	-	484
	7	344.26	7	0.772 to 3.268	10.5 to 47.7	-	484
	8	360.93	9	0.786 to 3.702	12.6 to 5.7	-	484
	9	298.15	9	1.103 to 5.171	21.4 to 113	-	484
	10	303.15	8	0.317 to 3.605	6.0 to 76.4	-	484
	11	274.35	8	0.567 to 2.806	25.8 to 114.2	-	484
	12	285.65	5	2.331 to 9.082	65.6 to 200	-	484
	13	283.37	4	1.765 to 7.046	56.2 to 185	-	485
	14	275.11	4	0.973 to 2.820	39.9 to 106.1	-	486

Table 7.4:
Continued…

	No.	T/K	a	c	d		b
	15	283.13	4	1.039 to 5.977	32.9 to 149.6	-	486
	16	313.11	4	1.025 to 17.998	20.4 to 232.5	-	486
	17	313.15	5	2.5 to 12.5	49.0 to 187	99697 to 99907	487
	18	338.15	5	2.5 to 12.5	40.0 to 162	99017 to 99702	487
	19	473.15	6	30 to 150	500.0 to 1300	81100 to 89000	488
	20	423.15	6	9.807 to 98.066	10.0 to 560	94000 to 98500	489
	21	473.15	5	19.613 to 98.066	380 to 1040	81000 to 96300	489
	22	298.15	5	2.5 to 12.5	59.0 to 221	99746 to 99941	489
L_w-H-E							
	23	278.10	7	5.79 to 19.35	96 to 114		490
	24	278.20	4	8.89 to 13.76	104 to 106		490
	25	273.10	8	4.98 to 14.81	76.5 to 77.5		490
	26	274.15	4	6 to 20	110.6 to 126.4		491
	27	278.15	4	6 to 20	132.2 to 145.2		491
	28	282.15	3	10 to 20	158.3 to 168.7		491
	29	286.15	2	15 to 20	179.9 to 182.6		491
	30	278.10	7	5.79 to 19.35	96 to 114		492
	31	278.20	4	8.89 to 13.76	104 to 106		492
	32	273.10	8	4.98 to 14.81	77.5 to 76.5		492

[a] *Number of experimental data points*

[b] *Reference of experimental data*

[c] *Solubility of gas in liquid phase*

[d] *Concentration of gas in vapor phase*

[*] *Liquid water- Gas/Vapor- Equilibria*

[**] *Liquid water- Hydrate- Equilibria*

[§] *Not available*

Table 7.5: Typical calculated/predicted results of solubilities in the carbon dioxide + water (mole fraction).

Set No.[a]	T/K	P/MPa	$x_2^{exp.} \times 10^2$ / mole fraction	$x_2^{calc./pred.} \times 10^2$ / mole fraction	$y_2^{exp.} \times 10/$ mole fraction	$y_2^{calc./pred.} \times 10/$ mole fraction	ARD[*] % / $x_2^{cal./pred.}$	ARD[**]% / $y_2^{cal./pred.}$
1	323.15	6.82	1.651	1.711	9.9661	9.9650	3.7	0.01
		7.53	1.750	1.812	9.9655	9.9651	3.5	0.00
		8.72	1.768	1.948	9.9636	9.9636	10	0.00
		10.13	2.081	2.061	9.9564	9.9578	1.0	0.01
		12.21	2.096	2.162	9.9457	9.9480	3.2	0.02
		14.75	2.215	2.249	9.9392	9.9413	1.5	0.02
		17.68	2.262	2.329	9.9357	9.9366	3.0	0.01
2	298.2	3.63	1.830	1.754	9.986	9.9871	4.2	0.01

		6.41	2.440	2.468	9.986	9.9879	1.1	0.02
		6.42	2.470	2.469	9.989	9.9878	0.0	0.01
3	323.2	4.05	1.090	1.183	9.954	9.9566	8.6	0.03
		5.06	1.370	1.401	9.964	9.9615	2.3	0.03
		6.06	1.610	1.588	9.963	9.9641	1.4	0.01
		7.08	1.760	1.749	9.966	9.9651	0.7	0.01
		8.08	1.900	1.878	9.966	9.9647	1.1	0.01
		9.09	2.000	1.982	9.959	9.9625	0.9	0.04
		10.09	2.050	2.058	9.955	9.9580	0.4	0.03
		11.1	2.100	2.113	9.95	9.9526	0.6	0.03
		12.1	2.140	2.157	9.945	9.9483	0.8	0.03
		14.11	2.170	2.228	9.939	9.9426	2.7	0.04
4	333.2	4.05	0.960	1.011	9.934	9.9318	5.3	0.02
		5.06	1.210	1.205	9.945	9.9402	0.4	0.05
		6.06	1.380	1.376	9.945	9.9450	0.3	0.00
		7.08	1.570	1.527	9.949	9.9476	2.7	0.01
		8.08	1.660	1.655	9.95	9.9485	0.3	0.02
		9.09	1.790	1.765	9.953	9.9479	1.4	0.05
		10.09	1.860	1.854	9.951	9.9459	0.3	0.05
		11.1	1.950	1.928	9.947	9.9424	1.1	0.05
		12.1	2.010	1.986	9.942	9.9381	1.2	0.04
		14.11	2.080	2.078	9.922	9.9301	0.1	0.08
5	353.1	4.05	0.800	0.776	9.857	9.8458	3.0	0.11
		6.06	1.140	1.079	9.891	9.8799	5.3	0.11
		7.08	1.280	1.213	9.896	9.8883	5.2	0.08
		8.08	1.400	1.331	9.903	9.8935	4.9	0.10
		9.09	1.510	1.438	9.908	9.8964	4.8	0.12
		10.09	1.600	1.533	9.907	9.8975	4.2	0.10
		11.1	1.720	1.617	9.91	9.8971	6.0	0.13
		12.1	1.760	1.691	9.904	9.8956	3.9	0.08
		13.1	1.840	1.756	9.9	9.8931	4.5	0.07

[a] Refer to Table 7.4 for observing the data set number.

$$^{*}ARD = 100 \times \frac{\left| x_2^{cal./\,pred.} - x_2^{exp.} \right|}{x_2^{exp.}} .\ ^{**}ARD = 100 \times \frac{\left| y_2^{calc./\,pred.} - y_2^{exp.} \right|}{y_2^{exp.}}$$

Table 7.6: Typical calculated/predicted results of solubilities in the methane + water (mole fraction).

Set No.[a]	T/K	P/MPa	$x_2^{exp.} \times 10^4$/mole fraction	$x_2^{cal./pred.} \times 10^4$/mole fraction	$y_2^{exp.} \times 10$/ mole fraction	$y_2^{calc./pred.} \times 10$/ mole fraction	ARD % /x_2 cal./pred.	ARD % / y_2 cal./pred.
1	298.15	2.351	4.97	5.43	-[§]	9.9852	9.2	
		3.165	7.17	7.11	-	9.9886	0.8	
		4.544	10.00	9.77	-	9.9916	2.3	
		6.44	13.17	13.04	-	9.9937	1	
		8.894	16.78	16.72	-	9.9949	0.3	
		13.307	22.35	22.09	-	9.9960	1.2	
		17.202	25.85	25.87	-	9.9965	0.1	
		24.235	31.10	31.29	-	9.9969	0.6	
		33.164	36.60	36.67	-	9.9972	0.2	
		44.402	41.70	42.14	-	9.9975	1.1	
2	310.93	2.275	4.40	4.53	-	9.9687	3	
		3.289	6.19	6.37	-	9.9776	2.9	
		4.578	8.39	8.55	-	9.9831	1.9	
		6.55	11.23	11.57	-	9.9874	3.1	
		8.756	14.40	14.58	-	9.9898	1.2	
		13.1	18.90	19.54	-	9.9921	3.4	
		17.754	22.90	23.81	-	9.9933	4	
		24.373	27.60	28.70	-	9.9942	4	
		33.853	33.30	34.24	-	9.9949	2.8	
		44.988	39.10	39.50	-	9.9954	1	
		54.262	41.70	43.23	-	9.9957	3.7	
		68.224	46.50	48.09	-	9.9960	3.4	
3	344.26	2.282	3.40	3.55	-	9.8463	4.4	
		3.22	4.70	4.92	-	9.8882	4.8	
		4.544	6.32	6.77	-	9.9178	7.1	
		6.502	9.09	9.30	-	9.9394	2.4	
		9.101	11.83	12.36	-	9.9536	4.4	
		12.962	15.00	16.33	-	9.9641	8.9	
		17.616	19.24	20.41	-[§]	9.9705	6.1	
		24.373	23.85	25.35	-	9.9754	6.3	
		33.957	27.70	31.03	-	9.9792	12	
		44.988	34.20	36.35	-	9.9817	6.3	
		56.675	37.50	41.07	-	9.9835	9.5	
		68.017	42.40	45.03	-	9.9847	6.2	
4	377.59	2.296	3.23	3.21	-	9.4474	0.6	
		3.213	4.32	4.49	-	9.5966	3.9	
		3.227	4.72	4.51	-	9.5982	4.5	
		4.495	6.11	6.21	-	9.7032	1.6	
		6.516	8.86	8.76	-	9.7859	1.1	

Table 7.6:
Continued…

Set No.	T/K	P						
		9.032	11.88	11.70	-	9.8370	1.5	
		13.1	15.60	15.96	-	9.8779	2.3	
		17.478	19.80	20.00	-	9.9005	1	
		24.614	25.10	25.63	-	9.9202	2.1	
		34.232	31.40	31.89	-	9.9341	1.6	
		44.988	36.10	37.67	-	9.9430	4.3	
		56.468	40.80	42.85	-	9.9493	5	
		68.086	45.10	47.35	-	9.9538	5	
19	473.15	20	50.00	35.00	8.110	8.8611	30	9.3
		30	60.00	49.06	8.460	9.1541	18	8.2
		40	70.00	60.73	8.690	9.3067	13	7.1
		50	80.00	70.54	8.850	9.4025	12	6.2
		70	90.00	86.05	8.880	9.5190	4.4	7.2
		100	110.00	102.35	8.900	9.6153	7	8
		150	130.00	118.62	8.900	9.6994	8.8	9
20	423.15	9.807	10.00	13.87	9.400	9.3952	39	0.1
		19.613	18.00	25.24	9.630	9.6487	40	0.2
		39.227	30.00	41.87	9.780	9.7791	40	0
		58.84	46.00	53.75	9.830	9.8265	17	0
		78.453	56.00	62.79	9.835	9.8527	12	0.2
		98.067	56.00	69.91	9.850	9.8699	25	0.2
21	473.15	19.613	38.00	34.39	8.915	8.8440	9.5	0.8
		39.227	67.00	59.90	9.350	9.2975	11	0.6
		58.84	87.00	77.98	9.480	9.4625	10	0.2
		78.453	10.00	91.35	9.545	9.5525	8.7	0.1
		98.067	10.40	101.48	9.630	9.6106	2.4	0.2

[a] Refer to Table 7.4 for observing the data set number. [§] Not available.

Table 7.7: Typical detailed results of thermodynamic consistency test on the experimental data of the solubility of carbon dioxide in water investigated in this work.

Set No.[a]	T/K	P/MPa	Z	φ_1^L	φ_2^L	A_p	A_φ	$\Delta A_i\%$	Test result
1	323.15	6.82	0.0495	0.013	50.074	48.478	53.189	9.7	TC
		7.53	0.0547	0.011	43.789				
		8.72	0.0634	0.010	36.387				
		10.13	0.0737	0.008	30.740				
		12.21	0.0889	0.007	25.601				
		14.75	0.1075	0.005	21.631				
		17.68	0.1288	0.004	18.594				
2	298.2	3.63	0.0281	0.007	67.203	14.55	22.694	56.0	TI
		6.41	0.0499	0.004	28.869				

		6.42	0.0500	0.004	28.813				
3	323.2	7.08	0.0514	0.012	47.611	30.702	38.172	24.3	TC
		8.08	0.0587	0.011	40.013				
		9.09	0.0661	0.009	34.679				
		10.09	0.0734	0.008	30.896				
		11.1	0.0808	0.007	28.049				
		12.1	0.0881	0.007	25.837				
		14.11	0.1028	0.006	22.498				
4	333.2	4.05	0.0286	0.127	68.918	87.855	399.217	354.4	TI
		5.06	0.0358	0.111	55.786				
		6.06	0.0429	0.094	47.329				
		7.08	0.0502	0.022	56.219				
		8.08	0.0573	0.018	47.604				
		9.09	0.0645	0.015	41.243				
		10.09	0.0716	0.013	36.568				
		11.1	0.0788	0.012	32.982				
		12.1	0.0860	0.010	30.216				
		14.11	0.1003	0.009	26.142				
5	353.1	4.05	0.0273	0.132	92.985	73.389	132.686	80.8	TI
		6.06	0.0410	0.108	62.937				
		7.08	0.0479	0.095	54.484				
		8.08	0.0548	0.082	48.478				
		9.09	0.0616	0.067	44.099				
		10.09	0.0685	0.050	41.486				
		11.1	0.0753	0.034	40.166				
		12.1	0.0822	0.027	37.753				
		13.1	0.0890	0.023	35.280				

[a] Refer to Table 7.4 for observing the data set number.

Table 7.8: Typical detailed results of thermodynamic consistency test on the experimental data of the concentration of carbon dioxide in gas phase investigated in this work.

Set No.[a]	T/K	P/MPa	Z	φ_1^G	φ_2^G	A_p	A_φ	ΔA%	Test result
1	323.15	6.82	0.6612	3.727	0.860	0.932	1.145	22.9	TC
		7.53	0.6152	3.246	0.796				
		8.72	0.5290	2.581	0.711				
		10.13	0.4221	1.809	0.636				
		12.21	0.3632	1.173	0.556				
		14.75	0.3724	0.846	0.489				
		17.68	0.4032	0.654	0.436				

4	333.2	4.05	0.8354	18.992	0.701	1.308	0.756	42.2	TI
		5.06	0.7907	19.859	0.676				
		6.06	0.7444	16.825	0.655				
		7.08	0.6948	14.206	0.641				
		8.08	0.6437	3.494	0.792				
		9.09	0.5899	3.135	0.732				
		10.09	0.5364	2.609	0.682				
		11.1	0.4875	2.129	0.639				
		12.1	0.4519	1.744	0.604				
		14.11	0.4232	1.073	0.547				
5	353.1	4.05	0.8671	9.163	0.733	0.978	0.552	43.5	NFC
		6.06	0.7990	9.777	0.688				
		7.08	0.7639	9.012	0.668				
		8.08	0.7293	8.319	0.652				
		9.09	0.6946	7.229	0.641				
		10.09	0.6610	5.325	0.642				
		11.1	0.6287	3.674	0.656				
		12.1	0.5996	2.718	0.645				
		13.1	0.5744	2.216	0.626				
6	308.8	1.17	0.9418	1.684	0.767	0.613	0.311	49.3	TI
		2.27	0.8836	2.599	0.725				
		3.8	0.7947	23.238	0.674				
		5.14	0.7053	69.842	0.641				
		5.26	0.6964	7.648	0.640				
		6.19	0.6210	0.670	0.828				
		7.96	0.3678	0.512	0.672				

[a] Refer to Table 7.4 for observing the data set number.

Table 7.9: Typical detailed results of thermodynamic consistency test on the experimental data of the solubility of methane in water investigated in this work.

Set No.[a]	T/K	P/MPa	Z	φ_1^L	φ_2^L	A_p	A_φ	$\Delta A\%$	Test result
22	298.15	2.5	0.0191	0.151	1359.345	1214.417	868.403	28.5	TC
		5	0.0383	0.112	721.499				
		7.5	0.0574	0.081	513.449				
		10	0.0766	0.057	413.267				
		12.5	0.0957	0.039	355.881				
1	298.15	2.351	0.0180	0.154	1440.584	6114.053	3365.225	45.0	TI
		3.165	0.0242	0.140	1090.400				
		4.544	0.0348	0.119	785.027				
		6.44	0.0493	0.093	581.289				
		8.894	0.0681	0.066	450.092				
		13.307	0.1019	0.035	342.255				
		17.202	0.1317	0.021	294.139				
		24.235	0.1855	0.011	243.281				
		33.164	0.2537	0.007	208.795				
		44.402	0.3395	0.005	187.384				
2	310.93	2.275	0.0168	0.159	1734.786	8774.705	4213.965	52.0	TI
		3.289	0.0243	0.144	1224.711				
		4.578	0.0339	0.126	904.786				
		6.55	0.0485	0.102	660.920				
		8.756	0.0648	0.079	521.156				
		13.1	0.0969	0.047	388.367				
		17.754	0.1313	0.029	320.724				
		24.373	0.1802	0.017	268.099				
		33.853	0.2502	0.010	228.279				
		44.988	0.3323	0.007	205.213				
		54.262	0.4005	0.006	195.896				
		68.224	0.5031	0.005	191.361				
19	473.15	19.613	0.1117	0.072	266.396	202.007	30.200	85.0	TI
		39.227	0.2217	0.076	155.805				
		58.84	0.3301	0.068	128.816				
		78.453	0.4369	0.062	120.899				
		98.067	0.5423	0.059	121.054				
26	274.15	6	0.0493	0.000	467.647	1052.33	1434.4	36.3	TC
		10	0.0821	0.000	280.588				
		15	0.1231	0.000	187.059				
		20	0.1640	0.000	140.294				

[a] Refer to Table 7.4 for observing the data set number.

Table 7.10: Typical detailed results of thermodynamic consistency test on the experimental data of the concentration of methane in gas phase investigated in this work.

Set No.[a]	T/K	P/MPa	Z	φ_1^G	φ_2^G	A_p	A_φ	$\Delta A\%$	Test result
22	298.15	2.5	0.9544	107.929	0.781	1.3	0.275	78.9	NFC
		5	0.9137	145.618	0.765				
		7.5	0.8798	141.530	0.755				
		10	0.8541	120.104	0.753				
		12.5	0.8378	95.284	0.755				
17	313.15	2.5	0.9624	48.265	0.788	1.3	0.36	72.3	TI
		5	0.9296	69.164	0.773				
		7.5	0.9027	72.781	0.764				
		10	0.8827	67.575	0.760				
		12.5	0.8701	58.024	0.760				

[a] Refer to Table 7.4 for observing the data set number.

7.1.6. Experimental data assessment test for composition of vapor phase in equilibrium with gas hydrate and liquid water for carbon dioxide + methane or nitrogen + water system

As described in chapter 6, experimental data for the composition of vapor phase in equilibrium with gas hydrate and liquid water in the systems containing carbon dioxide and nitrogen are of great significance particularly for designing the CO_2 capture processes utilizing gas hydrate formation technique.[436] The consistency of the corresponding scarce data is checked in this section applying the thermodynamic assessment tests.

Thermodynamic model

A previously checked gas hydrate thermodynamic model[462-464] containing the VPT EoS[465] with NDD mixing rules[466] has been used to calculate the compressibility factor, fugacity coefficients, and the mole fractions of components in the liquid and vapor phases, and the solid solution theory of vdW-P[319,320] has been employed to determine the fugacity of water in the hydrate phase. The equality of fugacities approach described in chapters 3 and 4 along with appropriate numerical methods for flash calculations in order to reach convergence of the algorithms for the investigated systems at the conditions of interest have been applied in this section.

The binary interaction parameters between the species of the investigated systems used for the VPT EoS[465] and NDD mixing rules[466] are reported in Tables 7.11 and 7.12. Moreover,

the critical properties and acentric factor of the compounds are reported in Table 4.6. The applied values of the Kihara[324,325] potential function parameters are shown in Table 7.13.

Table 7.11: Binary interaction parameters between the investigated gases and water using the VPT-EoS[465] with NDD mixing rule.[466]

Gas	H$_2$O(i)		
	$k_{ij}= k_{ji}$*	l_{ij}^{0}**	l_{ij}^{1}**
CH$_4$(j)	0.5028	1.8180	0.0049
CO$_2$(j)	0.1965	0.7232	0.0024
N$_2$(j)	0.4792	2.6575	0.0064

* Classical binary interaction parameters.

** Binary interaction parameters for the asymmetric term.

Table 7.12: Binary interaction parameters between the investigated gases using the VPT-EoS[465] with NDD mixing rule.[466]

Gas	k_{ij}		
	CH$_4$(j)	CO$_2$(j)	N$_2$(j)
CH$_4$(i)	0	0.092	0.035
CO$_2$(i)	0.092	0	-0.036
N$_2$(i)	0.035	-0.036	0

Table 7.13: The Kihara[324,325] potential parameters used in the thermodynamic model.[462-464]

Component	α,^{a} Å	σ*,^{b} Å	ε/k,^{c} K
CH$_4$	0.3834	3.165	154.5
CO$_2$	0.6805	2.9818	168.8
N$_2$	0.3525	3.0124	125.2

^{a} The radius of spherical molecular core.

^{b} $\sigma^* = \sigma - 2\alpha$, where σ is the collision diameter.

^{c} ε is the characteristic energy and k is the Boltzmann's constant.

The investigated experimental ranges of pressures and molar fractions of carbon dioxide in the vapor phase at various temperatures available in the open literature are presented in Table 7.14. The calculations demonstrate that the applied thermodynamic model[462-464] (accompanied by appropriate numerical methods) contributes to generally reliable predictions of vapor phase compositions for the investigated equilibrium conditions (except few data sets). The error propagation method[461] results in the range [0,20] % as the acceptable error range of calculated areas for probable thermodynamically consistent data. The consistency test calculation steps have been followed on the basis of the previously described algorithm.

Table 7.15 reports the final results of the thermodynamic consistency test for molar compositions of CO_2 in the vapor phase in equilibrium with gas hydrate and liquid water for the $CO_2 + CH_4/N_2 +$ water system. As can be seen, only one of the treated data sets seems to be thermodynamically consistent. It is worth it to point out that the three-phase compositional data of Belandria et al.[59,426] are, perhaps, the first comprehensive data/composition analysis reported in the literature to deal with the compositions of vapor + hydrate + aqueous phases.[436] As already mentioned, such data are indeed rare. In order to generate these kinds of data reported by Belandria et al.[59,426] (the data have been produced at CEP/TEP laboratory), we faced some technical problems (refer to the original article for observing the pursued measurements procedure).[56,436] This may be one of the reasons that some of these data seem to be inconsistent. Furthermore, measurements of data (such as those presented in the works of Belandria et al.[59,426]) are not experimentally easy and are subjected to non-negligible uncertainties.

7.1.7. Significant points on consistency tests

Some prominent factors about the performed consistency tests should be herein mentioned:[436]

1. It cannot be stated that we are completely sure about the validity of percentages (shares) of the uncertainties on area deviations, as they are model-dependent, to declare the data to be really inconsistent. Nevertheless, it is recommended to reduce the sources of the uncertainties by some precautions like more careful calibrations of the instruments, more precise measurements, more careful design of the apparatuses, and so forth.

2. Not all of the uncertainties and errors in the measurements are originated from the calibrations or design of the apparatuses. These errors may come from the performance of the person(s) who measure(s) the data or the operational conditions of the laboratory that may not be constant during the measurements. That is why we were very interested to perform such consistency tests, which are generally ignored by the researchers who are mainly concerned about the modeling issues.

3. The data, on which this kind of thermodynamic consistency test, is supposed to be applied, should be reported as isotherms because the main assumption in development of the employed expression (Eq. 7.1) is similar to that assumed in developing the original "Gibbs-Duhem equation"[440-443] at constant temperature. This fact assigns some limitations to choose the experimental data sets for the consistency test especially for scarce compositional data. One way of solving the problem of scarcity of data may be generating more data in a statistical form using a statistical software. The generated data can be treated as pseudo-experimental ones. Though, this is doubtful and seems to be incorrect for the data in the hydrate formation region because there is possibility of structure change of the clathrate hydrate, and this would

Table 7.14: The experimental data ranges used for consistency test of composition of vapor phase in equilibrium with gas hydrate and liquid water for carbon dioxide + methane or nitrogen + water system.

System	Set No.	T/K	N^a	Range of data		Ref.^{b}
				P/MPa	y_2 / mole fraction^c	
carbon dioxide + methane + water						
	1	280.3	30	3.77 to 4.36	0.143 to 0.384	217
	2	273.6	8	1.51 to 2.44	0.081 to 0.630	426
	3	275.2	8	1.792 to 2.766	0.086 to 0.657	426
	4	276.1	8	1.985 to 3.027	0.096 to 0.669	426
	5	278.1	7	2.450 to 3.802	0.103 to 0.694	426
	6	280.2	8	3.139 to 7.190	0.108 to 0.620	426
carbon dioxide + nitrogen + water						
	7	274	9	1.394 to 17.926	0 to 1	210, 220
	8	277	8	1.953 to 24.041	0 to 1	210, 220
	9	280	9	2.801 to 32.308	0 to 1	210, 220
	10	272.1	9	3.2 to 14.5	0.012 to 0.847	221
	11	275.3	7	1.6 to 3.5	0.436 to 1	222
	12	273.6	5	2.032 to 11.943	0.171 to 0.617	59
	13	275.2	7	2.29 to 12.745	0.16 to 0.729	59
	14	276.1	5	2.5 to 8.58	0.196 to 0.682	59
	15	278.1	5	2.974 to 14.260	0.127 to 0.729	59

^{a} *Number of experimental data points.*

^{b} *Refrence.*

^{c} *Mole fraction of carbon dioxide in vapor phase.*

result in inaccurate generation of the pseudo-experimental data. Apart from that, it is not recommended to generate such data based on doubtful data, which have not been yet theoretically checked for consistency.

4. The performed phase equilibrium data assessment tests are inevitably model-dependent. If there is a way that we could measure directly the required parameters for the consistency test including the fugacity coefficients, we could have employed this method only based on experimental measurements (we are sure at the moment that it is impossible). This conclusion is valid even at low pressures, when we can assume with high confidence that the fugacity coefficients and compressibility factors are unity. On the other hand, due to model

dependency of the consistency test, it can only be claimed that the data are thermodynamically consistent, inconsistent or not fully consistent based on the applied model

Table 7.15: The final results of thermodynamic consistency test on the investigated experimental data summarized in Table 7.14.

Set No.[*]	Test result
1	TI
3	TI
4	TI
5	TI
6	TI
7	TI
8	NFC[**]
9	NFC[**]
10	TI
11	TI
14	TC
15	TI

[*] The model has not resulted in acceptable deviations for the datasets 2, 12, and 13.

[**] The values of the integrals have been evaluated after elimination of about 25 % of the data in the corresponding data set.

and the assumptions made in the test. Therefore, some data which have not passed the consistency test may still be reliable data.

5. The thermodynamic consistency tests may provide only rough information about the data quality. The users must be very careful in keeping or removing these treated data from the database merely depending on the consistency test results. We recommend that the user keep all the data defined as fully consistent and some of the data declared as not fully consistent ones with the help of his/her own skills and experiences on the related subject.

Omitting one point from our discussion would be an oversight. In this work, we have studied many of isothermal phase equilibrium data available in open literature for the systems of interest. However, we are well aware that perhaps not all of the experimental data are fully trustable from an experimental point of view. This may be due to the inaccuracy of the used experimental techniques, as already mentioned. Furthermore, calibration of the pressure transducers, temperature probes, and gas chromatograph detectors are significant factors in defining the uncertainties of the experimental data, as explained previously. As a matter of fact, the results also suggest that new experimental techniques may lead to obtaining more reliable compositional data. However, we should be aware that PVT methods may have limitations. Non-destructive methods like RAMAN spectroscopy may contribute to more

promising results. However, these kinds of techniques are expensive. In the present work, as we were interested in defining only the data quality, consequently, we have focused on consistency tests while our objective has not been a comparison between the different experimental methods. More meticulous investigations should be made on the validity of the applied experimental techniques in future works.

7.2. Statistical evaluation for experimental hydrate dissociation data

With respect to the aforementioned criteria in the previous chapters/section, accurate and reliable phase equilibrium data are required to design the most efficient processes (either to prevent gas hydrate formation or to use it as a promising technique for other applications) and to adjust the parameters of the developed models (thermodynamic/numerical ones) for the corresponding phase equilibrium calculation/prediction.

Experimental phase equilibrium data (dissociation data) for simple clathrate hydrate systems e.g. CH_4, C_2H_6, C_3H_8, CO_2, N_2, H_2S, etc. have been extensively reported in the literature meanwhile the corresponding data for mixed hydrates (or those formed from binary hydrate formers) are more scarce.[2] Different experimental techniques such as phase equilibrium measurements using high pressure cell, Raman spectroscopy, nuclear magnetic resonance (NMR) spectroscopy, x-ray and neutron diffraction and so forth have been thus far applied for obtaining these data.[2,30]

Although the quantities of these reported data seem to be adequate for industrial applications, there may be no general method to check their qualities. However, two methods have been already employed to check the reliability of phase equilibrium data of the systems containing gas hydrates as follows:

I. The Clapeyron equation can be normally applied to determine the phase boundary of the clathrate hydrate systems.[2,9] The sketch of logarithm of dissociation pressure ($\log(P)$) vs. reciprocal temperature ($1/T$) generally exhibits a straight line (which shows the value of the enthalpy of hydrate formation). Thus, the hydrate dissociation data for any of the simple (or mixed) hydrate formers can be sketched to observe whether they show the same trends or not. However, it has been previously argued[30] that taking into account the effects of solubility of gases (especially for CO_2 and H_2S) and variation of the hydrate volume with temperature brings about a change in the slope of the $\log(P)$ vs. $1/T$ curve, as described in chapter 3. Therefore, a constant slope may not be expected particularly in the liquid water-hydrate-liquid hydrate former phase equilibrium region.[30]

II. Thermodynamic consistency tests are generally applied as a reliable method for assessment of the phase equilibrium data quality (refer to chapter 7.1). However, the applied consistency test method in this study is applicable only in the case of applicability of molar compositions

of equilibrium phases. It is worth pointing out that the studied phase equilibrium data include the molar compositions of the phases generally in three phase equilibrium conditions which are not necessarily the hydrate dissociation conditions. Such data are very scarce in the open literature. As a consequence, this method may not be an efficient technique of our concern in this work.

Hence, it is of much interest to propose a statistically-correct method for simultaneous detection of the doubtful data and their quality along with checking the validity and domain of applicability of available correlations[214,49] for representation/prediction of the phase equilibrium data of simple and mixed clathrate hydrates. In the present study, we use the Leverage approach [444-446] for this purpose. To the best of our knowledge, this is the first time that a statistical method is used for evaluation of such data.

7.2.1. Leverage approach

Outlier diagnostics (or detection) may be crucial in developing the mathematical models. Outlier detection is to identify individual datum (or groups of data) that may differ from the bulk of the data present in a dataset. The proposed methods for this purpose normally consist of numerical and graphical algorithms. One of the efficient and reliable statistical algorithm for outlier diagnostics is the Leverage approach.[444-446] The employed elements of this method includes the values of the residuals (i.e. the deviations of a model results from the experimental data) and a matrix known as Hat matrix composed of the experimental data and the represented/predicted values obtained from a correlation (or a model). Hence, a suitable mathematical model is also required to pursue the calculation steps of the algorithm.

The Leverage or Hat indices are determined as a Hat matrix (H) with the following definition:[444-446]

$$H = X(X^t X)^{-1} X^t \tag{7.33}$$

where X is a two-dimensional matrix composing n chemicals or data (rows) and k parameters of the model (columns) and t stands for the transpose matrix. The Hat values of the chemicals in the feasible region of the problem are, as a matter of fact, the diagonal elements of the H matrix.

The Williams plot is later sketched for graphical identification of the suspended data or outliers on the basis of the calculated H values through Eq. 7.33. This plot shows the correlation of Hat indices and standardized cross-validated residuals (R), which are defined as the difference between the represented/predicted values and the implemented data. A warning Leverage (H^*) is generally fixed at the value equal to $3n/p$, where n is number of training points and p is the number of model input parameters plus one. The leverage of 3 is normally considered as a "cut-off" value to accept the points within ± 3 range (two horizontal red lines)

standard deviations from the mean (to cover 99 % normally distributed data). Existence of the majority of data points in the ranges $0 \leq H \leq H^*$ and $-3 \leq R \leq 3$ reveals that both model development and its representations/predictions are done in applicability domain for a particular system. "Good High Leverage" points are located in domain of $H^* \leq H$ and $-3 \leq R \leq 3$. The Good High Leverage can be designated as the data, which are outside of applicability domain of the applied model. In other words, the model is not able to represent/predict the following data at all. The points located in the range of R < - 3 or 3 < R (whether they are larger or smaller than the H^* value) are designated as outliers of the model or "Bad High Leverage" points. These erroneous representations/predictions can be attributed to the doubtful data.

Correlations

Two generally acceptable correlations[214,492] for representation/prediction of the phase equilibria of simple/mixed clathrate hydrates in liquid water/ice-hydrate-vapor equilibrium region have been applied as follows:

I. For simple clathrate hydrates: [492]

$$P / \text{MPa} = 10^{-3} \exp(a' + b'(T/K)^{-1})$$ (7.34)

where a' and b' are the adjustable parameters of the correlation. The values of these parameters and the ranges of dissociation temperatures and the phase equilibrium regions, for which Eq. 7.34 has been recommended can be found elsewhere.[2,493]

II. For mixed clathrate hydrates of $CO_2 + CH_4/N_2$:[214]

$$\ln(P / \text{MPa}) = A + B(T/K)^{-1} + Cy + D(T/K)^{-2} + Ey(T/K)^{-1} + Fy^2$$ (7.35)

where y is the mole percent of CO_2 in the feed gas, A, B, C, D, E, and F are adjustable parameters. Adisasmito et al. [214] have reported the values of these parameters to determine the phase behavior of the clathrate hydrates of $CO_2 + CH_4$. In addition, the optimal values of the corresponding parameters for the $CO_2 + N_2 +$ water system have been herein evaluated. Both sets of the parameters are reported in Table 7.16.

Experimental data

Selected experimental gas hydrate dissociation data for the systems containing simple hydrate formers (CH_4, C_2H_6, C_3H_8, CO_2, N_2, and H_2S)[216,323,423,462,492-525] and mixed hydrate formers ($CO_2 + CH_4/N_2$) [214, 217,220,517,526-529] in L_w-H-V and/or I-H-V regions have been treated in this work. Table 7.17 reports the ranges of the experimental data along with their sources.

Table 7.16: Parameters in Eq. 7.35.

System	Parameters[*]					
	A	*B*	*C*	*D*	*E*	*F*
$CO_2 + CH_4$	175.3	-89009	0.07392	11307000	-23.392	0.000039566
$CO_2 + N_2$[**]	415.2	-219543	0.28337	29198870	-1330.392	1.969164551

[*] The numbers of the digits of the parameters have been determined by sensitivity analysis of the results to the values of these parameters.
[**] The parameters have been evaluated assuming no structural change of clathrate hydrates.

7.2.2. Results of the statistical approach

The absolute relative deviations of the correlations results from the experimental values for simple[216,323,423,462,492-525] and mixed clathrate hydrates[214, 217,220,517,526-529] show that the employed correlations[214,492,489] are generally acceptable to be used for the Leverage statistical approach.[444-446]

To pursue our objectives, the H values have been calculated through Eq. 7.33 and the Williams plots have been sketched in Figures 7.3 to 7.22. The warning Leverages (H^*) have been fixed at $3n/p$ for the whole data. In addition, the recommended cut-off value of 3 has been applied.

The following results are interpreted from application of the aforementioned methodology:

1. Accumulation of the data points in the ranges $0 \leq H \leq H^*$ and $-3 \leq R \leq 3$ for each dissociation datasets for clathrate hydrates of the investigated simple or mixed hydrate formers reveals that the applied correlations are statistically valid for representation/prediction of these experimental values.

2. The whole hydrate dissociation data points may be declared to within the applicability domain of the correlations except one point in the corresponding data of carbon dioxide in L_w+V+H region, three points of ethane hydrate dissociation data in L_w+V+H region, one point of hydrogen sulfide hydrate dissociation data in L_w+V+H region, and five points of methane hydrate dissociation data in L_w+V+H region. In addition, good high leverage points are accumulated in the domains of $H^* \leq H$ and $-3 \leq R \leq 3$. These points may be declared to be outside of applicability domain of the applied correlation; however, cannot be assigned as doubtful experimental data. It should be noted that, in the case of detecting good high leverage points, it is recommended to use/develop other models or correlations on the basis of different theoretical approaches for their calculations/estimations in order to avoid obtaining results through biased model calculations.

Table 7.17: The range of experimental data for simple[216,323,423,462,492-525] and mixed clathrate hydrates[2214, 217,220,517,526-529] treated in this work.

Hydrate former	Equilibrium region	T range / K	P range / MPa	Ref.[*]
Methane	(L_w+H+V)	273.49 to 297.58	2.716 to 42.35	323,489, 493-499
Methane	$(I+H+V)$	268.4 to 271.28	2.324 to 2.513	216
Ethane	(L_w+H+V)	278.3 to 287.61	1.300 to 3.244	462,500-507
Ethane	$(I+H+V)$	200.8 to 272.0	0.008 to 0.457	503,506,508
Propane	(L_w+H+V)	273.25 to 278.55	0.172 to 0.547	499,502,506, 509-514
Propane	$(I+H+V)$	251.4 to 272.9	0.058 to 0.172	506,514,515
Carbon dioxide	(L_w+H+V)	273.36 to 283.05	1.31 to 4.10	216,418, 516-520
Carbon dioxide	$(I+H+V)$	263.17 to 271.17	0.774 to 1.037	216,516
Nitrogen	(L_w+H+V)	273.67 to 309.43	16.54 to 425.19	423,494,499
Nitrogen	$(I+H+V)$	261.7 to 270.2	11.25 to 13.80	521
Hydrogen sulfide	(L_w+H+V)	272.8 to 302.7	0.093 to 2.239	521-525
Hydrogen sulfide	$(I+H+V)$	250.5 to 272.8	0.044 to 0.087	514,522
Carbon dioxide + Methane	(L_w+H+V)	272.66 to 287.60	1.45 to 10.95	214,217, 56-528
Carbon dioxide + Nitrogen	(L_w+H+V)	272.85 to 284.25	1.22 to 22.23	220,517,529

[*] Sources of the experimental data.

3. The data points located in the range of R < - 3 or 3 < R (ignoring their H values) are designated as outliers or bad high leverage points, as already described. All the hydrate dissociation data for the investigated systems seem to be valid (not outliers) except one point in the corresponding data of carbon dioxide in L_w+V+H region, two points of ethane hydrate dissociation data in L_w+V+H region, one point of methane hydrate dissociation data in L_w+V+H region, one point of nitrogen hydrate dissociation data in L_w+V+H region, three points in the experimental hydrate dissociation data of the $CO_2 + CH_4$ system, and one point in the corresponding data of the $CO_2 + N_2$ system. These erroneous representations/predictions may be attributed to the doubtful hydrate dissociation data.

4. The data points in the ranges $H^* \leq H$ and $R < -3$ or $3 < R$ may be designated as neither within the applicability domain of the applied correlation nor valid data. In other words, these data cannot be well calculated/estimated by the correlation and meanwhile attributed as suspended data points. There is one point of ethane hydrate dissociation data in L_w+V+H region, one point of methane hydrate dissociation data in L_w+V+H region, and one point of corresponding data for hydrogen sulfide in L_w+V+H region that can be categorized in this group.

Figure 7.3: Detection of the probable doubtful experimental data[323,489,493-499] and the applicability domain of the applied correlation for the CH_4 clathrate hydrate system in the L_w-H-V region. The H^* value is 0.073.

5. The quality of the treated data (even different data in the same dataset) are different. The data with lower absolute R values (near $R=0$ line) and lower H values may be declared as the more reliable experimental data.

One element should not be omitted from our discussion. Our aim herein has been to justify the quality of the investigated data in a statistical way. Conclusion about the accuracy and reliability of the applied experimental techniques and procedures for obtaining these data merits future detailed investigations.

Figure 7.4: Detection of the probable doubtful experimental data[216] and the applicability domain of the applied correlation for the CH_4 clathrate hydrate system in the I-H-V region. The H^* value is 1.500.

Figure 7.5: Detection of the probable doubtful experimental data[462,500-507] and the applicability domain of the applied correlation for the C_2H_6 clathrate hydrate system in the L_w-H-V region. The H^* value is 0.077.

Figure 7.6: Detection of the probable doubtful experimental data[503,506,508] and the applicability domain of the applied correlation for the C_2H_6 clathrate hydrate system in the I-H-V region. The H^* value is 0.545.

Figure 7.7: Detection of the probable doubtful experimental data[499,502,506,509-514] and the applicability domain of the applied correlation for the C_3H_8 clathrate hydrate system in the L_w-H-V region. The H^* value is 0.088.

Figure 7.8: Detection of the probable doubtful experimental data[506,514,515] and the applicability domain of the applied correlation for the C_3H_8 clathrate hydrate system in the I-H-V region. The H^* value is 0.316.

Figure 7.9: Detection of the probable doubtful experimental data[216,418,516-520]and the applicability domain of the applied correlation for the CO_2 clathrate hydrate system in the L_w-H-V region. The H^* value is 0.857.
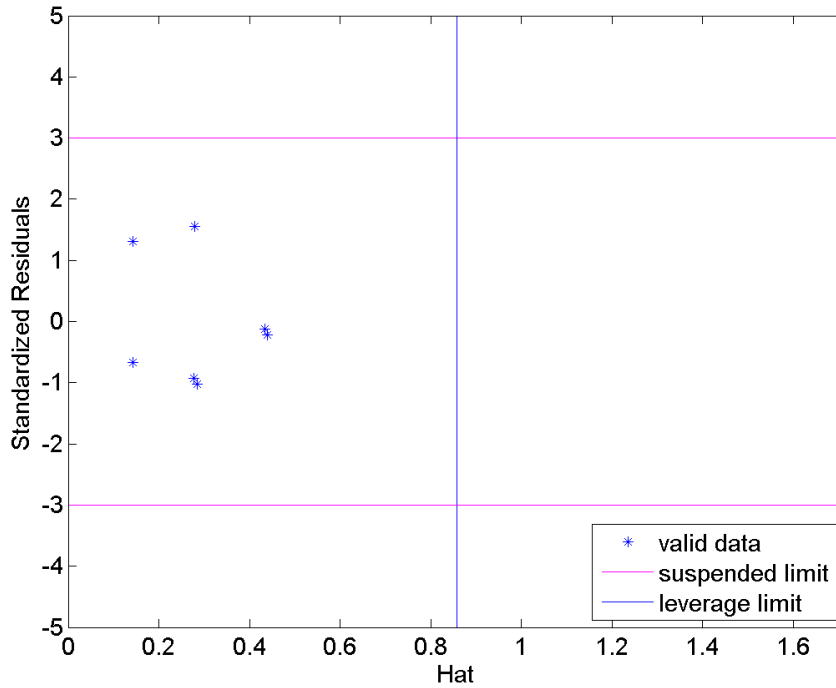
Figure 7.10: Detection of the probable doubtful experimental data[216,516] and the applicability domain of the applied correlation for the CO_2 clathrate hydrate system in the I-H-V region. The H^* value is 0.857.
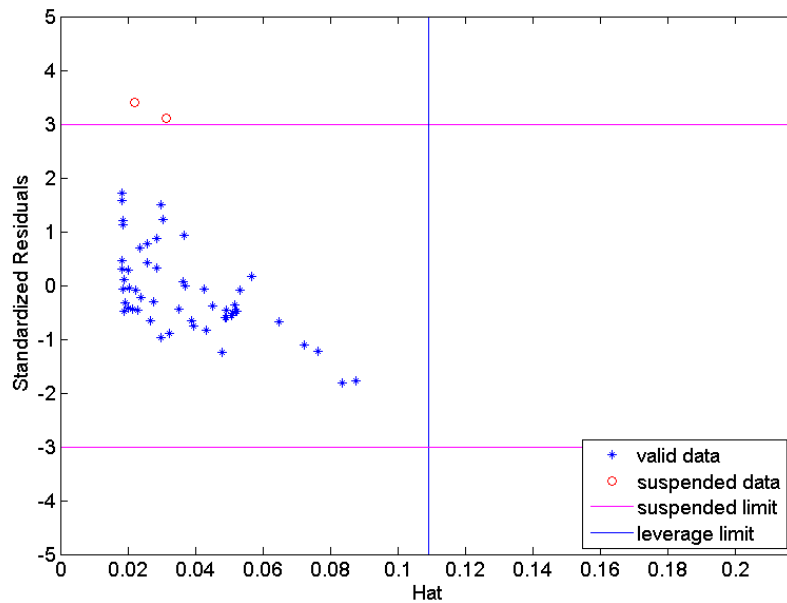
Figure 7.11: Detection of the probable doubtful experimental data[423,494,499] and the applicability domain of the applied correlation for the N_2 clathrate hydrate system in the L_w-H-V region. The H^* value is 0.109.
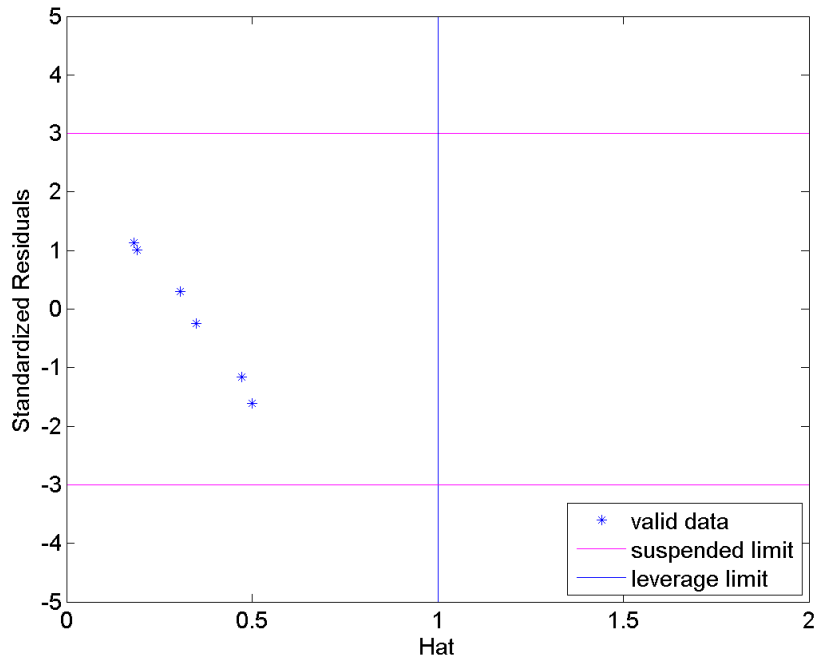
Figure 7.12: Detection of the probable doubtful experimental data[521] and the applicability domain of the applied correlation for the N_2 clathrate hydrate system in the I-H-V region. The H^* value is 1.000.
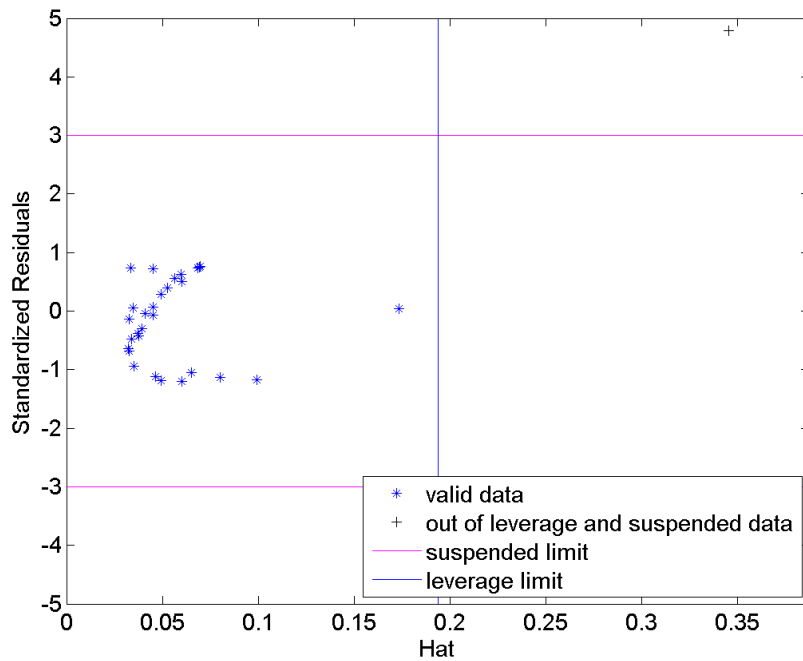
Figure 7.13: Detection of the probable doubtful experimental data[521-525] and the applicability domain of the applied correlation for the H_2S clathrate hydrate system in the L_w-H-V region. The H^* value is 0.194.
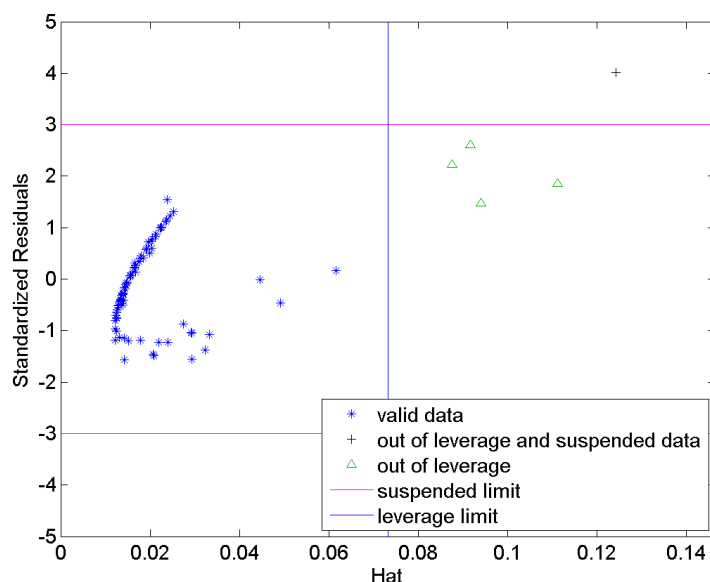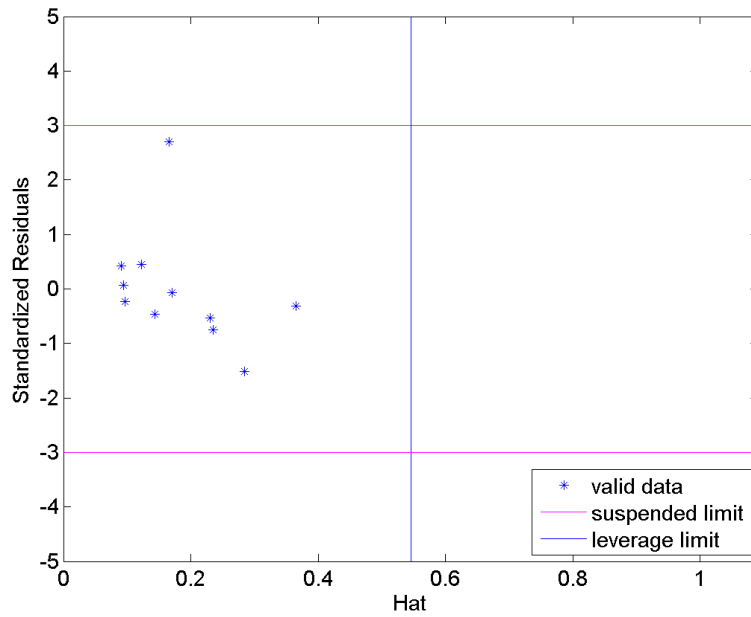
Figure 7.14: Detection of the probable doubtful experimental data[514,522] and the applicability domain of the applied correlation for the H_2S clathrate hydrate system in the I-H-V region. The H^* value is 0.545.
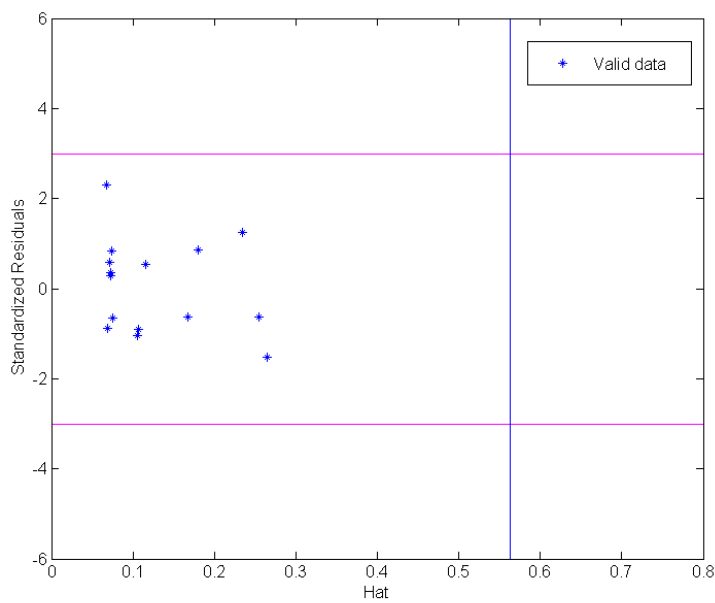
Figure 7.15: Detection of the probable doubtful experimental data[526] and the applicability domain of the applied correlation for the CO_2 + CH_4 clathrate hydrate system in the L_w-H-V region. The H^* value is 0.562.
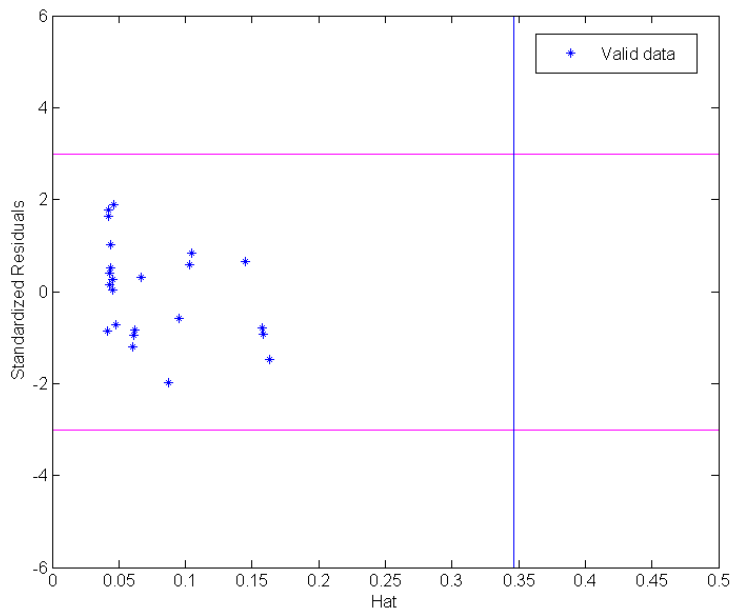
Figure 7.16: Detection of the probable doubtful experimental data[527] and the applicability domain of the applied correlation for the $CO_2 + CH_4$ clathrate hydrate system in the L_w-H-V region. The H^* value is 0.346.
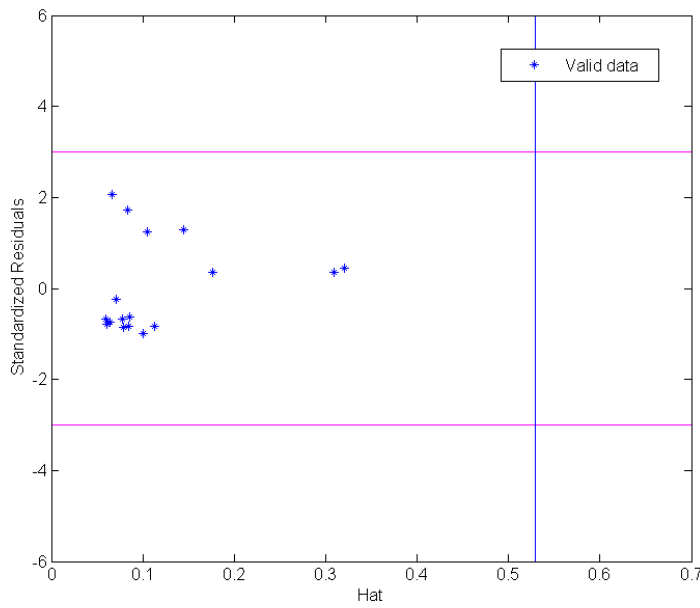
Figure 7.17: Detection of the probable doubtful experimental data[528] and the applicability domain of the applied correlation for the $CO_2 + CH_4$ clathrate hydrate system in the L_w-H-V region. The H^* value is 0.529.
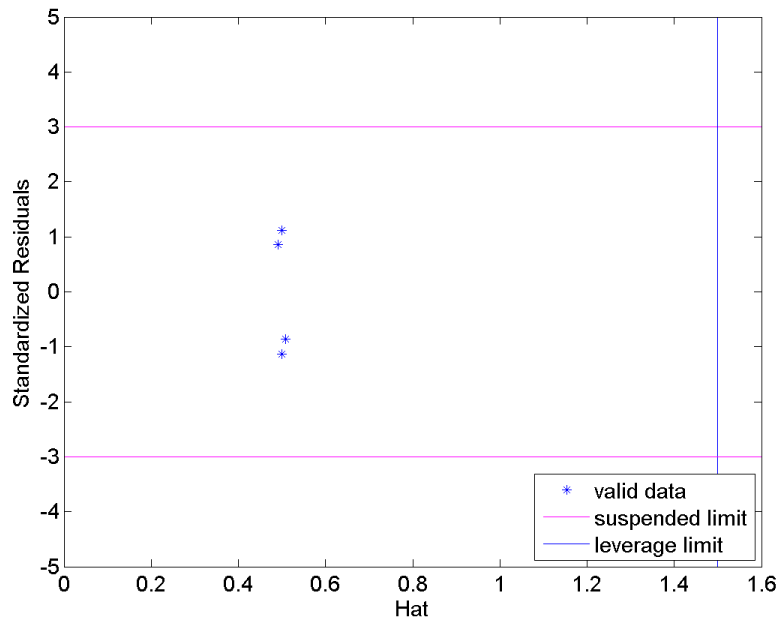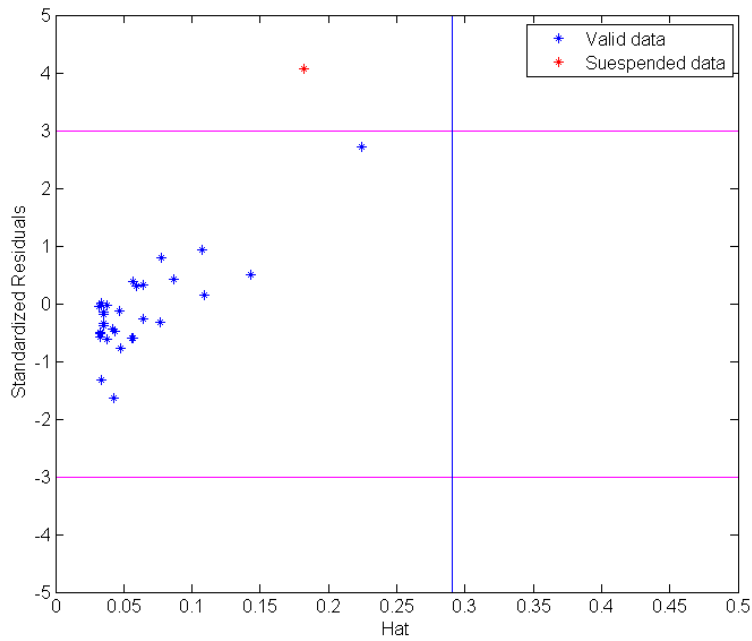
Figure 7.18: Detection of the probable doubtful experimental data[217] and the applicability domain of the applied correlation for the $CO_2 + CH_4$ clathrate hydrate system in the L_w-H-V region. The H^* value is 0.290.
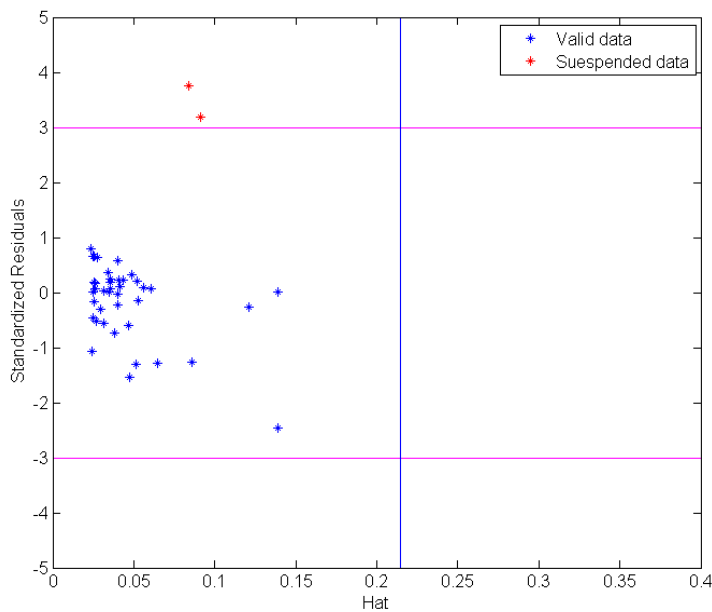
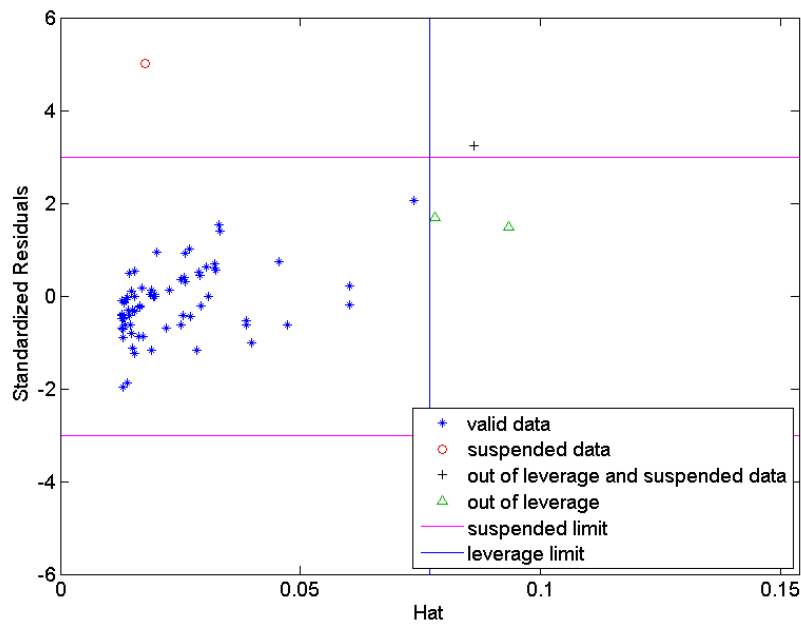**Figure 7.19:** Detection of the probable doubtful experimental data[214] and the applicability domain of the applied correlation for the $CO_2 + CH_4$ clathrate hydrate system in the L_w-H-V region. The H^* value is 0.214.
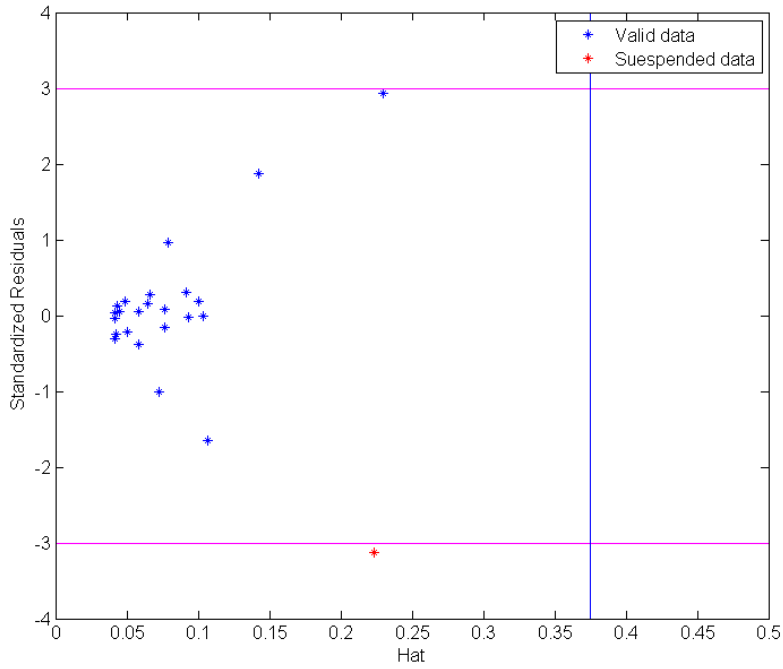
Figure 7.20: Detection of the probable doubtful experimental data[220] and the applicability domain of the applied correlation for the $CO_2 + N_2$ clathrate hydrate system in the L_w-H-V region. The H^* value is 0.375.
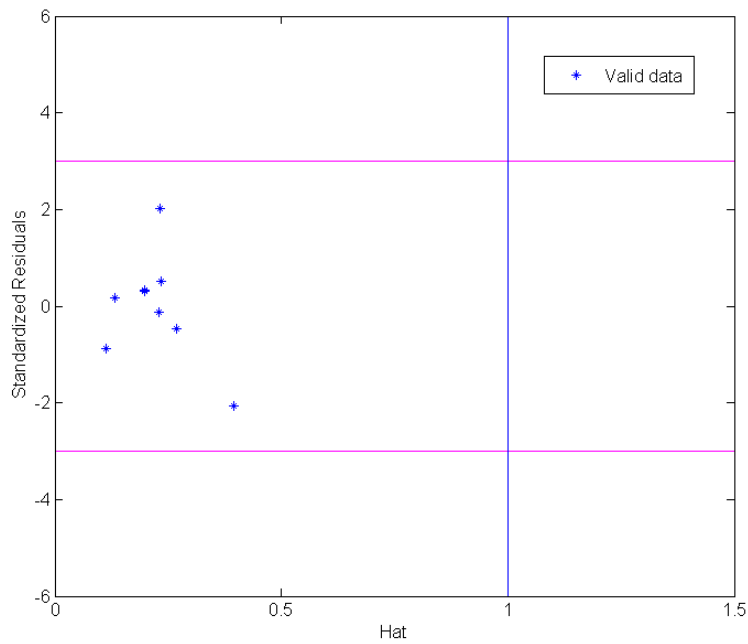
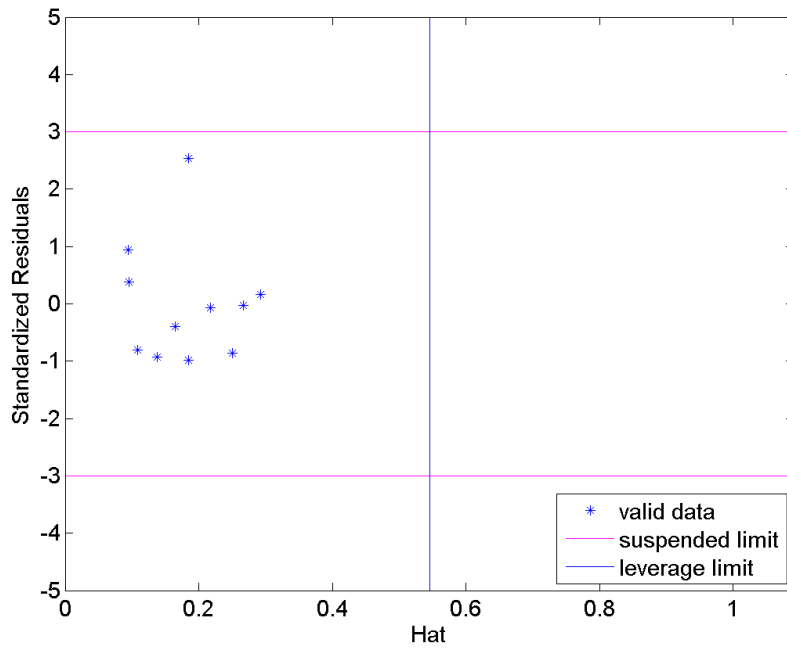**Figure 7.21:** Detection of the probable doubtful experimental data[517] and the applicability domain of the applied correlation for the $CO_2 + N_2$ clathrate hydrate system in the L_w-H-V region. The H^* value is 1.000.
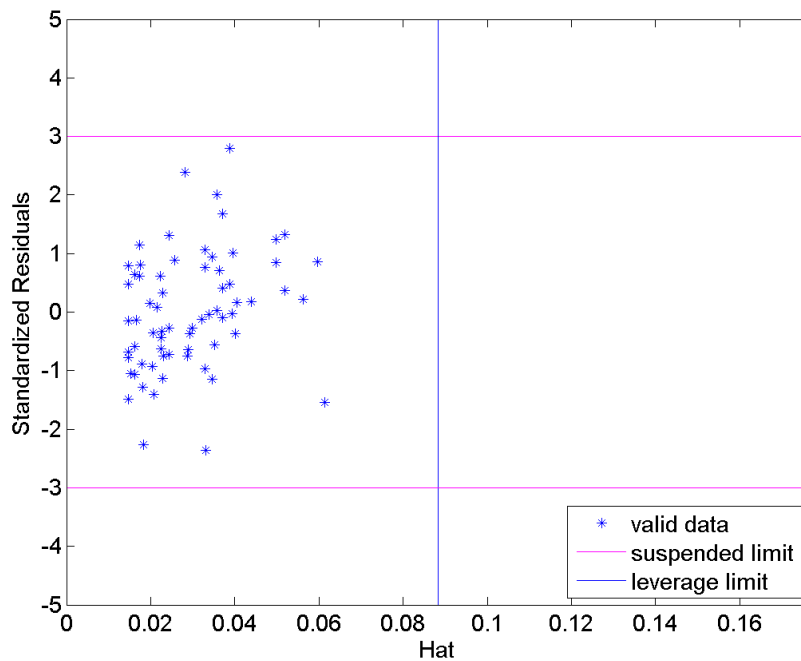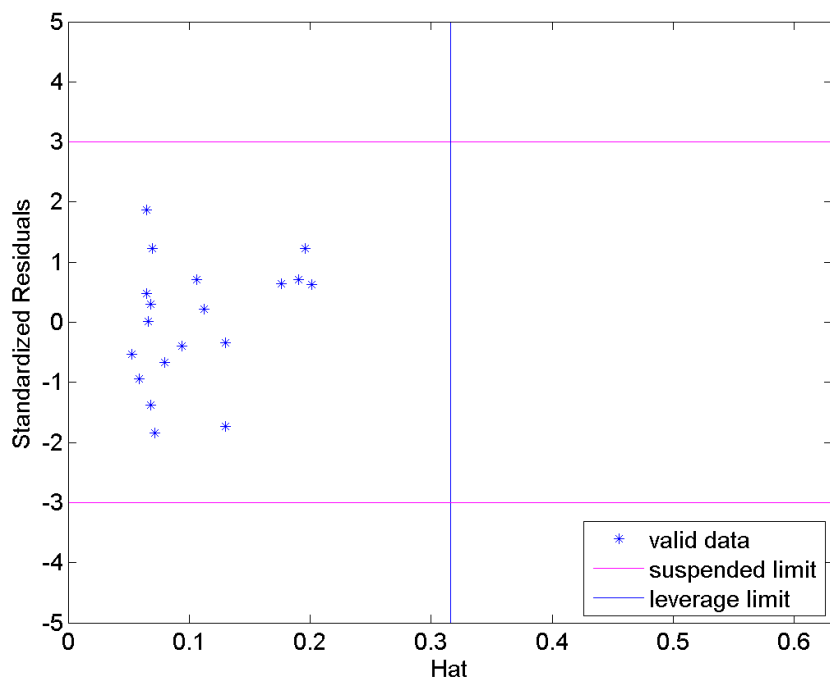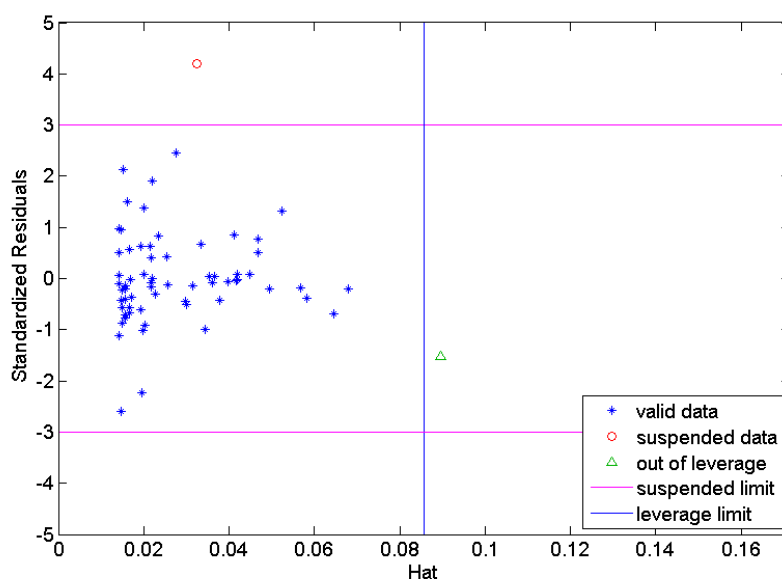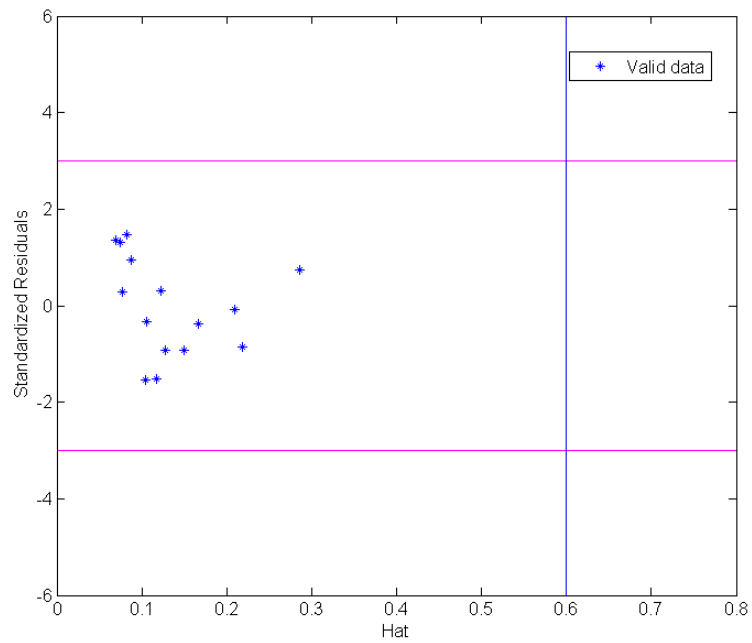
Figure 7.22: Detection of the probable doubtful experimental data[529] and the applicability domain of the applied correlation for the CO_2 + N_2 clathrate hydrate system in the L_w-H-V region. The H^* value is 0.600.

8. Conclusions

Conclusions

L'objectif principal de ce travail était d'effectuer diverses études thermodynamiques sur les équilibres de phases en présence de clathrates/semi-clathrates hydrates avec l'objectif final de leur utilisation potentielle en vue de la conception de procédés de capture et de séquestration du CO_2. Afin de poursuivre cet objectif, les étapes d´études suivantes, accompagnées, le cas échéant, par les conclusions correspondantes, ont été menées:

1. Tout d´abord nous avons fait une brève introduction sur hydrates de gaz, y compris sur leur découverte et sur leurs différentes caractéristiques.

2. Nous avons examiné et discuté en détail l´utilisation des clathrates hydrates et semi-clathrates hydrates pour les procédés de séparation ainsi que les études expérimentales sur la séparation des gaz à effet de serre, la séparation de l'hydrogène et de l'azote, le fractionnement du pétrole et du gaz, les procédés de dessalement, la séparation de différentes substances provenant d´organismes vivants, et la séparation de liquides ioniques de leurs solutions aqueuses diluées. On a montré que les études réalisées à ce jour concernent un domaine très diversifié de la recherche en chimie, physique, sciences de la terre et de l'environnement, bio-ingénierie et procédés pharmaceutiques pour n'en nommer que quelques-uns. Il est maintenant évident que la technologie de formation des hydrates de gaz jouera un rôle important dans l'avenir des procédés de séparation et a le potentiel d'être, peut-être, une technique plus durable que les technologies commerciales actuelles. Il faut noter que l'un des facteurs importants dans la prise de décisions pour les technologies de remplacement est l'aspect économique. Les nouvelles techniques ou méthodes proposées qui visent à remplacer les procédés traditionnels devraient être économiquement rentables. Cependant, il y a très peu d'études économiques détaillées disponibles dans la littérature sur les procédés de séparation via la technologie de formation d'hydrates de gaz. Par conséquent, il est impératif que plus d'études de cette nature soient entreprises dans un avenir proche pour démontrer la viabilité de cette technologie. Pour récapituler, notre revue justifie l'importance des mesures expérimentales (telles que celles du comportement de phases) pour les procédés de séparation utilisant la cristallisation des hydrates de gaz. Il est à noter que ces études expérimentales devraient être accompagnées de travaux théoriques (comme la modélisation thermodynamique) afin de clarifier les différents aspects nouveaux et applications des clathrates hydrates et semi-clathrates hydrates de gaz dans les technologies de séparation et donc convaincre l'industrie d´investir, à l'avenir, dans ces nouveaux procédés.

3. Par la suite, un examen concis des modèles thermodynamiques disponibles dans la littérature a été présenté. Les différentes caractéristiques de chaque groupe de modèles ont été

également brièvement discutées. Il a été démontré qu'il existe un besoin impératif de développement de modèles fiables pour la représentation et le calcul des équilibres de phases des semi-clathrates hydrates car encore très rares.

4. Un modèle thermodynamique a été proposé pour calculer/estimer les conditions de la dissociation des semi-clathrates hydrates de CO_2 et CH_4/N_2 en présence de solutions aqueuses de TBAB. Le modèle a été développé sur la base de la théorie des solutions solides de van der Walls et Platteeuw (vdW-P)[319,320] avec modification des expressions de détermination des constantes de Langmuir et de la pression de vapeur d'eau dans le réseau d´hydrates vides. En complément l´équation d´état cubique de Peng et Robinson (PR-EoS)[393] et la fonction alpha de Mathias-Copeman, (MC)[394] contenant des paramètres réajustés ont été utilisées pour le calcul de la fugacité en phase gazeuse des formeurs d'hydrates gazeux. La capacité du modèle à prévoir les équilibres de phases en présence d'eau des clathrates hydrates simples a été vérifiée avec succès avant son extension aux semi-clathrates hydrates. Les valeurs optimales des paramètres du modèle ont été obtenues en minimisant l´écart entre les résultats calculés par le modèle et les valeurs expérimentales obtenues pour les systèmes de CO_2 en solutions aqueuses de TBAB. Les paramètres ajustés ont été ensuite utilisés pour estimer les conditions de dissociation des semi-clathrates hydrates de CO_2 et CH_4/N_2 en présence de solution aqueuse de TBAB. On ainsi pu observer un accord acceptable entre les résultats du modèle et les données expérimentales sélectionnées dans la littérature et énoncer les remarques suivantes:

I. Le modèle développé peut ne pas être capable de prédire les changements structurels possibles des semi-clathrates hydrates sur de larges plages de températures-pressions-compositions de TBAB en solutions aqueuses.

II. Les effets de promotion ou d'inhibition de TBAB peuvent être bien représentés/prédits en utilisant le modèle proposé.

III. Le fait que ce modèle découle d´un développement simple et aussi le fait qu´il contient des paramètres faciles à utiliser sont parmi les avantages significatifs notables constatés.

IV. Le modèle thermodynamique peut ne pas être applicable pour la prévision des équilibres S-L du système eau + TBAB.

V. Il y a possibilité d'extension du modèle au calcul et à l´estimation du comportement de phases des semi-clathrates hydrates formés à partir de mélanges binaires de gaz.

5. Il a d'abord été constaté, suite à une recherche bibliographique préliminaire, que les données d'équilibres de phases de semi-clathrates hydrates dans le cas des solutions aqueuses de (CO_2 + N_2/CH_4/H_2 + TBAB) sont rares. Par conséquent, des mesures expérimentales de dissociation de semi- clathrates hydrates ont été réalisées (et tabulées), et ce, par utilisation de deux équipements développés en interne notamment pour les mesures d'équilibres de phases en présence d'hydrates de gaz sur les systèmes suivants:

1. CO_2 (fractions molaires : 0,151/0,399) + N_2 (fractions molaires : 0,849/0,601) + eau et + solutions aqueuses de TBAB (0,05/0,15/0,30 en fractions massiques).

2. CO_2 (fraction molaire : 0,399) + CH_4 (fraction molaire : 0,601) + solutions aqueuses de TBAB (fractions massiques : 0,05/0,10).

3. CO_2 (fractions molaires : 0,151/0,399/0,749) + H_2 (fractions molaires : 0,849/0,601/0,251) + eau et + solutions aqueuses de TBAB (0,05/0,30 en fractions massiques).

Les mesures d'équilibres de phases couvrent les gammes (275,1 à 293,2) K et (de 1,12 à 16,74) MPa, qui sont des domaines de conditions opératoires industrielles favorables pour les procédés de capture du CO_2 par formation d'hydrates de gaz. Il a également été discuté le fait que le type de semi-clathrates hydrates peut changer en fonction de la concentration en solution aqueuse du TBAB, en vertu d´une potentialité de transformation structurelle du type A vers le type B et vice versa. Ce phénomène de transformation de type rend les mesures d´équilibre particulièrement difficile à maitriser. Il a été déterminé à partir des résultats expérimentaux que l'augmentation de la concentration de TBAB en tant que promoteur (pour des valeurs des rapports TBAB / eau des clathrates hydrates inférieures à celle du rapport stœchiométrique) contribue à un procédé de séparation du CO_2 plus efficace qu´une technique classique de formation d'hydrates, en présence d'eau. Cependant, des études plus complètes et plus détaillées devraient être effectuées afin de déterminer la concentration optimale de la solution aqueuse de TBAB, en accord avec les conditions de séparation: pression et température.

6. La détermination de la composition molaire des clathrates hydrates mixtes contenant du dioxyde de carbone est d'une grande importance pour la conception de procédés de capture du CO_2 par la méthode de cristallisation sous forme d'hydrates de gaz. Dans ce travail, une approche par bilans de matière, a été suivie à cet effet. Afin de résoudre les équations non-linéaires de bilans de matière, un algorithme mathématique a été développé sur la base de la méthode numérique de Newton [431] associée à la « *differential evolution optimization strategy* ».[406,407] Les mesures d'équilibres de phases avec hydrate de gaz, précédemment réalisées dans notre laboratoire (CEP / TEP),[59,426] y compris celles des compositions de la phase vapeur en équilibre avec l'hydrate de gaz et l'eau liquide ont été utilisées comme banque de données expérimentales. Les compositions molaires déterminées en utilisant la méthode susmentionnée (et aussi les données expérimentales retenues concernant les conditions de dissociation des hydrates et les compositions de la phase vapeur)

ont été comparées aux prédictions du modèle thermodynamique fiable, à savoir CSMGem.[2] Il a ainsi été montré que ce modèle thermodynamique peut prédire de façon acceptable les conditions de dissociation d'hydrates pour les systèmes : $CO_2 + CH_4/N_2$ + eau, étudiées dans ce travail. Bien que le modèle CSMGem prédise de façon acceptable la composition de la phase gazeuse en équilibre avec de l'hydrate de gaz et celle de la phase aqueuse pour les systèmes $CO_2 + CH_4/N_2$ + eau, il semble peu fiable lorsqu'il s'agit de la prédiction des compositions de la phase hydrate.

7. Dans l'étape finale, il a été évoqué que les résultats des mesures d'équilibres de phases peuvent être entachées d´incertitudes considérables en raison de difficultés inévitables et des possibles sources d'erreurs lors des déterminations expérimentales. Par conséquent, deux approches ont été proposées dans ce travail afin de conclure quant à la qualité des données expérimentales d'équilibres de phases des systèmes contenant des clathrates hydrates. La première méthode appliquée utilise l´équation de Gibbs-Duhem à température constante. [440-443]. Cet algorithme a été suivi pour vérifier la fiabilité des données expérimentales d'équilibres de phases dans les cas suivants: teneur en eau du méthane en équilibre avec de l'hydrate de gaz, de l'eau liquide ou de la glace; données de solubilité du dioxyde de carbone et du méthane dans l'eau, à l'intérieur et l'extérieur de la région de formation des hydrates de gaz, et compositions de la phase vapeur en équilibre avec des hydrates de gaz et de l'eau liquide des systèmes : dioxyde de carbone + (méthane ou azote) + eau. Les données expérimentales traitées ont été finalement déclarées comme probablement thermodynamiquement cohérentes ou incohérentes, ou comme pas totalement cohérentes. Toutefois, il convient de souligner que l'évaluation des données d'équilibres de phases réalisée est inévitablement dépendante du modèle, car il n'y a aucun moyen de mesurer directement les paramètres requis pour le test de cohérence, y compris les coefficients de fugacité. En outre, les tests de cohérence thermodynamique ne peuvent fournir que des informations approximatives de la qualité des données.

La deuxième approche est une méthode statistique faisant appel au concept du levier. [444-446] Elle a été utilisée pour vérifier la fiabilité des données de dissociation concernant les hydrates de CH_4, C_2H_6, C_3H_8, CO_2, N_2, H_2S et celles concernant les clathrates hydrates mixtes de $CO_2 + CH_4/N_2$. Deux corrélations simples recommandées [214,492] ont été appliquées pour représenter / prédire ces données. Les résultats montrent que : - les corrélations appliquées sont valides et statistiquement correctes ; - parmi le domaine complet des données de dissociation d'hydrates, 10 sont jugées en dehors du domaine d'application des corrélations employées ; - 8 sont désignées comme probablement inacceptables. Les résultats mentionnés ci-dessus peuvent être utilisés pour conclure à propos de la qualité des données, qui sont censées intervenir lors de l´ajustement des modèles thermodynamiques de représentation/prédiction des équilibres de phases avec clathrates hydrates à partir des formeurs d'hydrates concernés.

Pour récapituler, nous recommandons aux utilisateurs de construire un ensemble comprenant toutes les données définies comme cohérentes et qui ne peuvent être déclarées comme aberrantes dans le cadre de l´approche statistique appliquée[444-446] ainsi qu´une partie des données pas entièrement cohérentes, en vue de l´ajustement des paramètres des modèles thermodynamiques et de leur application en conception de procédés. Ensuite, sur la base de leurs propres expériences, les utilisateurs pourront tirer certaines conclusions quant aux données thermodynamiques jugées incohérentes qui peuvent passer le test de l'approche statistique.[444-446] Toutefois, nous leur conseillons vivement de ne pas utiliser les données qui ne peuvent satisfaire aucun des tests.

The main objective of this work was to perform various thermodynamic studies on phase equilibria of clathrate/semi-clathrate hydrates with the final aim of their potential utilization in CO_2 capture and sequestration process. To pursue this goal, the following investigation steps were undertaken along with their eventual subsequent conclusions:

1. A brief introduction to gas hydrates including their discovery and different features was first presented.

2. The application of clathrate/semi-clathrate hydrates for separation processes including experimental studies on separation of greenhouse gases, separation of hydrogen and nitrogen, oil and gas fractionation, desalination processes, separation of different substances from living organisms, and separation of ionic liquids from their dilute aqueous solutions was later reviewed and discussed in details. It was argued that the studies preformed to date show a diverse field of research in chemistry, physics, earth and environmental sciences, bioengineering, and pharmaceutical processes to name a few. It is evident that gas hydrate formation technology will play a significant role in the future of separation processes and has the potential to be, perhaps, a more sustainable technique than current comparable commercial technologies for separation. It should be noted that one of the significant factors in decision making for alternative technologies is the economical aspect. The novel proposed techniques or methods which are meant to replace the traditional processes should be economically feasible. However, there are very few detailed economic studies on separation processes using gas hydrate formation technology available in the open literature. Hence, it is imperative that more studies of this nature are undertaken in near future to truly ascertain the sustainability of gas hydrate technology. To recapitulate, this review demonstrates the importance of experimental measurements (such as phase behavior) on separation processes utilizing gas hydrate crystallization. It should be noted that these experimental studies should be accompanied by theoretical investigations (like thermodynamic modeling) in order to clarify different novel aspects and applications of gas clathrate/semi-clathrate hydrates in separation technologies and consequently persuade the industry to invest in this in the future.

3. Later, a concise review on the thermodynamic models available in open literature was presented. The various characteristics of each group of models were also discussed in brief. It was shown that there is imperative need for developing reliable models for representation/prediction of phase equilibria of semi-clathrate hydrates since they are very scarce.

4. A thermodynamic model was proposed to calculate/estimate the dissociation conditions of the semi-clathrate hydrates of $CO_2/CH_4/N_2$ in the presence of TBAB aqueous solution. The model was developed on the basis of the solid solution theory of the vdW-P[319,320] with modification of the expressions to determine the vapor pressure of water in empty hydrate lattice and the Langmuir constants. Additionally the PR EoS[393] along with the Mathias-Copeman alpha function[394] containing re-tuned parameters were applied for calculation of the fugacity of the gaseous hydrate formers in the gas phase. The capability of

the model for prediction of the phase equilibria of the corresponding simple clathrate hydrates in the presence of water was successfully checked prior to extension to the semi-clathrate hydrates. The optimal values of the model parameters were obtained minimizing the deviation of the calculated model results compared to the selected data of the CO_2 + TBAB aqueous solution system. The tuned parameters were later used to estimate the semi-clathrate hydrate dissociation conditions of $CO_2/CH_4/N_2$ in the presence of TBAB aqueous solution. Acceptable agreement between the model results and selected experimental data from the literature were observed. In addition, the following factors have been observed from the model results:

I. The developed model may not be capable of prediction of the possible structural changes of the semi-clathrate hydrates in wide ranges of temperature-pressure-composition of the TBAB in aqueous solution.

II. The promotion or inhibition effects of the TBAB can be well-represented/predicted using the proposed model.

III. Easy-to-use model parameters and straight-forward development of this model are among significant advantages.

IV. The thermodynamic model is not applicable for prediction of the S-L equilibria of the TBAB + water system. In addition, the proposed model for the liquid phase cannot be used for complete liquid phase calculations.

V. There is a possibility for the extension of the model to calculate/estimate the phase behaviors of the semi-clathrate hydrates formed from binary mixtures of the investigated gases.

5. It was first inferred, through a preliminary literature survey, that phase equilibrium data of semi-clathrate hydrates for the (CO_2 + $N_2/CH_4/H_2$ + TBAB) aqueous solution systems are scarce. Therefore, experimental semi-clathrate hydrate dissociation data were measured and reported for the following systems using two equipment developed in-house particularly for gas hydrates phase equilibrium measurements:

I. CO_2 (0.151/0.399 mole fraction) + N_2 (0.849/0.601 mole fraction) + TBAB aqueous solution (0.05/0.15/0.30 mass fraction) or water.

II. CO_2 (0.399 mole fraction) + CH_4 (0.601 mole fraction) + TBAB aqueous solution (0.05/0.10 mass fraction).

III. CO_2 (0.151/0.399/0.749 mole fraction) + H_2 (0.849/0.601/0.251 mole fraction) + TBAB aqueous solution (0.05/0.30 mass fraction) or water.

The measured phase equilibrium data cover the (275.1 to 293.2) K temperature range and (1.12 to 16.74) MPa pressure range, which contain favorable industrial conditions for CO_2 capture processes applying gas hydrate formation technique. It was also discussed that the type of the semi-clathrate hydrates may change depending on the concentration of TBAB in aqueous solution i.e. the types have the potential of structural change from type A to B vice versa. This phenomenon may make such measurements to be generally difficult to manage.

It was determined from the experimental results that introducing TBAB as a promoter (below stoichiometric ratios of the clathrate hydrates of TBAB + water) contributes to a more efficient CO_2 separation process compared with a conventional hydrate formation technique in the presence of water. However, more detailed studies should be performed for determination of the optimal concentration of TBAB aqueous solution, and suitable pressure-temperature conditions for separation purposes.

6. Determination of the molar composition of the hydrate phase for mixed clathrate hydrates containing carbon dioxide is of great significance to design the CO_2 capture processes using gas hydrate formation method. A material balance approach was pursued for this purpose. In order to solve the non-linear mass balance equations, a mathematical algorithm was developed on the basis of the Newton's numerical method[431] coupled with the differential evolution optimization strategy.[406,407] Previously generated gas hydrate phase equilibrium data[59,426] in our laboratory (CEP/TEP) including the compositions of vapor phase in equilibrium with gas hydrate and liquid water were applied as experimental datasets. The determined molar compositions using the mentioned method (and also the applied experimental data of hydrate dissociation conditions and compositions of vapor phase) were compared with predictions of the reliable thermodynamic model, namely CSMGem.[2] It was shown that the aforementioned thermodynamic model can acceptably predict hydrate dissociation conditions for the CO_2 + CH_4/N_2 + water systems studied in this work. While the CSMGem[2] model acceptably predicts the composition of the gas phase in equilibrium with gas hydrate and aqueous phases for the CO_2 + CH_4/N_2 + water systems studied in this work, it seems that its prediction results for the compositions of the hydrate phase have generally high deviations.

7. In the final step, it was discussed that experimental phase equilibrium data may have considerable uncertainties due to inevitable difficulties and possible sources of errors during experimental measurements. Therefore, two approaches were proposed in this work to conclude about the quality of experimental phase equilibrium data for the systems containing clathrate hydrates. The first applied method benefits from the principles of the "Gibbs-Duhem equation"[440-443] at constant temperature. This algorithm was followed to check the reliability of the experimental phase equilibrium data of following systems: water content of methane in equilibrium with gas hydrate, liquid water or ice; solubility data of carbon dioxide and methane with water inside and outside gas hydrate formation region, and composition of vapor phase in equilibrium with gas hydrate and liquid water for carbon dioxide + methane or

191

nitrogen + water system. The treated experimental data were finally declared to be probable thermodynamically consistent/inconsistent, or not fully consistent data. However, it is worth pointing out that the performed phase equilibrium data assessment test is inevitably model-dependent because there is no way to measure directly the required parameters for the consistency test including the fugacity coefficients. Therefore, some data could not pass the consistency test but still be reliable ones from mathematical point of view.

The second approach was a statistical method using the Leverage concept.[444-446] The hydrate dissociation data for the CH_4, C_2H_6, C_3H_8, CO_2, N_2, and H_2S simple clathrate hydrates and the dissociation data for the $CO_2 + CH_4/N_2$ mixed clathrate hydrates data were treated to check their reliability. Two recommended simple correlations[214,492] were applied to represent/predict these data. The results show that: The applied correlations are valid for the purpose of this work; 10 points from the whole investigated hydrate dissociation data are found to be out of the applicability domain of the employed correlations and 8 hydrate dissociation data are designated as probable suspended experimental data. The aforementioned results can be further used to conclude about the quality of the data points, which are supposed to be applied in tuning the thermodynamic models to predict the phase equilibrium of clathrate hydrates of the treated hydrate formers/their mixtures.

To recapitulate, we recommend the users to keep all the consistent data that can be declared not to be outliers using the applied statistical approach[444-446] and some of the similar not fully consistent data, for tuning the thermodynamic models as well as application in design of the processes. Later, on the basis of their experiences, some conclusions should be made on thermodynamic inconsistent data which can pass the statistical approach.[444-446] However, we strongly advice the users not to use the data that can fulfill neither of the tests.

9. Prospective Works

Suggestions pour des travaux ultérieurs

1. Le modèle thermodynamique développé au cours de ce travail pourrait être étendu à la représentation et à la prédiction des équilibres de phases des mélanges de gaz formeurs de clathrates et semi-clathrates hydrates tels les systèmes $CO_2 + H_2/CH_4/N_2$.

2. Les comportements de phases des semi-clathrates hydrates dans des solutions aqueuses d'autres formeurs d´hydrates comme : TBAC, TBAF , etc. pourraient être estimées à l´aide du modèle proposé.

3. L'approche mathématique appliquée à la résolution les équations de bilans de masses pourrait être étendue à la détermination des compositions molaires des semi-clathrates hydrates.

4. Une méthode de test de cohérence thermodynamique pourrait être développée sur la base de l´équation de Gibbs-Duhem [440-443] à pression constante. Cette méthode pourrait alors être appliquée à la vérification de la fiabilité des données d'équilibres de phases isobares.

5. La méthode dite: "isochoric pressure search method" [58,59,199,312,425-429] pourrait continuer d´être utilisée pour la mesure des équilibres de phases des semi-clathrates hydrates de systèmes variés incluant différentes concentrations de TBAB en solutions aqueuses et de grandes variabilités de concentration de CO_2 dans les mélanges gazeux.

6. Finalement le développement de nouvelles techniques expérimentales de mesure des équilibres de phases, plus précises et plus rapides, est fortement recommandé. En effet, cela reste encore un challenge particulièrement intéressant et tout particulièrement en ce qui concerne la détermination de la structure et de la composition des hydrates.

1. The developed thermodynamic model can be extended to represent/predict the phase equilibria of semi-clathrate hydrates of mixed hydrate formers including the CO_2 + N_2/CH_4/H_2 systems.

2. Phase behaviors of the semi-clathrate hydrates containing the aqueous solutions of other hydrate promoters including TBAC, TBAF, etc. can attract attentions to be calculated/estimated by the proposed model.

3. The applied mathematical approach for solving the mass balance equations can be extended to determine the molar composition of semi-clathrate hydrates.

4. A thermodynamic consistency test method can be developed on the basis of the "Gibbs-Duhem equation"[440-443] at constant pressure. This method can be later applied for checking the reliability of isobaric phase equilibrium data.

5. The isochoric pressure search method[58,59,199,312,425-429] can be pursued for measurement of phase equilibria of semi-clathrate hydrates of various systems including different concentrations of TBAB in aqueous solutions or wider ranges of carbon dioxide in the feed gas.

6. The last but not the least is that developing new experimental phase equilibrium measurement techniques, more accurate and more rapid, is highly recommended. In fact, this is still a challenge especially interesting for those who are dealing with determination of the structure and composition of the hydrates.

Bibliography

1. Carroll, J. Natural Gas Hydrates, A Guide for Engineers. 2nd Ed., Gulf Professional Publishing, Burlington, MA, **2009**.

2. Sloan, E.D.; Koh, C.A. Clathrate Hydrates of Natural Gases. 3nd Ed., CRC Press, Taylor & Francis Group, New York, **2008**.

3. Jeffrey, G. A. Hydrate inclusion compounds. *J. Inclusion Phenom.* **1984**, *1*, 211-222.

4. Davy, H. On a combination of oxymuriatic gas and oxygene gas. *Phil. Trans. Roy. Soc. Lond.* **1811**, *101*, 155–162.

5. Faraday, M. On hydrate of chlorine. *Quart. J. Sci. Lit. Arts* **1823**, *15*, 71-74.

6. Pickering, S. U. X.–The hydrate theory of solutions. Some compounds of the alkyl-amines and ammonia with water. *J. Chem. Soc. Trans.* **1893**, *63*, 141-195.

7. Somerville, W. C. An investigation of the degrees of hydration of the alkyl amines in aqueous solution. *J. Phys. Chem.* **1931**, *35*, 2412-2433.

8. Hashemi, H.; Javanmardi, J.; Zarifi, M.; Eslamimanesh, A.; Mohammadi, A. H. Experimental study and thermodynamic modelling of methane clathrate hydrate dissociation conditions in silica gel porous media in the presence of methanol aqueous solution. *J. Chem. Thermodyn.* **2012**, *49*, 7-13.

9. Eslamimanesh, A.; Mohammadi, A. H.; Richon, D. An improved Clapeyron model for predicting liquid water–hydrate–liquid hydrate former phase equilibria. *Chem. Eng. Sci.* **2011**, *66*, 1759-1764.

10. Villard, P. Sur quelques nouveaux hydrates de gaz. *Compt. Rend.* **1888**, *106*, 1602-1603.

11. de Forcrand, R. Sur la composition des hydrates de gaz. *Compt. Rend.* **1902**, *135*, 959-961.

12. Schroeder, W. Die geschichte der gas hydrate. *Sammlung. Chem. Tech. Vortrage*, **1927**, *29*, 90-98.

13. Eslamimanesh, A.; Mohammadi, A. H.; Richon, D. Thermodynamic consistency test for experimental data of water content of methane. *AlChE J.* **2011**, *57*, 2566-2573

14. Eslamimanesh, A.; Mohammadi, A. H.; Richon, D. Thermodynamic consistency test for experimental solubility data in carbon dioxide/methane + water system inside and outside gas hydrate formation region. *J. Chem. Eng. Data* **2011**, *56*, 1573-1586.

15.   Campbell, J.M. Gas Conditioning and Processing. Volume 1: Phase Behavior, Physical Properties, Energy Changes, Vessel Sizing, Heat Transfer and Fluid Flow. 4th ed., Campbell Petroleum Series, John M. Campbell and Co, Norman, Oklahoma, **1976**.

16.   Eslamimanesh, A.; Gharagheizi, F.; Mohammadi, A. H.; Richon, D. Phase equilibrium modeling of structure H clathrate hydrates of methane + water "insoluble" hydrocarbon promoter using QSPR molecular approach. *J. Chem. Eng. Data* **2011**, *56*, 3775-3793.

17.   Eslamimanesh, A.; Gharagheizi, F.; Mohammadi, A. H.; Richon, D.; Illbeigi, M.; Fazlali, A.; Forghani, A. A.; Yazdizadeh, M. Phase equilibrium modeling of structure H clathrate hydrates of methane + water "insoluble" hydrocarbon promoter using group contribution-support vector machine technique. *Ind. Eng. Chem. Res.* **2011**, *50*, 12807-12814.

18.   Khokhar, A.A.; Gudmundsson, J.S.; Sloan, E.D. Gas storage in structure H hydrates. *Fluid Phase Equilib.* **1998**, *150*, 38-392.

19.   von Stackelberg, M. Solid gas hydrates. *Naturwissenschaften* **1949**, *36*, 327-33,359-62.

20.   Sugahara, T.; Mori, H.; Sakamoto, J.; Hashimoto, S.; Ogata, K.; Ohgaki, K. Cage occupancy of hydrogen in carbon dioxide, ethane, cyclopropane, and propane hydrates. *Open Thermodyn. J.* **2008**, *2*, 1-6.

21.   Dyadin, Y. A.; Larionov, E. G.; Manakov, A. Y.; Zhurko, F. V.; Aladko, E. Y.; Mikina, T. V.; Komarov, V. Y. Clathrate hydrates of hydrogen and neon. *Mendeleev Commun.* **1999**, *9*, L-LI.

22.   Florusse, L. J.; Peters, C. J.; Schoonman, J.; Hester, K. C.; Koh, C. A.; Dec, S. F.; Marsh, K. N.; Sloan, E. D. Stable low-pressure hydrogen clusters stored in a binary clathrate hydrate. *Science* **2004**, *306*, 469-471.

23.   (a)Belandria, V.; Eslamimanesh, A.; Mohammadi, A. H.; Richon, D. Study of gas hydrate formation in the carbon dioxide + hydrogen + water systems: Compositional analysis of the gas phase. *Ind. Eng. Chem. Res.* **2011**, *50*, 6455-6459. (b) Belandria, V.; Mohammadi, A. H.; Richon, D. Phase equilibria of clathrate hydrates of methane+carbon dioxide: New experimental data and predictions. *Fluid Phase Equilib.* **2010**, *296*, 60-65.

24.   McMullan, R. K.; Jordan, T. H.; Jeffrey, G. A. Polyhedral clathrate hydrates. XII. The crystallographic data on hydrates of ethylamine, dimethylamine, trimethylamine, n-propylamine (two forms), iso-propylamine, diethylamine (two forms), and tert-butylamine. *J. Chem. Phys.* **1967**, *47*, 1218-1222.

25.   Jeffrey, G. A. Water structure in organic hydrates. *Acc. Chem. Res.* **1969**, *2*, 344-352.

26.   Fukushima, S.; Takao, S.; Ogoshi, H.; Ida, H.; Matsumoto, S.; Akiyama, T.; Otsuka, T. JFE Steel Corporation, NKK Tech. Report, **1999**, *166*, 65-70 (in Japanese).

27.   Shimada, W.; Ebinuma, T.; Oyama, H.; Kamata, Y.; Takeya, S.; Uchida, T.; Nagao, J.; Narita, H. Separation of gas molecule using tetra-n-butyl ammonium bromide semi-clathrate hydrate crystals. *Jpn. J. Appl. Phys., Part 2* **2003**, *42*, L129-L131.

28.   Shimada, W.; Shiro, M.; Kondo, H.; Takeya, S.; Oyama, H.; Ebinuma, T.; Narita, H. Tetra-n-butylammonium bromide-water (1/38). *Acta Crystallogr., Sect. C: Cryst. Struct. Commun.* **2005**, *61*, o65-o66.

29.   Makino, T.; Yamamoto, T.; Nagata, K.; Sakamoto, H.; Hashimoto, S.; Sugahara, T.; Ohgaki, K. Thermodynamic stabilities of tetra-n-butyl ammonium chloride + H_2, N_2, CH_4, CO_2, or C_2H_6 semiclathrate hydrate systems. *J. Chem. Eng. Data* **2010**, *55*, 839-841.

30.   Eslamimanesh, A.; Mohammadi, A. H.; Richon, D.; Naidoo, P.; Ramjugernath, D. Application of gas hydrate formation in separation processes: A review of experimental studies. *J. Chem. Thermodyn.* **2012**, *46*, 62-71.

31.   Hammerschmidt, E. G. Formation of gas hydrates in natural gas transmission lines. *Ind. Eng. Chem.* **1934**, *26*, 851-855.

32.   Barker, J. W.; Gomez, R. K. Formation of hydrates during deepwater drilling operations. *J. Petrol Technol.* **1989**, *41*, 297-301.

33.   Hale, A. H.; Dewan, A. K. R. Inhibition of gas hydrates in deepwater drilling. *SPE Drilling Engineering* **1990**, *5*, 109-115.

34.   Ouar, H.; Cha, S. B.; Wildeman, T. R.; Sloan, E. D. Formation of natural gas hydrates in water-based drilling fluids. *Chem. Eng. Res. Des.* **1992**, *70*, 48-54.

35.   Katz, D. L.; Depths to which frozen gas fields may be expected. *J. Petrol Technol.* **1972**, May, 557-558.

36.   Verma, V. K.; Hand, J. H.; Katz, D. L.; Holder, G. D. Denuding hydrocarbon liquids of natural gas constituents by hydrate formation. *J. Petrol Technol.* **1975**, *27*, 223-226.

37.   Holder, G. D.; Katz, D. L.; Hand, J. H. Hydrate formation in subsurface environments. *AAPG Bulletin* **1976**, *60*, 981-988.

38.   Bishnoi, P. R.; Gupta, A. K.; Englezos, P.; Kalogerakis, N. Multiphase equilibrium flash calculations for systems containing gas hydrates. *Fluid Phase Equilib.* **1989**, *53*, 97-104.

39.   Sloan, E. D.; Khoury, F. M.; Kobayashi, R. Water content of methane gas in equilibrium with hydrates. *Ind. Eng. Chem. Fundam.* **1976**, *15*, 318-323.

40.   Piemonte, V.; Maschietti, M.; Gironi, F. A Triethylene Glycol–Water System: A study of the TEG regeneration processes in natural gas dehydration plants. *Energy Sources Part A* **2012**, *34*, 456-464.

41.   Ng, H. J.; Robinson, D. B. A method for predicting the equilibrium gas phase water content in gas-hydrate equilibrium. *Ind. Eng. Chem. Fundam.* **1980**, *19*, 33-36.

42.   Song, K. Y.; Kobayashi, R. Water content of CO_2 in equilibrium with liquid water and/or hydrates. *SPE Formation Evaluation* **1987**, *2*, 500-508.

43.   Mohammadi, A. H.; Chapoy, A.; Tohidi, B.; Richon, D. A semiempirical approach for estimating the water content of natural gases. *Ind. Eng. Chem. Res.* **2004**, *43*, 7137-7147.

44.   Sain, K.; Gupta, H. Gas hydrates in India: Potential and development. *Gondwana Res. Article in Press*, http://dx.doi.org/10.1016/j.gr.2012.01.007, **2012**.

45.   Mohammadi, A. H.; Chapoy, A.; Tohidi, B.; Richon, D. Water content measurement and modeling in the nitrogen + water system. *J. Chem. Eng. Data* **2005**, *50*, 541-545.

46.   Chapoy, A.; Mohammadi, A. H.; Tohidi, B.; Richon, D. Estimation of water content for methane + water and methane + ethane + n-butane + water systems using a new sampling device. *J. Chem. Eng. Data* **2005**, *50*, 1157-1161.

47.   Mohammadi, A. M.; Samieyan, V.; Tohidi, B. Estimation of water content in sour gases. *SPE* 94133, 2603-2612.

48.   Mohammadi, A. H.; Chapoy, A.; Tohidl, B.; Richon, D. Gas solubility: A key to estimating the water content of natural gases. *Ind. Eng. Chem. Res.* **2006**, *45*, 4825-4829.

49.   Mohammadi, A. H.; Chapoy, A.; Tohidi, B.; Richon, D. Advances in estimating water content of natural gases. Presented at the 85th Annual GPA Convention, 5-8 March Grape Vine, Texas, USA, **2006**.

50.   Mohammadi, A. H.; Richon, D. Use of artificial neural networks for estimating water content of natural gases. *Ind. Eng. Chem. Res.* **2007**, *46*, 1431-1438.

51.   Mohammadi, A. H.; Richon, D. In: Natural Gas Research Progress – IB: Chapter 4, ISBN: 978-1-60456-700-7, Nova Science Publishers, Inc., Editors: Nathan David and Theo Michel, **2008**.

52.   Chersky, N. J.; Makogon, Y. F. Solid gas world reserves are enormous. Oil Gas International **1970**, 8, 2-84.

53.   Makogon, Y. F.; Hydrates of Natural Gas; Penn Well Publishing: Tulsa, OK, **1981** (translated by W. J. Cieslewicz).

54.   Stoll, R. D.; Ewing, J.; Bryan, G. M. Anomalous wave velocities in sediments containing gas hydrates. *J. Geophys. Res.* **1971**, 76, 2090-2094.

55.   Miller, S.L. The occurrence of gas hydrates in the solar system. Proceeding of National Academy of Science, USA **1961**, 47, 1798-1808.

56.   Miller, S. L.; Smythe, W. D. Carbon dioxide clathrate in the Martian ice cap. *Science* **1970**, *170*, 531-533.

57.   Chatti, I.; Delahaye, A.; Fournaison, L.; Petitet, J. P. Benefits and drawbacks of clathrate hydrates: A review of their areas of interest. *Energy Convers. Manage.* **2005**, *46*, 1333-1343.

58.   Mohammadi, A. H.; Eslamimanesh, A.; Belandria, V.; Richon, D. Phase equilibria of semiclathrate hydrates of CO_2, N_2, CH_4, or H_2 + Tetra-n-butylammonium bromide aqueous solution. *J. Chem. Eng. Data* **2011**, *56*, 3855-3865.

59.   Belandria, V.; Eslamimanesh, A.; Mohammadi, A. H.; Richon, D. Gas hydrate formation in carbon dioxide + nitrogen + water system: Compositional analysis of equilibrium phases. *Ind. Eng. Chem. Res.* **2011**, *50*, 4722-4730.

60.   Englezos, P.; Lee, J. D. Gas hydrates: A cleaner source of energy and opportunity for innovative technologies. *Korean J. Chem. Eng.* **2005**, *22*, 671-681.

61.   Englezos, P. Clathrate hydrates. *Ind. Eng. Chem. Res.* **1993**, *32*, 1251-1274.

62.   Booth, J.S.; Rowe, M.M.; Fischer, K.M. Offshore gas hydrate sample database. U.S. Geological Survey, Open-File Report 96-272, **1996**.

63.   Mahajan, D.; Taylor, C. E.; Mansoori, G. A. An introduction to natural gas hydrate/clathrate: The major organic carbon reserve of the Earth. *J. Petrol. Sci. Eng.* **2007**, *56*, 1-8.

64.   Pierce, B.S.; Collett, T.S. Energy resource potential of natural gas hydrates. 5th Conference and Exposition on Petroleum Geophysics, Hyderabad, India, (2004) 899-903.

65.   Ruppel, C. Supplementary Paper 4, *MITEI Natural Gas Report*, Supplementary Paper on Methane Hydrates, **2011**, 1-25.

66.   Sloan, E. D. Clathrate Hydrates of Natural Gases, Dekker: NewYork, 1990.

67.   Judge, A. Natural gas hydrates in Canada Proceedings, Fourth Canadian Permafrost Conference, March 26, **1981**, Calgary, AB, French, H. M., Ed.; National Research Council of Canada: Ottawa, ON, **1982**, 320-328.

68.   McGuire, P.L. Methane hydrate gas production: An assessment of conventional production technology as applied to hydrate gas recovery. Los Alamos National Laboratory, LA-9102-MS, **1981**.

69.   Holder, G. D.; Angert, P. F.; John, V. T.; Yen, S. Thermodynamic evaluation of thermal recovery of gas from hydrates in the earth. *J. Petrol Technol.* **1982**, *34*, 1127-1132.

70.   Pearson, C. F.; Halleck, P. M.; McGuire, P. L.; Hermes, R.; Mathews, M. Natural gas hydrate deposits: A review of in situ properties. *J. Phys. Chem.* **1983**, *87*, 4180-4185.

71.   Weaver, J. S.; Stewart, J. M. In situ hydrates under the Beaufort sea shelf, Proceedings, Fourth Canadian Permafrost Conference, March 2-6, Calgary, AB; French, H. M., Ed.; National Research Council of Canada: Ottawa, ON, **1982**, 312-319.

72.   Bayles, G. A.; Sawer, W. K.; Anada, H. R.; Reddy, S. A steam cycling. model for gas production from a hydrate reservoir. *Chem. Eng. Commun.* **1986**, *47*, 225-245.

73.   Ridley, I.; Dominic, K. Gas hydrates keep energy on ice. *New Scientist* **1998**, *117*, 53-68.

74.   Sharma, G.D.; Kamath, V.A.; Patil, S.L. Natural gas hydrate resources of the Alaskan arctic and their recovery potential, Proceedings of the Second International Offshore and Polar Engineering Conference, Jun 14-19, San Francisco, CA, USA, **1992**, 652-659.

75.   Berner, D. Marine transport of natural gas in hydrate form Proceedings of the Second International Offshore and Polar Engineering Conference, Jun 14-19, San Francisco, CA, USA, **1992**, 636-643.

76.   Nogami, T.; Watanabe, S. Development of natural-gas supply chain by means of natural-gas hydrates. *J. Petrol Technol.* **2009**, *61*, 62-64.

77.   Stott, J. General interest: CERI: Arctic gas, LNG, hydrates key to gas supply gap. *Oil Gas J.* **2005**, *103*, 30.

78.   Mahajan, D.; Taylor, C. E.; Mansoori, G. A. An introduction to natural gas hydrate/clathrate: The major organic carbon reserve of the Earth. *J. Petrol. Sci. Eng.* **2007**, *56*, 1-8.

79.   Lowrie, A.; McGee, T.; Lerche, I. Natural gas hydrates: Geologic constituents from the birth of planet earth to the present, Offshore Technology Conference, May 6-9, Houston, TX, USA, **2002**, 359-366.

80.   Hatzikiriakos, S. G.; Englezos, P. The relationship between global warming and methane gas hydrates in the earth. *Chem. Eng. Sci.* **1993**, *48*, 3963-3969.

81.   Senger, K.; Bünz, S.; Mienert, J. First-order estimation of in-place gas resources at the Nyegga gas hydrate prospect, Norwegian Sea. *Energies* **2010**, *3*, 2001-2026.

82.   Thakur, N. K. Gas hydrates as alternative energy resource - seismic methods. *Current Science* **2010**, *99*, 181-189.

83.   Safronov, A. F.; Shits, E. Y.; Grigor'ev, M. N.; Semenov, M. E. Formation of gas hydrate deposits in the Siberian Arctic shelf. *Russ. Geol. Geophys.* **2010**, *51*, 83-87.

84.   Krey, V.; Canadell, J.G.; Nakicenovic, N.; Abe, Y.; Andruleit, H.; Archer, D.; Grubler, A.; Hamilton, N.T.M.; Johnson, A.; Kostov, V.; Lamarque, J.F.; Langhorne, N.; Nisbet, E.G.; O'Neill, B.; Riahi, K.; Riedel, M.; Wang, W.; Yakushev, V. Gas hydrates: Entrance to a methane age or climate threat? Environ. Res. Lett. **2009**, *4*, 1-6.

85.   Barone, G.; Chianese, E. Hydrates of natural gases and small molecules: Structures, properties, and exploitation perspectives. *ChemSusChem* **2009**, *2*, 992-1008.

86.   Moridis, G. J.; Collett, T. S.; Boswell, R.; Kurihara, M.; Reagan, M. T.; Koh, C.; Sloan, E. D. Toward production from gas hydrates: Current status, assessment of resources, and simulation-based evaluation of technology and potential. *SPE Reserv. Eval. Eng.* **2009**, *12*, 745-771.

87.   Gong, J. M.; Cao, Z. M.; Chen, J. W.; Zhang, M.; Li, J.; Yang, G. F. Simulation experiments on gas production from hydrate-bearing sediments. *Science in China, Series D: Earth Sciences* **2009**, *52*, 22-28.

88.   Azarinezhad, R.; Valko, I.; Chapoy, A.; Tohidi, B. Can gas hydrates provide a solution to gas utilisation challenges in Russian oil fields? SPE Russian Oil and Gas Technical Conference and Exhibition, 28-30 October **2008**, Moscow, Russia.

89.   Bai, Y.; Li, Q.; Li, X.; Du, Y. The simulation of nature gas production from ocean gas hydrate reservoir by depressurization. *Sci. China, Ser. E Eng. Mater. Sci.* **2008**, *51*, 1272-1282.

90.   Zhang, W. D.; Liu, Y. J.; Ren, S. R.; Wang, R. H. Thermal analysis on heat injection to natural gas hydrate (NGH) recovery. *Natural Gas Industry* **2008**, *28*, 77-79.

91.   Chen, D. F.; Su, Z.; Cathles, L. M. Types of gas hydrates in marine environments and their thermodynamic characteristics. *Terr. Atmos. Ocean Sci.* **2006**, *17*, 723-737.

92.   Wang, S.; Song, H.; Yan, W.; Shi, X.; Yan, P.; Fan, S. Stable zone thickness and resource estimation of gas hydrate in Southern South China Sea. *Tianranqi Gongye/Natural Gas Industry* **2005**, *25*, 24-27.

93.   Milkov, A. V. Global estimates of hydrate-bound gas in marine sediments: How much is really out there? *Earth Sci. Rev.* **2004**, *66*, 183-197.

94.   Xu, W. Modeling dynamic marine gas hydrate systems. *Am. Mineral.* **2004**, *89*, 1271-1279.

95.   Milkov, A. V.; Claypool, G. E.; Lee, Y. J.; Xu, W.; Dickens, G. R.; Borowski, W. S. In situ methane concentrations at Hydrate Ridge, offshore Oregon: New constraints on the global gas hydrate inventory from an active margin. *Geology* **2003**, *31*, 833-836.

96.   Müller, C.; Bönnemann, C.; Buttkus, B. Gas hydrates - A future energy resource? *Gashydrate - Eine zukünftige energieressource? DGMK Tagungsbericht* **2003**, 555-564.

97.   Collett, T. S. Energy resource potential of natural gas hydrates. *AAPG Bull.* **2002**, *86*, 1971-1992.

98.   Solov'ev, V. A. Global estimation of gas content in submarine gas hydrate accumulations. *Geol. Geofiz.* **2002**, *43*, 648-661.

99.   Collett, T. S. Natural-gas hydrates: Resource of the twenty-first century? *AAPG Mem.* **2001**, *74*, 85-108.

100.   Parlaktuna, M.; Erdogmuş, T. Natural gas hydrate potential of the Black Sea. *Energy Sources* **2001**, *23*, 203-211.

101.   Yoon, J. R.; Kim, Y. Reviews on Natural Resources in the Arctic: Petroleum, Gas, Gas Hydrates and Minerals. *Ocean and Polar Research* **2001**, *23*, 51-62.

102.   Smith, S. L. Natural gas hydrates. *Bulletin of the Geological Survey of Canada* **2001**, 265-280.

103.   Kvenvolden, K. A.; Lorenson, T. D. Global occurrences of gas hydrate. 1th International Offshore and Polar Engineering Conference Stavanger, Stavanger, **2001**, 462-467.

104.   Majorowicz, J. A.; Hannigan, P. K. Natural gas hydrates in the offshore Beaufort-Mackenzie basin - Study of a feasible energy source II. *Nat. Resour. Res.* **2000**, *9*, 201-214.

105.   Sawyer, W. K.; Boyer Ii, C. M.; Frantz Jr, J. H.; Yost Ii, A. B. Comparative assessment of natural gas hydrate production models. SPE/CERI GTS-2000: Creating Value - Extending Our Reach, Calgary, Alberta, Can, 2000; SPE: Calgary, Alberta, Canada, **2000**, 793-801.

106.   Mienert, J.; Posewang, J.; Baumann, M. Gas hydrates along the northeastern Atlantic margin: possible hydrate- bound margin instabilities and possible release of methane. *Geological Society, London, Special Publications*. **1998**, 275-291.

107.   Sloan, E. D. Physical/chemical properties of gas hydrates and application to world margin stability and climatic change. *Geol. Soc. Spec. Pub.* **1998**, *137*, 31-50.

108.   Dickens, G. R.; Paull, C. K.; Wallace, P. Direct measurement of in situ methane quantities in a large gas-hydrate reservoir. *Nature* **1997**, *385*, 426-428.

109.   Max, M. D.; Lowrie, A. Oceanic methane hydrates: A "Frontier" gas resource. *J. Pet. Geol* **1996**, *19*, 41-56.

110.   Nixdorf, V. J.; Oellrich, L. R. Natural gas hydrates - from bane to boon? Erdgashydrate - Vom Stoerenfried zum Hoffnungstraeger? *Urban Verlag Hamburg/Wien GmbH* **1995**, *111*, 458-462.

111.   Judge, A.; Smith, S. L.; Majorowicz, J. Current distribution and thermal stability of natural gas hydrates in the Canadian polar regions. *Int. Soc. Offshore and Polar Engineerns (ISOPE)*, Osaka, Jpn, **1994**, 307-314.

112.   Xie, Y.; Li, G.; Liu, D.; Liu, N.; Qi, Y.; Liang, D.; Guo, K.; Fan, S. Experimental study on a small scale of gas hydrate cold storage apparatus. *Appl. Energy* **2010**, *87*, 3340-3346.

113.   Komui, T.; Sakamoto, Y.; Tanaka, A. Enhanced CO_2 geological storage system using gas hydrates and environmental risk assessment. Proceedings of the Twentieth International Offshore and Polar Engineering Conference. Beijing, China, June 20-25, **2010**, 115-118.

114.   Brown, T.D.; Taylor, C.E.; Bernardo, M. New natural gas storage and transportation capabilities utilizing rapid methane hydrate formation techniques, AIChE Spring Meeting and 6th Global Congress on Process Safety, San Antonio, TX, **2010**.

115.   Kim, N. J.; Hwan Lee, J.; Cho, Y. S.; Chun, W. Formation enhancement of methane hydrate for natural gas transport and storage. *Energy* **2010**, *35*, 2717-2722.

116.   Tsuda, T.; Ogata, K.; Hashimoto, S.; Sugahara, T.; Moritoki, M.; Ohgaki, K. Storage capacity of hydrogen in tetrahydrothiophene and furan clathrate hydrates. *Chem. Eng. Sci.* **2009**, *64*, 4150-4154.

117.   Bi, Y.; Guo, T.; Zhang, L.; Chen, L.; Sun, F. Entropy generation minimization for charging and discharging processes in a gas-hydrate cool storage system. *Appl. Energy* **2010**, *87*, 1149-1157.

118.   Lee, J.; Shin, C.; Lee, Y. Experimental investigation to improve the storage potentials of gas hydrate under the unstirring condition. *Energy Fuels* **2010**, *24*, 1129-1134.

119. Cooper, A. I.; Wang, W.; Carter, B.; Bray, C.; Bacsa, J.; Steiner, A.; Su, F.; Adams, D. J.; Cropper, C.; Overend, G.; Weaver, J. V. M.; Jones, J. T. A.; Iggo, J. A.; Khimyak, Y. Z. Gas hydrates and semiclathrate hydrates for H_2 and CH_4 storage: Kinetics, capacity and stability. ACS National Meeting Book of Abstracts **2009**, 237.

120. Dou, B.; Jiang, G.; Wu, X.; Ning, F.; Zhang, L.; Research methane hydrate meta-stable property for application to natural gas storage and transportation. *SPE/IATMI Asia Pacific*, Oil Gas J. Conference and Exhibition, APOGCE **2009**, *1*, 42-47.

121. Seo, Y.; Lee, J. W.; Kumar, R.; Moudrakovski, I. L.; Lee, H.; Ripmeester, J. A. Tuning the composition of guest molecules in clathrate hydrates: NMR identification and its significance to gas storage. *Chem. Asian J.* **2009**, *4*, 1266-1274.

122. Ogawa, H.; Imura, N.; Miyoshi, T.; Ohmura, R.; Mori, Y. H. Thermodynamic simulations of isobaric hydrate-forming operations for natural gas storage. *Energy Fuels* **2009**, *23*, 849-856.

123. Ersland, G.; Husebø, J.; Graue, A.; Kvamme, B., Transport and storage of CO_2 in natural gas hydrate reservoirs. *Energy Procedia* **2009**, *1*, 3477-3484.

124. Belosludov, V. R.; Subbotin, O. S.; Belosludov, R. V.; Mizuseki, H.; Kawazoe, Y.; Kudoh, J. Thermodynamics and hydrogen storage ability of binary hydrogen + help gas clathrate hydrate. *Int. J. Nanosci.* **2009**, *8*, 57-63.

125. Husebø, J.; Ersland, G.; Graue, A.; Kvamme, B. Effects of salinity on hydrate stability and implications for storage of CO_2 in natural gas hydrate reservoirs. *Energy Procedia* **2009**, *1*, 3731-3738.

126. Javanmardi, J.; Nasrifar, K.; Najibi, S. H.; Moshfeghian, M. Economic evaluation of natural gas hydrate as an alternative for natural gas transportation. *Appl. Therm. Eng.* **2005**, *25*, 1708-1723.

127. Koh, C. A.; Sloan, E. D.; Sum, A. K.; Wu, D. T. Fundamentals and applications of gas hydrates. *Annual Review of Chemical and Biomolecular Engineering* **2011**, *2*, 237-257.

128. Gudmundsson, J. S.; Andersson, V.; Levik, O. I.; Mork, M. Hydrate technology for capturing stranded gas. 3rd. International Conference on Gas Hydrates, Salt Lake City, Utah, July 18-22, **1999**.

129. Gudmundsson, J. S.; Mork, M.; Graff, O. F. Hydrate non-pipeline technology. Proc. 4th Intl. Conf. Gas Hydrates, Yokohama, Japan, Tokyo: Keio University, **2002**, 997-1102.

130. Gudmundsson, J. S.; Parlaktuna, M. Storage of natural gas hydrate at refrigerated conditions. Presented at AIChE Spring National Meeting, New Orleans, LA, **1992**.

131. Kumar, R.; Linga, P.; Moudrakovski, I.; Ripmeester, J. A.; Englezos, P. Structure and kinetics of gas hydrates from methane/ethane/propane mixtures relevant to the design of natural gas hydrate storage and transport facilities. *AIChE J.* **2008**, *54*, 2132-2144.

132. Xie, Y.; Liu, D.; Liu, N.; Liang, D.; Guo, K.; Fan, S. Experimental research on performance of small scale cool storage apparatus with gas hydrate. *Hsi-An Chiao Tung Ta Hsueh/Journal of Xi'an Jiaotong University* **2008**, *42*, 573-577.

133. Cazares, Y.L. Storage of methane gas in propane hydrate, ACS National Meeting, Book of Abstracts, **2007**.

134. Xie, Y. M.; Liu, D. P.; Fan, Y.; Liu, N. Experimental research on natural gas hydrate storage process using water spraying. *Shanghai Ligong Daxue Xuebao/Journal of University of Shanghai for Science and Technology* **2007**, *29*, 368-372.

135. Stern, L. A.; Circone, S.; Kirby, S. H.; Durham, W. B. Anomalous preservation of pure methane hydrate at 1 atm. *J. Phys. Chem. B* **2001**, *105*, 1756-1762.

136. Belosludov, V. R.; Subbotin, O. S.; Krupskii, D. S.; Belosludov, R. V.; Kawazoe, Y.; Kudoh, J. I. Physical and chemical properties of gas hydrates: Theoretical aspects of energy storage application. *Materials Transactions* **2007**, *48*, 704-710.

137. Kvamme, B.; Graue, A.; Buanes, T.; Kuznetsova, T.; Ersland, G. Storage of CO_2 in natural gas hydrate reservoirs and the effect of hydrate as an extra sealing in cold aquifers. *Int. J. Greenhouse Gas Control* **2007**, *1*, 236-246.

138. Di Profio, P.; Arca, S.; Germani, R.; Savelli, G. Novel nanostructured media for gas storage and transport: Clathrate hydrates of methane and hydrogen. *J. Fuel Cell Sci. Technol.* **2007**, *4*, 49-55.

139. Bi, Y.; Guo, T.; Zhu, T.; Zhang, L.; Chen, L. Influences of additives on the gas hydrate cool storage process in a new gas hydrate cool storage system. *Energy Convers. Manage.* **2006**, *47*, 2974-2982.

140. Graue, A.; Kvamme, B.; Baldwin, B.A.; Stevens, J.; Howard, J.; Aspenes, E.; Ersland, G.; Husebø, J.; Zornes, D. Environmentally friendly CO_2 storage in hydrate reservoirs benefits from associated spontaneous methane production. Offshore Technology Conference, New Depths. New Horizons, **2006**, 1050-1058.

141. Savelli, G. ; Di Profio, P.; Arca, S.; Germani, R. Novel nanostructured media for gas storage and transport: Clathrate hydrates of methane and hydrogen. Proceedings of the 1st European Fuel Cell Technology and Applications Conference- Book of Abstracts, **2005**, 240.

142. Masoudi, R.; Tohidi, B. Gas hydrate production technology for natural gas storage and transportation and CO_2 sequestration, SPE Middle East Oil Gas J. Show and Conference, MEOS, Proceedings, **2005**, 745-751.

143. Bybee, K. Gas production technology: Gas-hydrate production for natural-gas storage and transportation. *J. Petrol Technol.* **2005**, *57*, 73-74.

144. Uchida, T.; Ikeda, I. Y.; Takeya, S.; Kamata, Y.; Ohmura, R.; Nagao, J.; Zatsepina, O. Y.; Buffett, B. A. Kinetics and stability of CH_4-CO_2 mixed gas hydrates during formation and long-term storage. *ChemPhysChem* **2005**, *6*, 646-654.

145. Liu, C.; Ye, Y.; Ren, H.; Diao, S.; Zhang, J. Experimental techniques of directly measuring the gas storage capacity in methane hydrate. *Tianranqi Gongye/Natural Gas Industry* **2005**, *25*, 44-47.

146. Li, K. N.; Tong, M. W.; Lin, K. Experimental research on the influence of jet pump on the cooling storage property of gas hydrates. *Int. J. Mod. Phys. B* **2005**, *19*, 507-509.

147. Ogawa, K.; Kawasoe, Y.; Haishi, T.; Utsuzawa, S. Devolopment of MRI-monitoring method to obtain the map of gas-storage ratio in gas-hydrate mash and MRI observation of time-evolution maps of gas-storage ratio in hydrate formation process. *Nihon Kikai Gakkai Ronbunshu, B Hen/Transactions of the Japan Society of Mechanical Engineers, Part B* **2004**, *70*, 3204-3211.

148. Sun, Z.; Ma, R.; Fan, S.; Guo, K.; Wang, R. Investigation on gas storage in methane hydrate. *J. Nat. Gas Chem.* **2004**, *13*, 107-112.

149. Bi, Y.; Guo, T.; Zhu, T.; Fan, S.; Liang, D.; Zhang, L. Influence of volumetric-flow rate in the crystallizer on the gas-hydrate cool-storage process in a new gas-hydrate cool-storage system. *Appl. Energy* **2004**, *78*, 111-121.

150. Chen, J.; Fan, S.; Liang, D.; Meng, Z.; Li, D. Experimental study on ice and HCFC-141b gas hydrate cool storage. *Wuhan Ligong Daxue Xuebao (Jiaotong Kexue Yu Gongcheng Ban)/Journal of Wuhan University of Technology (Transportation Science and Engineering)* **2004**, *28*, 190.

151. Tulk, C. A.; Wright, J. F.; Ratcliffe, C. I.; Ripmeester, J. A. Storage and handling of natural gas hydrate. *Bulletin of the Geological Survey of Canada* **2003**, 263-267.

152. Kobayashi, Y. Experimental research on the formation and storage of the methane gas hydrate, Proceedings of the fifth ISOPE Ocean Mining Symposium, Tsukuba, Japan **2003**, 185-187.

153. Seo, Y. T.; Lee, H. ^{13}C NMR analysis and gas uptake measurements of pure and mixed gas hydrates: Development of natural gas transport and storage method using gas hydrate. *Korean J. Chem. Eng.* **2003**, *20*, 1085-1091.

154. Sun, Z. G.; Wang, R.; Ma, R.; Guo, K.; Fan, S. Natural gas storage in hydrates with the presence of promoters. *Energy Convers. Manage.* **2003**, *44*, 2733-2742.

155. Sun, Z. G.; Ma, R. S.; Wang, R. Z.; Guo, K. H.; Fa, S. S. Experimental studying of additives effects on gas storage in hydrates. *Energy Fuels* **2003**, *17*, 1180-1185.

156. Sun, Z.; Wang, R.; Ma, R.; Guo, K.; Fan, S. Effect of surfactants and liquid hydrocarbons on gas hydrate formation rate and storage capacity. *Int. J. Energy Res.* **2003**, *27*, 747-756.

157. Zheng, X.; Sun, Z.; Fan, S.; Zhang, C.; Guo, Y.; Guo, K. Experimental investigation of storage capacity of natural gas hydrate. *Tianranqi Gongye/Natural Gas Industry* **2003**, *23*, 95-97.

158.   Ebinuma, T. Properties of gas hydrate and application to natural gas storage and transportation. *Nihon Enerugi Gakkaishi/Journal of the Japan Institute of Energy* **2002**, *81*, 908-914.

159.   Yan, L. J.; Liu, J.; Chen, G. J.; Guo, T. M. Kinetics of methane hydrate formation in active carbon. *Shiyou Xuebao, Shiyou Jiagong/Acta Petrolei Sinica (Petroleum Processing Section)* **2002**, *18*, 1-7.

160.   Zhigao, S.; Shuanshi, F.; Kaihua, G.; Ruzhu, W.; Rongshen, M. Storage technology of natural gas in the form of hydrate. *Tianranqi Gongye/Natural Gas Industry* **2002**, *22*, 87-90.

161.   Rogers, R.E.; Toghiani, R.K. Gas-hydrate storage of natural gas. ASEE Annual Conference Proceedings, **2001**, 5195-5201.

162.   Badakhshan, A.; Pooladi, E.M. Gas hydrates a new means for natural gas storage and transportation. World Petroleum Congress Proceedings **2000**, *4*, 145-157.

163.   Okui, T.; Kawasaki, T. Modification of gas hydrates for gas storage and transmission. International Gas Union World Gas Conference Papers, **2000**, 21.

164.   Tulk, C. A. Storage and handling of natural gas hydrate. *Bulletin of the Geological Survey of Canada* **1999**, 263-267.

165.   Khokhar, A.A.; Sloan, E.D.; Gudmundsson, J.S. Natural gas storage properties of structure H hydrate. *Ann. N.Y. Acad. Sci.* **2000**, *912*, 950-957.

166.   Guo, K. H.; Shu, B. F.; Zhang, Y.; Zhao, Y. L. Characterization of phase change and cool-storage processes of mixed gas hydrate. Guobang, C.; Steimle, F. W., Eds. Soc des Ingenieurs de l'Automobile: Hangzhou, China, **1998**, 345-348.

167.   Yevi, G. Y.; Rogers, R. E. Storage of fuel in hydrates for natural gas vehicles (NGVs). *J. Energy Res. Technol., Transactions of the ASME* **1996**, *118*, 209-213.

168.   Ohgaki, K.; Inoue, Y. A proposal for gas storage on the bottom of the ocean, using gas hydrates. *International Chemical Engineering* **1994**, *34*, 417-419.

169.   Hatzikiriakos, S. G.; Englezos, P. Gas storage through impermeation of porous media by hydrate formation. The Proceedings of the Fourth International Offshore and Polar Engineering Conference, J.S. Chung, B.J. Natvig and B.M. Das, Editors, Osaka, Japan, 10-15 April **1994**, 337-344.

170.   Utaka, Y.; Saito, A.; Seki, T. Gas hydrate cold storage using direct-contact heat transfer of liquid-vapor phase change and natural circulation of refrigerant in closed vessel. *JSME International Journal, Series B: Fluids and Thermal Engineering* **1993**, *36*, 150-155[99].

171.   Gudmundsson, J. S.; Parlaktuna, M.; Khokhar, A. A. Storage of natural gas as frozen hydrate. *Soc. of Petroleum Engineers of AIME*. Washington, DC, USA, **1992**, 699-707.

172.   Utaka, Y.; Saito, A.; Seki, T. Cool energy storage of gas hydrate using natural circulation of refrigerant with direct contact boiling and condensation. *Nippon Kikai Gakkai Ronbunshu, B Hen/Transactions of the Japan Society of Mechanical Engineers, Part B* **1991**, *57*, 3911-3915.

173. Mori, T.; Mori, Y. H. Characterization of gas hydrate formation in direct-contact cool storage process. *Int. J. Refrig* **1989**, *12*, 259-265.

174. Ternes, M. P. Characterization of refrigerant - 12 gas hydrate formation for heat pump cool storage applications. ASME: New Orleans, LA, USA, **1984**; New Orleans, LA, USA, 1984.

175. Papadimitriou, N. I.; Tsimpanogiannis, I. N.; Peters, C. J.; Papaioannou, A. T.; Stubos, A. K. Hydrogen storage in sH hydrates: A Monte Carlo study. *J. Phys. Chem. B* **2008**, *112*, 14206-14211.

176. Chapoy, A.; Anderson, R.; Tohidi, B. Low-pressure molecular hydrogen storage in semi-clathrate hydrates of quaternary ammonium compounds. *J. Am. Chem. Soc.* **2007**, *129*, 746-747.

177. Papadimitriou, N. I.; Tsimpanogiannis, I. N.; Stubos, A. K.; Martín, A.; Rovetto, L. J.; Florusse, L. J.; Peters, C. J. Experimental and computational investigation of the sII binary He-THF hydrate. *J. Phys. Chem. B* **2011**, *115*, 1411-1415.

178. Sabil, K.M. ; Nadia, O.; Witkamp, G.; Peters, C.J.; Bruining, J.M. hydrate-aqueous liquid-vapor equilibrium (H-L$_W$-V) for binary CO_2/H_2 mixture in aqueous solutions of water and tetrahydrofuran. International Conference on Chemical Engineering and Applications, 26-28 February, **2010**, 171-175.

179. Sabil, K. M.; Duarte, A. R. C.; Zevenbergen, J.; Ahmad, M. M.; Yusup, S.; Omar, A. A.; Peters, C. J. Kinetic of formation for single carbon dioxide and mixed carbon dioxide and tetrahydrofuran hydrates in water and sodium chloride aqueous solution. *Int. J. Greenhouse Gas Control* **2010**, *4*, 798-805.

180. Sabil, K. M.; Witkamp, G. J.; Peters, C. J. Phase equilibria in ternary (carbon dioxide + tetrahydrofuran + water) system in hydrate-forming region: Effects of carbon dioxide concentration and the occurrence of pseudo-retrograde hydrate phenomenon. *J. Chem. Thermodyn.* **2010**, *42*, 8-16.

181. Mooijer-Van Den Heuvel, M. M.; Witteman, R.; Peters, C. J. Phase behaviour of gas hydrates of carbon dioxide in the presence of tetrahydropyran, cyclobutanone, cyclohexane and methylcyclohexane. *Fluid Phase Equilib.* **2001**, *182*, 97-110[108].

182. Strobel, T. A.; Hester, K. C.; Koh, C. A.; Sum, A. K.; Sloan Jr, E. D. Properties of the clathrates of hydrogen and developments in their applicability for hydrogen storage. *Chem. Phys. Lett.* **2009**, *478*, 97-109.

183. Strobel, T. A.; Koh, C. A.; Sloan, E. D. Hydrogen storage properties of clathrate hydrate materials. *Fluid Phase Equilib.* **2007**, *261*, 382-389.

184. Shin, K.; Kim, Y.; Strobel, T. A.; Prasad, P. S. R.; Sugahara, T.; Lee, H.; Sloan, E. D.; Sum, A. K.; Koh, C. A. Tetra-n-butylammonium borohydride semiclathrate: A hybrid material for hydrogen storage. *J. Phys. Chem. A* **2009**, *113*, 6415-6418.

185. Strobel, T. A.; Sloan, E. D.; Koh, C. A. Raman spectroscopic studies of hydrogen clathrate hydrates. *J. Chem. Phys.* **2009**, *130*, 1-10.

186. Strobel, T. A.; Kim, Y.; Andrews, G. S.; Ferrell Iii, J. R.; Koh, C. A.; Herring, A. M.; Sloan, E. D. Chemical-clathrate hybrid hydrogen storage: Storage in both guest and host. *J. Am. Chem. Soc.* **2008**, *130*, 14975-14977.

187. Shin, K.; Choi, S.; Cha, J. H.; Lee, H. Structural transformation due to co-host inclusion in ionic clathrate hydrates. *J. Am. Chem. Soc.* **2008**, *130*, 7180-7181.

188. Strobel, T. A.; Hester, K. C.; Sloan Jr, E. D.; Koh, C. A. A hydrogen clathrate hydrate with cyclohexanone: Structure and stability. *J. Am. Chem. Soc.* **2007**, *129*, 9544-9545.

189. Rovetto, L. J.; Strobel, T. A.; Koh, C. A.; Sloan Jr, E. D. Is gas hydrate formation thermodynamically promoted by hydrotrope molecules? *Fluid Phase Equilib.* **2006**, *247*, 84-89.

190. Strobel, T. A.; Taylor, C. J.; Hester, K. C.; Dec, S. F.; Koh, C. A.; Miller, K. T.; Sloan Jr, E. D. Molecular hydrogen storage in binary THF-H_2 clathrate hydrates. *J. Phys. Chem. B* **2006**, *110*, 17121-17125.

191. Hester, K. C.; Strobel, T. A.; Sloan, E. D.; Koh, C. A.; Huq, A.; Schultz, A. J. Molecular hydrogen occupancy in binary THF-H_2 clathrate hydrates by high resolution neutron diffraction. *J. Phys. Chem. B* **2006**, *110*, 14024-14027.

192. Sugahara, T.; Haag, J. C.; Prasad, P. S. R.; Warntjes, A. A.; Sloan, E. D.; Sum, A. K.; Koh, C. A. Increasing hydrogen storage capacity using tetrahydrofuran. *J. Am. Chem. Soc.* **2009**, *131*, 14616-14617.

193. Bacher, P. Meeting the energy challenges of the 21st century. *International Journal of Energy Technology and Policy* **2002**, *1*, 1-26.

194. Hall, C.; Tharakan, P.; Hallock, J.; Cleveland, C.; Jefferson, M. Hydrocarbons and the evolution of human culture. *Nature* **2003**, *426*, 318-322.

195. International Panel on Climate Control (IPCC), 2005. Carbon dioxide capture and storage. Special report. International panel on climate (IPCC), February 5, 2007. Climate Change **2007**: The Physical Science Basis - Summary for Policy Makers.

196. Gough, C.; Shackley, S.; Cannell, M. G. R. Tyndall Centre for Climate Change Research, Technical Report 2, UMIST, Manchester, **2002**.

197. Yang, H.; Xu, Z.; Fan, M.; Gupta, R.; Slimane, R. B.; Bland, A. E.; Wright, I. Progress in carbon dioxide separation and capture: A review. *J. Environ. Sci.* **2008**, *20*, 14-27.

198. Peng, P.; Zhuang, Y. The evaluation and comparison of carbon dioxide capture technologies applied to FCC flue gas. Advanced Materials Research: Renewable and Sustainable Energy. **2012**; *347-353*, 1479-1482.

199. Belandria, V.; Mohammadi, A. H.; Eslamimanesh, A.; Richon, D.; Sánchez-Mora, M. F.; Galicia-Luna, L. A. Phase equilibrium measurements for semi-clathrate hydrates of the (CO_2+N_2 + tetra-n-butylammonium bromide) aqueous solution systems: Part 2. *Fluid Phase Equilib.* **2012**, *322–323*, 105-112.

200.   Kuramochi, T.; Ramírez, A.; Turkenburg, W.; Faaij, A. Comparative assessment of CO_2 capture technologies for carbon-intensive industrial processes. *Prog. Energy Combust. Sci.* **2012**, *38*, 87-112.

201.   Feron, P.H.M. ; Hendricks, C.A. CO_2 Capture Process Principles and Costs, Les différents procédés de capture du CO_2 et leurs coûts. Oil & Gas Science and Technology – Rev. IFP. **2005**, *60*, 451-459.

202.   Kang, S. P.; Lee, H. Recovery of CO_2 from flue gas using gas hydrate: Thermodynamic verification through phase equilibrium measurements. *Environ. Sci. Technol.* **2000**, *34*, 4397-4400.

203.   Linga, P.; Kumar, R.; Englezos, P. The clathrate hydrate process for post and pre-combustion capture of carbon dioxide. *J. Hazard. Mater.* **2007**, *149*, 625-629.

204.   Duc, N. H.; Chauvy, F.; Herri, J. M. CO_2 capture by hydrate crystallization - A potential solution for gas emission of steelmaking industry. *Energy Convers. Manage.* **2007**, *48*, 1313-1322.

205.   Kumar, R.; Wu, H. j.; Englezos, P. Incipient hydrate phase equilibrium for gas mixtures containing hydrogen, carbon dioxide and propane. *Fluid Phase Equilib.* **2006**, *244*, 167-171.

206.   Lee, H. J.; Lee, J. D.; Linga, P.; Englezos, P.; Kim, Y. S.; Lee, M. S.; Kim, Y. D. Gas hydrate formation process for pre-combustion capture of carbon dioxide. *Energy* **2010**, *35*, 2729-2733.

207.   Kumar, R.; Englezos, P.; Moudrakovski, I.; Ripmeester, J. A. Structure and composition of CO_2/H_2 and $CO_2/H_2/C_3H_8$ hydrate in relation to simultaneous CO_2 capture and H_2 production. *AlChE J.* **2009**, *55*, 1584-1594.

208.   Vorotyntsev, V. M.; Malyshev, V. M.; Mochalov, G. M.; Taraburov, P. G. Separation of gas mixtures by the gas hydrate crystallization method. *Teoreticheskie Osnovy Khimicheskoi Tekhnologii* **2001**, *35*, 128-133.

209.   Park, J.; Seo, Y. T.; Lee, J. w.; Lee, H. Spectroscopic analysis of carbon dioxide and nitrogen mixed gas hydrates in silica gel for CO_2 separation. *Catal. Today* **2006**, *115*, 279-282.

210.   Seo, Y. T.; Kang, S. P.; Lee, H.; Lee, C. S.; Sung, W. M. Hydrate phase equilibria for gas mixtures containing carbon dioxide: A proof-of-concept to carbon dioxide recovery from multicomponent gas stream. *Korean J. Chem. Eng.* **2000**, *17*, 659-667.

211.   Seo, Y.; Kang, S. P., Enhancing CO_2 separation for pre-combustion capture with hydrate formation in silica gel pore structure. *Chem. Eng. J.* **2010**, *161*, 308-312.

212.   Linga, P.; Adeyemo, A.; Englezos, P. Medium-pressure clathrate hydrate/membrane hybrid process for postcombustion capture of carbon dioxide. *Environ. Sci. Technol.* **2008**, *42*, 315-320.

213.   Unruh, C. H. ; Katz, D. L. Gas hydrates of carbon dioxide - methane mixtures. *Petroleum Transaction AIME* **1949**, *186*, 83-86.

214.   Adisasmito, S.; Frank Iii, R. J.; Dendy Sloan Jr, E. Hydrates of carbon dioxide and methane mixtures. *J. Chem. Eng. Data* **1991**, *36*, 68-71.

215.   Fan, S. S.; Chen, G. J.; Ma, Q. L.; Guo, T. M. Experimental and modeling studies on the hydrate formation of CO_2 and CO_2-rich gas mixtures. *Chem. Eng. J.* **2000**, *78*, 173-178.

216.   Hachikubo, A.; Miyamoto, A.; Hyakutake, K.; Abe, K.; Shoji, H. Phase equilibrium studies on gas hydrates formed from various guest molecules and powder ice. Fourth International Conference on Gas Hydrates, Japan, **2002**, 357-360.

217.   Ohgaki, K.; Takano, K.; Sangawa, H.; Matsubara, T.; Nakano, S. Methane exploitation by carbon dioxide from gas hydrates - Phase equilibria for CO_2-CH_4 mixed hydrate system. *J. Chem. Eng. Jpn.* **1996**, *29*, 478-483.

218.   Beltrán, J. G.; Servio, P. Morphological investigations of methane-hydrate films formed on a glass surface. *Cryst. Growth Des.* **2010**, *10*, 4339-4347.

219.   Bruusgaard, H.; Beltrán, J. G.; Servio, P. Solubility measurements for the CH_4 + CO_2 + H_2O system under hydrate-liquid-vapor equilibrium. *Fluid Phase Equilib.* **2010**, *296*, 106-109.

220.   Kang, S. P.; Lee, H.; Lee, C. S.; Sung, W. M. Hydrate phase equilibria of the guest mixtures containing CO_2, N_2 and tetrahydrofuran. *Fluid Phase Equilib.* **2001**, *185*, 101-109.

221.   Seo, Y. T.; Lee, H. Structure and guest distribution of the mixed carbon dioxide and nitrogen hydrates as revealed by X-ray diffraction and ^{13}C NMR spectroscopy. *J. Phys. Chem. B* **2004**, *108*, 530-534.

222.   Bruusgaard, H.; Beltrán, J. G.; Servio, P. Vapor-liquid water-hydrate equilibrium data for the system N_2 + CO_2 + H_2O. *J. Chem. Eng. Data* **2008**, *53*, 2594-2597.

223.   Sugahara, T.; Murayama, S.; Hashimoto, S.; Ohgaki, K. Phase equilibria for H_2 + CO_2 + H_2O system containing gas hydrates. *Fluid Phase Equilib.* **2005**, *233*, 190-193.

224.   Sugahara, T.; Mori, H.; Sakamoto, J.; Hashimoto, S.; Ogata, K.; Ohgaki, K. Cage occupancy of hydrogen in carbon dioxide, ethane, cyclopropane, and propane hydrates. *The Open Thermodynamics Journal* **2008**, *1*, 2-6.

225.   (a) Kim, D. Y.; Lee, H. Spectroscopic identification of the mixed hydrogen and carbon dioxide clathrate hydrate. *J. Am. Chem. Soc.* **2005**, *127*, 9996-9997. (b) Wang, X.; Chen, G.; Yang, L.; Zhang, L. Study on the recovery of hydrogen from refinery (hydrogen + methane) gas mixtures using hydrate technology. *Science in China, Series B: Chemistry* **2008**, *51*, 171-178.

226.   Rice, W. Hydrogen production from methane hydrate with sequestering of carbon dioxide. *Int. J. Hydrogen Energy* **2006**, *31*, 1955-1963.

227.   (a) Zhang, J.; Yedlapalli, P.; Lee, J. W. Thermodynamic analysis of hydrate-based pre-combustion capture of CO2. *Chem. Eng. Sci.* **2009**, *64*, 4732-4736. (b) Dong, T.; Wang, L.;

Liu, A.; Guo, X.; Ma, Q.; Li, G.; Sun, Q. Experimental study of separation of ammonia synthesis vent gas by hydrate formation. *Pet. Sci.* **2009**, *6*, 188-193.

228. (a) Surovtseva, D.; Amin, R.; Barifcani, A. Design and operation of pilot plant for CO2 capture from IGCC flue gases by combined cryogenic and hydrate method. *Chem. Eng. Res. Des.* **2010**, *89*, 1752–1757.(b) Lee, H. J.; Lee, J. D.; Kim, Y. D. Pre-combustion capture of carbon dioxide using principles of gas hydrate formation. *Korean Journal of Materials Research* **2008**, *18*, 650-654.

229. (a) Tajima, H.; Yamasaki, A.; Kiyono, F. Energy consumption estimation for greenhouse gas separation processes by clathrate hydrate formation. *Energy* **2004**, *29*, 1713-1729. (b) Li, S.; Fan, S.; Wang, J.; Lang, X.; Wang, Y. Clathrate hydrate capture of CO_2 from simulated flue gas with cyclopentane/water emulsion. *Chin. J. Chem. Eng.* **2010**, *18*, 202-206. (c) Lee, J.W.; Yedlapalli, P.; Mehta, R.; Lee, S. Thermodynamics-based design of H_2 storage, AIChE Spring National Meeting, Atlanta, GA, 2005, 3233.

230. Sun, C. Y.; Chen, G. J.; Zhang, L. W. Hydrate phase equilibrium and structure for (methane + ethane + tetrahydrofuran + water) system. *J. Chem. Thermodyn.* **2010**, *42*, 1173-1179.

231. (a) Wu, Q.; Zhang, B. Y. The effect of THF-SDS on separation of methane-hydrate from mine gas. *Zhongguo Kuangye Daxue Xuebao/Journal of China University of Mining and Technology* **2010**, *39*, 484-489. (b) Tajima, H.; Nagata, T.; Abe, Y.; Yamasaki, A.; Kiyono, F.; Yamagiwa, K. HFC-134a hydrate formation kinetics during continuous gas hydrate formation with a kenics static mixer for gas separation. *Ind. Eng. Chem. Res.* **2010**, *49*, 2525-2532.

232. (a) Zhang, B.; Wu, Q. Thermodynamic promotion of tetrahydrofuran on methane separation from low-concentration coal mine methane based on hydrate. *Energy Fuels* **2010**, *24*, 2530-2535. (b) Kondo, W.; Ogawa, H.; Ohmura, R.; Mori, Y. H. Clathrate hydrate formation from a hydrocarbon gas mixture: Evolution of gas-phase composition in a hydrate-forming reactor. *Energy Fuels* **2010**, *24*, 6375-6383.

233. (a) Lu, T.; Zhang, Y.; Li, X. S.; Chen, Z. Y.; Yan, K. F. Equilibrium conditions of hydrate formation in the systems of CO_2-N_2-TBAB and CO_2-N_2-THF. *Guocheng Gongcheng Xuebao/The Chinese Journal of Process Engineering* **2009**, *9*, 541-544 (in Chinese). (b) Ng, H. J. Hydrate phase composition for multicomponent gas mixtures. In **2000**; *912*, 1034-1039 *Ann. NY Acad. Sci.* **2000**, *912*, 1034–1039.

234. (a) Zhang, B. Y.; Wu, Q.; Zhu, Y. M. Effect of THF on the thermodynamics of low-concentration gas hydrate formation. *Zhongguo Kuangye Daxue Xuebao/Journal of China University of Mining and Technology* **2009**, *38*, 203-208. (b) Ma, Q.; Chen, G.; Zhang, L. Vapor-hydrate phases equilibrium of (CH_4+C_2H_6) and (CH_4+C_2H_4) systems. *Pet. Sci.* **2008**, *5*, 359-366.

235. (a) Zhao, J. Z.; Zhao, Y. S.; Shi, D. X. Experiment on methane concentration from oxygen-containing coal bed gas by THF solution hydrate formation. *Meitan Xuebao/Journal of the China Coal Society* **2008**, *33*, 1419-1424. (b) Lee, J. W.; Kim, D. Y.; Lee, H. Phase behavior and structure transition of the mixed methane and nitrogen hydrates. *Korean J. Chem. Eng.* **2006**, *23*, 299-302.

236. (a) Zhang, L. W.; Huang, Q.; Sun, C. Y.; Ma, Q. L.; Chen, G. J. Hydrate formation conditions of methane + ethylene + tetrahydrofuran + water systems. *J. Chem. Eng. Data* **2006**, *51*, 419-422.

237. Sun, Q.; Guo, X.; Liu, A.; Liu, B.; Huo, Y.; Chen, G. Experimental study on the separation of CH_4 and N_2 via hydrate formation in TBAB solution. *Ind. Eng. Chem. Res.* **2011**, *50*, 2284-2288.

238. Shimada, W.; Ebinuma, T.; Oyama, H.; Kamata, Y.; Takeya, S.; Uchida, T.; Nagao, J.; Narita, H. Separation of gas molecule using tetra-n-butyl ammonium bromide semi-clathrate hydrate crystals. *Jpn. J. Appl. Phys., Part 2* **2003**, *42*, L129-L131.

239. Xie, Y.; Gong, J.; Tang, T.; Liu, D.; Liu, N.; Qi, Y. Experimental research on hydrogen storage characteristics of TBAB hydrates. In Advanced Materials: Part 3, Second International Conference on Advances in Materials and Manufacturing Processes, Guilin, China, **2011**, *415-417*, 1697-1702.

240. Trueba, A. T.; Radović, I. R.; Zevenbergen, J. F.; Kroon, M. C.; Peters, C. J. Kinetics measurements and in situ Raman spectroscopy of formation of hydrogen-tetrabutylammonium bromide semi-hydrates. *Int. J. Hydrogen Energy* **2012**, *37*, 5790-5797.

241. Acosta, H. Y.; Bishnoi, P. R.; Clarke, M. A. Experimental measurements of the thermodynamic equilibrium conditions of tetra-n-butylammonium bromide semiclathrates formed from synthetic landfill gases. *J. Chem. Eng. Data* **2011**, *56*, 69-73.

242. Lee, S.; Lee, Y.; Park, S.; Seo, Y. Phase equilibria of semiclathrate hydrate for nitrogen in the presence of tetra- n -butylammonium bromide and fluoride. *J. Chem. Eng. Data* **2010**, *55*, 5883-5886.

243. Uchida, T.; Shiga, T.; Nagayama, M.; Gohara, K. Observation of sintering of clathrate hydrates. *Energies* **2010**, *3*, 1960-1971.

244. Chapoy, A.; Gholinezhad, J.; Tohidi, B. Experimental clathrate dissociations for the hydrogen + water and hydrogen + tetrabutylammonium bromide + water systems. *J. Chem. Eng. Data* **2010**, *55*, 5323-5327.

245. (a) Uchida, T.; Shiga, T.; Nagayama, M.; Gohara, K. Observation of sintering of clathrate hydrates. *Energies* **2010**, *3*, 1960-1971. (b) Johnson, A.; Osegovic, J. P.; Max, M. D. Hydrate gas separation - A new technology for removing nitrogen from natural gas. GPA Annual Meeting, Convention Proc., San Antonio, TX, **2009**.

246. Oshima, M.; Shimada, W.; Hashimoto, S.; Tani, A.; Ohgaki, K. Memory effect on semi-clathrate hydrate formation: A case study of tetragonal tetra-n-butyl ammonium bromide hydrate. *Chem. Eng. Sci.* **2010**, *65*, 5442-5446.

247. Rodionova, T.; Komarov, V.; Villevald, G.; Aladko, L.; Karpova, T.; Manakov, A. Calorimetric and structural studies of tetrabutylammonium chloride ionic clathrate hydrates. *J. Phys. Chem. B* **2010**, *114*, 11838-11846.

248. Deschamps, J.; Dalmazzone, D. Hydrogen storage in semiclathrate hydrates of tetrabutyl ammonium chloride and tetrabutyl phosphonium bromide. *J. Chem. Eng. Data* **2010**, *55*, 3395-3399.

249. Li, S.; Fan, S.; Wang, J.; Lang, X.; Wang, Y. Semiclathrate hydrate phase equilibria for CO_2 in the presence of tetra-n-butyl ammonium halide (bromide, chloride, or fluoride). *J. Chem. Eng. Data* **2010**, *55*, 3212-3215.

250. Sun, Z. G.; Sun, L. Equilibrium conditions of semi-clathrate hydrate dissociation for methane + tetra-n-butyl ammonium bromide. *J. Chem. Eng. Data* **2010**, *55*, 3538-3541.

251. Sugahara, T.; Haag, J. C.; Warntjes, A. A.; Prasad, P. S. R.; Sloan, E. D.; Koh, C. A.; Sum, A. K. Large-cage occupancies of hydrogen in binary clathrate hydrates dependent on pressures and guest concentrations. *J. Phys. Chem. C* **2010**, *114*, 15218-15222.

252. Li, X. S.; Xu, C. G.; Chen, Z. Y.; Wu, H. J. Tetra-n-butyl ammonium bromide semi-clathrate hydrate process for post-combustion capture of carbon dioxide in the presence of dodecyl trimethyl ammonium chloride. *Energy* **2010**, *35*, 3902-3908.

253. Li, X. S.; Xia, Z. M.; Chen, Z. Y.; Yan, K. F.; Li, G.; Wu, H. J. Equilibrium hydrate formation conditions for the mixtures of CO_2 + H_2 + tetrabutyl ammonium bromide. *J. Chem. Eng. Data* **2010**, *55*, 2180-2184.

254. Mayoufi, N.; Dalmazzone, D.; Fürst, W.; Delahaye, A.; Fournaison, L. CO_2 enclathration in hydrates of peralkyl-(Ammonium/Phosphonium) salts: Stability conditions and dissociation enthalpies. *J. Chem. Eng. Data* **2010**, *55*, 1271-1275.

255. Makino, T.; Yamamoto, T.; Nagata, K.; Sakamoto, H.; Hashimoto, S.; Sugahara, T.; Ohgaki, K. Thermodynamic stabilities of tetra-n-butyl ammonium chloride + H_2, N_2, CH_4, CO_2, or C_2H_6 semiclathrate hydrate systems. *J. Chem. Eng. Data* **2010**, *55*, 839-841.

256. Wenji, S.; Rui, X.; Chong, H.; Shihui, H.; Kaijun, D.; Ziping, F. Experimental investigation on TBAB clathrate hydrate slurry flows in a horizontal tube: Forced convective heat transfer behaviors. *Int. J. Refrig* **2009**, *32*, 1801-1807.

257. Deschamps, J.; Dalmazzone, D. Dissociation enthalpies and phase equilibrium for TBAB semi-clathrate hydrates of N_2, CO_2, N_2 + CO_2 and CH_4 + CO_2. *J. Therm. Anal. Calorim.* **2009**, *98*, 113-118.

258. Fan, S.; Li, S.; Wang, J.; Lang, X.; Wang, Y. Efficient capture of CO_2 from simulated flue gas by formation of TBAB or TBAF semiclathrate hydrates. *Energy Fuels* **2009**, *23*, 4202-4208.

259. Xiao, R.; Song, W. J.; Huang, C.; He, S. H.; Dong, K. J.; Feng, Z. P. Re-laminarization of TBAB hydrate slurry flow in tube. *Kung Cheng Je Wu Li Hsueh Pao/Journal of Engineering Thermophysics* **2009**, *30*, 971-973.

260. Schildmann, S.; Nowaczyk, A.; Geil, B.; Gainaru, C.; Böhmer, R. Water dynamics on the hydrate lattice of a tetrabutyl ammonium bromide semiclathrate. *J. Chem. Phys.* **2009**, *130*, 104505-1 104505-10.

261. Li, S.; Fan, S.; Wang, J.; Lang, X.; Liang, D. CO_2 capture from binary mixture via forming hydrate with the help of tetra-n-butyl ammonium bromide. *J. Nat. Gas Chem.* **2009**, *18*, 15-20.

262. Ma, Q. L.; Chen, G. J.; Ma, C. F.; Zhang, L. W. Study of vapor-hydrate two-phase equilibria. *Fluid Phase Equilib.* **2008**, *265*, 84-93.

263. Kim, S. M.; Lee, J. D.; Lee, H. J.; Lee, E. K.; Kim, Y. Gas hydrate formation method to capture the carbon dioxide for pre-combustion process in IGCC plant. *Int. J. Hydrogen Energy* **2011**, *36*, 1115-1121.

264. Kuramochi, T.; Ramírez, A.; Turkenburg, W.; Faaij, A. Techno-economic assessment and comparison of CO_2 capture technologies for industrial processes: Preliminary results for the iron and steel sector. *Energy Procedia* **2011**, *4*, 1981-1988.

265. Kamata, Y.; Oyama, H.; Shimada, W.; Ebinuma, T.; Takeya, S.; Uchida, T.; Nagao, J.; Narita, H. Gas separation method using tetra-n-butyl ammonium bromide semi-clathrate hydrate. *Jpn. J. Appl. Phys., Part 1: Regular Papers and Short Notes and Review Papers* **2004**, *43*, 362-365.

266. (a) Kamata, Y.; Yamakoshi, Y.; Ebinuma, T.; Oyama, H.; Shimada, W.; Narita, H. Hydrogen sulfide separation using tetra-n-butyl ammonium bromide semi-clathrate (TBAB) hydrate. *Energy Fuels* **2005**, *19*, 1717-1722. (b) Shiojiri, K.; Okano, T.; Yanagisawa, Y.; Fujii, M.; Yamasaki, A.; Tajima, H.; Kiyono, F. A new type separation process of condensable greenhouse gases by the formation of clathrate hydrates. Proc. ICGH4, **2004**; *153*, 507-512.

267. Happel, J.; Hnatow, M. A.; Meyer, H. The study of separation of nitrogen from methane by hydrate formation using a novel apparatus. *Ann. N.Y. Acad. Sci.* **1994**, *715*, 412-424.

268. Sun, C. Y.; Ma, C. F.; Chen, G. J.; Zhang, S. X. Experimental and simulation of single equilibrium stage separation of (methane + hydrogen) mixtures via forming hydrate. *Fluid Phase Equilib.* **2007**, *261*, 85-91.

269. Eslamimanesh, A.; Mohammadi, A. H.; Richon, D. Thermodynamic consistency test for experimental data of sulfur content of hydrogen sulfide. *Ind. Eng. Chem. Res.* **2011**, *50*, 3555-3563.

270. Cha, I.; Lee, S.; Lee, J. D.; Lee, G. W.; Seo, Y. Separation of SF_6 from gas mixtures using gas hydrate formation. *Environ. Sci. Technol.* **2010**, *44*, 6117-6122.

271. Østergaard, K. K.; Tohidi, B.; Danesh, A.; Burgass, R. W.; Todd, A. C.; Baxter, T. A novel approach for oil and gas separation by using gas hydrate technology. *Ann. N.Y. Acad. Sci.* **2000**; *912*, 832-842.

272. Dorsett, L. R. L T X Reapplication of Proven Technology. Presented at the SPE Gas Technology Symposium, Dallas, TX, **1989**, 239-246.

273. Chun, M. K.; Lee, H.; Ryu, B. J. Phase equilibria of R22 ($CHClF_2$) hydrate systems in the presence of NaCl, KCl, and $MgCl_2$. *J. Chem. Eng. Data* **2000**, *45*, 1150-1153.

274. Seo, Y.; Lee, H. A new hydrate-based recovery process for removing chlorinated hydrocarbons from aqueous solutions. *Environ. Sci. Technol.* **2001**, *35*, 3386-3390.

275. Javanmardi, J.; Moshfeghian, M. Energy consumption and economic evaluation of water desalination by hydrate phenomenon. *Appl. Therm. Eng.* **2003**, *23*, 845-857.

276. Eslamimanesh, A.; Hatamipour, M. S. Mathematical modeling of a direct contact humidification-dehumidification desalination process. *Desalination* **2009**, *237*, 296-304.

277. Eslamimanesh, A.; Hatamipour, M. S. Economical study of a small-scale direct contact humidification-dehumidification desalination plant. *Desalination* **2010**, *250*, 203-207.

278. Parker, A. Potable water from sea-water. *Nature* **1942**, *149*, 184-186.

279. McDermott, J. Desalination by freeze concentration, Noyes Data Corp.: Park Ridge, NJ, **1971**.

280. Tleilmat, B.W. Freezing methods. In Principles of Desalination, 2nd ed.; K.S. Spriengler, K. S., Ed.; Academic Press: New York, 1980, *7*, 359-400.

281. Khan, A. H. Freezing. In Desalination Processes and Multistage Flash Distillation Practice; Elsevier: Amsterdam, **1986**, *5*, 55-68.

282. Barduhn, A. J.; Towlson, H. E.; Hu, Y. C. The Properties of some new gas hydrates and their use in demineralizing seawater. *AIChE J.* **1962**, *22*, 176-183.

283. Pavlov, G.D.; Medvedev, I.N. Gas hydrating process of water desalination. Proceedings of 1st International Symposium on Water Desalination. **1967**, *3*, 123–127.

284. Sugi, J.; Saito, S. Concentration and demineralization of sea water by the hydrate process. *Desalination* **1967**, *3*, 27-31.

285. Barduhn, A.J.; Roux, G.M.; Richard, H.A. The rate of formation of the hydrates of F-31 (CH_3ClF) and F-142b (CH_3CClF_2) in a stirred tank reactor. Proceeding of International Symposium on Fresh Water from Sea **1976**, *3*, 253-261.

286. Vlahakis, J.G.; Chen, H.S.; Suwandi, M.S.; Barduhn, A.J. The growth rate of ice crystals: Properties of carbon dioxide hydrate, A Review of properties of 51 gas hydrates, Syracuse University Research and Development Report 830, Prepared for the Office of Saline Water, US. Department of the Interior, Nov., **1972**.

287. Barduhn, A. J., The state of the crystallization processes for desalting saline waters. *Desalination* **1968**, *5*, 173-184.

288. Morlat, M.; Pernolet, R.; Gerard, N.; Formation process of ethylene hydrate. Proceeding of International Symposium on Fresh Water from Sea, Alghero, Italy, May 16-20, **1976**, *3*, 263-269.

289. Rautenbach, R.; Seide, A. Technical problem and economics of hydrate process. Proceeding of International Symposium on Fresh Water from Sea, **1978**, 43-51.

290.   Delyannis, A. Fresh water sea. 2nd Proceeding of European Symposium on Fresh Water from Sea, May 9-12, Athens, Greece, **1967**.

291.   Delyannis, A.; Delyannis, E. Fresh water sea.   3rd Proceeding of International Symposium on Fresh Water from Sea, Dubrovnik, Yugoslavia, September, **1970**.

292.   Delyannis, A.; Delyannis, E. Fresh water sea. 4th Proceeding of International Symposium on Fresh Water from Sea, Athens, Greece, **1973**.

293.   Delyannis, A.; Delyannis, E. Fresh water sea, 5th Proceeding of International Symposium on Fresh Water from Sea, Alghero, Italy, May 16-20, **1976**.

294.   Delyannis, A.; Delyannis, E. Fresh water sea, 6th Proceeding of International Symposium on Fresh Water from Sea, Las Palmas, Gran Canaria, Spain, **1978**.

295.   Lund, D. B.; Fennema, O.; Powrie, W. D. Rotation apparatus for shell-freezing. *Cryobiology* **1968**, *5*, 26-28.

296.   Lund, D. B.; Fennema, O.; Powrie, W. D. Effect of gas hydrates and hydrate formers on invertase activity. *Arch. Biochem. Biophys.* **1969**, *129*, 181-188.

297.   Van Hulle, G.; Fennema, O. Gas hydrates in aqueous-organic systems. IV. Formation and detection of ethylene oxide hydrate in tissue. *Cryobiology* **1971**, *7*, 223-227.

298.   Van Hulle, G.; Fennema, O. Gas hydrates in aqueous-organic systems. VI. Effects of hydrate formers and hydrate crystals in carrot tissue. *Cryobiology* **1971**, *8*, 91-103.

299.   Nguyen, H.; Rao, A. M.; Phillips, J. B.; John, V. T.; Reed, W. F. Gas hydrate formation in reversed micelles - applications to bioseparations and biocatalysis. *Appl. Biochem. Biotechnol.* **1991**, *28-29*, 843-853.

300.   Rao, A. M.; Kommareddi, N.; John, V. T. Use of pressure to modify enzyme activity in reversed micelles. *Biotechnol. Progr.* **1992**, *8*, 514-520.

301.   John, V. T. Protein Recovery from reversed micellar solutions through contact with a pressurized gas phase. *Biotechnol. Progr.* **1991**, *7*, 43-48.

302.   Bayraktar, E.; Kocapiçak, O.; Mehmetoğlu, U.; Parlaktuna, M.; Mehmetoğlu, T. Recovery of amino acids from reverse micellar solution by gas hydrate. *Chem. Eng. Res. Des.* **2008**, *86*, 209-213.

303.   Aydoğan, Ö.; Bayraktar, E.; Parlaktuna, M.; Mehmetoğlu, T.; Mehmetoğlu, Ü. Production of L-aspartic acid by biotransformation and recovery using reverse micelle and gas hydrate methods. *Biocatal. Biotransform.* **2007**, *25*, 365-372.

304.   Fontes, N.; Harper, N.; Hailing, P. J.; Barreiros, S. Salt hydrates for in situ water activity control have acid-base effects on enzymes in nonaqueous media. *Biotechnol. Bioeng.* **2003**, *82*, 802-808.

305.   Berberich, J. A.; Kaar, J. L.; Russell, A. J. Use of salt hydrate pairs to control water activity for enzyme catalysis in ionic liquids. *Biotechnol. Progr.* **2003**, *19*, 1029-1032.

306. He, H. P.; Yang, L. R.; Zhu, Z. Q. Control of water activity of enzymatic reaction in organic solvent media using salt/salt hydrate pairs. *Chinese J. Org. Chem.* **2001**, *21*, 376-379.

307. Noritomi, H.; Hidaka, Y.; Kato, S.; Nagahama, K. Recovery of protein from reverse micelles through gas hydrate formation. *Biotechnol. Tech.* **1999**, *13*, 181-183.

308. Eslamimanesh, A.; Mohammadi, A. H.; Richon, D. Thermodynamic model for predicting phase equilibria of simple clathrate hydrates of refrigerants. *Chem. Eng. Sci.* **2011**, *66*, 5439-5445.

309. Huang, C. P.; Fennema, O.; Powrie, W. D. Gas hydrates in aqueous-organic systems. I. Preliminary studies. *Cryobiology* **1965**, *2*, 109-115.

310. Huang, C. P.; Fennema, O.; Powrie, W. D. Gas hydrates in aqueous-organic systems. II. Concentration by gas hydrate formation. *Cryobiology* **1966**, *2*, 240-245.

311. Eslamimanesh, A.; Gharagheizi, F.; Mohammadi, A. H.; Richon, D. Artificial Neural Network modeling of solubility of supercritical carbon dioxide in 24 commonly used ionic liquids. *Chem. Eng. Sci.* **2011**, *66*, 3039-3044.

312. Tumba, K.; Reddy, P.; Naidoo, P.; Ramjugernath, D.; Eslamimanesh, A.; Mohammadi, A. H.; Richon, D. Phase equilibria of methane and carbon dioxide clathrate hydrates in the presence of aqueous solutions of tributylmethylphosphonium methylsulfate ionic liquid. *J. Chem. Eng. Data* **2011**, *56*, 3620-3629.

313. Peng, X.; Hu, Y.; Liu, Y.; Jin, C.; Lin, H. Separation of ionic liquids from dilute aqueous solutions using the method based on CO_2 hydrates. *J. Nat. Gas Chem.* **2010**, *19*, 81-85.

314. Sun, R.; Duan, Z., Prediction of CH_4 and CO_2 hydrate phase equilibrium and cage occupancy from ab initio intermolecular potentials. *Geochim. Cosmochim. Acta* **2005**, *69*, 4411-4424.

315. Kamath, V. A. Study of Heat Transfer Characteristics during Dissociation of Gas Hydrates in Porous Media, Ph.D. Dissertation, University of Pittsburgh, University Microfilms No. 8417404, Ann Arbor, MI, **1984**.

316. Katz, D. L. Prediction of conditions for hydrate formation in natural gases. *Trans. AIME*, **1945**, *160*, *140*-149.

317. Wilcox, W. I.; Carson, D. B.; Katz, D. L. Natural gas hydrates. *Ind. Eng. Chem.* **1941**, *33*, 662-713.

318. Carson, D. B.; Katz, D. L. Natural Gas Hydrates. *Trans. AIME* **1942**, 146, 150-158.

319. van der Waals J. H.; Platteeuw J. C. Clathrate solutions. In *Advances in Chemical Physics* (Ed. Prigogine, I.), Interscience. **1959**, 1–57.

320. Platteeuw, J. C.; van der Waals, J. H. Thermodynamic properties of gas hydrates II: Phase equilibria in the system H$_2$S- C$_3$H$_8$-H$_2$O at −3°C. *Rec. Trav. Chim. Pays-Bas* **1959**, *78*, 126-133.

321. Parrish, W. R.; Prausnitz, J. M. Dissociation pressures of gas hydrates formed by gas mixtures. *Ind. Eng. Chem. Process Des. Develop.* **1972**, *11*, 26-35.

322. Holder, G.D.; Corbin., G.; Papadopoulos, K.D. Thermodynamic and molecular properties of gas hydrates from mixtures containing methane, argon and krypton. *Ind. Eng. Chem. Fundam.* **1980**, *19*, 282-286.

323. Mohammadi, A.H.; Anderson, R.; Tohidi, B. Carbon monoxide clathrate hydrates: equilibrium data and thermodynamic modeling. *AIChE J.* **2005**, *51*, 2825-2833.

324. Kihara, T. On Isihara-Hayashida's theory of the second virial coefficient for rigid convex molecules. *J. Phys. Soc. Japan* **1953**, *8*, 686-687.

325. Kihara, T. Virial coefficients and models of molecules in gases. *Rev. Mod. Phys.* **1953**, *25*, 831-840.

326. McKoy, V.; Sinanoğlu, O. Theory of dissociation pressures of some gas hydrates. *J. Chem. Phys.* **1963**, *38*, 2946-2956.

327. Clarke, M. A.; Pooladi-Darvish, M.; Bishnoi, P. R. A method to predict equilibrium conditions of gas hydrate formation in porous media. *Ind. Eng. Chem. Res.* **1999**, *38*, 2485-2490.

328. Trebble, M. A.; Bishnoi, P. R. Extension of the Trebble- Bishnoi Equation of State to Fluid Mixtures. *Fluid Phase Equilib.* **1987**, *40*, 1-21.

329. Lee, S.-Y; Holder, G.D. Model for Gas Hydrate Equilibria Using a Variable Reference Chemical Potential: Part 1. *AIChE. J.* **2002**, *48*, *161*-167.

330. Tohidi, B.; Burgass R.W.; Danesh A.; Todd, A.C. Hydrate inhibition effect of produced water, Part 1. Ethane and propane simple gas hydrates. *SPE* 26701. Proceeding of the SPE Offshore Europe 93 Conference, **1993**, 255-264.

331. Anderson. F.E.; Prausnitz, J.M.; Inhibition of gas hydrates by methanol. *AIChE J.* **1986**, *32*, 1321-1333.

332. Avlonitis, D.; Varotsis, N. Modelling gas hydrate thermodynamic behaviour: theoretical basis and computational methods. *Fluid Phase Equilib.* **1996**, *123*, 107-130.

333. Klauda, J.B.; Sandler, S.I. Phase behavior of clathrate hydrates: a model for single and multiple gas component hydrates. *Chem. Eng. Sci.* **2003**, *58*, 27-41.

334. Hashemi, S.; Macchi, A.; Bergeron, S.; Servio, P. Prediction of methane and carbon dioxide solubility in water in the presence of hydrate. *Fluid Phase Equilib.* **2006**, *246*, 131-136.

335.   Zhang, Y.; Debenedetti, P. G.; Prud'homme R. K.; Pethica, B.A. Accurate prediction of clathrate hydrate phase equilibria below 300 K from a simple model *J. Petrol. Sci. Eng.* **2006**, *51*, 45-53.

336.   Martín, Á.; Peters, C. J. Hydrogen storage in sH clathrate hydrates: thermodynamic model. *J. Phys. Chem. B* **2009**, *113*, 7558–7563.

337.   Ballard, L.; Sloan, E. D. The next generation of hydrate prediction: IV. A comparison of available hydrate prediction programs. *Fluid Phase Equilib.* **2004**, *216*, 257-270.

338.   Ballard, L.; Sloan, E. D. The next generation of hydrate prediction: I. Hydrate standard states and incorporation of spectroscopy. *Fluid Phase Equilib.* **2002**, *194-197*, 371-383.

339.   Ballard, A.L.; Sloan E. D. The next generation of hydrate prediction: Part III. Gibbs energy minimization formalism. *Fluid Phase Equilib.* **2004**, *218*, 15-31.

340.   Ballard, A.L.; Sloan E. D. The next generation of hydrate prediction V. A comparison of available hydrate prediction programs. *Fluid Phase Equilib.* **2004**, *216*, 257-270.

341.   Jager, M.D.; Ballard, A.L.; Sloan E.D. The next generation of hydrate prediction: II. Dedicated aqueous phase fugacity model for hydrate prediction. *Fluid Phase Equilib.* **2003**, *211*, 85-107.

342.   Lennard-Jones., J.E.; Devonshire, A.F. Critical phenomena in gases I. vapor pressures and boiling points. *Proc. Royal Soc. Lond. A* **1937**, *163*, 53-70.

343.   Cao, Z.; Tester, J. W.; Trout, B. L. Computation of the methane-water potential energy hypersurface via ab initio methods. *J. Chem. Phys.* **2001**, *115*, 2550-2559.

344.   Cao, Z.; Tester, J. W.; Sparks, K. A.; Trout, B. L. Molecular computations using robust hydrocarbon-water potentials for predicting gas hydrate phase equilibria. *J. Phys. Chem. B* **2001**, *105*, 10950-10960.

345.   Anderson, B. J.; Tester, J. W.; Trout, B. L. Accurate potentials for argon-water and methane-water interactions via ab initio methods and their application to clathrate hydrates. *J. Phys. Chem. B* **2004**, *108*, 18705–18715.

346.   Baker, L. E.; Pierce, A. C.; Luks, K. D. Gibbs energy analysis of phase equilibrium. *Soc. Pet. Eng. J.* **1982**, October, 731-742.

347.   Hagan, M.; Demuth, H. B.; Beale, M. H. Neural Network Design, International Thomson publishing Inc; Boston, MA, USA, **2002.**

348.   Gharagheizi, F.; Eslamimanesh, A.; Mohammadi, A. H.; Richon, D. Artificial neural network modeling of solubilities of 21 commonly used industrial solid compounds in supercritical carbon dioxide. *Ind. Eng. Chem. Res.* **2011**, *50*, 221-226.

349.   Mehrpooya, M.; Mohammadi, A. H.; Richon, D. Extension of an artificial neural network algorithm for estimating sulfur content of sour gases at elevated temperatures and pressures. *Ind. Eng. Chem. Res.* **2010**, *49*, 439-442.

350.   Chouai, A.; Laugier, S.; Richon, D. Modeling of thermodynamic properties using neural networks: Application to refrigerants. *Fluid Phase Equilib.* **2002**, *199*, 53–62.

351.   Piazza, L.; Scalabrin, G.; Marchi, P.; Richon, D. Enhancement of the extended corresponding states techniques for thermodynamic modelling. I. Pure fluids. *Int. J. Refrig.* **2006**, *29*, 1182-1194.

352.   Gu, X.; Han, X.; Wang, S.; Liu, F. Predicting gas hydrate formation by artificial neural networks. *Tianranqi Gongye/Natural Gas Industry* **2003**, *23*, 102-104.

353.   Kalogirou, S. A. Artificial neural networks in renewable energy systems applications: A review. *Renew. Sust. Energ. Rev.* **2001**, *5*, 373-401.

354.   Lee, M. J.; Chen, J. T., Fluid property predictions with the aid of neural networks. *Ind. Eng. Chem. Res.* **1993**, *32*, 995-997.

355.   Habiballah, W. A.; Startzman, R. A.; Barrufet, M. A. Use of neural networks for prediction of vapor/liquid equilibrium k values for light-hydrocarbon mixtures. *SPE Reservoir Engineering (Society of Petroleum Engineers)* **1996**, *11*, 121-125.

356.   Elgibaly, A. A.; Elkamel, A. M. A new correlation for predicting hydrate formation conditions for various gas mixtures and inhibitors. *Fluid Phase Equilib.* **1998**, *152*, 23-42.

357.   Mohammadi, A.H.; Richon, D. Hydrate phase equilibria for hydrogen + water and hydrogen + tetrahydrofuran + water systems: Predictions of dissociation conditions using an artificial neural network algorithm. *Chem. Eng. Sci.* **2010**, *65*, 3352-3355.

358.   Mohammadi, A.H.; Richon, D. A mathematical model based on artificial neural network technique for estimating liquid water − hydrate equilibrium of water − hydrocarbon System. *Ind. Eng. Chem. Res.* **2008**, *47*, 4966-4970.

359.   Mohammadi, A.H.; Richon, D. Use of artificial neural networks for estimating water content of natural gases. *Ind. Eng. Chem. Res.* **2007**, *46*, 1431-1438.

360.   Chapoy, A.; Mohammadi, A.H.; Richon, D. Predicting the hydrate stability zones of natural gases using Artificial Neural Networks. Oil & Gas Science and Technology – Rev. IFP **2007**, *62*, 701-706.

361.   Mohammadi, A.H.; Martínez-López, J.F.; Richon, D. Determining phase diagrams of tetrahydrofuran+methane, carbon dioxide or nitrogen clathrate hydrates using an artificial neural network algorithm. *Chem. Eng. Sci.* **2010**, *65*, 6059-6063.

362.   Mohammadi, A.H.; Belandria, V.; Richon, D. Use of an artificial neural network algorithm to predict hydrate dissociation conditions for hydrogen + water and hydrogen + tetra-n-butyl ammonium bromide + water systems. *Chem. Eng. Sci.* **2010**, *65*, 4302-4305.

363.   Eslamimanesh, A.; Gharagheizi, F.; Illbeigi, M.; Mohammadi, A. H.; Fazlali, A.; Richon, D. Phase equilibrium modeling of clathrate hydrates of methane, carbon dioxide,

nitrogen, and hydrogen + water soluble organic promoters using Support Vector Machine algorithm. *Fluid Phase Equilib.* **2012**, *316*, 34-45.

364. Suykens, J.A.K.; Van Gestel, T.; De Brabanter, J.; De Moor, B.; Vandewalle, J. Least Squares Support Vector Machines, World Scientific, Singapore, **2002**.

365. Suykens, J. A. K.; Vandewalle, J. Least squares support vector machine classifiers. *Neural Process. Lett.* **1999**, *9*, 293-300.

366. Curilem, M.; Acuña, G.; Cubillos, F.; Vyhmeister, E. Neural Networks and Support Vector Machine models applied to energy consumption optimization in semiautogeneous grinding. *Chemical Engineering Transactions* **2011**, *25*, 761-766.

367. (a) Tse, J. S.; Klein, M. L.; McDonald, I. R. Dynamical properties of the structure I clathrate hydrate of xenon. *J. Chem. Phys.* **1983**, *78*, 2096-2097 (b) Tse, J. S.; Klein, M. L.; McDonald, I. R. Molecular dynamics studies of ice and the structure I clathrate hydrate of methane. *J. Phys. Chem.* **1983**, *87*, 4198-4203. (c) Tse, J. S.; Klein, M. L.; McDonald, I. R. Computer simulation studies of the structure I clathrate hydrates of methane, tetrafluoromethane, cyclopropane, and ethylene oxide. *J. Chem. Phys.* **1984**, *81*, 6146-6153. (d) Tse, J. S.; McKinnon, W. R.; Marchi, M. Thermal expansion of structure I ethylene oxide hydrate. *J. Phys. Chem.* **1987**, *91*, 4188-4193.

368. Hwang, M. J.; Holder, G. D.; Zele, S. R. Lattice distortion by guest molecules in gas-hydrates. *Fluid Phase Equilib.* **1993**, *83*, 437-444.

369. Zele, S. R. Molecular Dynamics and Thermodynamic Modeling of Gas Hydrates. Ph.D. Thesis, University of Pittsburgh, Pittsburgh, PA, **1994**.

370. Pratt, R.M.; Sloan, E. D. A computer simulation and investigation of liquid-solid interfacial phenomena for ice and clathrate hydrates. *Mol. Sim.* **2005**, *15*, 247-264.

371. Carver, T. J.; Drew, M. G. B.; Rodger, P. M. Inhibition of crystal growth in methane hydrate. *J. Chem. Soc., Faraday Trans.* **1995**, *91*, 3449-3460.

372. Førrisdahl, O. K. R.; Kvamme, B.; Haymet, A. D. J. Methane clathrate hydrates: Melting, supercooling and phase separation from molecular dynamics computer simulations. *Mol. Phys.* **1996**, *89*, 819-834.

373. Makogon, T. Y. Kinetic Inhibition of Natural Gas Hydrates Formation. Ph.D. Dissertation, Colorado School of Mines, Golden, CO, **1997**.

374. Anderson, B. J.; Tester, J. W.; Borghi, G. P.; Trout, B. L. Properties of inhibitors of methane hydrate formation via molecular dynamics simulations. *J. Am. Chem. Soc.* **2005**, *127*, 17852-17862.

375. Tester, J. W.; Bivins, R. L.; Herrick, C. C. Use of Monte Carlo in calculating the thermodynamic properties of water clathrates. *AlChE J.* **1972**, *18*, 1220-1230.

376. Tse, J. S.; Davidson, D. W. Intermolecular potentials in gas hydrates. Proc 4th Can. Perm. Conf. Calgary, March 2-6, Alberta, **1981**, 329.

377.   Lund, A. The influences of gas-gas interactions on the stability of gas hydrates. Ph.D. Thesis, Norwegian Technical University, **1990**.

378.   Kvamme, B.; Lund, A.; Hertzberg, T. The influence of gas-gas interactions on the Langmuir constants for some natural gas hydrates. *Fluid Phase Equilib.* **1993**, *90*, 15-44.

379.   Natarajan, V.; Bishnoi, P. R. Langmuir constant computations for gas hydrate systems. *Ind. Eng. Chem. Res.* **1995**, *34*, 1494-1498.

380.   Todeschini, R.; Consonni, V. Molecular Descriptors for Chemoinformatics: Vol. I: Alphabetical Listing/Vol. II: Appendices, References, 2nd Revised and Enlarged Ed., Wiley-VCH: Weinheim, Gemany, **2009**.

381.   Talete srl, Dragon for Windows (Software for molecular Descriptor Calculation). Version 5.5, **2006**.

382.   Paricaud, P. Modeling the dissociation conditions of salt hydrates and gas semiclathrate hydrates: application to lithium bromide, hydrogen iodide, and tetra-n-butylammonium bromide + carbon dioxide systems. *J. Phys. Chem. B* **2011**, *115*, 288–299.

383.   Galindo, A.; Gil-Villegas, A.; Jackson, G.; Burgess, A.N.J. SAFT-VRE: Phase behavior of electrolyte solutions with the statistical associating fluid theory for potentials of variable range. *J. Phys. Chem. B* **1999**, *103*, 10272-10281.

384.   Chapman, W. G.; Gubbins, K. E.; Jackson, G.; Radosz, M. SAFT: Equation-of-state solution model for associating fluids. *Fluid Phase Equilib.* **1989**, *52*, 31-38.

385.   Mohammadi, A. H.; Richon, D. Thermodynamic model for predicting liquid water-hydrate equilibrium of the water-hydrocarbon system. *Ind. Eng. Chem. Res.* **2008**, *47*, 1346–1350.

386.   Mohammadi, A. H.; Richon, D. Development of predictive techniques for estimating liquid water-hydrate equilibrium of water hydrocarbon system. *J. Thermodyn.* **2009**, 1–12.

387.   Eslamimanesh, A.; Mohammadi, A. H.; Richon, D. Thermodynamic model for predicting phase equilibria of simple clathrate hydrates of refrigerants. *Chem. Eng. Sci.* **2011**, *66*, 5439-5445.

388.   Pahlavanzadeh, H.; Kamran-Pirzaman, A.; Mohammadi, A. H. Thermodynamic modeling of pressure-temperature phase diagrams of binary clathrate hydrates of methane, carbon dioxide or nitrogen+tetrahydrofuran, 1,4-dioxane or acetone. *Fluid Phase Equilib.* **2012**, *320*, 32-37.

389.   Eslamimanesh, A.; Mohammadi, A. H.; Richon, D. Thermodynamic modeling of phase equilibria of semi-clathrate hydrates of CO_2, CH_4, or N_2 + tetra-n-butylammonium bromide aqueous solution. *Chem. Eng. Sci. In Press*, **2012**.

390.   Anderson, F. E.; Prausnitz, J. M. Inhibition of gas hydrates by methanol. *AlChE J.* **1986**, *32*, 1321-1333.

391.   Krichevsky, I. R.; Kasarnovsky, J. S. Thermodynamical calculations of solubilities of nitrogen and hydrogen in water at high pressures. *J. Am. Chem. Soc.* **1935**, *57*, 2168–2172.

392.   Lin, W.; Delahaye, A.; Fournaison, L. Phase equilibrium and dissociation enthalpy for semi-clathrate hydrate of CO_2 + TBAB. *Fluid Phase Equilib.* **2008**, *264*, 220-227.

393.   Peng, D. Y.; Robinson, D. B. A new two-constant equation of state. *Ind. Eng. Chem. Fundam.* **1976**, *15*, 59-64.

394.   Mathias, P. M.; Copeman, T. W. Extension of the Peng-Robinson equation of state to complex mixtures: evaluation of the various forms of the local composition concept. *Fluid Phase Equilib.***1983**, *13*, 91-108.

395.   Shimada, W.; Ebinuma, T.; Oyama, H.; Kamata, Y.; Narita, H. Free-growth forms and growth kinetics of tetra-n-butyl ammonium bromide semi-clathrate hydrate crystals. *J. Cryst. Growth* **2005**, *274*, 246-250.

396.   Dharmawardhana, P.B.; Parrish, W.R.; Sloan, E.D. Experimental thermodynamic parameters for the prediction of natural gas hydrate dissociation conditions. *Ind. Eng. Chem. Fundam.* **1980**, *19*, 410-414.

397.   Oyama, H.; Shimada, W.; Ebinuma, T.; Kamata, Y.; Takeya, S.; Uchida, T.; Nagao, J.; Narita, H. Phase diagram, latent heat, and specific heat of TBAB semiclathrate hydrate crystals. *Fluid Phase Equilib.* **2005**, *234*, 131-135.

398.   Klauda, J.B.; Sandler, S.I. A fugacity model for gas hydrate phase equilibria. *Ind. Eng. Chem. Res.* **2000**, *39*, 3377–3386.

399.   Renon, H.; Prausnitz, J. M. Liquid-liquid and vapor-liquid equilibria for binary and ternary systems with dibutyl ketone, dimethyl sulfoxide, n-hexane, and 1-hexene. *Ind. Eng. Chem. Proc. Des. Dev.* **1968**, *7*, 220-225.

400.   Moore, J. C.; Battino, R.; Rettich, T. R.; Handa, Y. P.; Wilhelm, E. Partial molar volumes of "gases" at infinite dilution in water at 298.15 K. *J. Chem. Eng. Data* **1982**, *27*, 22-24.

401.   Lindenbaum, S.; Boyd, G. E. Osmotic and activity coefficients for the symmetrical tetraalkyl ammonium halides in aqueous solution at 25 °C. *J. Phys. Chem.* **1964**, *68*, 911-917.

402.   Amado G, E.; Blanco, L. H. Isopiestic determination of the osmotic and activity coefficients of dilute aqueous solutions of symmetrical and unsymmetrical quaternary ammonium bromides with a new isopiestic cell at 298.15 K. *Fluid Phase Equilib.* **2005**, *233*, 230-233.

403.   Söhnel, O.; Novotny, P. Densities of Aqueous Solutions of Inorganic Substances, Elsevier Science Pub. Co., Amsterdam, **1985.**

404.   Belandria, V.; Mohammadi, A. H.; Richon, D. Volumetric properties of the (tetrahydrofuran + water) and (tetra-n-butyl ammonium bromide + water) systems: Experimental measurements and correlations. *J. Chem. Thermodyn.* **2009**, *41*, 1382-1386.

405.   Component Plus, Ver. 3.0.0.0, Pure component database manager, ProSim SA, Released **2001**.

406.   Price, K.; Storn, R. Differential Evolution. *Dr. Dobb's J.*, **1997**, *22*, 18–24.

407. Babu, B.V.; Angira, R. Modified Differential Evolution (MDE) for optimization of non-linear chemical processes. *Comput. Chem. Eng.* **2006**, *30*, 989–1002.

408. Eslamimanesh, A. A semicontinuous thermodynamic model for prediction of asphaltene precipitation in oil reservoirs, M.Sc. Thesis, Shiraz University, Shiraz, Iran, **2009** (In Persian).

409. Eslamimanesh, A.; Shariati, A. A Semicontinuous thermodynamic model for prediction of asphaltene precipitation, Presented at VIII Iberoamerican Conference on Phase Equilibria and Fluid Properties for Process Design (Equifase), Praia da Rocha, Portugal, Oct. **2009**.

410. Eslamimanesh, A.; Esmaeilzadeh, F. Estimation of the solubility parameter by the modified ER equation of state, *Fluid Phase Equilib.* **2010**, *291*, 141–150.

411. Yazdizadeh, M.; Eslamimanesh, A.; Esmaeilzadeh, F. Thermodynamic modeling of solubilities of various solid compounds in supercritical carbon dioxide: Effects of equations of state and mixing rules. *J. Supercrit.* **2011**, *55*, 861-875.

412. Yazdizadeh, M.; Eslamimanesh, A.; Esmaeilzadeh, F. Applications of cubic equations of state for determination of the solubilities of industrial solid compounds in supercritical carbon dioxide: A comparative study. *Chem. Eng. Sci.* **2012**, *71*, 283-299.

413. Eslamimanesh, A.; Mohammadi, A. H.; Richon, D. Thermodynamic consistency test for experimental data of sulfur content of hydrogen sulfide. *Ind. Eng. Chem. Res.* **2011**, *50*, 3555–3563.

414. Deb, K. Multi-Objective Optimization Using Evolutionary Algorithms, Wiley, West Sussex, England, **2002.**

415. Project 801, Evaluated Process Design Data, Public Release Documentation; Design Institute for Physical Properties (DIPPR), AIChE: Provo, UT, **2006**.

416. Oyama, H.; Ebinuma, T.; Nagao, J.; Narita, H.; Shimada, W. Phase behavior of TBAB semiclathrate hydrate crystal under several vapor components, Proceedings of the 6th International Conference on Gas Hydrates (ICGH), Vancouver, Canada, **2008.**

417. NIST gas hydrate database, Thermodynamics Research Center (TRC) Thermophysical Properties Division, NIST, Boulder, Colorado, **2009**.

418. Ohgaki, K.; Makihara, Y.; Takano, K. Formation of CO_2 Hydrate in Pure and Sea Waters. *J. Chem. Eng. Jpn.* **1993**, *26*, 558-564.

419. Ng, H.-J.; Robinson, D. B. Hydrate formation in systems containing methane, ethane, propane, carbon dioxide or hydrogen sulfide in the presence of methanol. *Fluid Phase Equilib.* **1985**, *21*, 145-155.

420. Li, S.; Fan, S.; Wang, J.; Lang, X.; Wang, Y. Clathrate hydrate capture of CO_2 from simulated flue gas with cyclopentane/water emulsion. *Chin. J. Chem. Eng.* **2010**, *18*, 202-206.

421.   Arjmandi, M.; Chapoy, A.; Tohidi, B. Equilibrium data of hydrogen, methane, nitrogen, carbon dioxide, and natural gas in semi-Clathrate hydrates of tetrabutyl ammonium bromide. *J. Chem. Eng. Data* **2007**, *52*, 2153-2158.

422.   Mohammadi, A.H.; Richon, D. Phase equilibria of semi-clathrate hydrates of tetra-n-butylammonium bromide + hydrogen sulfide and tetra-n-butylammonium bromide + methane, *J. Chem. Eng. Data* **2010**, *55,* 982-984.

423.   Sugahara, K.; Tanaka, Y.; Sugahara, T.; Ohgaki, K. Thermodynamic stability and structure of nitrogen hydrate crystal. *J. Supramolecular Chemistry* **2002**, *2*, 365-368.

424.   SECOHYA (Separation of CO_2 by HYdrate Adsorption) project of Agence Nationale de la Recherche (ANR), internal reports, France, **2007** to **2011**.

425.   Eslamimanesh, A.; Mohammadi, A. H. Richon, D. Semi-clathrate hydrates phase equilibrium measurements for the CO_2 + H_2 + tetra-n-butylammonium bromide aqueous solution system. *Fluid Phase Equilib.* **2012**.

426.   Belandria, V.; Eslamimanesh, A. ; Mohammadi, A. H.; Théveneau, P.; Legendre, H.; Richon, D. Compositional analysis and hydrate dissociation conditions measurements for carbon dioxide + methane + water system. *Ind. Eng. Chem. Res.* **2011**, *50*, 5783–5794.

427.   Mohammadi, A. H.; Eslamimanesh, A.; Belandria, V.; Richon, D.; Naidoo, P.; Ramjugernath, D. Phase equilibrium measurements for semi-clathrate hydrates of the (CO_2 + N_2 + tetra-n-butylammonium bromide) aqueous solution system. *J. Chem. Thermodyn.* **2012**, *46*, 57-61.

428.   Tohidi, B.; Burgass, R. W.; Danesh, A.; Ostergaard, K. K.; Todd, A. C. Improving the accuracy of gas hydrate dissociation point measurements. *Ann. N.Y. Acad. Sci.* **2000**, *912*, 924–931.

429.   Ohmura, R.; Takeya, S.; Uchida, T.; Ebinuma, T. Clathrate hydrate formed with methane and 2-Propanol: Confirmation of structure II hydrate formation. *Ind. Eng. Chem. Res.* **2004**, *43*, 4964–4966.

430.   Meysel, P.; Oellrich, L.; Raj Bishnoi, P.; Clarke, M. A. Experimental investigation of incipient equilibrium conditions for the formation of semi-clathrate hydrates from quaternary mixtures of (CO_2 + N_2 + TBAB + H_2O). *J. Chem. Thermodyn.* **2011**, *43*, 1475-1479.

431.   Constantinides, A.; Moustofi, N. Numerical Methods for Chemical Engineers with Matlab Applications, Prentice Hall PTR, **1999**.

432.   Hoffman, J. D. *Numerical Methods for Engineering and Scientists*, 2nd Ed, Marcel Dekker: New York, **2001**.

433.   Gharagheizi, F.; Eslamimanesh, A.; Sattari, M.; Mohammadi, A. H.; Richon, D. Corresponding states method for determination of the viscosity of gases at atmospheric pressure. *Ind. Eng. Chem. Res.* **2012**, *51*, 3179-3185.

434.   Gharagheizi, F.; Eslamimanesh, A.; Sattari, M.; Tirandazi, B.; Mohammadi, A. H.; Richon, D. Evaluation of Thermal Conductivity of Gases at Atmospheric Pressure through a Corresponding States Method. *Ind. Eng. Chem. Res.* **2012**, *51*, 3844-3849**.**

435.   Gharagheizi, F.; Eslamimanesh, A.; Sattari, M.; Mohammadi, A. H.; Richon, D. Corresponding states method for evaluation of the solubility parameters of chemical compounds. *Ind. Eng. Chem. Res.* **2012**, *51*, 3826-3831.

436.   Eslamimanesh, A.; Babaee, S.; Mohammadi, A. H.; Javanmardi, J.; Richon, D. Experimental data assessment test for composition of vapor phase in equilibrium with gas hydrate and liquid water for carbon dioxide + methane or nitrogen + water system. *Ind. Eng. Chem. Res.* **2012**, *51*, 3819-3825.

437.   Mohammadi, A. H.; Eslamimanesh, A.; Richon, D. Wax solubility in gaseous system: Thermodynamic consistency test of experimental data. *Ind. Eng. Chem. Res.* **2011**, *50*, 4731-4740.

438.   Eslamimanesh, A.; Yazdizadeh, M.; Mohammadi, A. H.; Richon, D. Experimental data assessment test for diamondoids solubility in gaseous system. *J. Chem. Eng. Data* **2011**, *56*, 2655-2659.

439.   Mohammadi, A. H.; Eslamimanesh, A.; Yazdizadeh, M.; Richon, D. Glycol loss in a gaseous system: Thermodynamic assessment test of experimental solubility data. *J. Chem. Eng. Data* **2011**, *56*, 4012-4016.

440.   Prausnitz, J. M.; Lichtenthaler, R. N.; Gomez de Azevedo, E. Molecular Thermodynamics of Fluid Phase Equilibria. New Jersey: Prentice-Hall, Inc., **1999.**

441.   Smith, J. M.; Van Ness, H. C.; Abbott, M. M. Introduction to Chemical Engineering Thermodynamics. 6th Ed., New York: McGraw-Hill, **2003**.

442.   Van Ness, H. C.; Abbott, M. M. Classical Thermodynamics of Non-electrolyte Solutions. McGraw-Hill, New York, **1982**.

443.   Raal, J. D.; Mühlbauer, A. L. Phase Equilibria: Measurement and Computation. Washington: Taylor & Francis, **1998**.

444.   Rousseeuw, P. J.; Leroy, A.M. Robust Regression and Outlier Detection. John Wiley & Sons: New York, **1987**.

445.   Goodall, C. R. Computation Using the QR Decomposition, Handbook in Statistics. Vol. 9, Amsterdam: Elsevier/North-Holland, **1993**

446.   Gramatica, P. Principles of QSAR models validation: internal and external. *QSAR Comb. Sci.* **2007**, *26*, 694-701.

447.   Valderrama J. O.; Alvarez, V. H. A versatile thermodynamic consistency test for incomplete phase equilibrium data of high-pressure gas–liquid mixtures. *Fluid Phase Equilib.* **2004**, *226*, 149–159.

448.   Valderrama J. O.; Robles, P. A. Thermodynamic consistency of high pressure ternary mixtures containing a compressed gas and solid solutes of different complexity. *Fluid Phase Equilib.* **2006**, *242*, 93-102.

449.   Valderrama J. O.; Zavaleta J. Thermodynamic consistency test for high pressure gas–solid solubility data of binary mixtures using genetic algorithms. *J. Supercrit. Fluids* **2006**, *39*, 20-29.

450.   Valderrama J. O.; Reátegui, A.; Sanga, W. E. Thermodynamic consistency test of vapor-liquid equilibrium data for mixtures containing ionic liquids. *Ind. Eng. Chem. Res.* **2008**, *47*, 8416-8422.

451.   Valderrama, J. O.; Faúndez, C. A. Thermodynamic consistency test of high pressure gas–liquid equilibrium data including both phases. *Thermochimica Acta* **2010**, *499*, 85-90.

452.   Bertucco, A.; Barolo, M.; Elvassore, N. Thermodynamic consistency of vapor-liquid equilibrium data at high pressure. *AIChE J.* **1997**, *43*, 547-554.

453.   Mohammadi, A. H.; Richon, D. On estimating the water content of gas in equilibrium with gas hydrate or ice. *AIChE Journal* **2007**, *53*, 1601-1607.

454.   Mohammadi A. H., Richon D. Useful remarks to reduce experimental information required to determine equilibrium water content of gas near and inside gas hydrate or ice formation regions. *Ind. Eng. Chem. Res.* **2008**, *47*,7-15.

455.   Mohammadi A. H., Richon D. Determination of Water Content of Natural Gases: State of the Art. In: David, N, Michel T. Natural Gas Research Progress. New York: Nova Science Publishers, Inc., 2008.

456.   Von Stackelberg, M.; Müller, H. R. Feste gas hydrate II. Struktur und raumchemie. *Elektrochem.* **1954**, *58*, 25-39.

457.   Daubert, T. E.; Danner, R. P. *DIPPR* Data Compilation Tables of Properties of Pure Compounds. *AIChE*, New York, 1985.

458.   McCain W. D. J. The Properties of Petroleum Fluids (2nd Edition). Tulsa: Pennwell Publishing Co., **1990**.

459.   Mohammadi, A. H.; Chapoy, A.; Tohidi, B.; Richon, D. Gas solubility: A key to estimating the water content of natural gases. *Ind. Eng. Chem. Res.* **2006**, *45*, 4825-4829.

460.   Mohammadi, A. H.; Chapoy, A.; Tohidi, B.; Richon, D. A semiempirical approach for estimating the water content of natural gases. *Ind. Eng. Chem. Res.* **2004**, *43*, 7137-7147.

461.   Mickley, H. S.; Sherwood T. K.; Reed, C. E. Applied Mathematics in Chemical Engineering, New York: McGraw Hill, **1957**.

462.   Avlonitis, D. Thermodynamics of gas hydrate equilibria; Ph.D. Thesis, Department of Petroleum Engineering, Heriot-Watt University, Edinburgh, UK, **1992**.

463.   Tohidi-Kalorazi, B. Gas hydrate equilibria in the presence of electrolyte solutions; Ph.D. Thesis, Department of Petroleum Engineering, Heriot-Watt University, Edinburgh, UK, **1995**.

464.   Heriot–Watt University Hydrate model, Version 1.1, Accessed June **2007**.

465.   Valderrama, J. O. A generalized Patel-Teja equation of state for polar and non-polar fluids and their mixtures. *J. Chem. Eng. Japan* **1990**, *23*, 87-91.

466.   Avlonitis, D.; Danesh, A.; Todd, A. C. Prediction of VL and VLL equilibria of mixtures containing petroleum reservoir fluids and methanol with a cubic EoS. *Fluid Phase Equilib.* **1994**, *94*, 181-216.

467.   Mohammadi, A. H.; Chapoy, A., Richon, D.; Tohidi, B. Advances in estimating water content of natural gases. Presented at the 85th Annual GPA Convention held 5-8 March 2006, Grape Vine, Texas, USA, **2006**.

468.   Chapoy, A.; Coquelet, C.; Richon, D. Erratum: Revised solubility data and modeling of water in the gas phase of the methane/water binary system at temperatures from 283.08 to 318.12 K and pressures up to 34.5 MPa (Fluid Phase Equilibria (2003) 214 (101-117)). *Fluid Phase Equilib.* **2005**, *230*, 210-214.

469.   Chapoy, A.; Coquelet, C.; Richon, D. Solubility measurement and modeling of water in the gas phase of the methane/water binary system at temperatures from 283.08 to 318.12 K and pressures up to 34.5 MPa. *Fluid Phase Equilib.* **2003**, *214*, 101-117.

470.   Aoyagi, K.; Song, K. Y.; Kobayashi, R.; Sloan, E. D.; Dharmawardhana, P. B. (I). The water content and correlation of the water content of methane in equilibrium with hydrates (II). The water content of a high carbon dioxide simulated Prudhoe Bay gas in equilibrium with hydrates. *Gas Proc. Assn. Res. Report*, No. 45, Tulsa, OK, December, **1980**.

471.   Song, K. Y.; Yarrison, M.; Chapman, W. Experimental low temperature water content in gaseous methane, liquid ethane, and liquid propane in equilibrium with hydrate at cryogenic conditions. *Fluid Phase Equilib.* **2004**, *224*, 271-277.

472.   Mohammadi, A. H.; Chapoy, A.; Richon, D.; Tohidi, B. Experimental measurement and thermodynamic modeling of water content in methane and ethane systems. *Ind. Eng. Chem. Res.* **2004**, *43*, 7148-7162.

473.   Althaus K. Fortschritt - Berichte VDI; 1999. Reihe 3:350 (in German). Oellrich L.R.; Althaus K. GERG - Water Correlation (GERG Technical Monograph TM14) Relationship Between Water Content and Water Dew Point Keeping in Consideration the Gas Composition in the Field of Natural Gas. Fortschritt - Berichte VDI **2000**; Reihe 3: Nr. 679 (in English).

474.   Briones, J. A.; Mullins, J. C.; Thies, M. C.; Kim, B. U. Ternary phase equilibria for acetic acid-water mixtures with supercritical carbon dioxide. *Fluid Phase Equilib.* **1987**, *36*, 235-246.

475.   Nakayama, T.; Sagara, H.; Arai, K.: Saito, S. High pressure liquid-liquid equilibria for the system of water, ethanol and 1,1-difluoroethane at 323.2 K. *Fluid Phase Equilib.* **1987**, *38*, 109-127.

476.   Bamberger, A.; Sieder, G.; Maurer, G. High-pressure (vapor+liquid) equilibrium in binary mixtures of (carbon dioxide+water or acetic acid) at temperatures from 313 to 353 K. *J. Supercrit. Fluids* **2000**, *17*, 97–110

477.   Malinin, S. D. The system water-carbon dioxide at high temperatures and pressures (in Russian). *Geokhimiya* **1959**, *3*, 292–306.

478.   Muller, G. Ph.D. Dissertation, University of Kaiserslautern, **1983**.

479.   Takenouchi, S.; Kennedy, G. C. The binary system H_2O-CO_2 at high temperatures and pressures. *Am. J. Sci.* **1964**, *262*, 1055-1074.

480.   Servio, P.; Englezos, P. Effect of temperature and pressure on the solubility of carbon dioxide in water in the presence of gas hydrate. *Fluid Phase Equilib.* **2001**, *190*, 127-134.

481.   Yang, S. O.; Yang, I. M.; Kim, Y. S.; Lee, C. S. Measurement and prediction of phase equilibria for water + CO_2 in hydrate forming conditions. *Fluid Phase Equilib.* **2000**, *175*, 75-89.

482.   Culberson, O. L.; McKetta, J. J. The solubility of methane in water at pressures to 10000 psia: *AIME Petroleum Trans.* **1951**, *192*, 223-226.

483.   Davis, J. E.; McKetta J. J. Solubility of methane in water. *Petrol. Refiner* **1960**, *39*, 205-206.

484.   Lekvam, K.; Bishnoi, P. R. Dissolution of methane in water at low temperatures and intermediate pressures. *Fluid Phase Equilib.* **1997**, *131*, 297-309.

485.   Chapoy, A.; Mohammadi, A. H.; Richon, D.; Tohidi, B. Gas solubility measurement and modeling for methane–water and methane–ethane–n-butane–water systems at low temperature conditions. *Fluid Phase Equilib.* **2004**, *220*, 113-121.

486.   Yarym-Agaev, N. L.; Sinyavskaya, R. P.; Koliushko, I. I. Phase equilibrium in the binary systems water-methane and methanol-methane under high pressure (in Russian). *Zh. Prikl. Khim.* **1985**, *58*, 165-168.

487.   Sanchez, M.; De Meer, F. Equilibrio liquido-vapor del sistema metano-agua para altas presiones y temperaturas comprendidas entre 150 y 300°C. *An. Quim.* **1978**, *74*, 1325-1328.

488.   Sultanov, R. G.; Skripka, V. G.; Namiot, A. Y. Phase equilibria in the systems methane–n-hexadecane and nitrogen–n-hexadecane at high temperatures and pressures. *Viniti* **1971**, *2888-71*, 1.

489.   Yang, S. O.; Choa, S. H.; Leeb, H.; Lee, C. S. Measurement and prediction of phase equilibria for water + methane in hydrate forming conditions. *Fluid Phase Equilib.* **2001**, *185*, 53-63.

490.   Seo, Y.; Lee, H.; Uchida, T. Methane and carbon dioxide hydrate phase behavior in small porous silica gels: three-phase equilibrium determination and thermodynamic modeling. *Langmuir* **2002**, *18*, 9164–9170.

491. Lu, W. J.; Chou, I. M.; Burruss, R. C.; Yang, M. Z. In situ study of mass transfer in aqueous solutions under high pressures via Raman Spectroscopy : A new method for the determination of diffusion coefficients of methane in water near hydrate formation conditions. *Appl. Spectrosc.* **2006**, *60*, 122-129.

492. Kamath, V.A. Study of heat transfer characteristics during dissociation of gas hydrates in porous media, Ph.D. Dissertation, University of Pittsburgh, University Microfilms No. 8417404, Ann Arbor, MI, **1984**.

493. Nakamura, T.; Makino, T.; Sugahara, T.; Ohgaki, K. Stability boundaries of gas hydrates helped by methane - Structure-H hydrates of methylcyclohexane and cis-1,2-dimethylcyclohexane. *Chem. Eng. Sci.* **2003**, *58*, 269-273.

494. Mohammadi, A. H.; Tohidi, B.; Burgass, R. W. Equilibrium data and thermodynamic modeling of nitrogen, oxygen, and air clathrate hydrates. *J. Chem. Eng. Data* **2003**, *48*, 612-616.

495. Kharrat, M.; Dalmazzone, D. Experimental determination of stability conditions of methane hydrate in aqueous calcium chloride solutions using high pressure differential scanning calorimetry. *J. Chem. Thermodyn.* **2003**, *35*, 1489-1505.

496. Ohmura, R.; Kashiwazaki, S.; Shiota, S.; Tsuji, H.; Mori, Y. H. Structure-I and structure-H hydrate formation using water spraying. *Energy Fuels* **2002**, *16*, 1141-1147.

497. Jager, M. D.; Sloan, E. D. The effect of pressure on methane hydration in pure water and sodium chloride solutions. *Fluid Phase Equilib.* **2001**, *185*, 89-99.

498. Jager, M. D. High pressure studies of hydrate phase inhibition using Raman spectroscopy. Ph.D. Chemical Engineering Thesis, Colorado School of Mines, Golden, Colorado, USA. **2001**.

499. Nixdorf, J.; Oellrich, L. R. Experimental determination of hydrate equilibrium conditions for pure gases, binary and ternary mixtures and natural gases. *Fluid Phase Equilib.* **1997**, *139*, 325-333.

500. Servio, P.; Englezos, P.; Bishnoi, P. R. Kinetics of ethane hydrate growth on latex spheres measured by a light scattering technique. *Ann. N.Y. Acad. Sci.* **2000**, *912*, 576-582.

501. Guo, G. B., Bretz, R. E. and Lee, R. L. Gas hydrates decomposition and its modeling. International Gas Research Conference, Orlando, Florida, 16-19 November, **1992**, 231-240.

502. Reamer, H. H., Selleck, F. T.; Sage, B. H. Some prop. of mixed paraffinic & other olefinic hydrate. *Trans. Am. Inst. Min., Metall. Pet. Eng.* **1952**, *195*, 197-202.

503. Roberts, O. L.; Brownscombe, E. R.; Howe, L. S. Constitution diagrams and composition of methane and ethane hydrates. *Oil & Gas J.* **1940**, *39*, 37-43.

504. Englezos, P. Experimental study on the equilibrium ethane hydrate formation conditions in aqueous electrolyte solutions. *Ind. Eng. Chem. Res.* **1991**, *30*, 1655-1659.

505. Clarke, M.; Bishnoi, P. R. Determination of the intrinsic rate of ethane gas hydrate decomposition. *Chem. Eng. Sci.* **2000**, *55*, 4869-4883.

506.   Deaton, W. M.; Frost, E. M. Gas hydrates and their relation to the operation of natural-gas pipe lines. United States Department of the Interior Gas Hydrates and Their Relation to the Operation of Natural-Gas Pipe Lines, U18401 8653273, **1946**.

507.   Galloway, T. J.; Ruska, W.; Chappelear, P. S.; Kobayashi, R. Experimental measurement of hydrate numbers for methane and ethane and comparison with theoretical values. *Ind. Eng. Chem. Fundam.* **1970**, *9*, 237-243.

508.   Falabella, B. J. A study of natural gas hydrates. Ph.D. Chemical Engineering Dissertation, University of Massachusetts, **1975**.

509.   Den Heuvel, M. M. M. V.; Peters, C. J.; De Swaan Arons, J. Gas hydrate phase equilibria for propane in the presence of additive components. *Fluid Phase Equilib.* **2002**, *193*, 245-259.

510.   Robinson, D. B.; Mehta, B. R. Hydrates in the propane - carbon dioxide - water system. *J. Can. Petro.* **1971**, *10*, 33-35.

511.   Verma, V. K.; Hand, J. H.; Katz, D. L. Gas hydrates from liquid hydrocarbons (methane-propane-water system). *GVC/AIChE Joint Meeting*, Munich, **1975**, 10.

512.   Patil, S. L. Measurement of multiphase gas hydrate phase equilibria: Effect of inhibitors and heavier hydrocarbon components. Master of Science Thesis, University of Alaska, Fairbanks, Alaska, **1987**.

513.   Kubota, H.; Shimizu, K.; Tanaka, Y.; Makita, T. Thermodynamic properties of R13 ($CClF_3$), R_{23} (CHF_3), R152a ($C_2H_4F_2$), and propane hydrates for desalination of sea water. *J. Chem. Eng. Jpn.* **1984**, *17*, 423-429.

514.   Englezos, P.; Ngan, Y. T. Incipient equilibrium data for propane hydrate formation in aqueous solutions of NaCl, KCl, and $CaCl_2$. *J. Chem. Eng. Data* **1993**, *38*, 250-253.

515.   Holder, G. D.; Kamath, V. A. Experimental determination of dissociation pressures for hydrates of the cis- and trans-isomers of 2-butene below the ice temperature. *J. Chem. Thermodyn.* **1982**, *14*, 1119-1128.

516.   Goddard, J. D. Fluoro- and difluoro-vinylidenes and their rearrangements to acetylenes. *Chem. Phys. Lett.* **1981**, *83*, 312-316.

517.   Fan, S. S.; Guo, T. M. Hydrate formation of CO_2-rich binary and quaternary gas mixtures in aqueous sodium chloride solutions. *J. Chem. Eng. Data* **1999**, *44*, 829-832.

518.   Fan, S. S.; Chen, G. J.; Ma, Q. L.; Guo, T. M. Experimental and modeling studies on the hydrate formation of CO_2 and CO_2-rich gas mixtures. *Chem. Eng. J.* **2000**, *78*, 173-178.

519.   Yoon, J. H.; Lee, H. Clathrate phase equilibria for the water-phenol-carbon dioxide system. *AIChE J.* **1997**, *43*, 1884-1893.

520.   Komai, T.; Yamamoto, Y.; Ikegami, S. Equilibrium properties and kinetics of methane and carbon dioxide gas hydrate formation/dissociation. *ACS Division of Fuel Chemistry, Preprints* **1997**, *42*, 568-570.

521.   Mohammadi, A. H.; Richon, D. Ice-clathrate hydrate-gas phase equilibria for air, oxygen, nitrogen, carbon monoxide, methane, or ethane + water system. *Ind. Eng. Chem. Res.* **2010**, *49*, 3976-3979.

522.   Selleck, F. T.; Carmichael, L. T.; Sage, B. H. Phase behavior in the hydrogen sulfide-water system. *Ind. Eng. Chem.* **1952**, *44*, 2219-2226.

523.   Bond, D.; Russell, N. B. Effect of antifreeze agents on the formation of hydrogen sulphide hydrate. Petroleum Technology, November, **1948**, 192-198.

524.   Von Stackelberg, M. Solid gas hydrates. *Die Naturwissenschaften* **1949**, *36*, 359-362.

525.   Mohammadi, A. H.; Richon, D. Equilibrium data of carbonyl sulfide and hydrogen sulfide clathrate hydrates. *J. Chem. Eng. Data* **2009**, *54*, 2338-2340.

526.   Seo, Y. T.; Lee, H.; Yoon, J. H., Hydrate phase equilibria of the carbon dioxide, methane, and water system. *J. Chem. Eng. Data* **2001**, *46*, 381-384.

527.   Seo, Y. T.; Lee, H. Multiple-phase hydrate equilibria of the ternary carbon dioxide, methane, and water mixtures. *J. Phys. Chem. B* **2001**, *105*, 10084-10090.

528.   Servio, P.; Lagers, F.; Peters, C.; Englezos, P. Gas hydrate phase equilibrium in the system methane-carbon dioxide-neohexane and water. *Fluid Phase Equilib.* **1999**, *158-160*, 795-800.

529.   Olsen, B.; Majumdar, A. J.; Bishnoi, P. R. Experimental studies on hydrate equilibrium carbon dioxide and its systems. *Int. J. The Soc. of Mat. Eng. for Resources* **1999**, *7*, 17-23.

Appendix. A

The VPT EoS[465] is believed as a strong tool for modeling systems containing water and polar compounds.[466] This equation of state is written as follows:[13,323,465,472]

$$P = \frac{RT}{v-b} - \frac{a}{v(v+b)+c(v-b)}$$

(A.1)

where P is pressure, T is temperature, R denotes the universal gas constant, v stands for the molar volume, and a, b, and c are the parameters of the VPT EoS.[465]

In Eq. (A.1):

$$a = \bar{a}\,\alpha(T_r)$$

(A.2)

$$\bar{a} = \frac{\Omega_a R^2 T_c^2}{P_c}$$

(A.3)

$$b = \frac{\Omega_b R\, T_c}{P_c}$$

(A.4)

$$c = \frac{\Omega_c R\, T_c}{P_c}$$

(A.5)

where the alpha function is given as:

$$\alpha(T_r) = \left[1 + F\left(1 - T_r^\Psi\right)\right]^2$$

(A.6)

where $\Psi = 0.5$ and the coefficient F is given by:

$$F = 0.46286 + 3.58230(\omega Z_c) + 8.19417(\omega Z_c)^2$$

(A.7)

The subscripts c and r in the preceding equations denote critical and reduced properties, respectively, and ω is the acentric factor. Additionally, the coefficients Ω_a, Ω_b, Ω_c are calculated by:

$$\Omega_a = 0.66121 - 0.76105 Z_c$$

(A.8)

$$\Omega_b = 0.02207 + 0.20868 Z_c$$

(A.9)

$$\Omega_c = 0.57765 - 1.87080 Z_c$$

(A.10)

where Z_c is the critical compressibility factor, and ω is the acentric factor. Avlonitis et al.[466] relaxed the constraints on F and Ψ for water in order to improve the predicted vapor pressure and saturated volume for these compounds:

$$F = 0.72318, \qquad \Psi = 0.52084 \tag{A.11}$$

Later, Tohidi-Kalorazi[463] relaxed the alpha function for water, $\alpha_w(T_r)$, using experimental water vapor pressure data in the range of 258.15 to 374.15 K, in order to improve the predicted water fugacity:

$$\alpha_w(T_r) = 2.4968 - 3.0661\,T_r + 2.7048\,T_r^{\,2} - 1.2219\,T_r^{\,3} \tag{A.12}$$

Nonpolar - nonpolar binary interactions in fluid mixtures are described by applying classical mixing rules as follows:

$$a = \sum_i \sum_j x_i x_j a_{ij} \tag{A.13}$$

$$b = \sum_i x_i b_i \tag{A.14}$$

$$c = \sum_i x_i c_i \tag{A.15}$$

$$a_{ij} = \left(1 - k_{ij}\right)\sqrt{a_i a_j} \tag{A.16}$$

where k_{ij} is the standard binary interaction parameter and x stands for the mole fraction of the species.

For polar - nonpolar interaction, however, the classical mixing rules are not satisfactory and therefore more complicated mixing rules are necessary. In this work the *NDD* mixing rules developed by Avlonitis et al.[466] are applied to describe mixing in the *a*-parameter:

$$a = a^C + a^A \tag{A.17}$$

where a^C is given by the classical quadratic mixing rules (Eqs. A.13 and A.16). The term a^A corrects for asymmetric interaction which cannot be efficiently accounted for by classical mixing rules:[466]

$$a^A = \sum_p x_p^2 \sum_i x_i a_{pi} l_{pi} \tag{A.18}$$

$$a_{pi} = \sqrt{a_p a_i} \tag{A.19}$$

$$l_{pi} = l_{pi}^0 - l_{pi}^1\left(T - T_0\right) \tag{A.20}$$

where p is the index of polar components, and l represents the binary interaction parameter for the asymmetric term.

Using the preceding EoS[465] and the associated mixing rules, the fugacity of each component in fluid phases is calculated from:

$$f_i = y_i \varphi_i P \tag{A.21}$$

where y_i and φ_i are the mole fraction and the fugacity coefficient of component i, respectively.

Short Curriculum Vitae

Ali Eslamimanesh

INTRODUCTION

Date/place of birth: September 16, 1985/ Iran
Gender: Male

EDUCATION

2009 ~ 2012 **PhD**, Process Engineering
Laboratoire CEP/TEP,
École Nationale Supérieure des Mines de Paris (Mines ParisTech),
Fontainebleau/Paris, France

2012 **Research Stay**,
Department of Chemical and Biochemical Engineering (CERE),
Technical University of Denmark (DTU),
Lyngby, Denmark

2007 ~ 2009 **Master of Science**, Chemical Engineering,
(Natural Gas Engineering),
School of Chemical and Petroleum Engineering,
Shiraz University,
Shiraz, Iran

2003 ~ 2007 **Bachelor of Science**, Chemical Engineering
(Process Design Engineering),
Chemical Engineering Department,
The University of Isfahan,
Isfahan, Iran

1999 ~ 2003 **High School Diploma**, Mathematical Sciences
Tohid High School, Shiraz, Iran

PROFESSIONAL MEMBERSHIP

- Member of Society of Petroleum Engineers (SPE)

ACADEMIC ACHIEVEMENTS

- Henry Kehiaian Travel Award from the IACT (International Association of Chemical Thermodynamics), 2012.

- IACT and Elsevier PhD Student Award from IUPAC, 2011.

- 2 articles among the most-cited articles of Industrial & Engineering Chemistry Research Journal in 3 years.

- Around 400 citations by ISI articles (Scopus Reported).

- Author h-index = 13.

- Representative of Mines ParisTech in ParisTech Doctoral School, 2010-Present.

- Member of the Iranian National Elite Foundation (Bonyade Mellie Nokhbegan), 2010-Present.

- Member of the Office of Talented Students of Shiraz University, Iran (Daftare Esteedadhaie Derakhshan), 2007-2009.

- Highest GPA among all M.Sc. students in the School of Chemical and Petroleum Engineering,Shiraz University, 2008 and 2009.

- Ranked the 1st position among all M.Sc. students of School of Chemical and Petroleum Engineering, Shiraz University, 2007-2009.

- The only student among all B.Sc. students in Chemical Engineering Department, achieved publishing two ISI articles, The University of Isfahan, 2007.

- Ranked the 2nd position among all B.Sc. students in Chemical Engineering Department, The University of Isfahan, 2003-2007.

PUBLICATIONS

Book Chapters:

1) Mohammadi, A.H.; Eslamimanesh, A.; Richon, D. NITROUS OXIDE CLATHRATE HYDRATES, Book Chapter, In: Advances in Chemistry Research. Volume 11, Editor: James C. Taylor, pp. 1-10, **Nova Science Publishers, Inc.** 2011.
2) Mohammadi, A.H.; Eslamimanesh, A.; Richon, D. ASPHALTENE PRECIPITATION IN GAS CONDENSATE SYSTEM. In: Advances in Chemistry Research. Volume 15, Editor: James C. Taylor, **Nova Science Publishers, Inc.** 2012.

ISI Articles

1) Eslamimanesh, A.; Mohammadi A.H.; Richon D. Thermodynamic consistency test for experimental data of water content of methane. *AIChE J.* 2011, *57*, 2566-2573. (Related to Chapter 7 of this thesis)
2) Eslamimanesh, A.; Mohammadi, A. H.; Richon, D. Thermodynamic modeling of phase equilibria of semi-clathrate hydrates of CO_2, CH_4, or N_2 + tetra-n-butylammonium bromide aqueous solution. *Chem. Eng. Sci.* 2012, *81*, 319-328. (Related to Chapter 4 of this thesis)
3) Eslamimanesh, A.; Mohammadi, A.H.; Richon, D.; Naidoo, P.; Ramjugernath, D. Application of gas hydrate formation in separation processes: A review of experimental studies. *J. Chem. Thermodyn.* 2012, *46*, 62-71. (Related to Chapter 2 of this thesis)
4) Eslamimanesh, A.; Mohammadi, A.H.; Richon, D. An improved Clapeyron model for predicting liquid water-hydrate-liquid hydrate former phase equilibria. *Chem. Eng. Sci.* 2011, *66*, 1759-1764. (Related to Chapter 3 of this thesis)
5) Eslamimanesh, A.; Mohammadi, A.H.; Richon, D. Thermodynamic model for predicting phase equilibria of simple clathrate hydrates of refrigerants. *Chem. Eng. Sci.* 2011, *66*, 5439-5445. (Related to Chapter 4 of this thesis)
6) Eslamimanesh, A.; Gharagheizi, F.; Mohammadi, A. H.; Richon, D. A Statistical method for evaluation of the experimental phase equilibrium data of simple clathrate hydrates. *Chem. Eng. Sci.* 2012, *80*, 402-408. (Related to Chapter 7 of this thesis)
7) Eslamimanesh, A.; Gharagheizi, F.; Mohammadi, A.H.; Richon, D.; Illbeigi, M.; Fazlali, A.; Forghani, A. A.; Yazdizadeh, M. Phase equilibrium modeling of structure H clathrate hydrates of methane + water "insoluble" organic promoters using group contribution-support vector machine technique. *Ind. Eng. Chem. Res*. 2011, *50*, 12807-12814. (Related to Chapter 3 of this thesis)
8) Eslamimanesh, A.; Mohammadi, A. H.; Richon, D. Thermodynamic consistency test for experimental solubility data in carbon dioxide/methane + water system inside and outside gas hydrate formation region. *J. Chem. Eng. Data* 2011, *56*, 1573-1586. (Related to Chapter 7 of this thesis)
9) Eslamimanesh, A.; Gharagheizi, F.; Mohammadi, A.H.; Richon, D. Phase equilibrium modeling of structure H clathrate hydrates of methane + water insoluble hydrocarbon promoters using QSPR molecular-based approach. *J. Chem. Eng. Data* 2011, *56*, 3775-3793. (Related to Chapter 3 of this thesis)

10) Eslamimanesh, A.; Babaee, S.; Mohammadi, A.H.; Javanmardi, J.; Richon, D. Compositional analysis of vapor phase in equilibrium with liquid water + hydrate for carbon dioxide + methane/nitrogen + water system: Experimental data assessment test. ***Ind. Eng. Chem. Res***. 2012, *51*, 3819-825. (Related to Chapter 7 of this thesis)

11) Eslamimanesh, A.; Gharagheizi, F.; Illbeigi, M.; Mohammadi, A.H.; Fazlali, A.; Richon, D. Phase equilibrium modeling of clathrate hydrates of methane, carbon dioxide, nitrogen, and hydrogen + water soluble organic promoters using support vector machine algorithm. ***Fluid Phase Equilib.*** 2012, *316*, 34-45. (Related to Chapter 3 of this thesis)

12) Eslamimanesh, A.; Mohammadi, A. H.; Yazdizadeh, M.; Richon, D. Chrastil-type approach for representation of glycol loss in gaseous system. ***Ind. Eng. Chem. Res.*** 2011, *50*, 10373-10379.

13) Eslamimanesh, A.; Esmaeilzadeh, F. Estimation of solubility parameter by the modified ER equation of state. ***Fluid Phase Equilib.*** 2010, *291*, 141-150.

14) Eslamimanesh, A.; Gharagheizi, F.; Mohammadi, A. H.; Richon, D. Artificial neural network modeling of solubility of supercritical carbon dioxide in 24 commonly used ionic liquids. ***Chem. Eng. Sci.*** 2011, *66*, 3039-3044.

15) Eslamimanesh, A.; Mohammadi, A.H.; Richon, D. Determination of sulfur content of various gases using Chrastil-type equations. ***Ind. Eng. Chem. Res***. 2011, *50*, 7682-7687.

16) Eslamimanesh, A.; Mohammadi, A. H.; Richon, D. Thermodynamic consistency test for experimental data of sulfur content of hydrogen sulfide. ***Ind. Eng. Chem. Res***. 2011, *50*, 3555-3563.

17) Eslamimanesh, A.; Yazdizadeh, M.; Mohammadi, A. H.; Richon, D. Experimental data assessment test for diamondoids solubility in gaseous system. ***J. Chem. Eng. Data*** 2011, *56*, 2655-2659.

18) Eslamimanesh, A.; Hatamipour, M.S. Mathematical modeling of a direct contact humidification-dehumidification desalination process. ***Desalination*** 2009, *237*, 296-304.

19) Eslamimanesh, A.; Hatamipour, M.S. Economical study of a small-scale direct contact humidification-dehumidification desalination plant. ***Desalination*** 2010, *250*, 203-207.

20) Gharagheizi, F.; Eslamimanesh, A.; Mohammadi, A. H.; Richon, D. QSPR approach for determination of parachor of non-electrolyte organic compounds. ***Chem. Eng. Sci.*** 2011, *66*, 2959-2967.

21) Gharagheizi, F.; Eslamimanesh, A.; Tirandazi, B.; Mohammadi, A.H.; Richon, D. Handling a very large data set for determination of surface tension of chemical compounds: a quantitative structure-property relationship strategy. ***Chem. Eng. Sci.*** 2011, *66*, 4991-5023.

22) Gharagheizi, F.; Eslamimanesh, A.; Mohammadi, A.H.; Richon, D. Empirical method for estimation of Henry's law constant of non-electrolyte organic compounds in water. ***J. Chem. Thermodyn.*** 2102, *47*, 295–299.

23) Mohammadi, A.H.; Eslamimanesh, A.; Belandria, V.; Richon, D. Phase equilibria of semi-clathrate hydrates of CO_2, N_2, CH_4, and H_2 + tetra-n-butylammonium bromide aqueous solutions. ***Chem. Eng. Data*** 2011, *56*, 3855-3865. (Related to Chapter 5 of this thesis)

24) Tumba, K.; Reddy, P.; Naidoo, P.; Ramjugernath, D.; Eslamimanesh, A.; Mohammadi, A.H.; Richon, D. Phase equilibria of methane and carbon dioxide clathrate hydrates in the presence of aqueous solutions of tributylmethylphosphonium methylsulfate ionic liquid. ***J. Chem. Eng. Data*** 2011, *56*, 3620-3629. (Related to Chapter 4 of this thesis)

25) Mohammadi, A.H.; Eslamimanesh, A.; Richon, D.; Gharagheizi, F.; Yazdizadeh, M.; Javanmardi, J.; Hashemi, H.; Zarifi, M.; Babaee, S. Gas hydrate phase equilibrium in porous media: Mathematical modeling and correlation. *Ind. Eng. Chem. Res***.** 2012, *51*, 1062-1072. (Related to Chapter 3 of this thesis)

26) Mohammadi, A.H.; Eslamimanesh, A.; Richon, D. Monodisperse thermodynamic model based on chemical + Flory- Hüggins theories for estimating asphaltene precipitation. *Ind. Eng. Chem. Res***.** 2012, *51*, 4041-4055.

27) Mohammadi, A.H.; Eslamimanesh, A.; Belandria, V.; Richon, D.; Naidoo, P.; Ramjugernath, D. Phase equilibrium measurements for semi-clathrate hydrates of the (CO_2 + N_2 + Tetra-n-Butylammonium Bromide) aqueous solution system. *J. Chem. Thermodyn.* 2012, *46*, 57-61. (Related to Chapter 5 of this thesis)

28) Belandria, V. ; Mohammadi, A.H.; Eslamimanesh, A.; Richon, D.; Sánchez, M.F.; Galicia-Luna, L.A. Phase equilibrium measurements for semi-clathrate hydrates of the (CO_2 + N_2 + tetra-n-butylammonium bromide) aqueous solution systems. *Fluid Phase Equilib.*, Accepted manuscript, 2011. (Related to Chapter 5 of this thesis)

29) Belandria, V.; Eslamimanesh, A.; Mohammadi, A. H.; Richon, D. Study of gas hydrate formation in the carbon dioxide + hydrogen + water systems: Compositional analysis of the gas phase. *Ind. Eng. Chem. Res***.** 2011, *50*, 6455-6459. (Related to Chapter 5 of this thesis)

30) Belandria, V.; Eslamimanesh, A.; Mohammadi, A. H.; Richon, D. Gas hydrate formation in carbon dioxide + nitrogen + water system: Compositional analysis of equilibrium phases. *Ind. Eng. Chem. Res***.** 2011, *50*, 4722-4730. (Related to Chapters 5 and 6 of this thesis)

31) Belandria, V.; Eslamimanesh, A.; Mohammadi, A. H.; Théveneau, P.; Legendre, H.; Richon, D. Compositional analysis and hydrate dissociation conditions measurements for carbon dioxide + methane + water system. *Ind. Eng. Chem. Res***.** 2011, *50*, 5783-5794. (Related to Chapters 5 and 6 of this thesis)

32) Hashemi, H.; Javanmardi, J.; Zarifi, M.; Eslamimanesh, A.; Mohammadi, A. H. Experimental study and thermodynamic modeling of methane clathrate hydrate dissociation conditions in porous media in the presence of methanol aqueous solution. *J. Chem. Thermodyn.* 2012, *49*, 7-13. (Related to Chapter 3 of this thesis)

33) Gharagheizi, F.; Eslamimanesh, A.; Sattari, M.; Mohammadi, A. H.; Richon, D. Corresponding states method for evaluation of the solubility parameter of chemical compounds. *Ind. Eng. Chem. Res***.** 2012, *51*, 3826-3831.

34) Gharagheizi, F.; Eslamimanesh, A.; Farjood, F.; Mohammadi, A.H.; Richon, D. Solubility parameter of non-electrolyte organic compounds: Determination using quantitative structure–property relationship strategy. *Ind. Eng. Chem. Res***.** 2011, *50*, 11382-11395.

35) Gharagheizi, F.; Eslamimanesh, A.; Ilani Kashkooli, P. Mohammadi, A. H.; Richon, D. QSPR molecular approach for representation/prediction of very large vapor pressure dataset. *Chem. Eng. Sci.*, 2012, 76, 99-107.

36) Gharagheizi, F.; Eslamimanesh, A.; Sattari, M.; Mohammadi, A. H.; Richon, D. Development of corresponding states model for estimation of the surface tension of chemical compounds. *AIChE J.* In Press, 2012.

37) Gharagheizi, F.; Eslamimanesh, A.; Sattari, M.; Mohammadi, A. H.; Richon, D. Corresponding states method for determination of the viscosity of gases at atmospheric pressure. *Ind. Eng. Chem. Res***.** 2012, *51*, 3179-3185.

38) Gharagheizi, F.; Eslamimanesh, A.; Mohammadi, A. H.; Richon, D. Determination of critical properties and acentric factors of pure compounds using the artificial neural network group contribution algorithm. *J. Chem. Eng. Data* 2011, *56*, 2460-2476.

39) Gharagheizi, F.; Eslamimanesh, A.; Mohammadi, A. H.; Richon, D. Representation and prediction of molecular diffusivity of nonelectrolyte organic compounds in water at infinite dilution using the artificial neural network-group contribution method. *J. Chem. Eng. Data* 2011, *56*, 1741-1750.

40) Gharagheizi, F.; Eslamimanesh, A.; Mohammadi, A. H.; Richon, D. Use of artificial neural network-group contribution method to determine surface tension of pure compounds. *J. Chem. Eng. Data* 2011, *56*, 2587-2601.

41) Gharagheizi, F.; Eslamimanesh, A.; Mohammadi, A. H.; Richon, D. Empirical method for representing the flash-point temperature of pure compounds. *Ind. Eng. Chem. Res.* 2011, *50*, 5877-5880.

42) Gharagheizi, F.; Eslamimanesh, A.; Mohammadi, A.H.; Richon, D. A group contribution-based method for calculation/estimation of solubility parameter of organic compounds. *Ind. Eng. Chem. Res.* 2011, *50*, 10344-10349.

43) Gharagheizi, F.; Eslamimanesh, A.; Sattari, M.; Tirandazi, B.; Mohammadi, A. H.; Richon, D. Evaluation of thermal conductivity of gases through a corresponding states method. Submitted to *Ind. Eng. Chem. Res.*, 2012, *51*, 3844-3849.

44) Gharagheizi, F.; Eslamimanesh, A.; Mohammadi, A. H.; Richon, D. Determination of parachor of various compounds using an artificial neural network-group contribution method. *Ind. Eng. Chem. Res.* 2011, *50*, 5815-5823.

45) Gharagheizi, F.; Eslamimanesh, A.; Mohammadi, A. H.; Richon, D. Representation/Prediction of solubilities of pure compounds in water using artificial neural network-group contribution method. *J. Chem. Eng. Data* 2011, *56*, 720-726.

46) Gharagheizi, F.; Eslamimanesh, A.; Mohammadi, A. H.; Richon, D. Group contribution model for determination of molecular diffusivity of non-electrolyte organic compounds in air at ambient conditions. *Chem. Eng. Sci.* 2012, *68*, 290-304.

47) Gharagheizi, F.; Eslamimanesh, A.; Mohammadi, A. H.; Richon, D. Artificial neural network modeling of solubilities of 21 commonly used industrial solid compounds in supercritical carbon dioxide. *Ind. Eng. Chem. Res.* 2011, *50*, 221-226.

48) Mohammadi, A. H.; Eslamimanesh, A.; Richon, D. Wax solubility in gaseous system: Thermodynamic consistency test of experimental data. *Ind. Eng. Chem. Res.* 2011, *50*, 4731-4740.

49) Javanmardi, J.; Babaee, S.; Eslamimanesh, A.; Mohammadi, A.H. Experimental measurements and predictions of gas hydrate dissociation conditions in the presence of methanol and ethane-1,2-diol aqueous solutions. *J. Chem. Eng. Data*, 2012, 57, 1474-1479. (Related to Chapter 3 of this thesis)

50) Yazdizadeh, M.; Eslamimanesh, A.; Esmaeilzadeh, F. Applications of cubic equations of state for determination of the solubilities of industrial solid compounds in supercritical carbon dioxide: A comparative study. *Chem. Eng. Sci.* 2012, *71*, 283-299.

51) Mohammadi, A. H.; Eslamimanesh, A.; Yazdizadeh, M.; Richon, D. Glycol loss in natural gas system: Thermodynamic assessment test of experimental solubility data. *J. Chem. Eng. Data* 2011, *56*, 4012–4016.

52) Yazdizadeh, M.; Eslamimanesh, A.; Esmaeilzadeh, F. Thermodynamic modeling of solubilities of various solid compounds in supercritical carbon dioxide: Effects of equations of state and mixing rules. *J. Supercrit. Fluids* 2011, *55*, 861-875.

53) Gharagheizi, F.; Eslamimanesh, A.; Ilani-Kashkooli, P.; Mohammadi, A. H.; Richon, D. Determination of vapor pressure of chemical compounds: A group contribution model for an extremely large database. *Ind. Eng. Chem. Res.* 2012, *51*, 7119-7125.

54) Mohammadi, A. H.; Eslamimanesh, A.; Gharagheizi, F.; Richon, D. A novel method for evaluation of asphaltene precipitation titration data. *Chem. Eng. Sci.* 2012, 78, 181-185.

55) Salamat, Y.; Moghadassi, A.; Illbeigi, M.; Eslamimanesh, A.; Mohammadi A. H. Experimental investigation of hydrogen sulfide clathrate hydrate formation induction time in the presence/absence of kinetic inhibitor. *J. Nat. Gas Chem.* Accepted manuscript, 2012.

56) Mohammadi, A. H.; Gharagheizi, F.; Eslamimanesh, A.; Richon, D. Evaluation of experimental data for wax and diamondoids solubility in gaseous systems. *Chem. Eng. Sci.* 2012, *81*, 1-7.

57) Chamkalani, A.; Amir H. Mohammadi, A.H.; Eslamimanesh, A.; Gharagheizi, F.; Richon, D. Diagnosis of asphaltene stability in crude oil through ''two parameters'' SVM model. *Chem. Eng. Sci.* 2012, *81*, 202-208.

58) Babaee, S.; Hashemi, H.; Javanmardi, J.; Eslamimanesh, A. ; Mohammadi, A. H. Thermodynamic model for prediction of phase equilibria of clathrate hydrates of hydrogen with different alkanes, alkenes, alkynes, or cycloalkanes. *Fluid Phase Equilib.* Accepted manuscript, 2011.

Notes

Études Thermodynamiques sur les Semi-Clathrate Hydrates de TBAB + Gaz Contenant du Dioxyde de Carbone

RESUME : Capturer le CO_2 est devenu un domaine de recherche important en raison principalement des forts effets de serre dont il est jugé responsable. La formation d'hydrate de gaz comme technique de séparation montre un potentiel considérable, d'une part pour sa faisabilité physique et d'autre part pour une consommation énergétique réduite. En bref, les hydrates de gaz (clathrates) sont des composés ″cages″ non-stœchiométriques, cristallins comme la glace et formés par une combinaison de molécules d'eau et de molécules hôtes convenables, à basses températures et pressions élevées. Puisque la pression exigée pour la formation d'hydrate de gaz est généralement forte, il est judicieux d'ajouter du bromure tétra-n-butylique d'ammonium (TBAB) comme promoteur de formation d'hydrate de gaz. En effet, le TBAB permet généralement de réduire la pression exigée et/ou d'augmenter la température de formation aussi que de modifier la sélectivité des cages d'hydrates au profit des molécules de CO_2. TBAB participe à la formation des cages par liaisons ″hydrogène″. De tels hydrates sont nommés "semi-clathrate hydrates". Évidemment, des données d'équilibres de phase fiables et précises, des modèles thermodynamiques acceptables, et d'autres études thermodynamiques sont requises pour concevoir des procédés de séparation efficaces utilisant la technologie mentionnée ci-dessus. Dans ce but, des équilibres de phase de clathrate/semi-clathrate hydrates de de divers mélanges avec des gaz contenant CO_2 (CO_2 + CH_4/N_2/H_2) ont été mesurés, ici, en présence d'eau pure et de solutions aqueuses de TBAB. La partie théorique de la thèse présente un modèle thermodynamique développé avec succès sur la base de la théorie des solutions solides de van der Waals et Platteeuw (vdW-P) associée aux équations modifiées de la détermination des constantes de Langmuir des promoteurs d'hydrates pour la représentation/prédiction des équilibres en présence de ″semi-clathrate hydrates″ de CO_2, CH_4, et N_2. Plusieurs tests de cohérence thermodynamique basés soit sur l'équation de Gibbs-Duhem, soit sur une approche statistique ont été appliqués aux données d'équilibre de phase des systèmes de ″clathrate hydrates″ simples/mélanges afin de statuer sur leur qualité.

Mots clés : Semi-clathrate hydrate, Équilibres de phase, Appareillage expérimental, Modèle thermodynamique, Capture de CO_2, tests de cohérence.

Thermodynamic Studies on Semi-Clathrate Hydrates of TBAB + Gases Containing Carbon Dioxide

ABSTRACT : CO_2 capture has become an important area of research mainly due to its drastic green-house effects. Gas hydrate formation as a separation technique shows tremendous potential, both from a physical feasibility as well as an envisaged lower energy utilization criterion. Briefly, gas (clathrate) hydrates are non-stoichiometric, ice-like crystalline compounds formed through a combination of water and suitably sized guest molecule(s) under low-temperatures and elevated pressures. As the pressure required for gas hydrate formation is generally high, therefore, aqueous solution of tetra-n-butyl ammonium bromide (TBAB) is added to the system as a gas hydrate promoter. TBAB generally reduces the required hydrate formation pressure and/or increases the formation temperature as well as modifies the selectivity of hydrate cages to capture CO_2 molecules. TBAB also takes part in the hydrogen-bonded cages. Such hydrates are called "semi-clathrate" hydrates. Evidently, reliable and accurate phase equilibrium data, acceptable thermodynamic models, and other thermodynamic studies should be provided to design efficient separation processes using the aforementioned technology. For this purpose, phase equilibria of clathrate/semi-clathrate hydrates of various gas mixtures containing CO_2 (CO_2 + CH_4/N_2/H_2) in the presence of pure water and aqueous solutions of TBAB have been measured in this thesis. In the theoretical section of the thesis, a thermodynamic model on the basis of the van der Waals and Platteeuw (vdW-P) solid solution theory along with the modified equations for determination of the Langmuir constants of the hydrate formers has been successfully developed to represent/predict equilibrium conditions of semi-clathrate hydrates of CO_2, CH_4, and N_2. Later, several thermodynamic consistency tests on the basis of Gibbs-Duhem equation as well as a statistical approach have been applied on the phase equilibrium data of the systems of mixed/simple clathrate hydrates to conclude about their quality.

Keywords : Semi-clathrate hydrate, Phase equilibria, Experimental set-up, Thermodynamic model, CO_2 capture, Consistency test.

MINES ParisTech

ParisTech
INSTITUT DES SCIENCES ET TECHNOLOGIES
PARIS INSTITUTE OF TECHNOLOGY